Luís Miguel Paredes Blanco

Licenciado em Engenharia Geológica

Compaction quality control on site of earthworks - A comparative study

Dissertação para obtenção do Grau de Mestre em Engenharia Geológica (Geotecnia)

Orientadora: Prof. Doutora Ana Paula Fernandes da Silva (FCT/UNL)

Co-orientador: Mestre Eng.º Alexandre M. Gameira dos Santos Ferreira (DGRM)

Júri:

Presidente: Prof. Doutor Pedro Calé da Cunha Lamas

Arguente: Prof. Doutora Maria da Graça Azevedo Brito

Vogal: Prof. Doutora Ana Paula Fernandes da Silva

FACULDADE DE CIÊNCIAS E TECNOLOGIA
UNIVERSIDADE NOVA DE LISBOA

Março 2015

Luís Miguel Paredes Blanco

Licenciado em Engenharia Geológica

Compaction quality control on site of earthworks - A comparative study

Dissertação para obtenção do Grau de Mestre em
Engenharia Geológica (Geotecnia)

Orientadora: Prof. Doutora Ana Paula Fernandes da Silva
(FCT/UNL)

Co-orientador: Mestre Eng.º Alexandre M. Gameira dos Santos Ferreira (DGRM)

Júri:

Presidente: Prof. Doutor Pedro Calé da Cunha Lamas
Arguente: Prof. Doutora Maria da Graça Azevedo Brito
Vogal: Prof. Doutora Ana Paula Fernandes da Silva

Março 2015

Compaction quality control on site of earthworks - A comparative study

ACKNOWLEDGMENTS

A presente dissertação representa o culminar de um percurso académico que não poderia ter sido ultrapassado sem a ajuda de algumas pessoas e entidades. Desde já quero deixar um enorme obrigado a todos os que, de alguma forma contribuíram para a elaboração desta dissertação.

Ao engenheiro Santos Ferreira, por toda a disponibilidade e paciência demonstrados durante a realização deste trabalho.

À professora Ana Paula Silva, pela oportunidade de realizar este projecto, assim como pela partilha de conhecimentos, amizade e compreensão demonstrados durante a realização desta dissertação e percurso académico. Agradeço, ainda, a extensa e cuidada revisão desta dissertação.

Às intuições Instituto Portuário e dos Transportes Marítimos (IPTM) e Direção Geral dos Recursos Marítimos (DGRM), pela possibilidade de realizar o estágio nas mesmas.

Aos meus pais, por todo o amor e carinho demonstrados, bem como por todos os sacrifícios que realizaram para me poderem facultar as melhores condições de vida.

A todos os meus familiares.

À Bárbara Carreira, por toda ajuda, compreensão, carinho e atenção demonstrada.

Aos meus amigos, Andreia Barbas, André Costa, Diana Silva, Henrique Lopes, Luís Conceição pelo apoio, momentos de diversão proporcionado ao longo deste percurso académico.

Às minhas colegas de estágio Liliana Ribeiro, Cláudia Santos pela amizade e apoio demonstrados durante esta fase.

ABSTRACT

The capacity to use geologic materials (soil and rock) that are available in the surrounding environment is inherent to the human civilization and has contributed to the evolution of societies throughout the course of history. The use of these materials in the construction of structures such as houses, roads, railways or dams, stirred the improvement of socioeconomic and environmental conditions.

Several reports of structural problems on embankments can be found throughout history. A considerable number of those registers can be linked to inadequate compaction, demonstrating the importance of guaranteeing a suitable quality of soil compaction. Various methodologies and specifications of compaction quality control on site of earthworks, based on the fill moisture content and dry unit weight, were developed during the 20th century. Two widely known methodologies are the conventional and nuclear techniques. The conventional methods are based on the use of the field sand cone test (or similar) and sampling of material for laboratory-based testing to evaluate the fill dry unit weight and water content. The nuclear techniques measure both parameters in the field using a nuclear density gauge.

A topic under discussion in the geotechnical community, namely in Portugal, is the comparison between the accuracy of the nuclear gauge and sand cone test results for assessing the compaction and density ratio of earth fills, particularly for dams. The main purpose of this dissertation is to compare both of them. The data used were acquired during the compaction quality control operations at the Coutada/Tamujais dam trial embankment and core construction. This is a 25 m high earth dam located in Vila Velha de Rodão, Portugal. To analyse the spatial distribution of the compaction parameters (water content and compaction ratio), a 3D model was also developed.

The main results achieved are discussed and finally some considerations are put forward on the suitability of both techniques to ensure fill compaction quality and on additional research to complement the conclusions obtained.

Keywords: Embankment dams; Compaction control; Sand cone test; Nuclear density meter

RESUMO

A capacidade de recorrer a materiais geológicos (solo e rocha) presentes no meio envolvente é inerente à civilização humana e tem contribuído para o seu desenvolvimento ao longo da história. A utilização destes materiais na construção de infraestruturas como estradas, habitações ou barragens, estimulou uma melhoria gradual das condições socioeconómicas e ambientais.

Ao longo da história podem ser encontrados diversos relatos sobre problemas estruturais em aterros que podem ser associados a processos de compactação inadequados, demonstrando-se assim a importância de controlar a qualidade da compactação. Para esse propósito foram desenvolvidas diversas metodologias e especificações durante o séc. XX, baseadas no peso específico e o teor em água do solo após colocação no aterro.

Duas metodologias amplamente utlizadas nas operações de controlo são designadas por convencional e nuclear. Na metodologia convencional usa-se o ensaio da garrafa de areia (ou similar) através do qual se colhem amostras que são enviadas para laboratório para determinar o seu peso volúmico e teor em água *in situ*. Na técnica nuclear recorre-se ao gamadensímetro nuclear para determinar ambos os parâmetros.

Um tópico debatido na comunidade geotécnica, nomeadamente em Portugal, é a comparação do grau de exactidão dos resultados obtidos pelos ensaios com o gamadensímetro nuclear e a garrafa de areia para obter o grau de compactação e o peso volúmico, *in situ,* durante o controlo de compactação de aterros, particularmente em barragens de aterro. O principal objectivo da presente dissertação consiste em comparar os resultados obtidos pelos ensaios acima referidos durante o controlo de compactação. Para realizar este estudo foram utilizados dados referentes ao empreendimento da barragem de Coutada/Tamujais, que consiste numa barragem de terra com 25 m de altura situada em Vila Velha de Rodão, Portugal. Adicionalmente, foram realizados modelos tridimensionais para analisar a distribuição espacial dos parâmetros de compactação (teor em água e grau de compactação).

Os resultados obtidos são discutidos, e tecem-se considerações sobre a aplicabilidade de ambas as técnicas durante o controlo de compactação. Adicionalmente, sugerem-se trabalhos futuros a desenvolver sobre o presente tema.

Palavras-chave: Barragens de aterro; Controlo de compactação; Garrafa de areia; Gamadensímetro nuclear

TABLE OF CONTENTS

LIST OF ILLUSTRATIONS

List of Tables

LIST OF ACRONYMS

AS	Australian standards
ASBNT	Associação Brasileira de Normas Técnicas
ASTM	American Society for Testing Materials
BSM	Backscatter mode
CEN	European Committee for Normalization
CPNI	Centre for the Protection of the National Infrastructure
CIGB	Comissão Internacional de Grandes Barragens
DM	Direct transmission mode
EDG	Electrical density gauge
EL	Equality line
ESCS	European Soil Classification System
FCT-UNL	Faculdade de Ciências e Tecnologia - Universidade NOVA de Lisboa
IDW	Inverse distance weightening
ISAC	Inert steel aggregate
ISO	International Society of Standardization
ICOLD	International Commission of Large Dams
IQR	Interquartile range
IST	Instituto Superior Técnico
LNEC	Laboratório Nacional de Engenharia Civil
MADRP	Ministério da Agricultura do Desenvolvimento Rural e das Pescas
MDI	Moisture density indicator
NDG	Nuclear densimeter gauge
NP	Norma Portuguesa
NRC	National Research Council
OMC	Optimum moister content
OVM	Oven method
SCT	Sand cone test
SDG	Soil density gauge
SPT	Standard penetration test
SS	Steel shot
USACE	United States Army Corps of Engineers
USBR	United Sates Bureau of Reclamation
USCS	United Soil Classification System
USDI-BR	United States Department of the Interior-Bureau of Reclamation
UTL	Universidade Técnica de Lisboa
WB	Water Balloon
WSDOT	Washington State Department of Transportation
ZCI	Zona Centro Ibérica

LIST OF SYMBOLS

Greek alphabet

γ	In situ or natural unit weight (kN/m^3)
γ'	Submerged unit weight (kN/m^3)
γ_ω	Water unit weight (kN/m^3)
$\gamma_{\omega c}$	Cylinder wet unit weight (kN/m^3)
$\gamma_{\omega fill}$	Fill wet unit weight (kN/m^3)
γ_d	Dry unit weight (kN/m^3)
γ_{dc}	Cylinder dry unit weight (kN/m^3)
$\gamma_{d,field}$	Field dry unit weight (kN/m^3)
γ_{dfill}	Fill dry unit weight (kN/m^3)
$\gamma_{d,ref}$	Dry unit weight from the reference sand (kN/m^3)
γ_{dmax}	Maximum dry unit weight (kN/m^3)
$\gamma_{dmax,laboratory}$	Maximum dry unit weight obtained in laboratory (kN/m^3)
$\gamma_{dmax,ref}$	Maximum dry unit weight for reference sample (kN/m^3)
γ_{sample}^{max}	Maximum wet unit weight for the sample (kN/m^3)
γ_{dmin}	Minimum dry unit weight for purely (kN/m^3)
γ_{fill}	Fill unit weight (kN/m^3)
γ_{max}	Converted maximum wet unit weight (kN/m^3)
γ_s	Solids unit weight (kN/m^3)
η	Viscosity of the water (kg/m.s)
ρ_s	Density of the soil particles (kg/m^3)
ρ_w	Density of the water (kg/m^3)
ρ_{wet}	Wet density of compacted specimen (kg/m^3)
ρ_{wet_c}	Converted wet density of compacted specimen (kg/m^3)
ω	Water content (kN/m^3)
ω_{fill}	Fill water content (%)
ω_L	Liquid limit value (%)
ω_{opt}	Optimum water content (%)
ω_P	Plastic limit (%)
ω_{ref}	Optimum water content for the reference sample (%)

Latin alphabet

A	Coefficient of seismicity
C	Relation between the fill and laboratory compactive efforts
CL	Inorganic clay with low to medium plasticity
D	Diameter (m)
DC	Degree of compaction (%)
e	Void ratio
e_{max}	Maximum void index for sand
e_{min}	Minimum void index for sand
g	Gravitacional acceleration (m/s^2)
G_s	Specific gravity of the solid particles
GC-GM	Clayey gravel with silt
GP-GC	Poorly graded gravel with clay
GW-GC	Well graded gravel with clay
h_d	Height of fall of the hammer (m)
v	Velocity (m/s)
M_c	Mass of container (kg)
M_{cs}	Mass of container and oven dry specimen (kg)
M_{cws}	Mass of container and wet specimen (kg)
M_h	Mass of the hammer (kg)
M_s	Mass of solid particles (kg)
M_w	Mass of water (kg)

n	Porosity (%)
N_b	Number of blows given by the hammer
N_t	Number of layers used on the test
PI	Plasticity index (%)
R	Pearson coefficient
R^2	Coefficient of determination
RC	Relative compaction (%)
S	Degree of saturation (%)
SC	Clayey sand
SC-SM	Clayey sand with silt
SM	Silty sands
SW	Well graded sand
SP-SM	Poorly graded silty sands
V	Volume of compacted soil (m^3)
V_a	Volume of air in the voids (m^3)
V_f	Volume of water that remains in the cylinder at the end of the test (m^3)
V_i	Volume of liquid in the cylinder when in the beginning of the test (m^3)
V_s	Volume of solids (m^3)
Vs	Versus
V_T	Total volume of a soil sample (m^3)
V_v	Volume of voids (m^3)
V_w	Volume of water in the voids (m^3)
$W_{a/r}$	Weight of water that was added or removed to the soil sample (kN)
W_{C+J}	Weight of the device composed by the jar and cone when filled with sand, during the sand cone test (kN)
W_{ES}	Weight of the excavated soil (kN)
W_{FC}	Weight of sand that used to fill the cone, during the sand cone test (kN)
W_{FH}	Weight of the sand that is used to fill the hole during the sand cone test (kN)
W_W^{samp}	Wet weight from the soil sample (kN)
W_{RJ}	Weight of sand remaining in the jar, during the sand cone test (kN)
W_S	Weight of soil solids (kN)
W_ω	Weight of water (kN)
Z	Amount of water added or removed to soil before compacting specimen (%)
z_m	Abscise correspondent to the peak point (%)

1. INTRODUCTION

The ability to use soils and rocks from surrounding environment as construction materials is inherent to humans and this has contributed to the development of the first civilizations, which used them to build shelters. Nowadays, these geologic materials are used to build more complex structures, such as embankments.

Embankment can be defined as structure generally with a trapezoidal section, in which geological materials (soil or rock) are used as construction materials. Depending on the type of material, there are two types of embankments: earth and rock fills.

These structures can be used in a wide range of geotechnical projects, such as dams, slope stability, highways or landfills. However, its design and mechanical proprieties must be adapted in conformity with the type of project, since the desired behaviour for each type of embankment depends on the project purpose.

A typical example of this situation is the difference between the acceptable behaviour for earth dams and road embankments. An embankment dam is constructed to store water, therefore the existence of cracks in the embankment is unacceptable, since cracks allow water seepage and, in extreme cases, can lead to failure. On the other hand, this type of structures can support minor deformations, which are not tolerable in road construction once any minor deformations can create cracks in the road surface. Nonetheless, the presence of minor cracks in a road embankment will not affect its serviceability. Figure 1.1 represents typical profiles of embankments for different types of project. This dissertation focuses on the earth embankments associated to dam projects designated as earth fill dams.

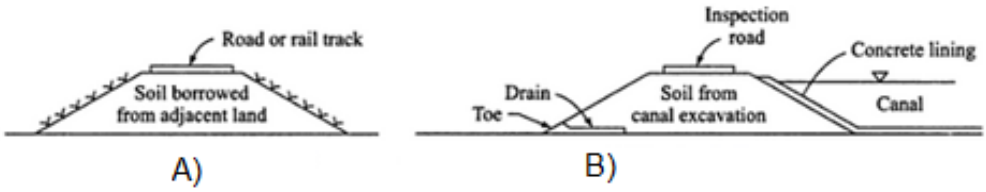

A) Homogenous embankment for road/railway; B) Canal embankment.

Figure 1.1 - Typical sections for embankments (Gulhati & Datta, 2008)

The construction process of an earth dam implicates a considerable number of stages, one of them is designated as soil compaction. This process intends to improve mechanical proprieties of the soil within ranges defined in the project, making it suitable to be used as construction material. Through the course of human history, it is possible to find various reports of early dam failures that can be linked to an inappropriate soil compaction, since compaction can control the deformability, shear strength and permeability of the construction materials.

Those failures showed the importance of ensuring the quality of the soil compaction, and stimulated the development of techniques to measure the results from soil compaction, which are mostly based on two properties:

- Fill water content;
- Fill unit weight.

There are a wide variety of techniques that can be used during the compaction quality control operations; two commonly used methodologies are the conventional and the nuclear. The conventional methodology consists in using a sand cone test - SCT (or similar) and sampling of material for laboratory-based testing to evaluate the control parameters (fill water content and dry unit weight); in the nuclear methodology these parameters are measured by a nuclear density gauge (NDG).

The sand cone test is a time consuming and destructive method to access the control parameters in the field, in contrast to the nuclear gauge, which is a rapid and non-destructive test. However the accuracy of the nuclear gauge measurement relatively to the sand cone test has been questioned since their introduction during the 60s.

Nevertheless, the technical and technologic evolution witnessed in the last decades, allied to the short time period that is necessary to measure the control parameters with the nuclear gauge, and the fact that it is a non-destructive test, contributed to an increase of its popularity. Nowadays, it is a widely accepted method in compaction control operation but in some countries, namely in Portugal, the problem about which method is more accurate remains contemporary and is still discussed by the technical and scientific community.

1.1. OBJECTIVES AND METHODOLOGY

This dissertation falls within the scope of the *Mestrado em Engenharia Geológica (Geotecnia)* from the *Universidade NOVA de Lisboa- Faculdade de Ciências e Tecnologia* (FCT-UNL). The main purpose of this work is to study the suitability of using the conventional (SCT) and nuclear methodologies (NDG) during compaction control operations, by comparing the accuracy of the results obtained during the construction of an earth dam (test fill and core).

It uses the results from the compaction quality control operations developed during the construction of the Coutada/Tamujais dam core and trial embankment, a 22.5 m high earthfill dam located in municipality of Vila Velha de Rodão, Portugal, comprising an area of 322 ha. The data from the trial embankment and core were analysed as two different case studies.

The methodology applied to compare the results from both methodologies can be divided in 2 stages (Figure 1.2). In the first stage, the Hilf method was applied to the results from the conventional and nuclear methodologies (fill unit weight and water content) to access the degree of compaction for both cases. Afterwards, the results from both methodologies (fill unit weight, water content, and degree of

compaction) were compared through three types of bivariate analysis, which differed for each case study.

Complementarily, the results from the dam core quality control were plotted in three-dimensional models using Rockworks® (version15) software to study the spatial variation of the control parameters.

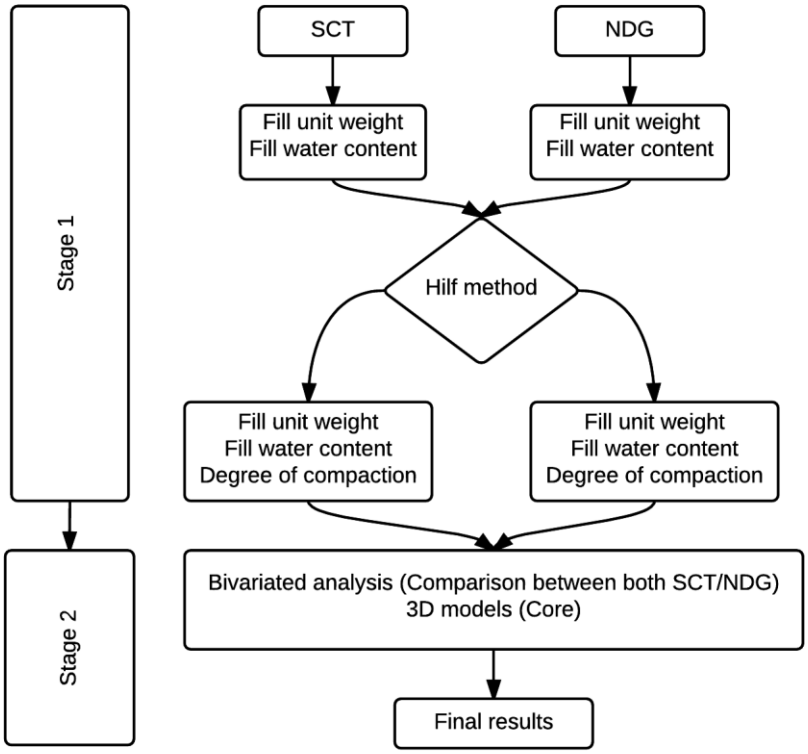

Figure 1.2 - Methodology used for the comparison between the conventional and nuclear methodologies

1.2. ORGANIZATION

The dissertation is divided into five chapters, as summarized in the following paragraphs:

- First chapter comprises the description of dissertation subject, objectives and organization;
- Second chapter consists in a state of the art about the history, types of earthfill dams and their construction techniques;
- Third chapter is a literature review about soil compaction that can be divided in two sections: in the first one, the aspects related to soil compaction are described, and the other section discusses aspects related to the compaction control;

- Fourth chapter comprises all the aspects referent to the case study, the results achieved during the comparison between both methodologies for compaction control, the 3D model, and the discussion of the results;
- Fifth chapter encompasses the final considerations, and suggestions about future researches that might be taken to complement the conclusions.

The volume encompasses a set of five annexes with complementary data to understand the research developed.

2. EARTH DAMS

This chapter consists in a brief review of general aspects related to earth dams, such as their concept and evolution through the course of the Human history, classification systems, construction phases and structural elements, and most usual designs.

2.1. DEFINITION AND CLASSIFICATION

2.1.1. TYPES OF EMBANKMENT DAMS

The dams described in this work can be defined as manmade structures built across valleys that act as barriers to store water. These structures can be classified by their construction materials, dimensions and storage capacity, hydraulic design, construction methods, and purpose (Figure 2.1). Taking into account the construction materials, these structures can be divided essentially in two types: rock fill, and earth fill dams. As the names indicate, an earth fill dam is predominately composed by soil materials; on the other hand, rock fill is mostly composed by rock materials. As mentioned before, this dissertation will focuses of the first type.

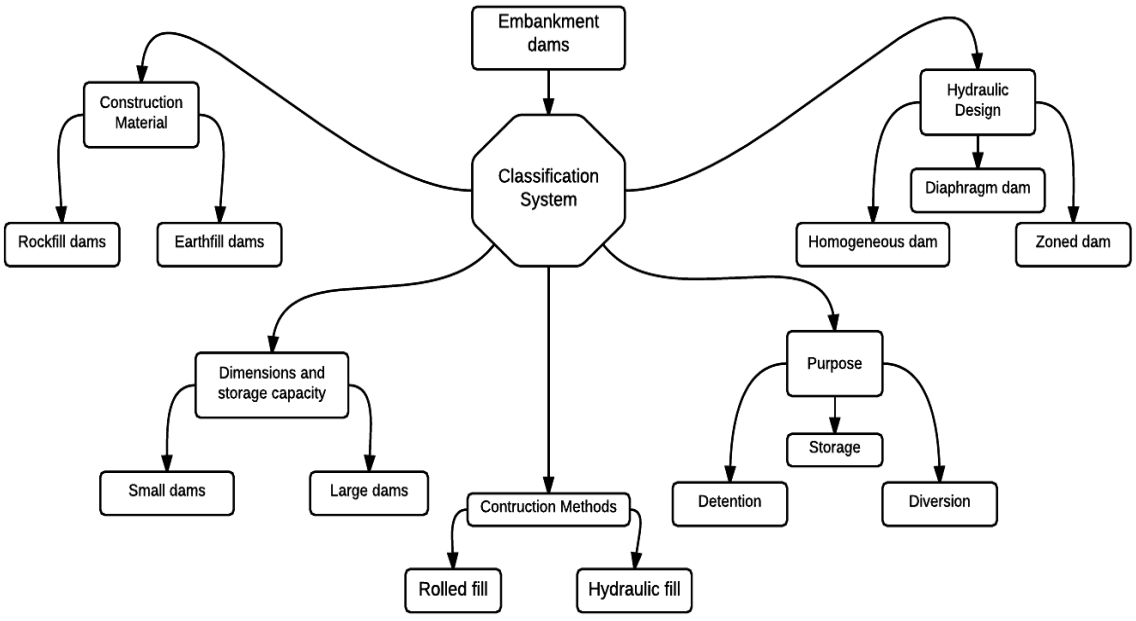

Figure 2.1 – Embankment dam classification systems

An advantage of embankment dams relatively to concrete dams is the capacity of reusing natural materials from the surrounding areas that do not need substantial processing, instead of using a more expensive manufactured material, as concrete. Another important characteristic associated to earth dams is the aptitude to be constructed in areas with weaker foundations and/or topographic

characteristics that are not adequate to other types of dams, like the ones made of concrete. This factors contribute to the popularity of earth fill dams (USBR, 2011).

A classification system regarding the dam dimensions and reservoir capacity was defined by international committee of large dams (ICOLD), this system divides dams in two types: large and small dams. This institution defines large dams as “a dam with a height of 15 m or greater from lowest foundation to crest or a dam between 5 m and 15 m impounding more than 3 million cubic meters” (ICOLD, 2011 *apud* ICOLD, 2012).

This definition is commonly recognized in the world, however the Portuguese distinction between small and large dams, presented in the Decree-Law, n.º 344/2007 of 15 October by the *Subcomissão dos Regulamentos de Barragens*, differs from ICOLD, since it groups dams in two categories, with the following characteristics:

- Large dams, structures with a height equal or higher to 15 m, or dams with an height equal or higher than 10 m with an reservoir capacity above 1 million m^3;
- Dams with a height lower than 15 m that cannot be included in the large dams category, and with a reservoir capacity lower than 100,000 m^3.

Depending on the dam purpose, they can be divided into three classes: storage dams, diversion dams and detention dams. Storage dams as the name indicates are constructed to impound water for supply; diversion dams are used for carrying water into ditches, canals or other transportation systems, and detention dams retard and minimize the consequences of sudden floods (USBR, 1987).

2.1.2. TYPES OF EARTH DAMS

In each earth dam project, the adopted design “must be realistic. It should reflect actual foundations conditions at the site and the material available for embankment construction. It should not be patterned after a successful design used at a site with different conditions or material, or even at a site with similar conditions. It should be designed for its specific site geology” (USBR, 1987). In other words, design should be adapted to the construction site, and based on the information retrieved during the investigation phase. In compliance with Moum *et al.* (1985) and Raj (2008), a design based classification for embankment dams, divides earth dams in three generic classes: diaphragm, homogeneous and zoned (Figure 2.2).

Fell *et a*l (2015), defines seven types of earth dams, which include the three generic classes defined above and some of their variations. The typical section, main characteristics, and applicability of these dams are expressed in Table 2.1.

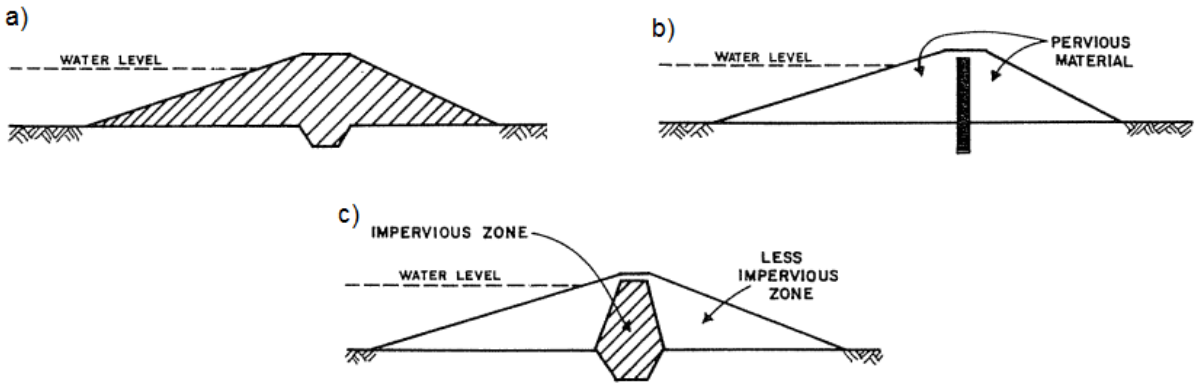

a) Homogenous earthfill; b) Homogeneous dam with diaphragm; c) Zoned embankment dam.

Figure 2.2 - Earthfill dams types (Moum, *et al.*, 1985)

Table 2.1 - Types of embankment dams (adapted from Zackaria *et al*., 2006; Fell *et al*., 2015)

Dam type	**Typical section**	**Degree of filter control of internal erosion and piping**	**Degree of control of pore pressures for stability**	**Applicability**
Homogeneous earth fill	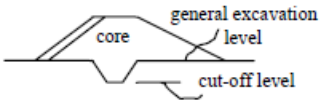	Non-existent	Poor	Low hazard areas
Earth fill with toe drain	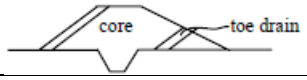	Poor	Poor	
Zoned earth fill	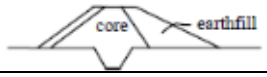	Moderate	Good	Very low to significant hazard areas
Earth fill with horizontal drain	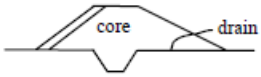	Poor	Poor	Very low and low to significant if no population at risk
Earth fill with vertical and horizontal drain	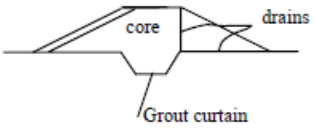	Very good to good	Good	Significant to extreme hazard areas
Earth and rock fill, central core	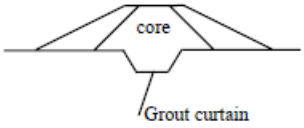	Very good	Very good	Significant to extreme hazard areas. May be costly and complicated for dams less than 20m high
Earth and rock fill, sloping upstream core	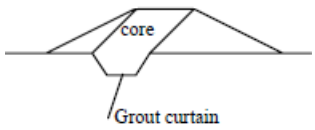	Very good	Very good	Significant to extreme hazard areas. May be costly and complicated for dams less than 20m high. Adequate for staged construction

2.2. HISTORICAL EVOLUTION

Dams played an unquestionable role in the human evolution, and the first ones to be constructed were mainly used to store water for agriculture, but currently dams usually have multiple purposes, for example: water supply, recreation, irrigation, and hydropower generation. Singh (1996) states that the oldest archaeological findings related to dams are located in Jawa, Jordan, and are dated from 4000 B.C.; this findings indicate the presence a structure used to store water constructed of earth with a masonry facing.

According to Singh & Varshey (1995) and Jesus (2011), the first significant developments in dam construction were set by the earliest civilization in the valleys of the Nile, Tigris and Euphrates and the Indus; all these cultures benefited from a climate and topography that were adequate for rain water storage. The dams constructed by these civilizations, with particular reference to the Egyptian civilization (2950 - 2750 B.C.), were earth embankments used for agriculture irrigation. One of the oldest dams recorded in this period is the *Sadd-El-Kafara* dam, in Egypt, with 4800 years old, composed of two rubble walls separated by a central fill formed by sand and gravel; this dam is represented in the Figure 2.3.

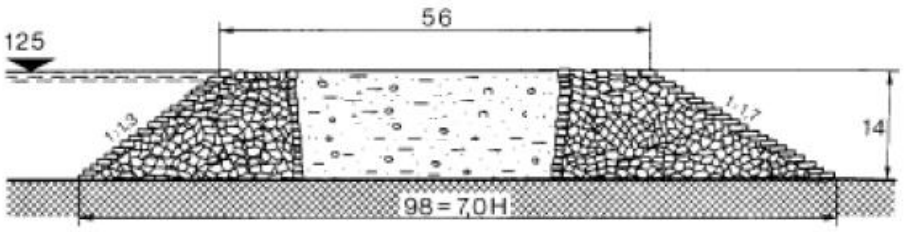

Figure 2.3 - Sadd-El-Kafarra dam (adapted from Jesus, 2011)

The next ground-breaking steps in dam construction were taken during the Roman Civilization, even though Romans used the same hydraulic concepts as the firsts civilizations mentioned above. They developed the capacity to construct more complex dams, and some of them are still functional, nowadays. This civilization introduced the construction of arc dams, in the 1st century A.D. Nero ordered the construction of a 40 m high arch dam for recreational purposes (Bretas *et al.,* 2012). From all the dams constructed during this period, one must emphasize the *Cornalvo* dam (Figure 2.4-1) and the Prosperina dam (Figure 2.4-2), both located in the vicinity of *Badajoz*, Spain, which are both gravity dams dated from the 1st and 2nd centuries A.D., respectively.

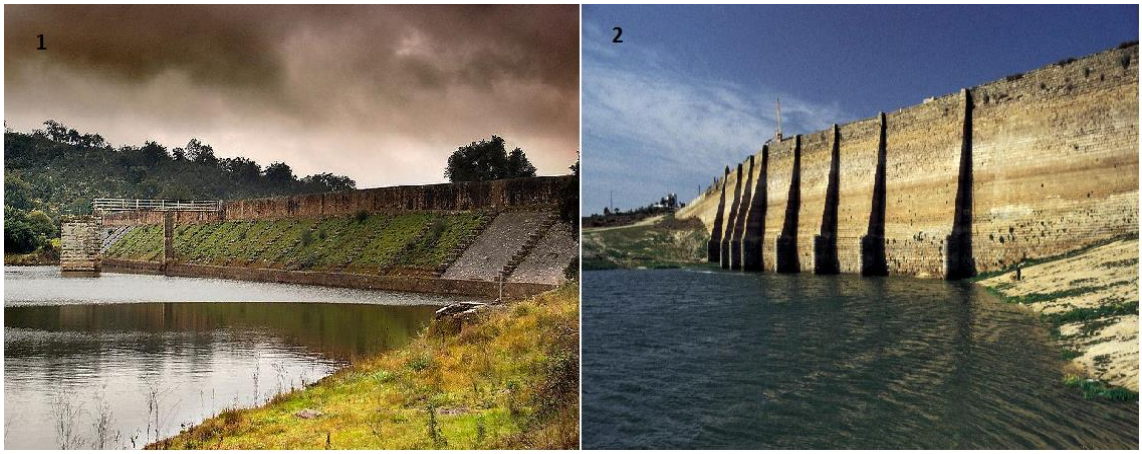

Figure 2.4 - View of the Cornalvo (1) and the Prosperina (2) dams (Jesus, 2011)

According to Singh & Varshey (1995), until the 19th century embankment dam design was mostly based on empirical knowledge. The inexistence of appropriate design methodologies led to various dam failures throughout history, creating a disbelief in this type of dams and some limitations related to their maximum height. Usually and before 1925, the maximum height for these structures did not exceed 30 m; however, in that year, the USBR constructed an earth dam that exceeded 40 m in height. From this year forward, an increase of the knowledge associated to soil mechanics stimulated the resolution of problems associated to embankment dams construction and increased their popularity. The improvements in embankment dam construction where the following *(op. cit*):

- Development of investigation techniques for the study of dam foundations and construction materials, and laboratory techniques to identify this materials proprieties. The information obtained with these techniques enable the creation of dam designs based on the foundation characteristics and materials proprieties;
- The theoretical knowledge on soil mechanics developed from 1925 onwards was used to improve the dams design preserving it against the potential sources of failure;
- Quality control specifications were defined to guarantee that any desired fill characteristics specified in the project were achieved;
- Development of monitoring equipment and practises which enable the study of the post-construction structural behaviour, and an increase of knowledge about dam behaviour that was used in the design of future dams.

These innovations associated to a demographic growth and an increasing demand for electric energy production, which started after the end of the Second World War (1939-1945), increased the acceptance of embankment dams and encouraged the development of higher structures and, in some cases, in places that in the past were not adequate for embankment dams, like valleys with steep abutment slopes or deep pervious foundations (Singh & Varshey, 1995). Figure 2.5 represents the number of dams inaugurated per decade during the 20th century, in accordance with the works of the Comissão Internacional das Grandes Barragens (CIGB, 2008). It can be observed that the number of dam inaugurations started to increase considerably during the 50's, and this period corresponds to the

end of the Second World War which, as emphasised above, was an important factor to the evolution of dam construction.

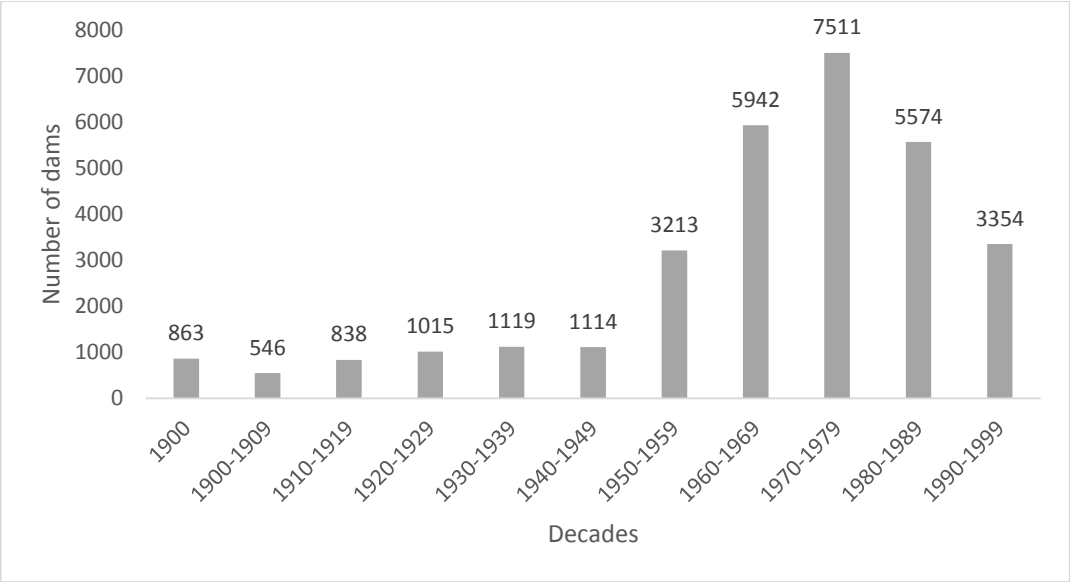

Figure 2.5 - Number of dams inaugurated per each decade of the 20th century (adapted from CIGB, 2008)

Presently, the ICOLD (2014) specifies the existence of 58,266 large dams in their member states; the majority of these dams are earth dams (63%), as demonstrated in the Figure 2.6.

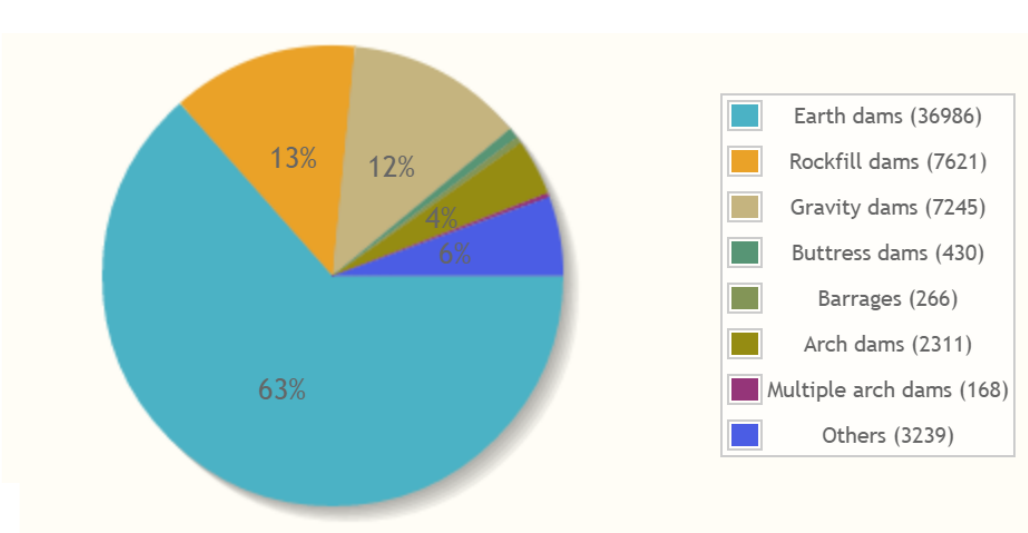

Figure 2.6 - World distribution of each type of dam (ICOLD, 2014)

According to a CIGB (2008), 90% of the world large dams are located in three continents: Asia, North America and Europe, as illustrated in the Figure 2.7. This study also refers that, in 2008, earth dams represent 43.7% of the total; therefore, between 2008 and 2014, the significance of earth dams in the world increased 20%, demonstrating their importance nowadays.

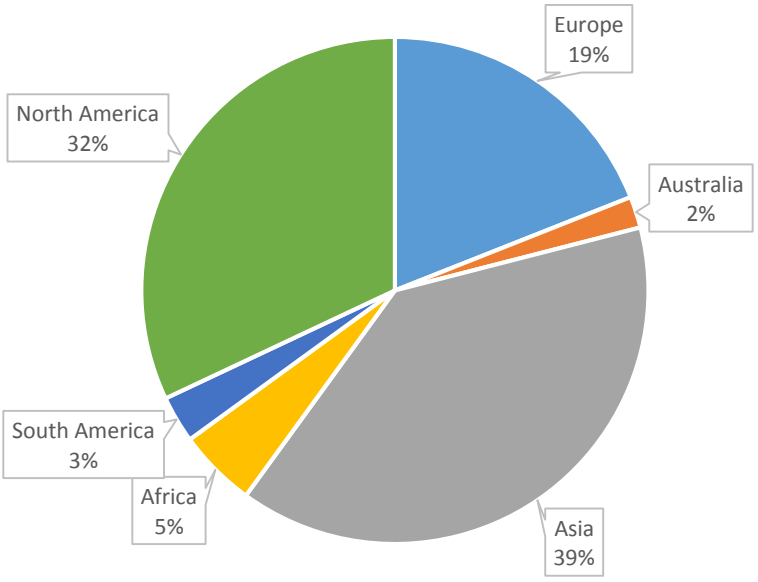

Figure 2.7 - Distribution of large dams in the world (adapted from CIGB, 2008)

The dams can be divided in two types: single purpose and multipurpose - Figure 2.8; in both of them, the majority are used for irrigations purposes.

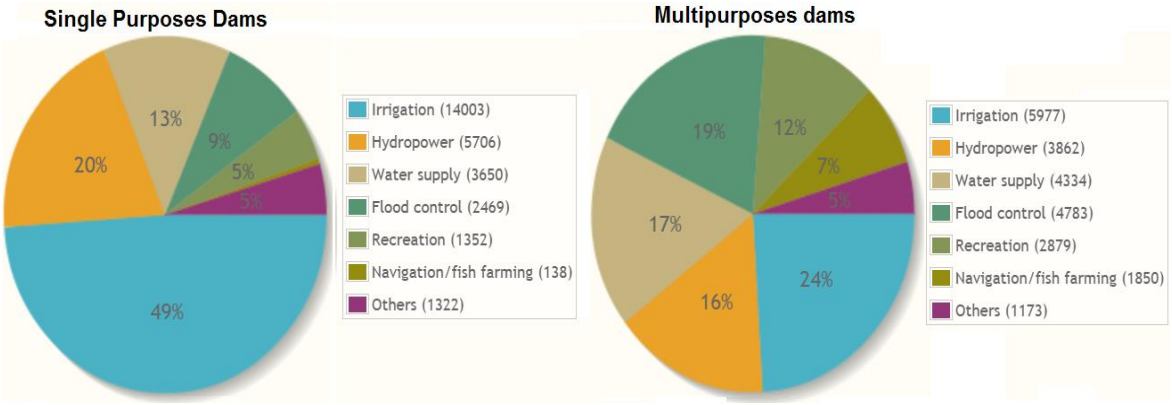

Figure 2.8 - Dams purpose (ICOLD, 2014)

In Portugal, the most ancient archaeological evidences that can be associated to dams are dated from the Roman period. Quintela *et al.* (1989) published several works about this subject, in which 20 dams from this period were identified.

Jesus (2011) states that, in Portugal, the construction of dams reached a peak during the 50s. According to Pimenta (2008 *apud* Faustino 2009) in 2007, there were 231 large dams in Portugal from which 66% (153) were earth fill and/or rock fill dams.

2.3. DAM FAILURES

Despite the important role that dams had in human evolution is always imperative to refer the considerable number of dam failures that occurred throughout human history, since each one of this accidents can be a reminder of the risks associated to dam construction and, also, a highlight of what must be improved and avoided during dam construction. Some historical examples of earth dams failures are listed in Table 2.2

Table 2.2 - Examples of embankment dam failures (adapted from Chanson, 2009)

Dam	Construction date	Date of the accident	Description of failure	Loss of life
Black Brook dam, UK	1797	1799	Collapsed caused by dam settlement and spillway inadequacy.	none
South Fork (Jonhstown) dam, USA	1839	1889	Overtopping and break of earth dam caused by spillway inadequacy	over 2000
Bilberry dam, UK	1843	1852	Failure of earth dam caused by poor construction quality	81
Dale Dyke dam, UK	1863	1863	Earth embankment failure attributed to poor construction work. Surge wave volume ~0.9 Mm^3	150
Dolgarrog dams, UK	1910	1925	Sequential failure of two earth dams following undermining of the upper structure	25
Belci dam, Romania	1962	1991	Dam overtopping and breach (caused by a failure of gate mechanism)	97
Teton Dam, USA	1976	1976	Dam failure caused by cracks and piping in the embankment near completion	11
Glashütte dam, Germany	1953	2002	Earth dam overtopping during a large flood because of inadequate spillway capacity	none

One of the most studied failures is the case of the Teton dam, located in the Teton River, Idaho, United States. This dam was constructed by the Bureau of Reclamation (USBR) and completed in 1975. The failure occurred on June 5, 1976 during the first filling and one of the causes was internal erosion of the core. This accident killed 14 people and caused damages equivalent to hundreds of millions of dollars (Solava & Delatte, 2003).

Due to the destructive effects of dam failures, several studies on this subject had been developed in the last decades, since that information can be used to prevent new accidents and diminish their negative effects. Xu *et al*. (2007) released a study that compiles literature information relative to more than 900 dam failures through the world, excluding China. 593 (65.5%) of those failures referred to earth dams. According to Figure 2.9, the majority of the documented failures occurred in the United States (70.1%), followed by India (4.2%) and United Kingdom (3.6%).

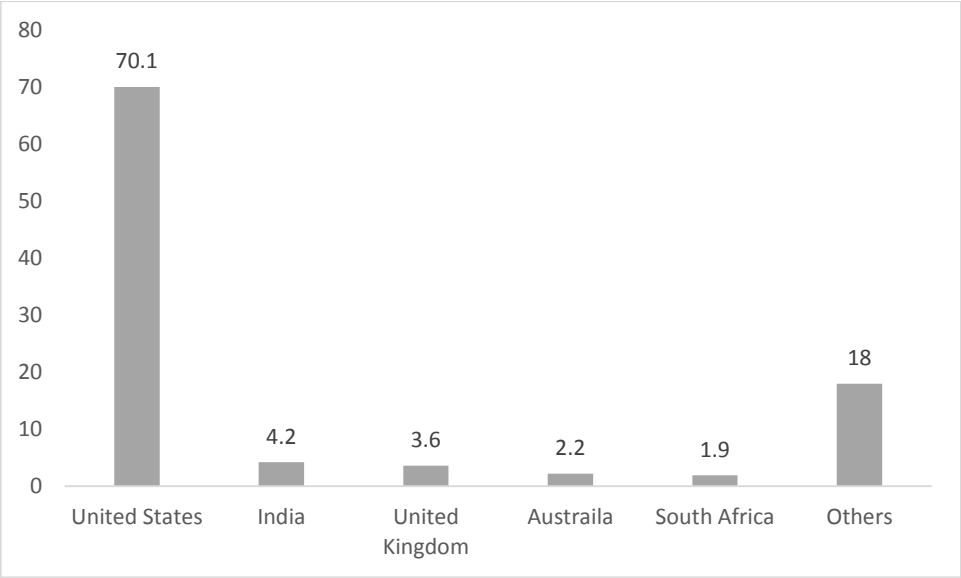

Figure 2.9 - Geographic distribution of dam failures (Xu *et al.*, 2007)

The results from this study were grouped into five categories: reservoir capacity, height of the dam, construction time, age, and dam type. In relation to the reservoir capacity, this study demonstrates that 16.2% (96 cases) of the failures were associated to dams with a reservoir capacity inferior to 1×10^8 m^3; however, dams with a capacity range between $1\text{-}10\times10^8$ and $10\text{-}100\times10^8$ m^3 represent 10.6% (63) and 10.5% (62) of the reports, respectively.

Dams with a height inferior to 15 m represent 50.8% of the failures; from this information it is comprehensible that, in the past, dam failures generally were associated with smaller dams; however, at least 31.5% (187) of the 593 accidents occurred before 1925. As previously referred, this date can be associated to the first advances in soil mechanics, allowing the use of safer construction methodologies and higher earth dams, which to the date did not exceed 30 m of height. Therefore, the predominance of failures in this range and in the range between 15-30 m, which represents 22.8% of the occurrences, may be associated to the construction techniques and the basic soil mechanics knowledge that existed before that date. The diminution of failures in higher ranges of dam's height may also be associated to these developments, since dams with a height superior to 30 m only became common afterwards.

Regarding the construction time, it is possible to identify two periods, 1890-1939 and 1950-1979, representing 32.3% and 21.4%, respectively. The first five year service represent 30.5% of the documented failures. The results regarding the type of dam are not conclusive, since 89.8% of the earth dams are defined as unknown; however, it is possible to denote a predominance of failures in homogenous earth fill dams.

Generally, a dam failure is not a result from a single factor, but rather a combination of factors that may or may not be related; therefore, identifying the failure causes can be difficult. According to *Foster et al.* (2000, 2002 *apud* in Wan, *et al.* 2004), the two most usual types of failures on earth dams are overtopping, internal erosion and piping, which may be associated to inadequate compaction, since

compaction affects the permeability, shear strength resistance, and deformability of the embankment. The results from the Xu *et al.* (2007) study support this affirmation, since the most common types of failure are overtopping and quality problems (Figure 2.10) which include:

- Piping in dam body;
- Sliding of dam body;
- Piping in foundation;
- Piping around spillway;
- Quality issues in spillway;
- Piping around culvert and other embedded structures;
- Quality issues in culvert and other embedded structures.

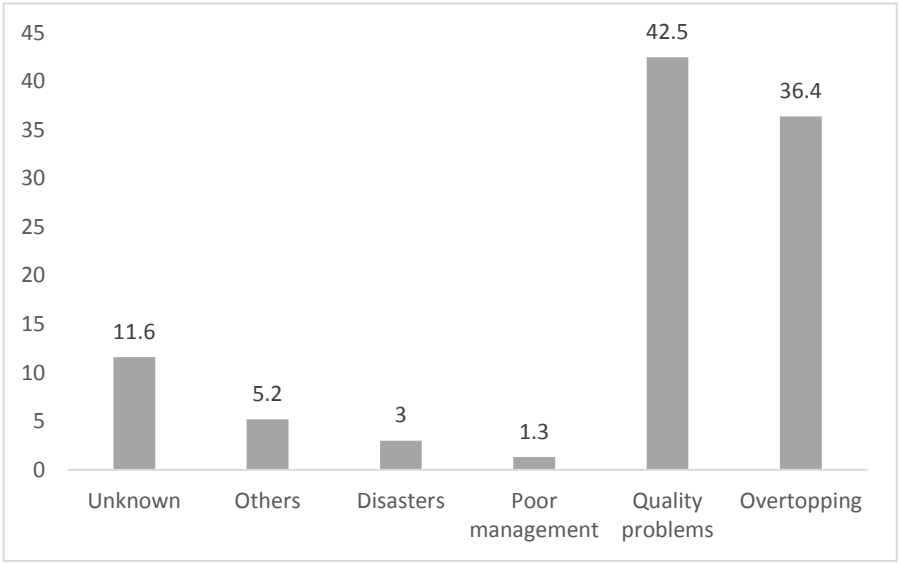

Figure 2.10 - Percentages of causes for earth dam failures (Xu *et a*l. 2007)

Piping problems represent 61.1% of the quality issues, as expressed in Figure 2.11.

In 1983, ICOLD and the National Research Council (NRC, 1983 *apud* Fell *et al.,* 1992) published two studies referent to this subject. When those results are compared to those obtained by Xu *et al.* (2007), it is perceptible that 1983 results are similar to those from 2007; however, there are some differences between the studies that should be considered. ICOLD study do not differentiate any type of dam and the NRC encompasses rock dams and earth dams as fill dams. An additional detail that can be observed from this comparison is that the most common type of dam presently still is the earth dam.

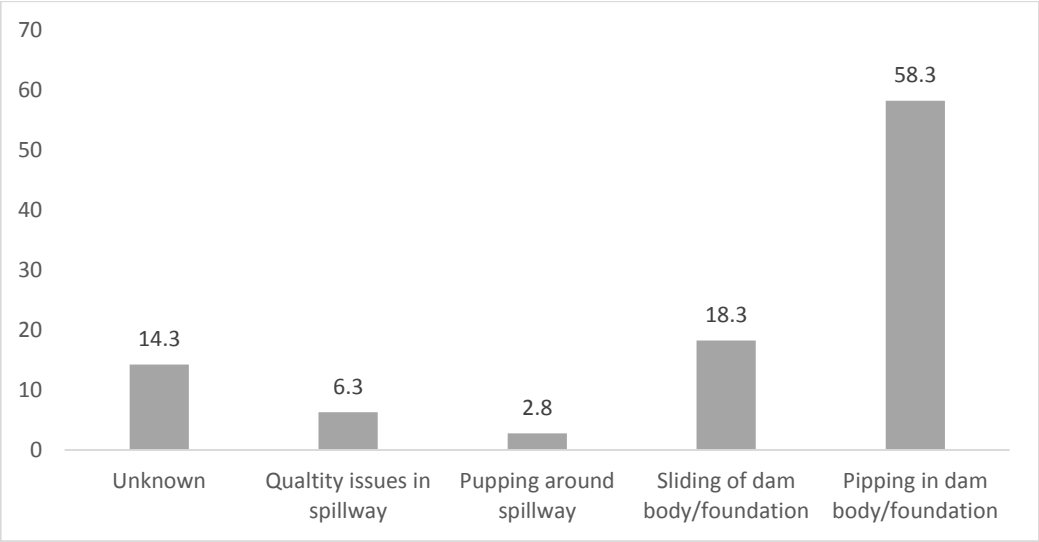

Figure 2.11 - Percentages of sub-cases of quality problems for earth dam failures (Xu *et al.* 2007)

2.4. EARTH DAMS COMPONENTS

An earth dam system is composed by a set of structural elements, each one with a specific purpose. Therefore the necessity to include a specific element on the dam body must be studied during the design stage. As illustrated in the previous section, the different types of profiles are composed by different elements.

These structural elements can be identified in the figures presented in Table 2.1 the presence of these elements on the dam body and their role are a result of the evolution of embankment dams throughout the course of history. These component are illustrated and described in Figure 2.12 and Table 2.3, respectively.

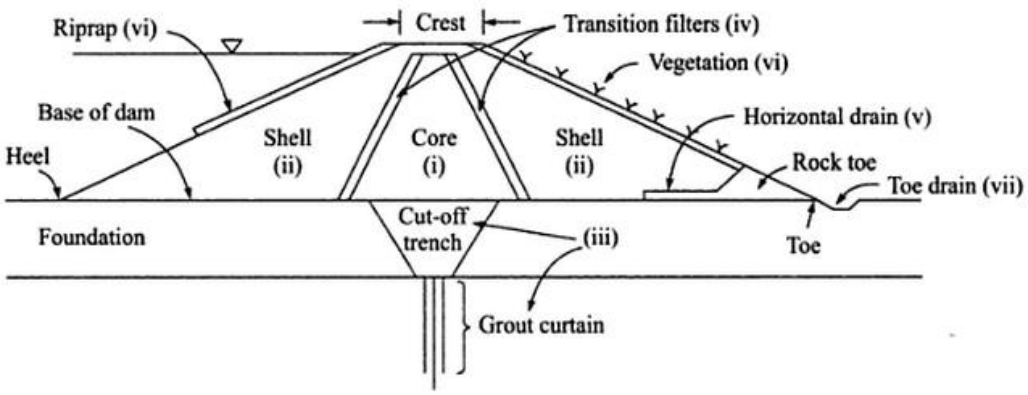

Figure 2.12 - Earth dam components (Gulhati & Datta 2008)

Table 2.3- Function of the structural elements represented in the Figure 2.12 (adapted from Gulhati & Datta, 2008)

Code	Structural element	Function
i	Core	Composed by fine grained material, controls the seepage through the dam body
ii	Shells	Composed by coarse grained material, provide stability to the dam
iii	Cut-off barrier	Prevents under-seepage through a permeable foundation
iv	Filters	Prevent the migration of fine soil particles between zones with this type of material and a zone with coarser material
v	Drains	Intercept the water table to transmit the seepage water
vi	Vegetation and rip rap	Protects the slopes from erosion
vii	Toe drainage	Carry away seepage water and surface run off

2.5. Construction phases

According to the Department of Transport (1982), embankment construction processes can be divided into three phases: investigation, design and construction (Figure 2.13). Each one of these stages dependents on the results of the previous one. As formerly referred, embankment construction reuses geologic materials from the surrounding environments, so it is logical that the first phase of an embankment project embraces an adequate research of the construction site and surrounding areas, which include:

- Bibliographic research;
- Geophysical exploration;
- Mechanical exploration and soil sampling;
- Laboratory tests to establish an adequate identification and characterization of the sampled materials.

The information obtained during this stage should be used in the design stage to define project specifications, such as dimension, construction specifications, types of equipment that should be required during the construction and the structural application of the available materials. The construction stage can be initiated when the design is defined; embankment construction includes six fundamental processes, listed below:

- Exploitation of the construction materials;
- Transportation;
- Placing;
- Spreading;
- Compaction;
- Compaction control.

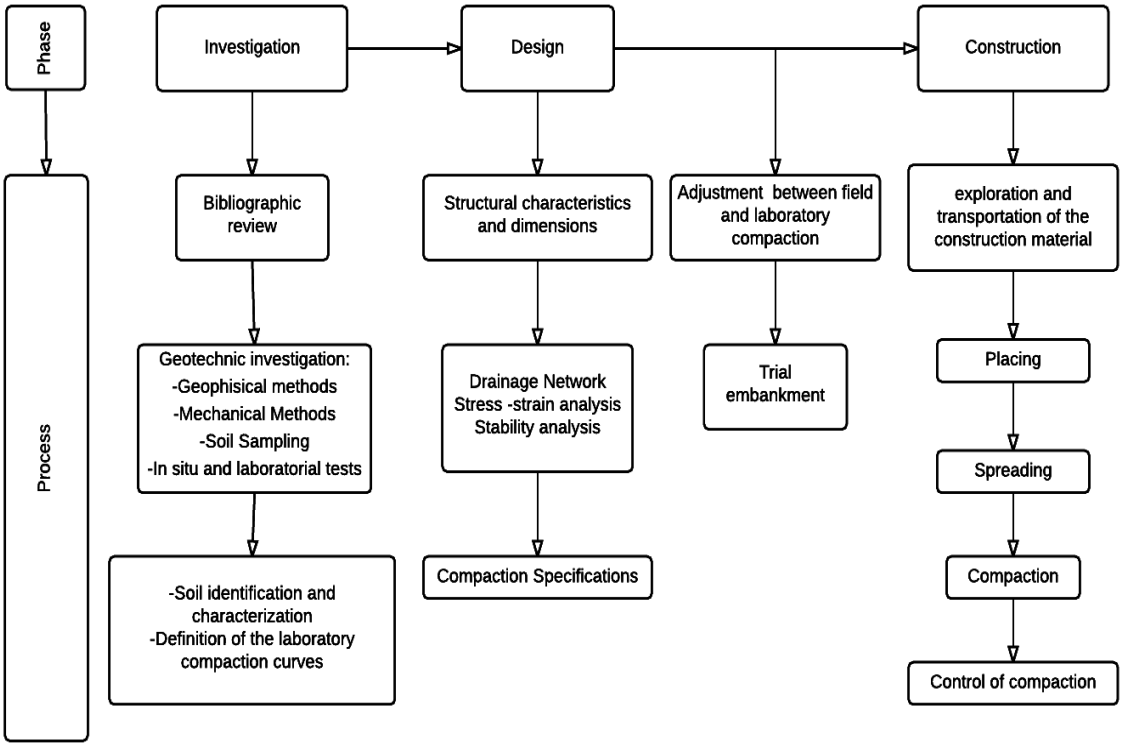

Figure 2.13- Construction processes for embankments (adapted from Fernandes, 2011)

2.6. CONSTRUCTION TECHNIQUES AND QUALITY CONTROL OF FILLS

From Section 2.5, it can be understood that embankment projects are composed by a succession of interconnected processes. Several construction techniques can be used during the construction phase; however, not all of them are suitable for earth dam construction. According to USBR (1987) and Raj (2008) the rolled fill and hydraulic fill techniques are the most adequate for earth dam construction, and these methods can be combined with soil improvement procedures such as selecting, controlling moisture content, mixing, stabilizing using several admixtures, and compacting to improve the soil engineering proprieties. These two construction methods can also be used to classify teh structures as rolled fill and hydraulic fill dams.

The rolled fill and hydraulic fill techniques are described in the following paragraphs.

In the rolled fill construction technic, the majority of the embankment is built in successively mechanically compacted layers and the materials from the borrow areas are transported to the embankment site and placed generally by trucks or scrapers. Afterwards, these materials are spread by motor graders and bulldozers and, if necessary, sprinkled to form lifts that have a previously specified water content. The final step of this process is to thoroughly compact these lifts with the exact rollers that were defined in the construction specifications (*op. cit.)*.

USBR (1998) states that this method can be applied to soils with inadequate engineering proprieties that need to be improved to the maximum practical extent through selection, compaction, moisture control, and special processing. This improvement is necessary in structures such as canals and earth embankments to prevent failure or functioning problems (for example: excessive leakage on the foundation) which can result in economic and social losses. The construction specifications for embankment dams generally define a moisture content range and density, and the compaction requirements which include type of roller, thickness of lifts and number of passes (*op. cit.*). The definition of these parameters should be based in statistical data and empirical knowledge.

Construction specifications for earthfill dams define that the water content should be uniform in the layer extent and often is slightly inferior to the optimum water content determined in laboratory with the Proctor test (*op. cit*). The inspection of the fill should guarantee:

- The material uniformity and the nonexistence of oversized particles;
- The compaction equipment is functioning correctly and fulfils the specifications;
- The thickness of the layers and number of passes respect the parameters defined in the specifications;
- Moisture uniformity.

An extended approach to soil compaction and its control is defined in Chapter 3. In compliance with USBR (1987) , this is the most popular method for earthfill dams construction, and presently hydraulic fills are rarely constructed therefore this dissertation will only consider rolled fill dam in the further sections.

The majority of embankment construction techniques implicate the control of water content; however, in some circumstances, it is necessary to place the material in conditions that involve an excess of water content. In this case, it may be necessary to use a technique designated as hydraulic fill, which involves excavation and transportation of the material using flowing water, which consists in pumping a soil-water suspension (typically around 85% of water) to a previously defined site and allowing it to settle. With an adequate control of the suspension and settling processes it is possible to construct a uniform embankment (USBR, *op. cit.*, and Raj, *op. cit.*).

This construction method has some restrictions which may make it inadequate for embankment construction. According to USBR (1998), active densification techniques should be applied to uniform granular or cohesionless soils, or the resultant fills will have very low degrees of compaction. Mejia *et al.* (2005) refer the existence of several hydraulic earth fill dam failures associated to seismic actions; one of the most emblematic cases referred by both authors is an earthquake-induced liquefaction witnessed at the Norman dam, during the 1971 San Fernando earthquake. Fine graded soils placed with this method will be weak and highly compressible and it may require several years to improve this materials by natural consolidation (*op. cit.*). The use of high water contents in the construction of large fills may result in considerable pore pressures and, consequently, intolerable deformations or shear failures (*op. cit.*). All these limitations associated to the evolution of compactive equipment, resulted in a decrease of popularity after the 30s.

Economic viability of this type of construction is determined by the availability of geologic materials previously sorted by the action of following water into two zones: one composed by impervious material and the other with previous materials; a large volume operation; and a source of inexpensive power (USBR, 1998).

3. SOIL COMPACTION

This chapter consists of a literature review on soil compaction and is divided in two main sections: the first one accesses the generalities about soil compaction, as follows:

- Soil origins and its effects on their proprieties;
- General principles of soil compaction in non-cohesive soils and cohesive soil;
- Proctor test;
- Compaction parameters and equipment;
- Trial embankments.

The second section consists in a description of the processes associated to control compaction operations performed during an earth dam construction, field tests executed during the control operations to access the control parameters, comparison between the sand cone test (SCT) and the nuclear gauge (NDG), and the most common methods that are used to analyse the results of the quality control operations.

3.1. SOIL ORIGIN AND PROPRIETIES

In order to comprehend the mechanisms associated to soil compaction it is necessary to understand the soil origin and, consequently, its effect on soil proprieties. The soil definition from an engineering point of view is different from the definition used by a geologist; these are synthetized in Table 3.1

Table 3.1- Soil definitions from the points of view of an engineer and a geologist

Engineer definition	Braja (2007)	"(…) uncemented aggregate material of mineral grains and decayed organic matter (solid particles) with liquid and gas in the empty spaces"
	Terzaghi & Peck (1996)	"a natural aggregate of minerals grains that can be separated by such gentle mechanical means as agitation in water"
Geologist definition	Selley, (2000 *apud* Martini and Cesworth, 1992)	"rock debris and humus, which is decaying organic matter largely of plant origin"

The two main soil origins on Earth are physical or chemical rock weathering. Physical weathering consists in a single or group of physical processes that lead to the mechanical disaggregation of a rock, resulting in debris with the same chemical composition as the original rock. The agents responsible for this type of weathering comprise running water, wind, water, ocean waves, glacier ice, frost, and expansion and contraction caused by temperature variations. The physical agents responsible for rock weathering are dependent on the local climate; for example, in Polar regions, the most common weathering agent is glacier ice; however in arid regions weathering can be caused by wind or significate temperature variations.

Chemical weathering processes consist in oxidation and dissolution of the rock minerals, the chemical composition from the resultant products may be different from the original rock; for example feldspars weathering will produce clay minerals such as laterite, kaolinite, and bauxite. Chemical weathering is almost entirely dependent on water; therefore, it is commonly associated to warm and humid climates typical from tropical regions (Selley, 2000; Braja, 2007).

The products resultant from the weathering can be transported and subsequently deposited by physical agents, the soils formed by this process are designated as transported soils. The most common transportation agents are gravity, ice, water, and wind, each one of this agents is dependent on the laws of physics. Weathering products can be transported in a fluid such as wind, water or ice (in compliance with Galopim de Carvalho (2003), ice can be considered as a liquid with great viscosity) by suspension, bouncing, rolling, or as a solute (for soluble materials); the first three processes are represented in Figure 3.1.

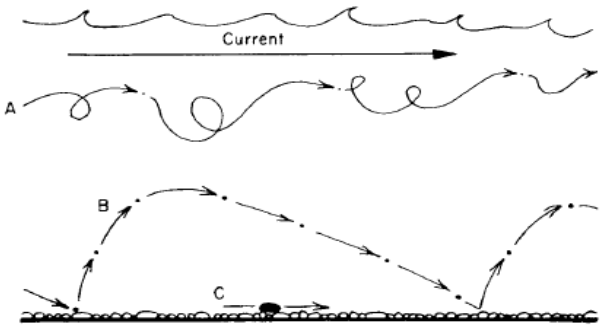

A) Suspension; B) Bouncing; C) Rolling

Figure 3.1 - Transportation processes of weathered materials (adapted from Selley, 2000)

Deposition occurs when an agent loses its transportation capacity. Hjulström diagram, represented in Figure 3.2, expresses the relation between the transportation capacity and the energy of a flow.

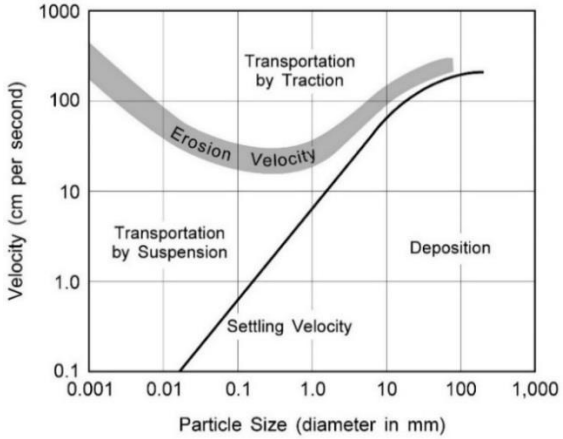

Figure 3.2 - Hjulström diagram, retrieved in 23 September 2014 from http://echo2.epfl.ch/e-drologie/resumes/chapitre5/resume5.html

This loss of transportation capacity by a physical agent will lead to a gradual selection of the particle sizes that can be transported, since heavier (larger) materials will be deposited and smaller (lighter) materials will continue to be transported; therefore energy variations can control the deposit genesis

(Selley, 2000). Consequently, deposits resulting from high energy mass movements such as rock falls (which is a type of transport trigged exclusively by gravity) or avalanches can origin deposits composed by particles from different sizes, and deposits formed by low energy agents like wind generally originate deposits with a range of sizes from sand to clay (Selley, 2000; Galopim de Carvalho, 2003; Braja, 2007). The transportation processes and types of deposits that can be originate are defined in Table 3.2.

Table 3.2 - Transportation processes and the types of deposits formed by each process (adapted from Selley, 2000)

Transportation process	**Originated deposit**	
Subaerial	Traction deposits	Predominantly cross-beded sands
	Density deposits	*Nuées ardentes*, etc
	Suspension deposits	Loess
Subaqueous	Traction deposits	Predominantly cross-beded sands
	Density (turbidity) deposits	Graded sands, silts and clays
	Suspension deposits	Nepheloid clays
Mass gravity transport	Subaerial	Generally unstratified poorly sorted deposits of boulder to clay grade (diactamictites)
	Subaqueous	
Glacial transport	Moraine deposits	

If the products resultant from weathering do not suffer transportation, are designated as residual soils. This type of soils are commonly associated to warm and humid climates, since the weathering rate in this climates might be higher comparatively to semiarid or temperate climates. Rahardjoa *et al*. (2004) states that these soils have a heterogeneous nature and highly variable degree of weathering, their proprieties are dependent on the climatic and topographic conditions, and nature of the bedrock. Weslie (2009) defines the main factors that contribute to the heterogeneity and behaviour of a residual soil as follow:

- The inexistence of a sorting process which forms homogeneous deposits, gerenally this process is associated to transportation;
- The nature of the soil particles (size, shape, mineralogical composition);
- The state of the soil particles on the ground.

In summary, the formation of a soil deposit is a result from an interaction between the following conditions:

- Composition of the parent rock;
- Local climate;
- Type of weathering;
- The existence of transportation, and the type of transportation agent;
- Depositional environment;
- Geological events.

Atkinson (1993) defines that the type of weathering, and the existence or not of a transportation and the transportation agents mostly control the particle size distributions, shape of grains, and its

mineralogy. The depositional environment and eventual geological events that may occur after the soil deposition mostly control the state of the soil and its fabric. The regional variability of these conditions guarantees that each soil deposit is singular, therefore it is important to establish an adequate description of a soil deposit before using it as a source of material for earth dam construction. A diagram illustrating the soil formation processes and factors affecting the soil behaviour is represented in the Figure 3.3.

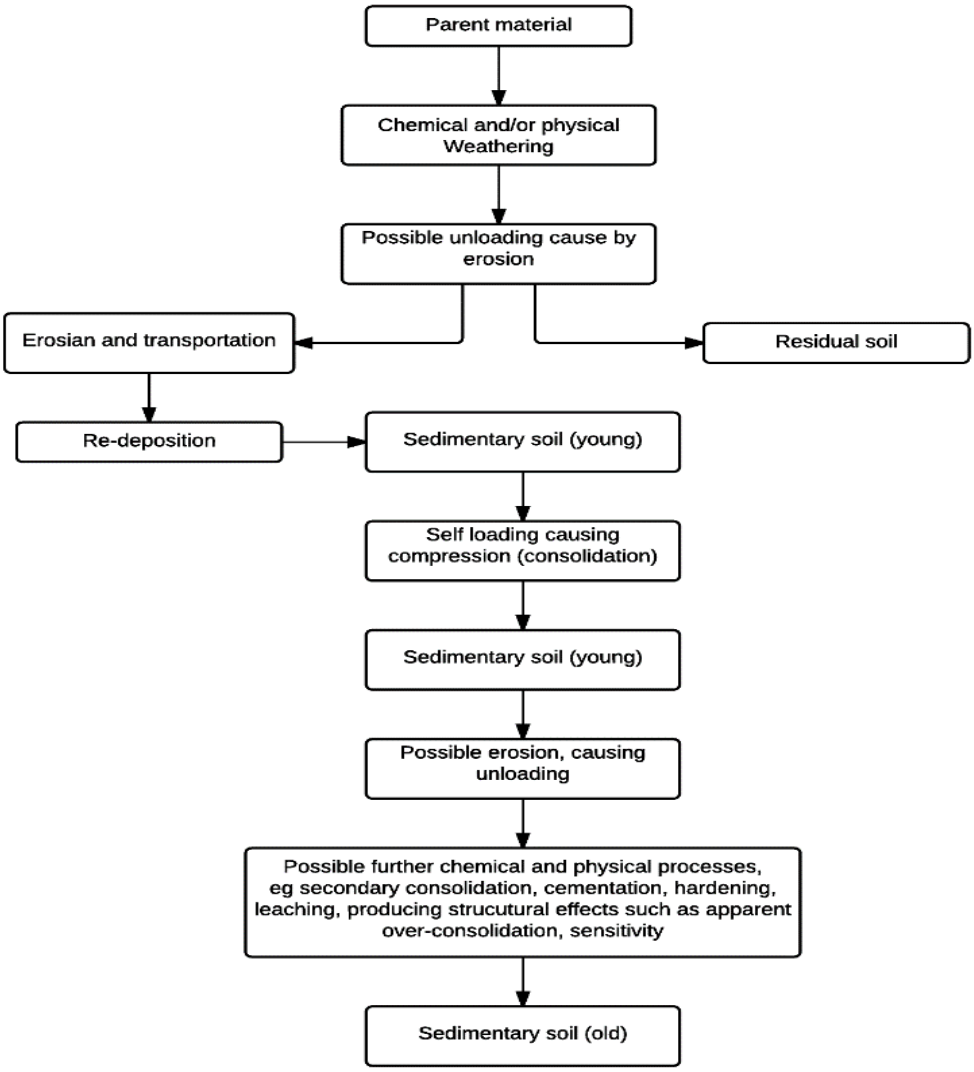

Figure 3.3 - Soil formation processes (Weslie, 2009)

3.1.1. SOIL DESCRIPTION AND CLASSIFICATION

A correct soil description must be based on a physical analysis of the soil. This analysis includes information about the grain size distribution and consistency, which is provided by laboratory tests. The grain size distribution of the coarse grained soil fractions is assessed with a set of sieves, and the hydrometer test is used for the fine graded fraction. Consistency is characterized by the Atterberg

Limits (Liquid Limit and Plastic Limit). The Portuguese, European and American standards for each one of those tests are defined in Table 3.3, their results are used as input in soil classification systems.

Table 3.3 - Portuguese, European and American Standards for soil identification

	Portuguese standards	**European standards**	**American standards**
Grain size distribution (sieve and hydrometer analysis)	NP EN-196 (1966)	ISO/TS 17892-4:2004/Cor1(2004)	ASTM D422-63 (2007)
Consistency limits	NP-143 (1969)	ISO/TS 17892-12: 2004/Cor1(2006)	ASTM D4318-10e1(2010)

There are several classification systems, one of the most used by geotechnical engineers is the United Soil Classification Systems (USCS) developed in 1952, and described by the American Society for Testing Materials (ASTM), in the D2487-11 standard. More recently, the European Committee for Normalization (CEN) developed a new system designated European Soil Classification System (ESCS), which is outlined in ISO14688-2 from 2013.

Classification systems can be used to obtain a simplified description from the soil proprieties, this information can be useful in any type of geotechnical engineering project; however should only be used as an indicator of the soil behaviour, since its behaviour cannot be predicted without in situ and laboratory tests (Venkatramaiah, 2006).

3.1.2. VOLUMETRIC RELATIONS

As defined by Lambe *et al.*, (1969) and Budhu (2011) soils are particulate systems formed by three phases: solid (minerals, organic matter or both), gas (usually air) and liquid (usually water). Budhu, (2011) states that the physical properties of soils are dependent on the relative proportions of solid, gas and liquid. Figure 3.4 is a simplified representation from the three soil phases and their volumetric relations.

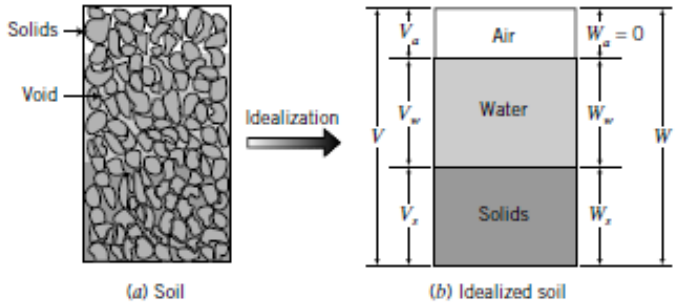

Figure 3.4 - Soil phases (Budhu, 2011)

The total volume of a soil can be calculated by the Equation 3.1.

$$V_T = V_s + V_v = V_s + V_w + V_a \quad (m^3) \quad (3.1)$$

Where:

V_T - Total volume of a soil sample (m³);

V_s - Volume of solids (m³);

V_v - Volume of voids, (m³);

V_w- Volume of water in the voids, (m³);

V_a - Volume of air in the voids (m³).

The total weight of a soil sample, considering the weight of the air negligible, can be calculated by Equation 3.2.

$$W = W_s + W_w = m_s \times g + m_w * g \quad (kN) \quad (3.2)$$

Where:

W - Total weight of a soil sample (kN);

W_s - Weight of soil solids (kN);

W_w- Weight of water (kN);

m_s - Mass of solid (kg);

m_w - Mass of water (kg);

g - Gravitational acceleration ($\cong 9.81$) (m/s²)

Volumetric and weight relations can be used to determinate several soil index proprieties, using the equations expressed in Table 3.4.

Table 3.4 - Volume and weight relationships

Volume relationships		**Weight relationships**	
Void ratio (e)	$e = \frac{V_v}{V_s}$ (3.3)	Water Content (ω)	$w = \frac{W_w}{W_s}$ (kN/m^3) (3.7)
		In situ or wet unit weight (γ)	$\gamma = \frac{W}{V}$ (kN/m^3) (3.8)
Porosity (n)	$n = \frac{V_v}{V_s}$ (3.4) $n = \frac{e}{1+e}$ (3.5)	Dry unit weight (γ_d)	$\gamma_d = \frac{W_s}{V}$ (kN/m^3) (3.9) $\gamma_d = \frac{\gamma}{1+w}$ (kN/m^3) (3.10)
		Solids unit weight (γ_s)	$\gamma_s = \frac{W_s}{V_s}$ (kN/m^3) (3.11)
		Water unit weight (γ_w)	$\gamma_w = \frac{W_w}{V_w}$ (kN/m^3) (3.12)
Degree of saturation (S)	$S = \frac{V_w}{V_v}$ (3.6)	Submerged unit weight (γ')	$\gamma' = \gamma_{sat} - \gamma_w$ (kN/m^3) (3.13)
		Specific gravity from the solid particles (G_s)	$G_s = \frac{\gamma_s}{\gamma_w}$ (3.14)

3.2. SOIL COMPACTION - GENERAL PRINCIPLES

Usually in geotechnical engineering the soils available for construction do not fit the technical requirements for the desired purpose. They may be weak, highly compressible or have a higher permeability than the one intended; in these circumstances, it may seem practical to relocate the construction site. However in some instances, there are other considerations apart from the geotechnical considerations making the relocation of the construction site unmanageable and in this situations it may be necessary to improve the engineering proprieties of the soils using a technique known as soil compaction.

Soil compaction consists in mechanically densifying a soil through the expulsion of the air present in the voids reducing its volume and increasing the dry unit weight. This process will also increase the saturation degree, since the void ratio decreases due to the expulsion of air. The main effects of compaction in the soil engineering proprieties are:

- Increases shear strength;
- Decreases permeability;
- Reduces compressibility.

This capacity to improve the soil engineering proprieties makes compaction one of the most important and also least expensive procedures that can be used on the construction of fills for different purposes. However, an inappropriate compaction can affect the durability and stability of a structure, and in most severe cases can lead to its failure; for example if during the construction of an earth dams soils were dumped or randomly placed into a fill without any attempt to compact them, the resultant embankment may present problems related to stability and settlements. This type of situation was common before the 1930´s in highway and railway fills causing failures, namely in considerable high embankments.

Holtz & Kovacs (1981) and Venkatramaiah (2006) stated that in the 30´s, Proctor developed the fundaments of compaction, through his research works, defining that compaction is a function of four variables, namely:

- Dry density;
- Water content;
- Compactive effort in the field, which can be defined as a combined result from the number of passages and the weight of the roller;
- Soil type.

Proctor also demonstrated the existence of a relation between moisture content and the dry density, and that for a specific type of soil specific and compactive effort, there is a certain moisture content which corresponds to the maximum dry density, the moisture content is designated as optimum moisture content (OMC). This relation was used to establish the concept of the compaction curve (Figure 3.5), which is essential for compaction control.

A peak point can be identified in the compaction curve defined on Figure 3.5, representing the maximum dry density at the OMC, and divides the compaction curve in two parts: on the left side, the dry of optimum and, on the right side, the wet of optimum (Venkatramaiah, 2006). This behaviour is explained in the paragraph bellow.

When water is added to a dry soil, the particles became more close due to the water film that forms around them. At low water content the soil tends to be stiff and its more difficult to compact. An increase of the soil water content will performe as a lubricant, the paricles became more close due to an higher workability. In this condition, under a certain increase of compactive effort, the mixture formed by soil, water and air starts occupying a smaller volume and as, a response form this, the dry density increases. If water continues to be added the soil reaches a plateau in which the soil attains a minmum volume, and therefore the dry density will be maximum. Adding water beyond this level, which is called optimum water content (ω_{opt}) will cause a decrease of the dry unit wheight, since the water starts occupying space that should be occupied be the soil (*op. cit.*).

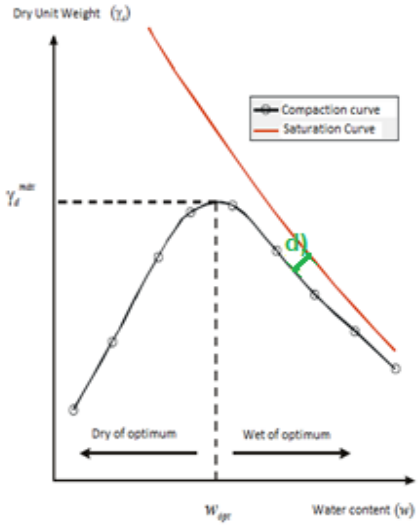

Figure 3.5 - Compaction curve (translated from Santos, 2008)

The wet side of optimum (Figure 3.5) is parallel to the saturation curve that expresses the relation between water content and dry density at a constant degree of saturation, and can be calculated through Equation 3.15.

$$\gamma_d = \frac{G_s \gamma_w}{\left(1 + \frac{w G_s}{S}\right)} \qquad (3.15)$$

Guedes de Melo (1985) defines that the distance “d” illustrated in Figure 3.5 can be used to quantify the volume of air present in the soil.

Compaction curves can be obtained on laboratory and in the field. At the laboratory, this curves can be determined by the Proctor test and, in the field they can be determined using several in situ tests. Laboratory and in situ tests will be described in Sections 3.2.1 and 3.6.1.3, respectively.

The relation determined by Proctor allows to understand that variations of the compactive effort and/or soil type, will result in a different compaction curves. Consequently, if two compactive efforts with different energy levels are applied to the same soil, the resulting curves will be different. The curve which represents the compactive effort with higher energy will have a higher maximum dry density at a lower water content, as represented in the Figure 3.6. Santos (2008) states that every soil as a limit for the maximum dry density that can be achieved regardless of the amount of compactive energy used, when this value is reached any increase of energy will be wasted as elastic deformation.

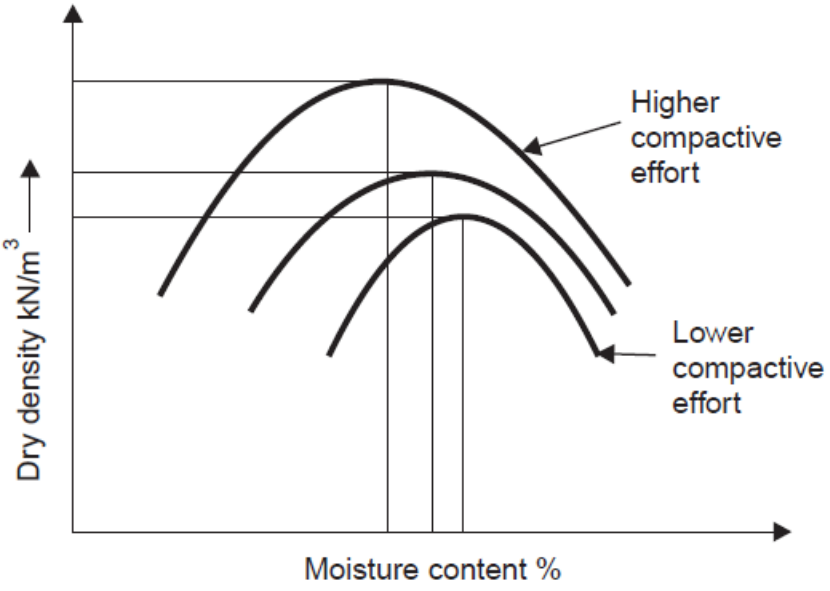

Figure 3.6 - Effects of the compactive effort on compaction characteristics (Venkatramaiah, 2006)

3.2.1. PROCTOR TEST

As referred in Section 3.2, the compaction curve can be obtained through laboratory and field tests, this Section is dedicated to the first type of tests. The most common method to evaluate behaviour of a soil after compaction in laboratory is the standard Proctor test. This test was developed by Ralph Proctor, at the United States of America in 1933, and has the purpose of determining an acceptable state of compaction for the soils used in the construction of fills, and providing the engineers with a tool for monitoring the degree of compaction during the construction. The procedure for the standard Proctor test is described below:

A soil sample at selected water content is placed in three layers into a mould with standardized dimensions (Table 3.5) and compacted with 25 or 56 blows of a 2.5 kg rammer dropped from a distance of 0.35 m.

When this procedure is over, the dry unit weigh from the sample is calculated using Equation 3.16.

$$\gamma_d = \frac{\gamma}{1+w} \quad (kN/m^3) \qquad (3.16)$$

The unit weight of the soil is calculated using the equation 3.16 and the water content is determined using the drying oven method with a sample of the material used in the test, this method will be discussed in Section 3.6.3.

This procedure is repeated at least three times to establish a relation between the dry unit weight and the water content. The resultant information is plotted in a graphic of dry unit weight *versus* water content.

A variation to this test designated as modified Proctor test was developed afterwards, to simulate the heavier compaction used in airfield construction (Venkatramaiah, 2006). The proceedings are similar to those of the standard test, but the modified method uses a rammer with 4.54 kg with a drop distance of 0.46 m to compact five soil layers in a mould of given dimensions producing a compactive effort of 270 N.cm/cm^3.

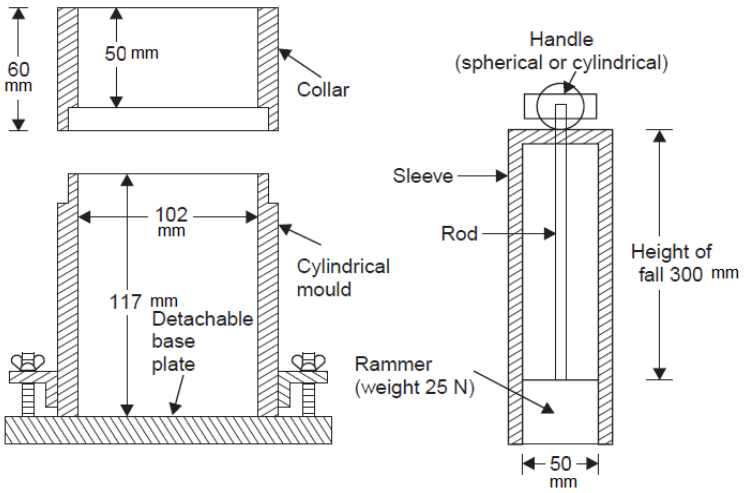

Figure 3.7 - Apparatus for the Proctor test (adapted from Venkatramaiah, 2006).

The energy transmitted to the soil by the rammer can be calculated using the following equation:

$$E_{comp} = m_h g \frac{h_d}{V} N_b N_t \quad (\mathrm{N.cm/cm3}) \qquad (3.17)$$

Where:

m_h - Mass of the rammer (kg);

g - Gravitational acceleration (m/s^2);

h_d - Height of fall of the rammer (m);

V - Volume of compacted soil (m$^{3)}$;

N_b - Number of blows given by the rammer;

N_t - Number of layers used on the test.

There are two types of mould: a smaller one with a volume of 9.44x10^{-4} m^3, and a larger one with 20.68X10^{-4} m^3. The larger mould should be used if more than 20 % mass of the material is retained on the 9.53 mm sieve and less than 30% by mass of the material is retained on the 19 mm sieve (ASTM 1557:2012). All the test variations are defined in Table 3.5.

Table 3.5 - Characteristics of the Proctor tests

Equipment	**Characteristics**	**Standard Proctor**		**Modified Proctor**	
		Small Mould	Large Mould	Small Mould	Large Mould
Mould	Inner diameter (mm)	101.6	152.4	101.6	152.4
	Height (mm)	116,4			
	Volume (cm^3)	944	2124	944	2124
Rammer	Weight (kg)	2.5		4.54	
	Drop distance (cm)	30.5		45.7	
Blows	Nº/layers	25	36	25	56
	Nº layers	3		5	
Specific energy	N (cm/cm^3)	60		270	

The energy of compaction (weight of the rammer) used during the Proctor depends on the type of project, and subsequently the intended mechanical and hydraulic characteristics for the construction materials. For example, a high earth dam supports higher loads than a canal embankment, therefore the dam must be compacted with an higher compactive effort, however an higher effort will implicate higher cost (Fernandes, 2011). Portuguese and American specifications are defined in Table 3.6

Table 3.6- Portuguese and American Standards for the Proctor test

		Portuguese standards	**American standards**
Proctor Test	Standard	NP EN-197 (1966a)	ASTM D698 (2012)
	Modified		ASTM D1557 (2012b)

Once the laboratorial compaction curves are defined for each type of material available in the borrow areas, the Proctor test methodology will be used to create the samples for the mechanical and hydraulic characterization tests.

3.2.2. COMPACTION OF COHESIVE SOILS

Cohesive soils are composed by a significate fraction of clay particles with lamellar geometry, clay particles have a larger surface area when compared to the larger particles in coarser soils (sands and gravel). Another important characteristic that controls the behaviour of cohesive soil is the clay-water

interaction, an explication for this characteristic presented below is based on the works of Guedes de Melo (1985), Braja (2007), and Budhu (2011).

Clay particles carry a net electric charges formed by negative charges (anions) on its surface, and positive charges (cations) on their edges (Figure 3.8). when this particles interact with water molecules, which are dipolar (formed by a negative charge on one side and a positive charge on the other) these molecules will be attracted to the ions on clay particles forming a thin film of water designated as diffuse double layer, the inner layer of this fil is known as adsorbed water. The concentration of cations is higher near the particle surface and decreases exponentially with the distance from the surface of the particle (Figure 3.8 B).

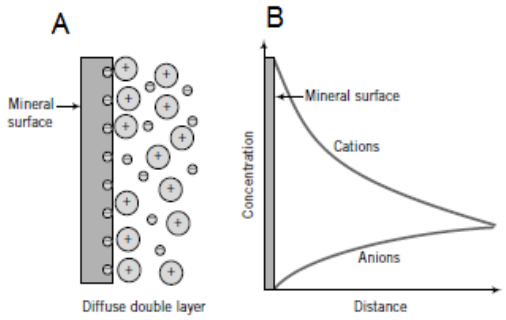

A) Diffuse Double Layer; B) Relation between distance and ions concentration.

Figure 3.8 - Water-clay relation (Budhu, 2011)

The electric charges on the surface of clay minerals will generate attracting forces and repelling forces between particles. Attracting forces decrease in inverse proportion to the square of the distance between particles. The repelling forces are caused by the double layer which forms an ionic cloud surrounding each particle. When two particles are at a considerable distance from each other the electric charge is neutralized, however when this distance decreases substantially both clouds interact and the negative charges originate repelling forces.

Particles in a soil sample have a random orientation and several types of bonds between them. Compaction breaks this electrical bonds between particles leading to a soil with an inferior void ratio, in a first phase the energy created by the compactive effort his used to break this bonds afterwards in a second phase there is an effort to bring this particles together (*op.cit.*).

As demonstrated in the previous paragraphs, the water content and the electric charges in the surface of the particles have an important role on the soil behaviour during the compaction of cohesive soils. Therefore, it seems natural that the fraction of clay in a soil will affect the compaction curve. The Figure 3.9, representing the compaction curves of various types of soil with different clay fractions, denotes that for soils with higher contents of clay and silt (higher plasticity), the OMC is higher causing a lower dry unit weight. This type of soils has flatter compaction curves.

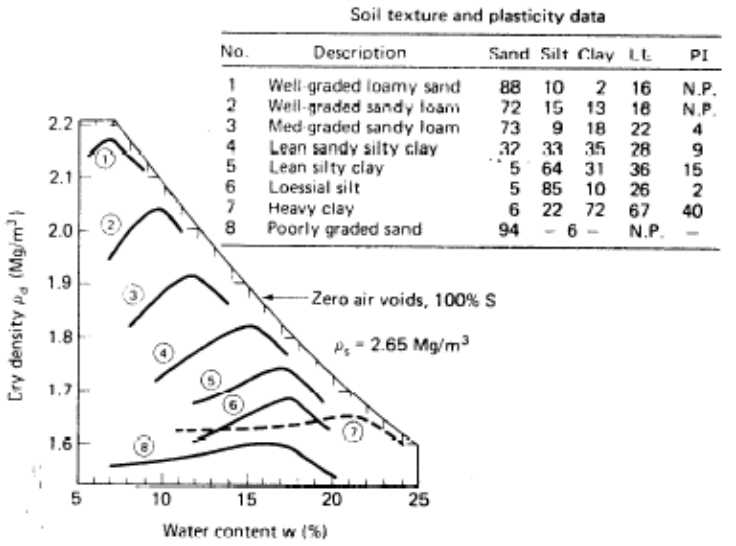

Figure 3.9 - Compaction curves for six types of soil, compacted with the Standard Proctor test (adapted from Holtz & Kovacs 1981)

3.2.3. COMPACTION OF COHESIONLESS SOILS

This soils can be characterized by a small fraction of fine grained material or even a total inexistence in the case of a purely cohesionless soil and, consequently, these particles have a smaller surface area which contributes to a smaller influence of the water content in their behaviour, and a larger permeability when compared to cohesive soils. This differences are reflected in their compaction curve - Figure 3.10.

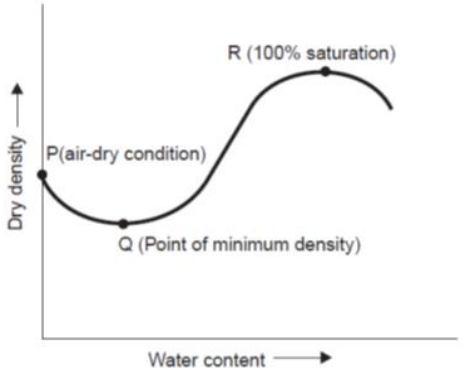

Figure 3.10 - Generic compaction curve for cohesionless soils (Venkatramaiah, 2006)

In this soils (Figure 3.10), the dry unit weight, in an initial phase, decreases with an increase of water content until it reaches a minimum value (Q), according to Venkatramaiah (2006) and Fernandes (2011), this behaviour is designated as apparent cohesion and can be explained by the occurrence of negative water pressures (capillarity) associated to low water contents; it can affect the reassortment of the soil particles during the compaction process. After that point, any increase of water content will result in an increase of the dry unit weight until it reaches its maximum (R), which corresponds to the complete saturation.

Fernandes (2011) defines that well graded soils can be compacted without major difficulties, when these soils are compacted near to a minimum void ratio can form an embankment with suitable mechanical proprieties. In contrast, the compaction of poorly graded soil may present some difficulties.

3.2.4. COMPACTION OF SOILS AND WATER CONTENTS

The shape of the laboratorial compaction curve obtained with the Proctor test shows the existence of two values of water content for each dry unit weight, with the exception of the OMC point, as illustrated in the Figure 3.11. One of the values is located on the dry wet of optimum (left side) and the other on the wet of optimum (right side), despite the fact that both values have the same dry unit weight, the mechanical behaviour of a soil compacted on dry of optimum is different from the one of a soil compacted on the wet of optimum side.

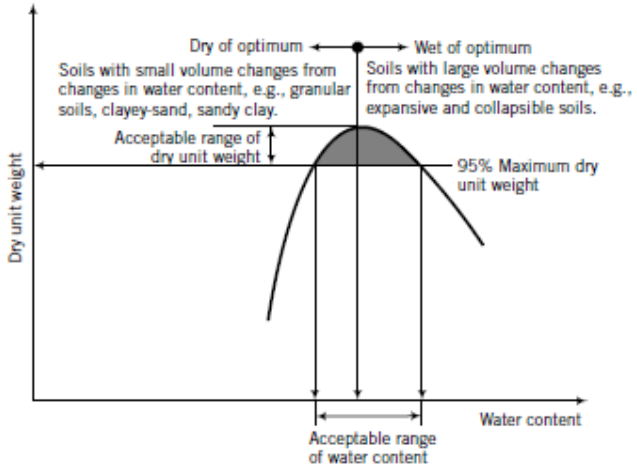

Figure 3.11 - Wet and dry side of optimum in soils (adapted from Budhu, 2011)

It seems natural that these differences in the soil behaviour between soils compacted on both sides of the compaction curve, will result in soils with different engineering proprieties. The characteristics from the soils compacted on both sides of the compaction curve are defined in Table 3.7.

Table 3.7 - Characteristics from soils compacted on both sides of the compaction curve (based on Holtz & Kovacs, 1981, Guedes de Melo, 1985, Santos, 2008 and Budhu, 2011)

Wet of optimum	Dry of optimum
• Higher shear strength resistance, this tends to increase with an increase of compactive effort; • Variations of pore pressures practically null when subjected to external loads; • Possible appearance of cracks; • Volume variations when subjected to an increase of shear strength; • Higher permeability when compared with the soils compacted with the dry of optimum	• Inferior shear strength resistance comparatively to the dry side; • Possible occurrence of high pore pressures; • Plastic behaviour; • Volume variations almost inexistent;

As explain in Section 3.2.2, the proprieties from a compacted cohesive soil, will mostly be influenced by the compactive effort, soil type, and moulding water content. However, researches by Seed & Chan (1959 *apud* Holtz & Kovacs, 1981) showed that when clays are compacted on the dry side of optimum, the soil structure will be independent from the type of compaction, although when they are compacted on the wet of optimum the response of the soil structure when subjected to different types of compaction is reversed.

Through their works, Lambe & Whitman (1969) demonstrated that for a cohesive soil with a certain water content, increasing compactive effort tends to originate a more disperse soil, with particularly incidence on the dry side of optimum, as illustrated in the Figure 3.12 (Points: A-E; C-D). Guedes de Melo (1985) states that an excess of compaction can create modifications in the orientation of the particles without reinforcing the bonds between them, resulting in layers with low shear strength resistance and those zones can cause structural problems in the embankment.

Lamb and Whitman (*op.cit.*) also stated that if a constant compactive effort with increasing water content is applied to a soil, the fabric tends to be more oriented if compacted on the wet side (Figure 3.12 - Points A-C, and E-D), increasing the compactive effort in the same conditions will result in a more oriented soil (Figure 3.12, points A-E and C-D), however this effect is less visible for soils compacted on the dry side.

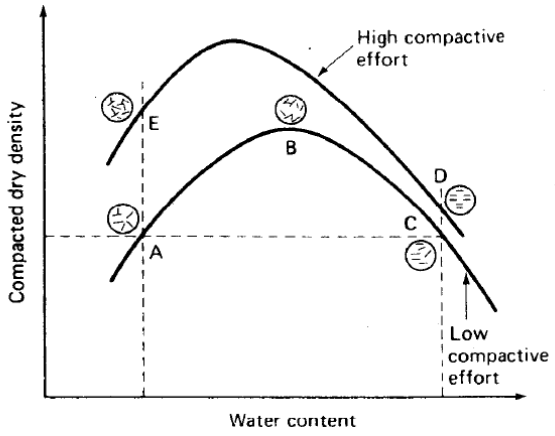

Figure 3.12 - Effects of compaction on the structure of the soil (Venkatramaiah, 2006)

Earth structures such as embankment dams are susceptible to the presence of water, therefore it is important to study the influence of water on its resistance. According to Santos (2008), an increase of water content will result in a reduction of resistance. This variation of resistance will be higher in soils compacted on the dry side. When completely saturated, a soil compacted on the dry size will have a similar resistance to a soil compacted on the wet size. For this reason it is important to perform laboratory tests in the samples retrieved during the investigation stages.

3.3. COMPACTION EQUIPMENT

The compactive effort can be transmitted to the soil through by pressure, vibration, kneading and impact. In accordance with Ministry of Railways (2005) and Santos (2008), the choice of the type of equipment used during soil compaction relies on the following conditions:

- Size of the embankment and the number of passes;
- Proprieties of the soils being compacted;
- Characteristics and availability of the equipment;
- The preference of the contractor.

The most common types of compaction equipment in embankment construction are defined in Table 3.8.

Presently, as a result from the technologic evolution experienced in the last decades, it is possible to use vibratory rollers with integrated technology to continuously measure the compaction during the construction process, known as intelligent compaction. A more extended approach to this subject is presented in the works of Mooney *et al*. (2007) and USBR (2014).

Table 3.8 -Main features and Applicability of compaction Equipment (based on the Works of Railways (2005), Venkatramaiah (2006), Braja (2007), Santos (2008), and Fernandes (2011))

Equipment	Main Features	Compactive Effort	Applicability

Smooth wheel rollers	• Two versions of this equipment:
	  ○ Steel drum in the front;
	  ○ Two steel drums (front and rear).
	• Weight between 6-8 and 8-10 tons, can be increased to 20t by filling the drums with water or sand;
	• This rollers provide 100% coverage under their wheels;
	• Non-reversible
	• Lack of efficiency for depths above 15 cm;
	• Unpopular in the Construction of embankment dams.
		• Pressures between 310-380 kN/m^2;
		• Transmits compactive effort to the soil through pressure;
		• 8 passes are adequate to achieve a result similar to the standard Proctor test
			Cohesionless soils

Sheepsfoot rollers	• Structure similar to the smooth wheel roller;
	• Two Versions;
	• Projections similar to a sheepsfoot on the drums;
	• Weight between 15-40 tons, can be increased by filling the drums with sand or water;
	• The thickness of the layer should not exceed by more than 50 mm the length of the feet;
	• Not able to compact the superficial zone of the layer (firsts 0.05 - 0.06 m)
		• Generated pressure depends of:
		  ○ Weight of the roller,
		  ○ Pressure generated by each foot.
		• Transmits compactive effort to the soil through kneading;
		• higher pressures, due to the smaller area of contact between soil surface and the slug;
		• Pressures between 1380 to 6900 kN/m^2;
		• The lugs penetrate the soil compacting the lower zones (compaction from bottom to top)
			Cohesive soils

Rubber tyre rollers	• Two axis fitted with pneumatic smooth wheels on both axles;
	• Weight 11 tons can be increased up to 25 tons by ballasting;
	• Percentage of coverage 70-80%.
		• Compaction process is a combination of pressure and kneading;
		• Generated pressure depends of:
		  ○ Pressure of the tyre
		  ○ Area of contact between the soil and the tyre
		• Pressure between 600-700 kN/m^2
			Most types of soil, but has particular advantages for wet cohesive materials

Vibratory rollers;	• Similar structure to each one of the previous rollers;
	• Drums Cans Produce Vibrations;
	• Vibrations break the bonds between particles;
		• The compactive effort depend of:
		  ○ Thickness of the lift;
		  ○ Pressure generated by the equipment
			Cohesionless soils

Vibratory Plate.	• Weigh between 50 and 100 kg and are manually guided; • Formed by an engine connected to a spring and a plate;	• The engine produces vibrations which in a first stage are transmitted to the spring and lastly to the plate;	Cohesionless soils in restrained spaces
Rammer	• Compaction by impact through an interaction between ascendant/descendent force • This force is repeatedly generated by an engine and will lead to the sock between the metallic plate and a soil a metallic plate	• Compactive effort transmitted by impact	Cohesive soils in restrained spaces

3.4. COMPACTION SPECIFICATIONS

Once the proprieties from the construction materials are determined it is necessary to establish the project dimensions and specifications, (Figure 2.13). The specifications depend on the type of project and should be based on the laboratorial compaction curves defined for each construction through the Proctor test. Holtz & Kovacs (1981) and Ranjan & Rao (2005) delineate the existence of two types of specifications: method specification and end-product specifications.

In the first type, specific instructions referent to the machine type, lift depths, number of passes, machine speed and moisture content are specified and must be fulfilled. It may be necessary to construct trial embankments with different types of equipment, procedures, and construction materials. However, the construction of these structures can represent significant expenses and therefore this type of specification may only be adequate for large projects.

In end-product specifications, the degree of compaction that must be achieved by the Contractor is previously specified, but the construction procedures and equipment are not defined. Providing more flexibility to the contractor to choose the most economical solution for fulfilling the specifications. Nevertheless and according to both authors (*op.cit.*) this condition can create some problems since, for example, a fill compacted on the wet side of optimum as different characteristics from a fill compacted on the dry side of optimum, even if both fills were compacted to the same degree of compaction. To avoid this problem, it may be recommendable to define a range of deviation for the water content. This type of specifications is common for highway projects and building foundations.

Hall *et al.* (2012) stated that, in earth dam construction, is common to use a combination of both types, once generally these specifications include information about the degree of compaction, water content, construction materials, construction equipment, and layer thickness.

Fell *et al.* (2015) defines that it is a common procedure in earth dams construction to specify a dry unit weight ratio ≥ 98% of the maximum dry unit weight determined with standard Proctor test, and a water content range between $\omega_{opt} \pm 1\%$, or $\omega_{opt} \pm 2\%$.

The use of the standard Proctor test as a reference for field compaction guarantees moist compaction producing more flexible fills with lower permeability. A compaction at a water content proximate to the ωopt will generate high densities (*op. cit.*). Another reason, defined by Guedes de Melo (1985), is associated to the fact that sheepsfoot rollers, which are a popular equipment in embankment dam construction, since they can produce a degree of compaction similar to the obtained through the standard Proctor test.

The use of a density ratio ≥ 98% is not a strict rule. USBR (1987) and Guedes de Melo (1985) specify a minimum of 95% content with a moisture content between $\omega_{opt} \pm 2\%$, nevertheless (*op. cit.*) defines that the desirable average unit weight of each layer should be ≥ 98%. Even Fell *et al.*, (2015) states that this condition can be suitable for some types of dams, namely the ones constructed in wet climates, and with soils difficult to compact, on condition that compaction will be executed with an

water content above the ωopt. Compacting a soil in this conditions with a water content below the optimum could lead to a permeable embankment susceptible to failure (*op. cit.).*

Guedes de Melo (*op. cit*) specifies that is a common procedure to adopt a final layer thickness of 0.15m after the compaction is completed, however, and due to the characteristic of the compaction equipment nowadays the construction of such thin layers may be exaggerated. USBR (1991) suggests the use of 0.15-0.2mm for loose thickness before compaction with sheepsfoot rollers, and 0.2-0.3m before compaction with 50 t rubber tired rollers.

Field compaction curves obtained are not perfectly adjustable with laboratory curves, since the degree of compaction achieved in the field is not uniform as the one obtained in lab test; in other words, the results from the compaction in laboratory are not completely replicable in the field. Therefore, specifying a density ratio of 100% (Equation 3.18) is not practical, once this condition do not consents a margin of error that contemplates the differences between field and laboratory conditions (Guedes de Melo, 1985; Braja, 2007). The construction of a trial embankment to obtain information that will be used in the adjustment between both curves is a common procedure in embankment dams projects, an extended approach to this subject is presented in the following section.

$$\gamma_{d,field} = 100 * \gamma_{dmax,laboratory} \qquad (3.18)$$

3.5. TRIAL EMBANKMENT

Trial embankments or also known as test fills, can be used to define construction methodologies such as the number of passes that guarantees a maximum efficiency for the compaction equipment, the layer thickness that provides a minimal heterogeneity in the embankment. As mentioned before, this structures offer to engineers an opportunity to study the effects produced by variations of soil compaction techniques on the embankment characteristics.

The information retrieved during the construction of these structures is used to adjust the field compaction curves to the compaction curves obtained in laboratory, the adjustment should be gradual and based on in situ tests performed during the construction of the trial embankment (Guedes de Melo, 1985; Santos, 2008).

A modification in the compaction equipment or type of soil used during the dam construction implicates the construction of a new embankment (*op. cit.*), denoting that situations where the constructor wants to use different types of rollers in simultaneous to compact the same layer are common in dam construction. However, this condition creates a complex solution from which conclusions cannot be drawn, since each type of equipment has specific conditions of use which are disregarded with this type of construction.

The authors define that the construction of the trial embankment should be implemented over one or more layers of fill, and follow all the construction procedures that were defined by the designer for the

embankment dam. A brief description of the construction procedures based on the work of the author is described in the paragraph bellow:

- This structures should be implemented in area that allows the delimitations of 5 stripes with a length between 50 and 80 m, and a width between 3 and 5 m. Each stripe should be compacted with a different water content ranging between the dry of optimum and the wet of optimum, with one of them having a water content similar to the optimum.
- The compaction process is initiated after the soil placement. It is a common procedure to start compaction with a small number of passes, followed by an evaluation of the achieved results through in situ tests. This procedure is successively repeated for an increased number of passages. With this methodology engineers can measure the effects of increasing the compactive effort;
- The results from these in situ tests are used to plot the field compaction curve. An extended approach to this tests will be defined in the next Section.

3.6. COMPACTION CONTROL

Compaction control can be defined as the group of operations that is performed on an embankment to assure that the field compaction specifications defined in the project are being fulfilled, through a comparison between the results from in situ tests and the compaction curves obtained in laboratory. The purpose of this operations is to define if a layer is accepted or not; if a layer is not accepted, it will be removed. To evaluate the effects of soil compaction it is necessary to measure the following proprieties in the field:

- Fill unit weight - γ_{fill};
- Fill water content - ω_{fill}.

There are several devices that can be used to access these properties, some of them can be employed to measure both proprieties. A list of the most commonly used devices is defined in Table 3.9.

Table 3.9 - Commonly used devices to access the fill unit weight and water content (adapted from Berney *et al*., 2011)

Fill water content		**Fill unit weight**	**Fill unit weight and water content**
Direct Heat	Chemical		
Laboratory oven Laboratory Microwave Gas stove Moisture analyser	"Speedy" moisture	Sand Cone Test (SCT) Water Balloon (WB) Steel Shot (SS)	Moisture Density Indicator (MDI) Nuclear Density Gauge (NDG) Soil Density Gauge (SDG) Electrical Density Gauge (EDG)

The SCT, NDG, laboratory microwave, laboratory oven, and "speedy" moisture, will be described in the following sections. The other methods are beyond the scope of this dissertation since are not yet used in Portugal. The values from those proprieties must be compared with the laboratory maximum dry density and ω_{opt} to verify that soil compaction fulfils the technical specifications.

This comparison can be established using mathematical indicators, like the degree of compaction (Equation 3.19) or relative density (Equations 3.20 and 3.21) depending on the type of soil.

The results from the compaction procedures in cohesive soils can be evaluated using a parameter designated as relative compaction (RC) or degree of compaction (DC), which is defined by Equation 3.19.

$$DC = \frac{\gamma_{dfill}}{\gamma_{dmax}} \times 100 \qquad (\%) \qquad (3.19)$$

Where,

γ_{dfill} - Dry unit weight from the fill;

γ_{dmax} - Maximum dry unit weight from the laboratorial compaction curve obtained with the Proctor test.

Fernandes (2011), states that the Equation 3.19 as no significance for cohesionless of soils, with particular significance for poorly-graded soils, since for these soils the interval between $e_{max} - e_{min}$ is small, and consequently the relation $\gamma_{d,min}/\gamma_{d,max}$ is proximate to 1.Therefore this will always be proximate to 100%. The normal procedure for this soil is to use the relative density (RD), defined by Equations 3.20 and 3.21.

$$RD = \frac{e_{max} - e}{e_{max} - e_{min}} \times 100\% \qquad (\%) \qquad (3.20)$$

$$RD = \frac{\gamma_{d,max}}{\gamma_d} \times \frac{\gamma_d - \gamma_{d,min}}{\gamma_{d,max} - \gamma_{d,min}} \times 100\% \qquad (\%) \qquad (3.21)$$

Where:

e_{max} - Maximum void index for a sand;

e_{min} - Minimum void index for a sand;

$\gamma_{d,max}$ - Maximum dry unit weight (kN/m^3);

$\gamma_{d,min}$ - Minimum dry unit weight (kN/m^3).

The dry unit weight of the fill is determined with Equation 3.10 using the fill unit weight and water content.

3.6.1. DETERMINATION OF THE FILL UNIT WEIGHT

As explained previously, the γ_{fill} can be determined using the SCT or the NDG, both method are described in the following sections.

3.6.1.1. SAND CONE TEST

The sand cone apparatus is formed by a jar made of plastic or glass with a metal cone attached to its top. The jar is filled with a reference sand (Ottawa or similar). The equipment used in this test is illustrated in the Figure 3.13.

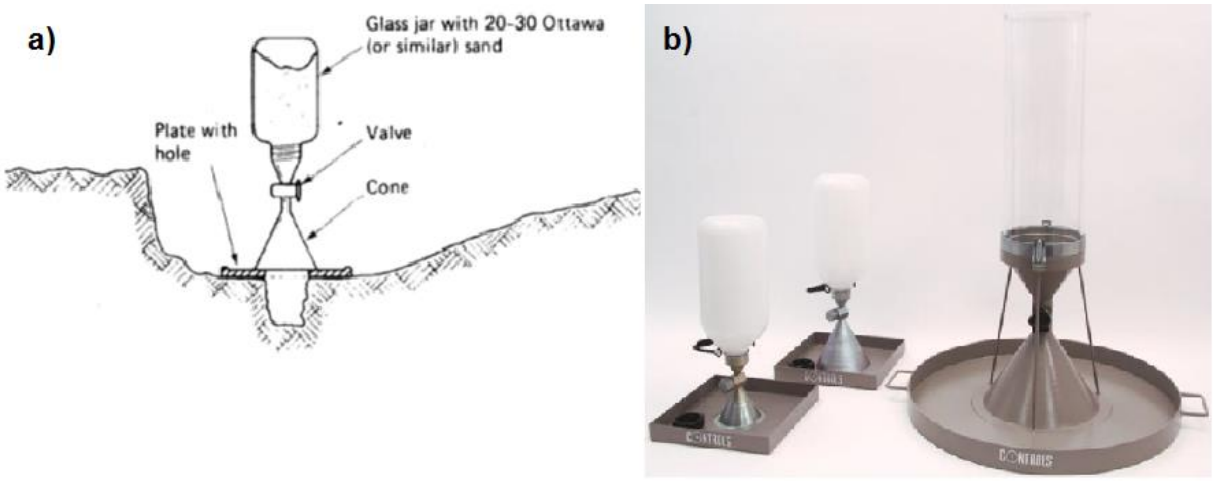

SCT: a) parts (Holtz & Kovacs, 1981); b) equipment (Center for the Protection of the National Infrastruture - CPNI, 2015)

Figure 3.13 - Sand cone test apparatus

The principle used by the SCT to measure the fill unit weight resides in obtaining the volume of a hole excavated in the field by filling it with a previously calibrated sand (known unit weight), and then determining the weight of the amount of sand that was required to fill the hole (Venkatramaiah, 2006).

Santos (2008) states the SCT is the most used method in Portugal to access the fill unit weight. A summarized description of the test procedure is provided on the specification ASTM D1556 (2015). A test hole is excavated in the fill by an operator, the material retrieved from this hole is protected against water losses and preserved in an adequate container. The hole is filled with a sand of known unit weight and the volume is determined. The in situ unit weight is calculated by dividing the weight of the removed by the volume of the hole (Equation 3.8). The water content from the excavated material is determined and the fill dry unit weight is determined with Equation 3.25.

The weight of the sand that is used to fill the hole can be calculated through Equation 3.22.

$$W_{FH} = W_{C+J} - \left(W_{FC} + W_{RJ}\right) \qquad (kN) \qquad (3.22)$$

Where:

W_{FH} - Weight of the sand that is used to fill the hole (kN);

W_{C+J} - Weight of the device composed by the jar and cone when filled with sand (kN);

W_{FC} - Weight of sand used to fill the cone (kN);

W_{RJ} - Weight of sand remaining in the jar (kN).

Once the values of W_{FH} and γ_{dref} are known, the volume of the hole can be obtained through Equation 3.23.

$$V = \frac{W_{FH}}{\gamma_{dref}} \quad (m^3) \qquad (3.23)$$

Where:

γ_{dref} - Dry unit weight from the reference sand (kN/m³).

If the weight of dry soil can be calculated with the Equation 3.2.

$$\gamma_d = \frac{\gamma}{1+w} \Leftrightarrow \frac{W_d}{V} = \frac{\frac{W_{ES}}{V}}{1+w} \Leftrightarrow W_d = \frac{W_{ES}}{1+w} \quad (kN) \qquad (3.24)$$

Where:

W_{ES} - Weight of the excavated soil (kN).

The dry unit weight can be defined by the Equation 3.25.

$$\gamma_{d=} \frac{W_d}{V} \quad (kN/m^3) \qquad (3.25)$$

The Portuguese and American standards for this test are listed in the Table 3.10.

Table 3.10 - Portuguese and American Standards for the SCT

	Portuguese standards	**American standards**
SCT	LNEC E-204 (1967)	D1556-15 (2015)

3.6.1.2. NUCLEAR METHOD

In this method, a device known as nuclear density gauge (Figure 3.14) is used to obtain the in situ dry unit weight and the water content, this section addresses the determination of the fill unit weight, the water content determination will be described in the following section. In a simplified way it can be said that this equipment is composed by three main elements:

- A nuclear source - responsible for the emission of gamma rays or neutrons;
- A radiation detector;
- A counters with provisions - to detect an automatic and precise timing for the arrival of the modified gamma ray.

According to Maregesi (n.d.) and Environment Agency (2014) this test uses the interaction between gamma radiation and soil to measure the dry density; this propriety can be measured through two modes, direct transmission or backscatter, as follows.

- Direct transmission (DM): In this method the source rod is introduced into hole in the embankment that was previously drilled. The gamma rays transmitted from the source pass

through soil and are counted by the equipment detectors, the number of counts is used to determinate the density (Figure 3.15 a)). This process is suitable for earth fill construction.

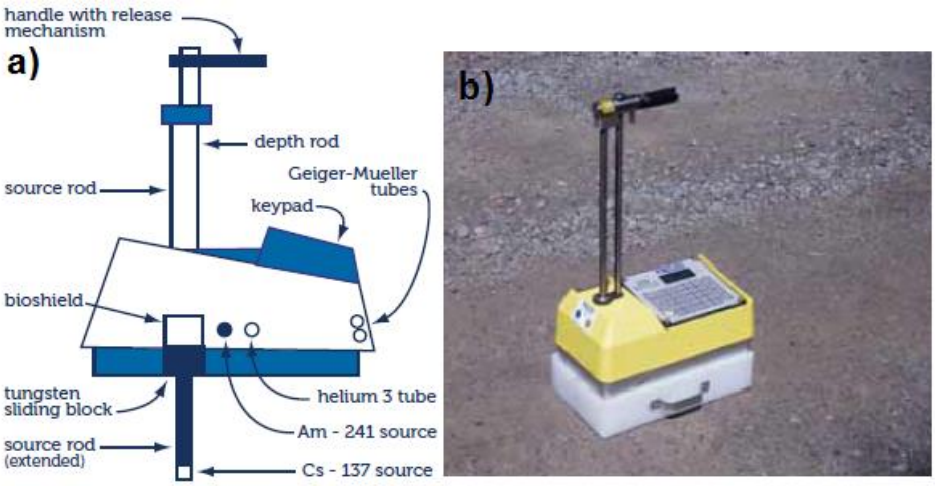

a) parts; b) equipment.

Figure 3.14 - NDG equipment and its main parts (Vicroads, 2011)

- Backscatter (BSM): The equipment is placed on the embankment surface, and the gamma source remains inside the equipment, (Figure 3.15 b)). The source initiates the emission of gamma rays into the soil, those that are scattered back to the surface are counted, and then density is measured. This method can test the materials to a depth of approximately 10 cm (depending on the soil hydrogen content), and is commonly used to measure the density of asphalt concrete and cement concrete.

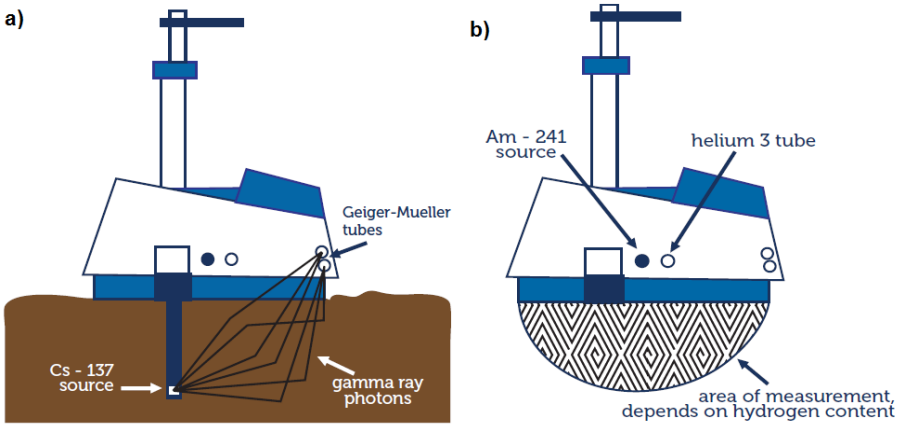

a) Direct transmission mode b) Backscatter mode.

Figure 3.15 - Control of compaction using the nuclear gauge (Vicroads, 2011)

The test is based on the following principle: the amount of gamma rays counted by the equipment during a certain period (usually 1 min) is inversely proportional to the density of the material. The

relation between the number of rays counted and density is calculated using calibration constants. Usually nuclear gauges have a factory calibration based on the characteristics of a material with a well-known mineralogical/chemical composition. However, using this type of calibration for field measurements can lead to unreliable gauge readings, since embankment and reference materials may have different compositions. A solution for this problem is to use an *in situ* calibration based on the characteristics of the embankment materials measured by other field tests, like the sand cone method (ASTM, 2008b). According to Maregesi (n.d.), the common procedure for calibrating the nuclear gauge consists in finding the mean error (shift coefficient) of the nuclear gauge results and add or subtract the results from the sand cone method.

In Europe, there is no specification for this method; however, the test procedure is described in the specification ASTM D6938-10 (2010c).

3.6.2. DETERMINATION OF THE WATER CONTENT

The water content can be determined in laboratory and in the field. In laboratory, the most common methods to measure the water content are the direct oven (OVM) and the microwave method. The basic principles are the same for both methods; the main difference is the duration of the process. A simplified description for the procedure used in the oven method (OVM) is defined in the next paragraph:

A sample is placed in an oven and dried at a temperature of 110º±5ºC to a constant mass, the loss of mass resultant from this process is considered to be water. The water content is determined using the mass of the sample before and after being dried (ASTM, 2010).

The water content can be calculated by Equation 3.26.

$$\omega = \left[\frac{M_{cws} - M_{cs}}{M_{cs} - M_c}\right] \times 100 = \frac{M_w}{M_s} \times 100 \quad (\%) \qquad (3.26)$$

Where:

ω - Water content (%);

M_{cws} - Mass of container and wet specimen (kg);

M_{cs} - Mass of container and oven dry specimen (kg);

M_c - Mass of container (kg)

M_w - Mass of water (kg);

M_s - Mass of solid particles (kg).

The Portuguese, European and American standards for this test are listed in Table 3.11 and according to the Portuguese specification, this test has a duration of 24h.

Table 3.11- Portuguese, European and American Standards for the Oven Method

	Portuguese standards	European standards	American standards
Water content determination	NP-84 (1965)	ISO/TS 17892-1 (2014)	ASTM D2216-10 (2010)

As previously referred, the oven method is identic to the microwave method, but the drying process takes less time; however and according to the ASTM D4643 (2008a), the results obtained with this test are less accurate than the direct heating method.

In the field, two commonly used methods to measure the water content are:

- Calcium carbide gas pressure tester method ("speedy" test);
- Nuclear density meter (NDM) method.

The calcium carbide gas pressure tester method is generally designated as "speedy" method and is based on the principle that when calcium carbide is used as a reagent, it reacts with water producing acetylene gas. In Portugal, there is no specification for this method, nevertheless the test procedure can be consulted in ASTM D4944-11 (2011b). A summarized description for the test procedure is transcribed in the paragraphs bellow.

A measured volume of calcium carbide along with two steel balls and a soil sample that has all particles smaller than the nº4 sieve size are placed in the testing apparatus. The equipment is shaken in a rotating motion to guarantee that the calcium carbide reagent contacts with all the water present in the sample. The apparent water content is read from a pressure gauge present on the equipment.

The equipment must be calibrated for each type of soil, a calibration curve can be defined by plotting the pressure gauge reading and the water content determined by the oven method.

According to Guedes de Melo (1985), the "speedy" is a fast simple method to indirectly estimate the water content. Santos (2008), however refers that this method should only be applied in granular soil, since it has an inferior precision in fine graded soils. In his studies, Berney *et al*. (2011) tested several types of equipment to determinate the water content, in this study the authors concluded that the "speedy" method was the most precise but least accurate method, and should only be applied as a last resource method.

The nuclear method was described in the previous section; however, the water content determination has some differences since it is measured using a neutron source instead of a gamma ray source. The principle used in this measurement is based on a process designated as thermalisation, which occurs when neutrons pass through soil and collide with water molecules, the hydrogen in this molecules will slow down the neutrons. The amount of thermalized neutrons counted by the equipment is directly proportional to the water content (Maregesi, n.d.).

3.6.3. COMPARISION BETWEEN SCT AND NDG

As explained in the previous sections, there are several tests that can be employed to measure the fill unit weight and water content. Therefore the identification of the most adequate solution to be used during the control operations is an important subject. In this dissertation, non-nuclear methods (SCT and OVM) will be compared with the nuclear ones (NDG), to evaluate the accuracy of the late.

The SCT and OVM compose the conventional approach to compaction control, however this procedures have some limitations. The sand cone is a low cost but time consuming and destructive method that implicates the excavation of a hole with considerable dimensions which can create some future problems, such as cracks, in the embankment (Kim *et al.,* 2011). In accordance with the works of Holtz *et al.* (1981) and Budhu (2011) the determination of the hole volume can be affected by:

- Densification of the sand in the hole due to vibration produced by working equipment, resulting in a larger hole volume;
- The size of the hole can be altered through soil movement; in granular soils there is the possibility of collapse;
- The existence of void space beneath the plate.

Maregesi (n.d.) states that the results from these test have low reproducibility and repeatability. The use of the SCT implicates the determination of the water content through the OVM (or similar), and this process takes 24 hours. Another common approach is to use the “speedy” method as an expeditious technique to determinate an approximate value of the fill water content. However, the results obtained with this method have some limitations as expressed in section 3.6.3. The value of the fill dry unit weight from this test needs to be computed through Equation 3.25.

Compaction control using nuclear gauges can be defined as a non-destructive methodology. Although the direct method implicates the drill (by percussion) of a hole, the dimensions of this hole are substantially inferior when compared to the hole excavated during the SCT. The nuclear methods are a rapid and direct methods of obtaining both control parameters and, therefore, a larger amount of tests can be performed increasing the amount of information that is available for control. However this methods also have some disadvantages, which are defined bellow in compliance with the works of Maregesi (*op. cit.*) and Fernandes (2011):

- The equipment is more expensive than the sand cone, and a radiation certification is obligatory;
- There could be some operator errors;
- The embankment surface must be prepared;
- Radiation can cause serious health damages to the operator;
- This equipment cannot be applied to very coarse grained soils (gravels).

Despite being a rapid and direct way to control the compaction, the reliability of the nuclear method has been a subject of discussion by specialists during the last decades. LeFevre (1984) defines a detailed literature review on the evolution of this subject between 1940 and 1984. A summary from this review is expressed in Table 3.12.

Table 3.12 - Evolution of the comparison between NDG and SCT between 1940 and 1981

Date	Event
40´s	First investigations regarding the use of nuclear methods in control operations, developed by geologists and geophysics in petroleum explorations
1960	First commercial NDG, launched by Nuclear-Chicago.
1960	Gnaedinger compared the results obtained with of one NDG launched by the Nuclear-Chicago firm with the SCT, stipulating that: • NDG calibration was affected by the type of material, therefore the calibration curves provided by the manufacturer were not adequate; • Nuclear gauges should be calibrated for each soil type by comparisons with field and laboratory tests. • NDG results gave lower density readings than the SCT for granular soils, and higher readings for clayey soils. • The NDG provided more reliable results for granular materials
1963	Ralston & Anday, (1963) investigated three NDGs and stated that none could be recommend for the Virginia Department of highways, since even with the calibration obtained from the field data the variation of the nuclear densities relatively to the conventional methods was above the acceptable limits. Weber, (1963) obtained similar results to those described by Gnaedinger and concluded the NDG were as time consuming as the conventional methods due to the necessity of establishing a calibration curve for each type of soil. Arkansas State Highway Department published a report in which was stated that the NDG was inadequate from stone base materials. Kuhn presented the air gap method as a solution to eliminate the effect of soil type in density measurements, which could only be applied to the backscatter configuration.
1966	Todor & Gartner Jr. published the results from an evaluation using the DM method, which provided more accurate and faster than the balloon test, and the principle of this method removed the necessity of several calibration curves.
1967	Truesdale & Selig compared NDG and SCT results and concluded that: • The densities measured with the SCT were inferior to those obtained by the NDG; • The NDG results were not accurate when using the calibration curves defined by the manufacturer, and sustained the importance of defining standard operation procedures Gardner, et al. presented a model of gauge response to explain and optimize the air-gap method defined by Kuhn.
1971-72	ASTM published two procedures for the calibration and testing with nuclear gauges
1973	Hatano et al (1973) published a study comparing both methodologies, one of the purpose of this report was to identify the effects of concrete walls and pipes on nuclear gauge measurements. The author concluded that: • The NDG results did not reveal any effect produced by the concrete wall; • The comparison between both methodologies showed that the SCT results were slightly higher.
1979-78	Revision of the ASTM procedures
1981	The California Transportation Department presented the autoprobe, which was a prototype backscatter nuclear gauge installed in a motor vehicle together with a hydraulic operator mechanism that automatically positions the gauge This equipment could measure the in situ moisture and density values in 3 min

In his researches, LeFevre (*op. cit*) investigated the correlation between nuclear and actual density and moisture on gravel bases from Nashville Arkansas. The nuclear tests were performed on laboratory compacted samples and their results were compared with the samples natural density (relation between the soil weight and volume) and water content measured through the oven method. The conclusions of this comparison were as follow:

- Nuclear and actual wet density have a linear correlation, and their difference increases with the wet density;

- The values of moisture content obtained by the nuclear gauge can be higher or lower than those from the oven method, and also have a linear correlation;
- The nuclear and actual dry density have a low correlation.

The author also compared the field density and moisture content obtained by nuclear methods with the results from the sand cone test and oven method, the conclusion that can be taken from this comparison are:

- Nuclear gauge provided lower values of wet density;
- The majority of the water contents measured by the nuclear gauge were higher;
- In both comparisons there was no correlation between results.

In a report published in 2005, the Division & Gas Technology Institute compared the results from the NDG with other types of soil compaction measuring devices. Even though the sand cone test and oven method were not directly used in this comparison, their results were used to calibrate the nuclear gauge - Figure 3.16.

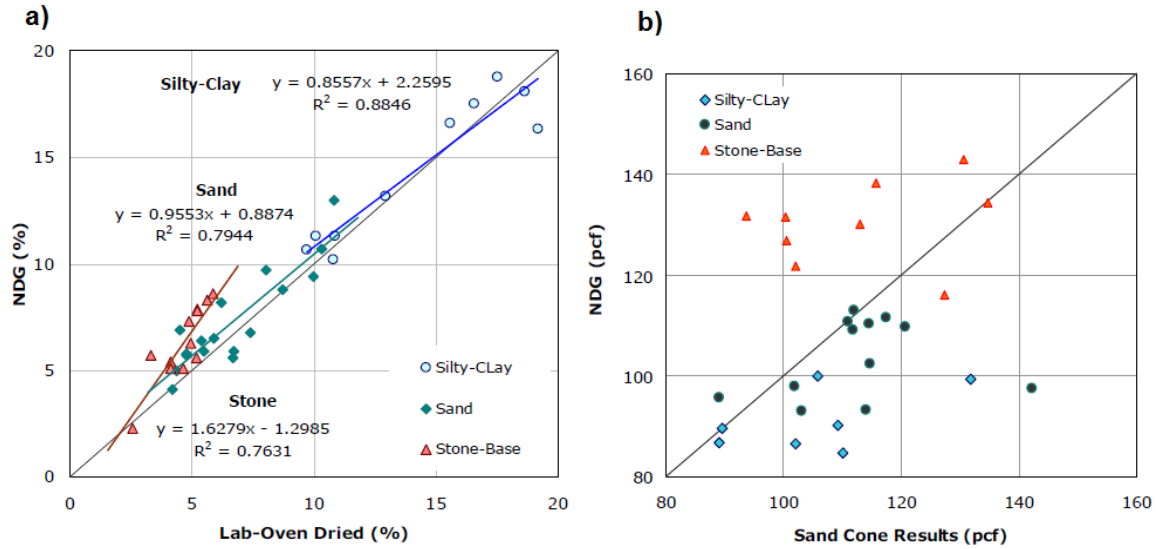

a) Measurements of soil moisture content using the NDG and OVM;
b) Measurements of soil dry density using NDG and SCT[1]

Figure 3.16 - Comparison between the results from the conventional and nuclear approach (Division & Gas Technology Institute 2005)

From these results, it is possible to verify that the majority of the water contents obtained with the NDG are higher than those from the oven method (Figure 3.15a)). Correlation between results depends on the type of soil and is higher for fine graded soils. The author states that the amount of hydrogen in the gypsum, lime, and fly ash particles may had affected the moisture readings resulting in higher moisture contents.

The dry density results illustrated in Figure 3.15b) shown that the NDG present lower readings for the sands and silty-clay soils, and the SCT higher results for stone-based soils. The higher results from

[1] The fill dry density in this study was expressed in pound per cubic foot (lb/ft^3), 1 kN/m^3 = 0.1571 lb/ft .

the SCT can be explained by a difficulty in achieving accurate densities from this test in this type of soil (*op. cit.*).

Altun *et al.* (2008) published a study that compared the parameters of field compaction obtained by the SCT and OVM with the results from the nuclear density gauge. The parameters of soil compaction considered in this work where the density, water content and degree of compaction. In this works, the authors tried to determine the relationship between the γ_d of the SCT by means of the γ_d and ω_{fill} obtained with the NDG through linear relationships, non linear relationships, and neural networks. The data used study was collected from 87 in situ tests taken in 3 different locations from the sub base layer of a road construction in Afyon, Turkey. The majority of the soils were classified as SM - silty sands with the exception of two soils, which were defined as SP-SM - poorly graded silty sand.

The authors demonstrated that the best solution to express the relationship between both parameters could be achieved using artificial neural networks.

Martins (2011) used both methodologies on the construction of trial embankments and compared the results. The tests were employed during the construction of the Évora trial railway embankment and Fafe trial road embankment to study the respective state parameters. The materials used on the Évora embankment were a clayey sand (SC) and a crushed aggregate (CA 31.5).

Initially, that author compared the results from the tests performed in the same grid. Values of density were disperse and usually higher for the SCT, Figure 3.17 (a). In contrast, the water content results had a high correlation, Figure 3.17 (b).

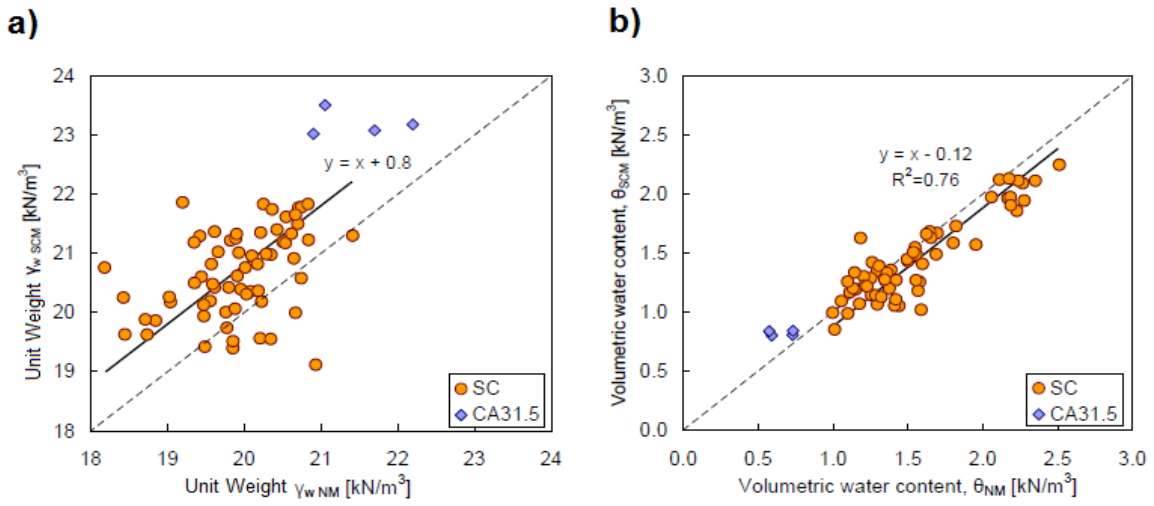

a) Measurements of soil fill unit weight NDG and SCT;
b) Measurements of soil volumetric water content using the NDG and OVM.

Figure 3.17 - Comparison of soil parameters obtained from NDG and conventional methodology performed on the same grid (Martins, 2011)

To minimize the dispersion from density results, he established a relationship between average values per energy level for each layer, as illustrated in Figure 3.18 (a).

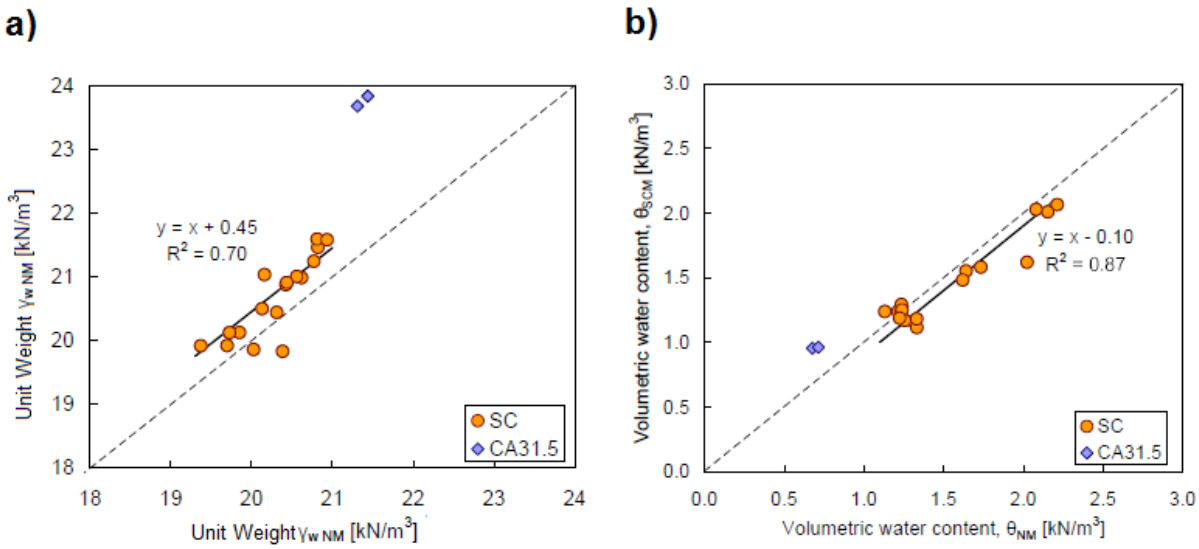

a) Measurements of soil fill density using NDG and SCT;
b) Measurement of soil water content using the NDG and OVM.

Figure 3.18 - Comparison of soil parameters per layer obtained from nuclear and conventional methodology (Martins, 2011)

The materials employed on the Fafe embankment construction were inert steel aggregate (ISAC) and poorly graded sands (SP). The same process was used to study the correlation between both methodologies in this new materials; the results from the tests performed on the same grid are plotted in Figure 3.19. It is evident that the outputs for SP material have a reasonable correlation between both methodologies (R^2=0.53 and R^2=0.55). On the other hand ISAC material showed a poor correlation (*op. cit.*).

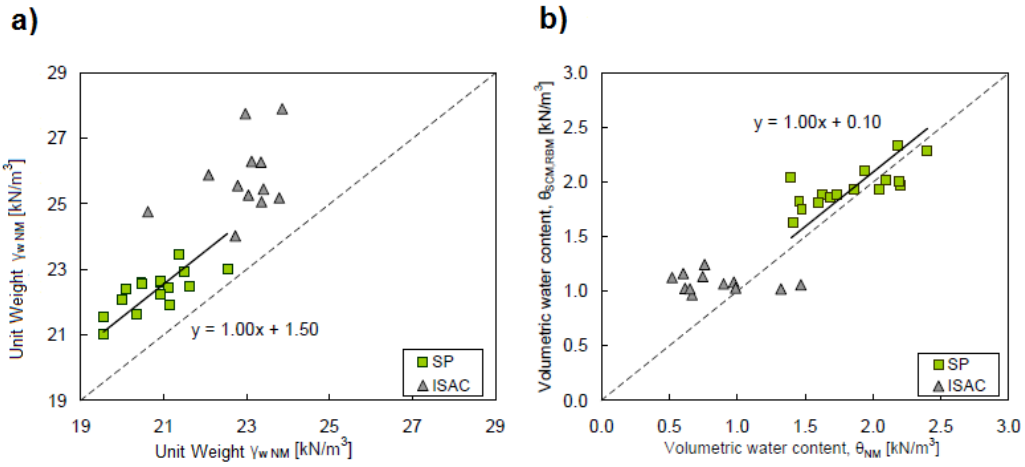

a) Measurement of soil fill density using NDG and SCT;
b) Measurement of soil volumetric water content using the NDG and OVM[1]

Figure 3.19 - Comparison of soil parameters per layer obtained from nuclear and conventional methodology (Martins, 2011)

As in the previously, it was established a relationship between average values per energy level for each layer, with the purpose of minimizing the ISAC scatter. However the ISAC values plotted in Figure 3.20 conserved low correlations, concluded that NDG may not be appropriate to measure the moisture content, in this materials (*op. cit.*).

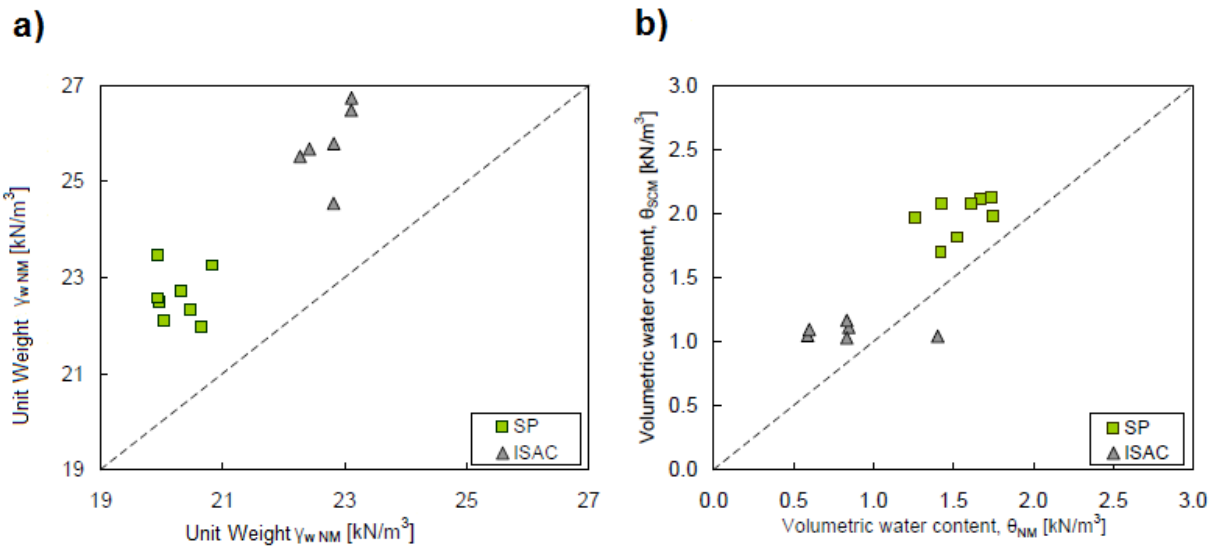

a) Measurements of soil fill density using NDG and SCT;
b) Measurements of soil volumetric water content using the NDG and OVM.

Figure 3.20 - Comparison of state parameters per layer obtained from nuclear and conventional methodology (Martins, 2011)

The United States Army Corps of Engineer (USACE) research and Development Center published a report about this subject in 2011, in which they compared several devices for determining the fill water content (Berney *et al*., 2011). The purpose of that study was to determine a suitable alternative to the NDG by comparing the accuracy and precision of eight testing devices to the results from the oven method. Since this dissertation only considers the results from the comparison between nuclear and oven methods, only this results will be highlighted. The research comprised a full-scale construction of test sections with seven soils, which are considered as representative from a range of materials considered as commonly used in construction activities, varying in range from fine-grained silts and clays to coarse-grained gravels and crushed limestone.

The scattering of the comparison between both methods is defined in Figure 3.21 and is near 1. It can be concluded that the NDG and OVM presented high correlations, being the NDG from all the equipment tested in this work the one that presented highest correlations with the SCT. The only calibration required for this equipment was performed against a reference platform provided by the manufacturer (*op. cit.*). However, as described in section 3.6.1.2, this procedure can lead to inconsistent results. The main disadvantage of the nuclear gauge highlighted was the safety and bureaucratic required for its use.

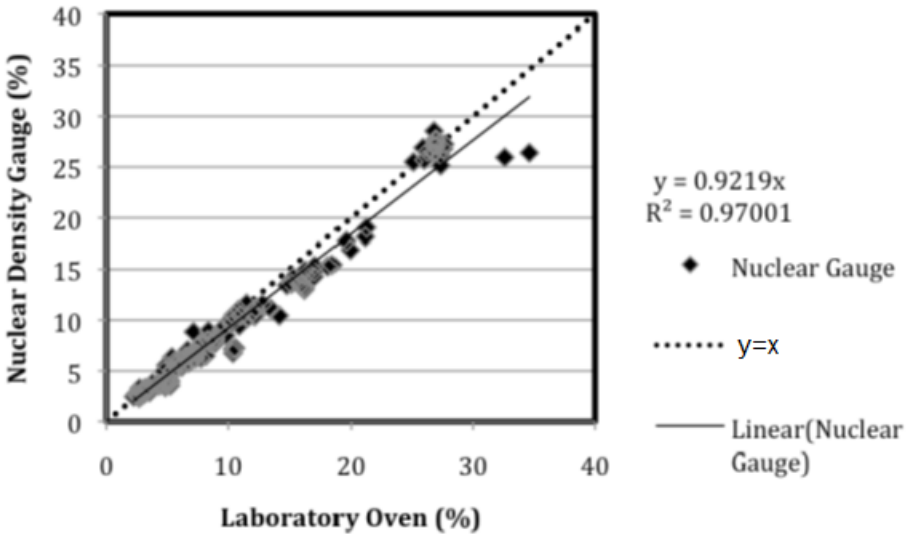

Figure 3.21 - Comparison of field moisture measurements with NDG with the OVM (Berney *et al.*, 2011)

Berney & Kyzar (2012) presented a comparison of the results of 11 compaction measuring devices, that were employed in the test sections described in the works of Berney *et al*., (2011). The overall conclusions stated that the SCT and SDG were the most adequate devices to replace the nuclear method.

Maregesi (n.d.) discussed this subject and the use of “multiple shift coefficients” to adjust the NGD readings against the sand replacement method. These test were performed during the construction of Dar Es Salaam (Wazo Hill) - Bagamoyo project in Tanzania. The methodology and experiment design used in this study are described on the following paragraph.

Three density and moisture measurements were taken with the NDG. The test result considered in this work was the average of these three nuclear gauge measurements. Thereafter, the determination of wet density and moisture content using the SCT were taken at the same location where density and moisture content were determined previously using the NDG. Samples for water content determination were preserved in water thigh plastic bags ant taken to the laboratory for oven drying for 24 hours. (op.cit.)

The experience was divided into three phases, in each phase the tests were performed on a different material. The tests in the first phase were performed on a reddish brown clayey/sitly sand with low plasticity which formed a topping (improved subgrade). In the second phase the test were executed on a crushed coral limestone that was used as a natural gravel sub-base. The material tested in the third phase was crushed-run material obtained after crushing massive granite gneiss. The author concluded that using multiple shift parameters to adjust the nuclear gauge readings will improve, as follow:

- The coefficient of determination (R^2), is improved;
- The slope of bets-fit line becomes unit;
- The dispersion of the results is reduced;
- The error sum of square is reduced.

Neves *et al.* (2013) presented a study about laboratory and field tests related to soil compaction in sandy clayey soils (SC). This work can be divided into two sections, the first described the repeatability and reproducibility of the test results, and the other focused on the following practical aspects from the test methods:

- The influence of manual or mechanical devices in the modified test results;
- Comparison between the water content results obtained by direct transmission and backscatter modes;
- Correlation between the results from nuclear and conventional methods;
- Inter laboratory performance evaluation.

The results from the comparisons between direct transmission and backscatter modes, and between the results from nuclear and conventional methods are illustrated in the Figures 3.22 and Figure 3.23.

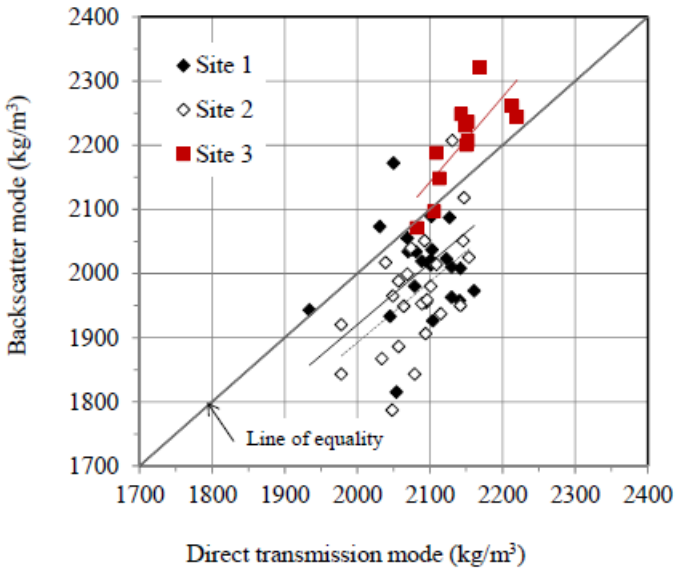

Figure 3.22 - Comparison of the wet density results obtained with backscatter and direct mode (Neves et al., 2013)

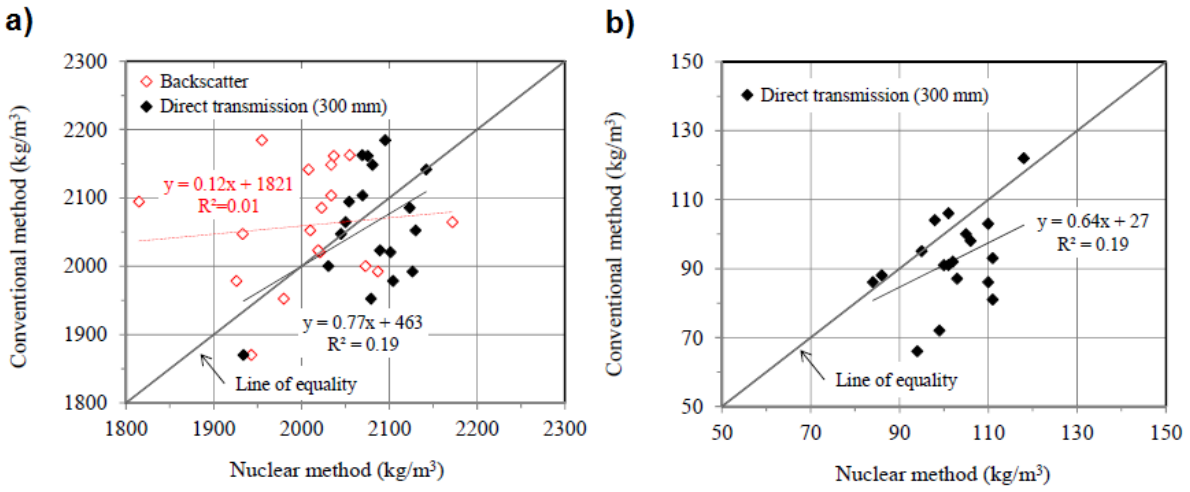

a) Measurements of soil dry unit weight using NDG and SCT;
b) Measurements of volumetric water content using the NDG and OVM.

Figure 3.23 - Comparison of soil parameters per layer obtained within nuclear and conventional methodologies (Neves et al., 2013)

The overall conclusions from this study were the following:

- The differences between the results from both methods demonstrated in Figure 3.23a) were expected;
- The results from the nuclear method should be validated according to the results from the conventional methodology;
- As can be seen in Figure 3.23a), wet density results from the direct transmission are closer to the SCT results, and the regression analysis was more adequate;
- The wet density readings from the nuclear methodology are different for each operating mode;
- The results from direct transmission mode were more accurate;
- In accordance with the results from the statistical parameters, repeatability and reproducibility were more acceptable for the nuclear method.

In conclusion, the knowledge associated to nuclear methods evolved considerably during the last decades and, presently, are one of the most used tests for compaction control of soils. The most significant advantages of this gauge when compared to conventional methods are the non-destruction of the fill and its quickness, allowing to perform a considerable number of nuclear tests during the execution time of a SCT.

However some authors consider that this method should not be used without using the conventional tests, since the accuracy of the nuclear gauge readings can be improved using a correction based on the results from the convention methodology. Another disadvantages from the nuclear methods are associated with the price of the device, bureaucratic demands, and the effects of radiation on humans.

Therefore, the most adequate solution may be to employ the SCT and NDG simultaneously to obtain a reasonable amount of information about the compaction parameters during an amount of time that must be compatible with construction schedules. This solution is commonly used in embankment construction.

Finally it must be referred that all the conclusions described on previously paragraphs, should not be applied to other types of materials besides those employed on the studies, since the results from soil compaction depend on the type of soil and as explained by a considerable number of authors, the accuracy of the NDG is influenced by the chemical composition of the soils.

3.6.4. COMPARISON BETWEEN FIELD AND LABORATORY COMPACTION CONTROL

Control operations intend to verify if the results form laboratory compaction are being replicated in the field, through a comparison between the results from in situ tests and the compaction curves obtained in laboratory. The purpose of this operations is to define if a layer is accepted or not, if a layer is not accepted it will be removed.

According to Hilf (1959) the classical approach to the control of compaction implicates the determination of the fill wet density without nuclear methods, the water content, and the compaction curve for each controlled point. The compaction curve is defined by compacting fill samples at the fill water content and at other water contents. The operations for converting wet to dry density take approximately one hour, and the determination of water contents involve a period of 24 hours (*op. cit.*). These periods of time, especially the 24 hours needed to determine the water content, are impracticable in the scope of a construction project. Two commonly used methodologies to solve this problem are: the family of curves method and the Hilf method.

3.6.4.1. HILF METHOD

This method was developed by Hilf in 1959 as an expeditious technique to evaluate compaction in cohesive soils without knowing the absolute values of water content and dry density, the degree of compaction is obtained by comparing the fill density with the results from a Proctor test. The principles of this method are (*op. cit.*):

- A laboratorial wet density curve can be obtained by compacting various specimens from the fill in the Proctor test and recording the variations of water content as percent of fill wet weight (Figure I.A - Annex I);
- The laboratorial wet density curve can be converted to wet density on a fill water content basis, from which the exact percentage of fill dry density relatively to the laboratory maximum density (degree of compaction) can be obtained (Figure I.B - Annex I).

The results obtained by this methodology are the compaction degree and the deviation between the fill and optimum water contents. According to *Associação Brasileira de Normas Técnicas* (ASBNT, 1991) both parameters can be calculated by equations 3.27 and 3.28.

$$DC = \frac{\gamma_{fill}}{\gamma_{max}} \times 100 \qquad (\%) \qquad (3.27)$$

Where:

γ_{max}- converted maximum wet unit weight, obtained with the Proctor test;

$$\Delta\omega = -\frac{z_m}{1+z_m}\left[\frac{1.6\gamma_{fill}^{max}}{2.6\gamma_{fill}^{max}-2.537}\right]\times 100 \quad (\%) \qquad (3.28)$$

Where:

z_m- z parameter for the γ_{max} point obtained with the Proctor test, this parameter expresses the amount of water added or removed to the soil sample in percentage of the fill wet weight, and can be calculated by Equation 3.29.

$$z = \frac{W_{a/r}}{W_{w,samp}}\times 100 \quad (\%) \qquad (3.29)$$

Where:

$W_{a/r}$: Weight of water that was added or removed to the soil sample (kN);

W_W^{samp}: Wet weight from the soil sample (kN).

γ_{sample}^{max}- Maximum wet unit weight for the sample (kN/m³), can be calculated by Equation 3.30.

$$\gamma_{sample}^{max} = \gamma_{max}(1+z_m) \quad (kN/m^3) \qquad (3.30)$$

These parameters can be obtained within an hour after the laboratory tests, since this method does not requires the determination of the water content through the oven method. Which is a significant improvement relatively to the classical approach. Fernandes (2011) stated that the methodology used in this method can be simplified in the following four steps:

1. A soil sample protected against evaporation is retrieved from the fill;
2. The sample is divided into *n* fragments, and the weight from each fragment is determined;
3. A know weight of water is added to a fragment and mixed until an homogeneous mass is formed;
4. Each fragment is compacted with the methodology used for the Proctor test, and its unit weight is measured;

This method was originally developed for cohesive soils; however in their works Abadi (2010) and Caldeira & Brito (2011) demonstrated that it remains valid for coarser grained materials. The methodology for this test can be consulted in the works of Hilf (1959), Guedes de Melo (1985), and in the following standards: AS 1289.5.7.1 (2006) from Australian Standards (AS) and MB-3443 (1991) from Associação Brasileira de Normas Técnicas (ASBNT).

The demonstration of this method in accordance with Hilf (1959) and Guedes de Melo (1985) is explained in Annex I.

3.6.4.2. FAMILY OF CURVES METHOD

This method is used to obtain the maximum density and optimum moisture content of a soil sample sing a family of curves and a single-point determination. The definition of those curves requires an exhaustive characterization of the materials available in the borrow areas. These families are defined

using the Proctor test and each family is composed by a group of curves with similar proprieties and origin (Colorado Department of Transportation, 2003).

This method is described in the specification T272 from AASHTO (2004) and in Guedes de Melo (1985).

The description of is method presented hereafter is based upon the documents of Guedes de Melo (1985). Before applying this method, it is necessary to establish a correct and extensive characterization of the soils that form each borrow area, and to perform a considerable number of compaction tests on the embankment.

A simplified description from the procedure is written bellow (*op. cit.*):

1. Three pits are excavated in the embankment, and the volume of soil retrieved from each pit should be estimated using the sand cone test;
2. Three determinations of the water content through the “speedy" test are applied to the soil excavated from the pits;
3. The soil is taken to the laboratory and is passed through a ASTM Nº4 (4.75 mm) sieve size,
4. The dry unit weight of the soil fraction from the last pit that passes through the No.4 sieve is estimated through a Proctor test;
5. The water content from the fraction that passes through the No.4 sieve is estimated by one of the methods referred in 2.10;
6. The material retained on the No.4 sieve is washed, dried and weighted, the volume of coarse elements is estimated;
7. The coarse material is dried and weighted.

The values of dry unit weight and water content obtained with the field tests are plotted in a graphic of water content versus dry unit weight where the reference curves from the soils that form each borrow area were previously plotted, and to each point is associated a family of curves. Figure 3.25 represents an example from the family of curves method that has three arbitrary points (A, B, and C) resulting from the field test and the reference curves graphic.

Point A can easily be associated to the family of curves number 1, once it coincides with one of the curves. Its point B belongs to the family 1, the compaction curve correspondent to this point will have a shape that fits between the compaction curves from family 1, as illustrated by the dashed curve in Figure 3.24.

Point C situation corresponds to a more complex situation, the decision about which family can be associate to this point will be based in the operator experience. This decision is associated to a risk factor nevertheless with a considerable knowledge and experience about the soils that are being used in the construction it is possible to minimize this risk.

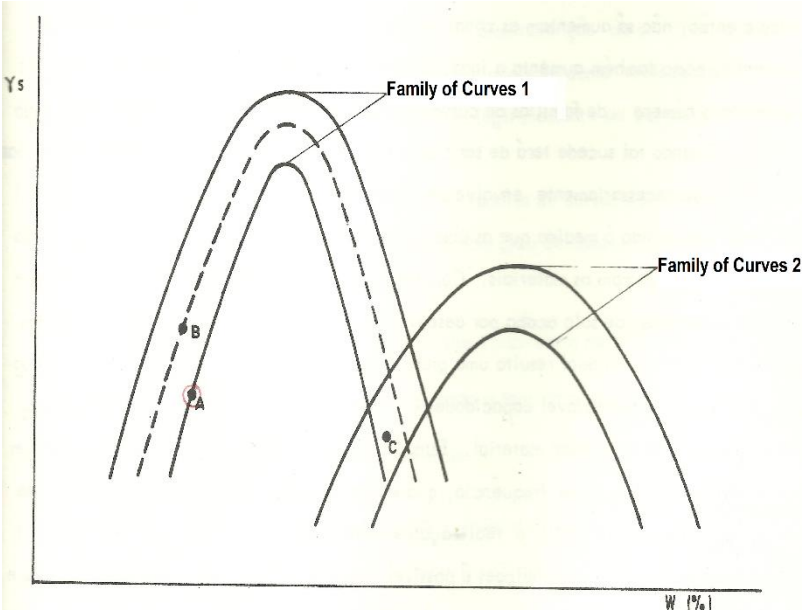

Figure 3.24 - Family of curves (adapted from Fernandes, 2011)

This method is practical and expedite, and its efficiency depends on (*op. cit.*):

- the homogeneity of construction materials (suitable for homogenous fills),

- the degree of accuracy of the water content measurements taken in the field, and

- the experience of field operators.

4. CASE STUDY

This chapter is initiated by a description of the following aspects related to the Coutada/Tamujais dam:

- Structural characteristics;
- Morphology;
- Geology and tectonic settings;
- Hydrogeology and seismicity main features;
- Construction materials;
- Construction and compaction control procedures (trial embankment and core).

Subsequently, the results from the conventional and nuclear methodologies obtained during the compaction control operations employed for the construction of the trial embankment are compared and discussed, and some final remarks about the results are established.

In the last part of this chapter, the comparison between both methodologies is applied to the results from the dam core, and 3D models of the dam core are offered. These results are discussed, and some considerations about the use of both methodologies during the core quality control are presented.

4.1. COUTADA/TAMUJAIS DAM

4.1.1. MAIN CHARACTERISTICS

The case study described in this dissertation is referent to the Coutada/Tamujais dam, illustrated in Figure 4.1. The data recovered through the compaction control operations during the construction of its trial embankment and core are used to compare the results obtained by the SCT and nuclear density meter test.

Figure 4.1 - General view of Tamujais/Coutada dam

In accordance with the information presented by Ferreira & Dias (2007), this dam was built as part of the Coutada/Tamujais irrigation project and is located in the streams of Prior, Locriz and Tamujais. This irrigation project comprises an area of 390 ha in the municipality of Vila Velha de Rodão, Portugal. The infrastructures that integrate this project are:

- Coutada/Tamujais dam;
- Retaxo's weir and derivation channel;
- Water pumping station;
- Irrigation and drainage networks;
- Road network.

Coutada/Tamujais dam is a zoned earthfill dam with a central core composed by arkoses and shells formed by alluvial materials. The dam have a maximum height of 22.5 m above the foundations and a crest length of 412 m. The maximum storage capacity is 3.9×10^6 m^3, with an useful volume of 3.8×10^6 m^3, the flooded area at the maximum storage capacity is 43,6 ha. The dam axis has an E-W orientation, the building contractor was Edifer and the construction ended in 2007.

4.1.2. MORPHOLOGY

In accordance with Ferreira & Dias (2007a) the Coutada/Tamujais dam was implemented in a wide valley with gentle and almost symmetric slopes 130 m high above the sea level. The bottom of the valley is almost flat and has flood a channel 120 m wide. The stream on the axis of the dam site has a North-South orientation and flows to South in a valley with 22 m wide. The dam reservoir area has a smooth relief, which creates a difference of approximately 20 m for the hydrographic network between the dam axis and the hydrographic network head. The stream in this area has a meander geometry (Figure 4.1).

The hydrographic network is composed by streams with gentle slopes. The characteristics from this streams can vary from downstream to upstream, due to a lithological modification from a relatively weak sedimentary formation to a metamorphic rock such as schist. As a consequence from this alteration the valley morphology changes from a wide valley to a narrow valley.

4.1.3. REGIONAL GEOLOGY AND TECTONIC

The area under study is integrated in a region of the Hesperic Massif designated as *Zona Centro-Ibérica* (ZCI), and can be characterized by the presence of flysh type metassediments that are included in the Super Group *Dúrico-Beirão* (Schist-greywack Complex that has been dated previously to the Ordovician period), and constitute the superior member of the *Malpica do Tejo* Formation (Ferreira & Dias, 2007). Built with layers of pelitic schists and metagreywackes, these deposits are deformed by tectonic structures, such as folds and overthrusts.

The *Malpica do Tejo* Formation is overlaid by a series of arkosic deposits (Cenozoic) belonging to the stratigraphic unit of *Cabeço do Infante.* The contact between these formations is made through an unconformity. The *Cabeço do Infante* unit is a series usually formed by friable arkoses with coarse

grain and clayey cement alternating with consolidated arkoses with a finer gradation, and having intercalations of sandstone beds. The studied dam is located in this formation.

The studied area is represented in Portuguese geologic map designated 24-D- Castelo Branco with a scale of 1/50,000 published by the *Serviços Geológicos de Portugal*, an excerpt from this map is represented in Figure 4.2.

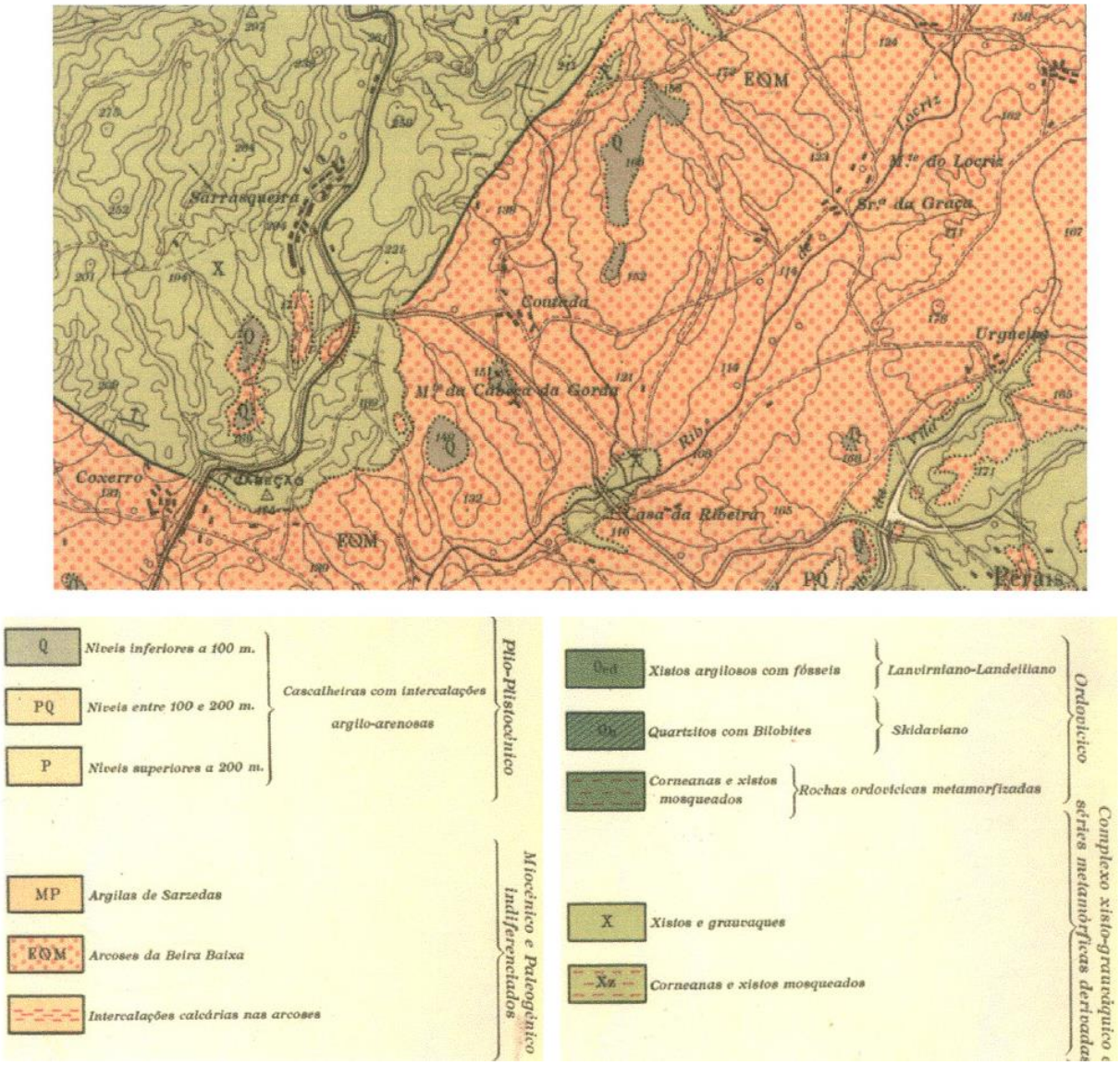

Figure 4.2 - Excerpt from the Carta Geológica de Portugal, Folha 24-D- Castelo Branco at the original scale of 1/50 000, (adapted from Ribeiro,*et al.*, 1967; Santos-Ferreira & Dias, 2007a)

The regional tectonic is based on the information sustained by Ferreira & Dias (2007a; 2007b) in the scope of the project. This region was affected by three stages of deformation, the first stage formed folds sediments dated between the late Precambrian and the early Paleozoic, the second stage (Hercynian cycle) originated second order folds on the materials previously deformed and first order folds in sediments dated from the later Paleozoic; the third stage originated faults.

4.1.4. HYDROGEOLOGY AND SEISMICITY

The presence of a topsoil layer with a low thickness in conjunction with the clayey genesis from the sub-superficial arkosic formations in the region, favour the predominance of superficial runoff over infiltration. However, in some situations, friable arkoses and/or sandstones occur on the surface and water circulation in these formations is made through porosity, and this type of permeability depends on the geometry of the clasts and nature of the cement (*op. cit.*, 2007a).

The majority of seismic events witnessed in Portugal can be originated by interplate seismicity or intraplate seismicity. The first type refers to seismic events with a focus in the border between the Eurasian plate and the African Plate, the second origin encompasses events with focus in the interior of the Eurasian plate. Therefore the proximity to active faults such as Ponsul and Segura need to be considered.

4.1.5. LOCAL GEOLOGY

The construction areas can be divided into 2 distinct zones based on the project characteristics: the dam axis and dam reservoir, the description from each of these zones established in this work is based on the information present in the document of Ferreira & Dias (2007b).

4.1.5.1. DAM RESERVOIR

The outcropping units that occur in the dam site belong to the *Cabeço do Infante* Formation, as referred in section 4.1.3 this formation is composed by arkoses and sandstones. A blanket composed by colluvium and alluvial deposits dated from the Quaternary overlays this formation.

The topsoil layer is formed by a sandy-clay soil with fragments of schist, usually the thickness of this layer do not exceed 0.5 m and occurs in the slopes of the valley. The structural unconformities identified in this area were parting planes.

4.1.5.2. DAM AXIS

The estimated thickness in this area for topsoil, colluvium deposits, and decompressed massif (sandy clay material with cobbles of quartz) usually did not exceed 2 m.

Alluvial deposits cover a considerable area in the region under study, these deposits were mapped at 700 m downstream from the dam axis, and between 500 and 600 m upstream the dam axis. The maximum thickness for these deposits was estimated at 3 m.

4.2. EARTH MATERIALS

According to the *Ministério da Agricultura do Desenvolvimento Rural e das Pescas (MADRP*, 2000) the identification of the borrow areas was based on the results from two phases:

1st phase- feasibility study stage: during this period, 9 pits were excaveted;

2nd phase- execution project stage: during this period 27 pits were excaveted.

From the information retrieved in the first stage alongside with the smooth topography, the thickness of decomposed massif and the presence alluvial material enabled the identification of three potential borrow areas: A, B and C. These are described below.

- Borrow area A - located in the flood plain upstream the dam axis and composed by alluvial deposits;
- Borrow area B - covers the stream margins, and is formed by the unit "*Arcoses da Beira Baixa*";
- Borrow area C - located 600 m to the west of the dam axis, outside the reservoir area, and is located in the Schist-greywacke Complex.

With the information obtained during second stage the hypothesis of using the area C was abandoned, since the estimated volume of material that was available in the other areas was not enough to be used in the construction of the embankment, and those materials were adequate from a geotechnical point of view. A borrow area designated as B' was defined in this phase to prevent an eventual insufficiency of the material in the area B, that could result from an overestimation of the volume of material available.

The characterization of those areas is described in Table 4.1, and it was based upon the information retrieved during the site investigation stage and laboratory tests.

Table 4.1 - Borrow areas description (based on *MADRP*, 2000)

Area designation	Number of pits	Area description
Area A	10	Generally the thickness of the topsoil Layer in this area is inferior to 0.5m; The topsoil layer overlays an alluvial deposit with a sandy-clay matrix; occasionally this deposit has fragments of decomposed schist and quartz rolled cobbles. The depth reached by this materials varies between 0.5 m and 4.7 m; Fairly compacted or decompressed arkoses underlie the alluvial deposit; The depth of the water table was detected in 3 wells (from P2 to P4) and varies between 1,5 m and 3,5 m.
Area B	11	Usually the thickness of the topsoil layer in this area is proximate to 0.3 m; The layer is formed by decompressed arkoses reaches a depth around 3,5m; Compacted arkoses occur bellow this layer.
Area B'	3	Usually in this area the thickness of the topsoil layer is around 0.3 m, and this one overlays a layer formed by decompressed arkoses; As in the Area B, a series of compacted arkoses occurs inferiorly to the decompressed arkoses.

4.3. SITE INVESTIGATION AND LABORATORY TESTS

These works were executed during the project phase and intended to complement the information retrieved in the preliminary study. The geophysical and mechanical prospection methods used in this project and their location are defined in Table 4.2.

Table 4.2 - Site investigation works associated to each dam zone *(MADRP*, 2000)

	Seismic Refraction Profiles		**Prospection pits**		**Geological surveys resorting to rotation with continues sampling**		**Standard Penetration Test (SPT)**	**Permeability Test/Lugeon Test**
	Used	Number profiles	Used	Number	Used	Number Surveys	Used	Used
Dam axis	Yes	5	Yes	-	Yes	4	Yes	Yes
Ancillary structures	Yes	5	No	0	Yes	1	No	No
Borrow areas	No	-	Yes	30	No	-	No	No

Samples were retrieved from the prospection wells executed in the borrow areas, in compliance with previously referred author the following laboratory tests were executed on this samples to establish a geological and geotechnical characterization:

- Particle size distribution (sieves analysis and hydrometer test);
- Atterberg limits;
- Compaction tests (Proctor test);
- Triaxial tests and determination of permeability (the results from these tests were not considered in this work since they transcend the purpose of this study).

The results obtained through this tests will be discussed in the following sections.

4.4. CONSTRUCTION MATERIALS

With the information retrieved during the prospection stages it was possible to identify two types of construction material: alluvial deposits and arkoses. Both materials are described in the following sections.

Rockfill materials for the rip rap, drains and filters were extracted from quarries in the proximity of the construction site. Sandy materials for the filters were retrieved from sand extractions in the vicinity of the construction site.

4.4.1. BORROW AREA A - ALLUVIUM MATERIALS

As described in Table 4.1 in this area occur alluvial deposits with a sandy-clay matrix, the mechanical prospection techniques and laboratories tests defined in Section 4.3 were applied to characterize these materials. The results are presented in Annex II.

The classification of the samples obtained during the prospection campaigns ranged in terms of particles sizes between clayey sands (SC), and well graded gravels with clay (GW-GC), Tables II.A and Figures IIA and IIB - Annex II. An average γ_{dmax} of 20.14 kN/m^3 (Table II.B and Figure II.C - Annex II) was obtained for the samples tested with the Proctor test. According to MADRP (2000) the

results from the geotechnical characterizations indicate that this materials were suitable for being used as a shell construction material.

Considering the dimensions of the prospected area and the thickness of the deposit varying between 2 and 4 m as observed in prospection pits, it was possible to estimate the volume of material available in this area at 265,000 m^3 approximately *(op.cit.)*.

4.4.2. BORROW AREA B AND B'- ARKOSIC MATERIALS

As defined on Table 4.1, this area was characterized by the occurrence of arkosic deposits, the mechanical prospection techniques and laboratories tests defined in Section 4.3 were applied to study these materials. The results are represented in Annex III.

The majority of the samples retrieved from this area were classified as clayey sands (SC) Tables III.A and Figures III.A and III.B - Annex III, and an average γ_{dmax} of 18.73 kN/m^3 (Table III.B and Figure III.C - Annex III) was obtained for the samples tested with the Proctor test. The geotechnical proprieties from this materials indicate that they are adequate to be used as core construction material (MADRP, *op. cit.*).

Due to the dimension of the prospected area and the thickness of the deposits identified on the prospection pits the volume of available material for this area was estimated at 200,000 m^3, approximately. To prevent core material scarcity, an additional area, designated as B', was defined *(op.cit.).*

4.5. TRIAL EMBANKMENT

The information about the construction of the trial embankment is based on the texts from Ferreira & Dias (2007a). The trial embankment was located on the east side of the spill way tunnel (Figure 4.3), and it was constructed in a flat platform 30x40m that had previously been stripped from the top soil layer, and compacted parallel to the dam axis, as prescribed on the project specifications. This structure was integrated in the dam body in a posterior construction stage.

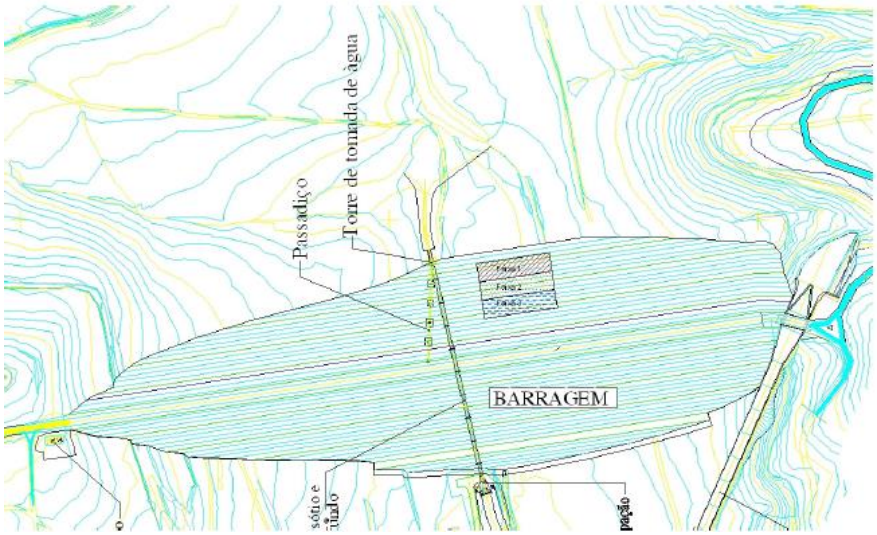

Figure 4.3- Location of the trial embankment within the structure, rescaled from the original of 1:500 (Ferreira & Dias, 2007a)

The purpose of this structure was the definition of the placing and compaction parameters (layer thickness, water content, and number of passes) for each type of soil and equipment used in the dam. This structure had 9 layers, each one divided in 3 adjacent stripes, overlapping passes of 0.5 m each, with a total volume of approximately 4,500 m^3.

The materials described in section 4.4.1 and 4.4.2 were used in the construct it. Borrow area A was used as a preferential source for the construction material, since its natural water content for the materials was more similar to the optimum water content obtained in Proctor test.

4.5.1. CONSTRUCTION PROCEDURES

As explained in section 2.5, the construction of an earth dam implicates several construction stages and in each one several types of equipment are required. The equipment used in each construction stage at Tamujais dam are listed below:

- A bulldozer to spread the soil;
- A 14 cat sheepsfoot roller model CS573 with a motor potency of 145 hp, and a 17 tons Bitelli smooth wheel roller model C170 with a motor potency of 224 hp were used during soil compaction; the smooth wheel roller was used to compact both types of soil, and the shepsfoot roller was used on finer materials;
- A farm tractor equipped with a water deposit to increase the soil water content.

As previously described, the trial embankment was constructed in a 30x40 m platform that had been previously stripped from the top soil layer and compacted. This platform was divided in three 10 m wide stripes, each one had a different thickness (0.3, 0.4 or 0.5 m), as represented in Figure 4.4.

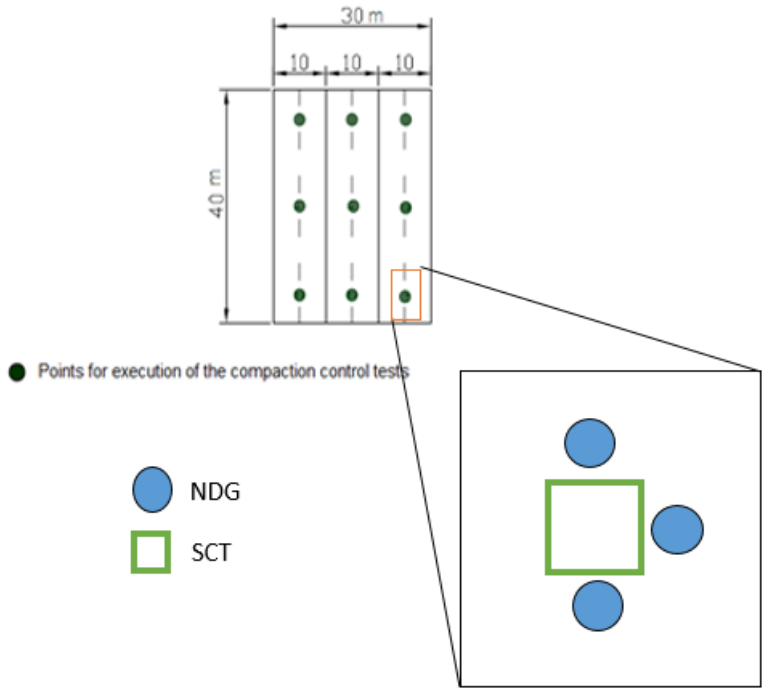

Figure 4.4 - Location of the compaction control tests performed

The construction process was considered to be divided in three stages, each one with three layers, depending on the type of soil and compaction equipment employed. The type of soil and equipment used in each layer are defined in the Table 4.3. The construction procedures used in each stage were similar, and are defined below:

1. In the first layer of each stage the soil was placed, spread and compacted with a water content 2% below the optimum (ω_{op}-2%);
    a. The compaction process in each stripe was executed using the predefined roller in a come and go motion over a track with a width equal to the roller.
    b. When the desired number of passes was reached, the roller passed to the adjacent track with a superposition of 0.5 m (Figure 4.5);
    c. This practice was stopped when the 10 m wide stripe was reached.
2. These construction processes were repeated for the second and third layers of each stage, however the water content used on these layers was the optimum (ω_{op}) and 2% above the optimum (ω_{op}+2%), respectively.

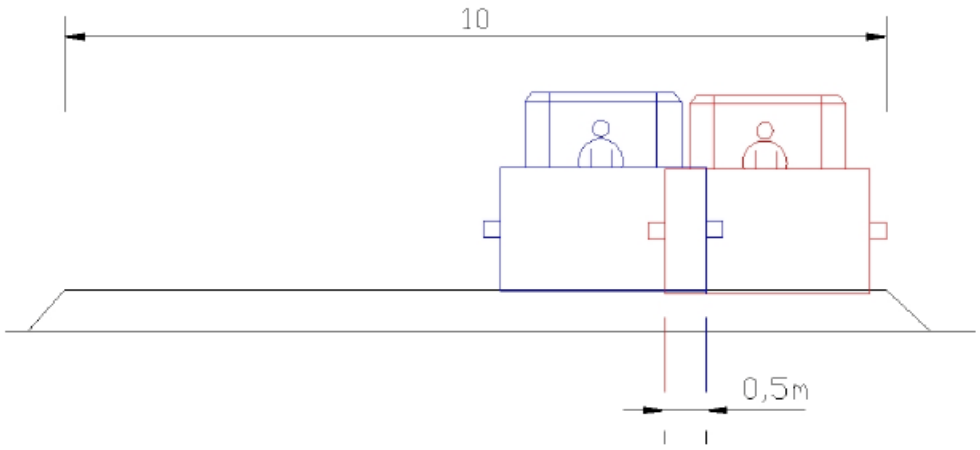

Figure 4.5 - Procedure for the compaction of each 10 m stripes, with the equipment overlapping 0.5m

Table 4.3-Equipment and type of soil used in each construction stage

Stage	Layers	Equipment	Number of passes	Soil type
1	1 to 3	Sheepsfoot roller	8	Arkoses (SC)
2	4 to 6	Smooth wheel roller	8	Arkoses (SC)
3	7 to 9	Smooth wheel roller	8	Alluvium (SC to GW-GC)

4.5.2. COMPACTION CONTROL

As referred in section 4.5, the purpose of the trial embankment was to define the placing and compaction parameters that would be used during the dam construction. The definition of this parameters is based on the results from the tests executed to evaluate degree of compaction in each layer.

Two methodologies were employed during the quality control operations to measure the fill, unit weight and fill, be designated as A and B:

Methodology A - It corresponded to the conventional methodology; the fill water content was accessed in the field with the “speedy” method to obtain an expedite value for this parameter, and the OVM was applied in laboratory to determinate a more precise value for the water content. The fill unit weight in the field was accessed with the SCT.

Methodology B - It corresponded to nuclear methodology; the NDG was used to measure both parameters. In the trial embankment the nuclear gauge measurements were taken at three depths, 0 (backscatter), 0.15 and 0.3 m in each testing site.

The tests from both methodologies were executed in each lane at the end of 4, 6 and 8 roller passes, their location is represented in Figure 4.4. For each SCT performed during quality control operations, three additional tests were taken with the NDG in the vicinity of sand cone testing site. As represented

in Figure 4.4, a total of three measurements were taken on each lane, considering that each layer has three lanes and the trial embankment is composed by nine layers.

During the construction of the trial embankment, the samples retrieved with the SCT (methodology A) were prepared and sent to laboratory, where the methodology described in the Hilf method (section 3.6.5.1) was applied. The application of this method resulted in a laboratory compaction curve for each sample that is used to calculate the water content deviation and the degree of compaction for each control point.

With methodology B, the quality control parameters were obtained by comparing the field measurements with the results of a previously defined reference sample, which was characterized in laboratory during the geotechnical characterization stages. The parameters were calculated by Equations 4.1 and 4.2.

$$CD = \frac{\gamma_{d_{fill}}}{\gamma_{dmax_{ref}}} \quad (4.1)$$

$$D_h = \omega_{fill} - \omega_{ref} \quad (4.2)$$

Where:

$\gamma_{d_{fill}}$ - Test fill dry unit weight (kN/m^3);

$\gamma_{dmax_{ref}}$ - Maximum dry unit weight for the reference sample (kN/m^3);

ω_{ref} - Optimum water content for the reference sample (%).

The $\gamma_{d_{fill}}$ can be calculated using the Equation 3.10. The values of $\gamma_{dmax_{ref}}$ and ω_{ref} used to calculate the control parameters (reference value) where 19.3 kN/m^3 and 13% respectively.

During the compaction control operations, a total of 324 measurements for each compaction control parameter (fill unit weight and water content) were obtained, 81 with methodology A (OVM and SCT), and 243 with methodology B (NDG). This results were analyzed and the main outcomes are displayed and discussed in the following sections.These results were used to define the placing and compaction parameters that were used during the construction of the dam.

The equipment used in the field during these operations needed to be calibrated for each type of soil. The calibration of each equipment is described in the following paragraphs:

- The SCT used calibrated sand in accordance with the specification LNEC E-204 (1967);
- The calibration curve for the “speedy” device was calculated using the results from a series of tests performed with the oven method;
- The NDG was used to determine the fill water content unit weight, therefore it was necessary to calculate two calibration curves for each type of soil:

- The calibration curve used for the determination of the water content was obtained by establishing a correlation between the results accessed with the “speedy” and the NDG;
- The calibration curve used for the determination of the DC was obtained by establishing a correlation between the results accessed with the SCT and the NDG.

The calibration curves obtained for the NDG were used to define the correction factor that should be entered in the equipment. The corrections used can differ for each soil type and equipment.

4.5.3. DATA ANALYSIS – METHODOLOGY

This dissertation intends to compare the results from both methodologies; however instead of using the original results from methodology B, which were obtained as explained in section 4.5.2, the original results were modified through the application of the Hilf method to the NDG measurements.

This method requires the existence of a sample that must be compacted in laboratory to obtain a field compaction curve. However, the NDG test does not provide a sample, to solve this problem the Hilf method was applied by considering that the laboratorial compaction curve defined for each SCT was valid for all the NDG performed in the vicinity of a SCT testing site.

To ensure the quality of data presented hereafter, the calculus from the application of the Hilf method to the SCT results were also redone by the author using the direct inputs from the field tests and data from the laboratorial tests described in Section 4.5.2.

After applying the Hilf method modified as explained above, the data was organized and the abnormal results were identified through the interquartile method using the software SPSS ® of IBM. The abnormal values can have several origins such as misspelling or inappropriate measuring procedures, and the software identifies as an outlier any value that fulfills the condition defined by Equation 4.3.

$$Q_1 - 1.5IQR \leq x_i \leq Q_3 - 1.5IQR \qquad (4.3)$$

Where:

Q_1 - First quartile;

Q_3 - Third quartile;

IQR - Interquartile range, which can be calculated through Equation 4.4:

$$IQR = Q_3 - Q_1 \qquad (4.4)$$

Three types of bivariate analysis were defined to compare the results from both methodologies:

1. Comparison between each methodology A measurement and all the NDG measurements taken in the vicinity of the SCT testing site, by considering the measurements taken at different depths, and different placing water contents as individual populations;

2. Comparison between both methodologies, by considering all the measurements taken at different depths and different placing water contents as a single population;
3. Comparison between each methodology A measurement and the NDG measurements taken in its vicinity at depths of 0.15 and 0.30 m (DM), the measurements taken at different depths, and different placing water contents were considered as a single population.

As described in Section 4.5.1, the construction was considered to be divided in three stages, therefore the results will be presented separately for each one of those stages. The comparison between both methodologies in each one of the analysis was established by plotting the results in SCT/OVM measurements *Versus* (*Vs*) NDG measurements scattergrams. A linear regression was applied to each one of the populations represented in those scatters and the coefficient of determination (R^2) was calculated. This coefficient measures how well a model (in this case a linear equation) fits the results, and it varies between 0 a 1, being 1 the maximum fit.

Additionally, a correlation matrix using the Pearson coefficient (*r*) was defined. This parameter is used to measure the correlations, and varies between -1 and 1, being 1 the maximum correlation. Different *r* ranges express different correlations. Evans (1996) proposed empirical classifications for interpreting this correlations which are defined in Table 4.4 and were adopted in this dissertation.

Table 4.4 – *r* ranges and their correlation (based on Evans, 1996)

$\|r\|<0.2$	Very weak correlation
$0.2<\|r\|<0.39$	Weak correlation
$0.4<\|r\|<0.59$	Moderate correlation
$0.6<\|r\|<0.79$	Strong correlation
$\|r\|>0.8$	Very strong correlation

4.5.4. RESULTS

4.5.4.1. COMPARISON BETWEEN SCT AND NDG RESULTS FOR STAGE 1

The three layers that compose the first stage were built with arkosic materials (SC) and compacted with a sheepsfoot roller. The control operations were carried out between 17 and 23 of April 2007. The descriptive statistics of the results obtained by both methodologies are described in Table 4.5, the histograms from the variables defined in this stage are defined in Annex IV.

Each set of graphics represented in Figure 4.6 is a comparison between both methodologies obtained for each compaction parameter (γ_{fill},ω_{fill}, and *DC*), at the three depths of the nuclear gauge measurements (0, 0.15, and 0.3 m) and three different water contents ($\omega_{opt} - 2\%$, ω_{opt}, $\omega_{opt} + 2\%$).

From the descriptive statistics presented in Table 4.5 it is possible to verify that methodology A results for each control parameter showed a tendency to show higher values, since all the control parameters measured with these methodology presented higher values for the central tendency parameters. This aspect can be enhanced by the results presented in Figure 4.6, in which the majority of the (SCT/OVM, NDG) points presented in the graphics are above the equality line (EL)

Therefore, any point above that line will correspond to a pair of results with higher values for methodology A.

In terms of dispersion, a distinctive pattern cannot be identified when comparing the results from both methodologies. The water contents measured by the NDG with the BSM have higher dispersions which may be caused by variations in the soil water content due to climatic conditions, which tend to be more intense at the surface and decrease with depth.

The skewness coefficient is negative for the majority of the NDG results indicating that the data is skewed left, resulting a histogram with a longer left tail (Annex IV). The majority of the kurtosis values are negative indicating a flatter distribution curve for the histogram formed by this results, with an exception for the DC data in the ω_{opt}*-2%* layer. The histograms for this stage presented in Annex IV demonstrate that the distribution of the numerical data varies with the depth of measurement and placing water content.

The highest values of R^2 in this stage were obtained for the DC parameter, reaching values up to 0.9 (Figure 4.6 i)) meaning a very strong correlation between both methodologies for this population. The majority of the lowest R^2 results were obtained for the measurements taken with BSM, Figure 4.6 a),d),g). This results are in accordance with previous works of Neves *et al*. (2013), (Figure 3.23).

From the comparison between the OVM and NDG results (Figures 4.6 e)f)g)) it is possible to perceive that both methodologies present very weak to strong correlations, being the ω_{opt}-2% populations the one that presents the highest values of R^2 (0.57-0.61).

This correlation between methodologies had an inversely proportional relation with the depth of the NDG measurements and water content, since the populations ω_{opt}+2% presented the lower values of R^2, and the ω_{opt}-2% and ω_{opt} populations presented in Figure 4.6f) (BSM) had lowest values of R^2, than those from Figure 4.6d) (DM measurement at 0.3m).

A correlation matrix using the Pearson coefficient (*r*) was defined in Table 4.6. Two types of interpretations can be expressed based on the correlation coefficients expressed in this table:

- Correlation between both methodologies, which can be compared with R^2 values presented in Figure 4.6;
- Correlation between the NDG measurements taken at different depths.

Table 4.5- Descriptive statistics for both methodologies obtained with the stage 1 results

		Methodology A			Methodology B											
		γ_{fill} (kN/m^3)	ω_{fill} (%)	DC (%)	γ_{fill} (kN/m^3)				ω_{fill} (%)				DC (%)			
	Depth (m)	0.25	0.25	0.25	0	0.15	0.3	Mean	0	0.15	0.3	Mean	0	0.15	0.3	Mean
ω_{opt}-2 %	Mean	20.89	10.77	100.17	20.85	20.81	20.70	20.76	9.98	9.91	9.98	9.98	100.33	100.46	99.88	100.12
	Median	20.90	10.72	100.33	20.90	20.81	20.74	20.80	10.00	10.20	10.00	10.10	100.61	100.55	100.05	100.37
	Standard Deviation	0.27	0.68	1.21	0.22	0.25	0.25	0.25	0.82	0.68	0.83	0.77	1.13	1.05	1.22	1.15
	Variance	0.07	0.46	1.45	0.05	0.06	0.06	0.06	0.67	0.46	0.68	0.60	1.27	1.11	1.50	1.33
	Minimum	20.30	9.23	96.67	20.48	20.13	20.23	20.14	8.60	8.70	8.50	8.60	97.34	98.26	96.98	96.98
	Maximum	21.30	11.93	101.67	21.24	21.09	21.15	21.11	11.70	10.90	11.80	11.60	101.64	103.23	102.17	102.02
	Kurtosis	-0.28	-0.31	2.04	-0.91	1.26	-0.72	0.41	-0.39	-1.00	0.09	-0.22	0.86	1.49	0.15	1.20
	Skewness coefficient	-0.26	-0.37	-1.21	0.00	-1.07	-0.05	-0.88	0.05	-0.56	-0.11	-0.18	-1.14	0.33	-0.32	-0.98
ω_{opt}%	Mean	21.46	13.33	102.55	21.23	21.33	21.22	21.25	12.52	12.31	12.50	12.43	101.51	101.81	101.41	101.55
	Median	21.50	13.31	103.23	21.20	21.35	21.24	21.27	12.60	12.30	12.60	12.50	101.48	102.03	101.57	101.80
	Standard Deviation	0.32	0.41	1.49	0.28	0.23	0.22	0.24	0.46	0.31	0.37	0.35	1.14	1.21	0.99	1.01
	Variance	0.10	0.17	2.21	0.08	0.05	0.05	0.06	0.21	0.09	0.13	0.12	1.30	1.46	0.97	1.03
	Minimum	20.70	12.59	99.86	20.59	20.84	20.74	20.65	11.50	11.80	11.70	11.70	99.62	98.99	99.52	99.62
	Maximum	22.00	14.43	105.16	21.67	21.69	21.51	21.58	13.20	12.90	13.00	13.00	104.29	103.63	103.24	103.34
	Kurtosis	-0.39	0.45	-1.30	-0.38	-0.15	-0.29	0.52	-0.50	-0.84	-0.30	-0.78	-0.01	-0.16	-1.02	-0.71
	Skewness coefficient	-0.42	0.63	-0.13	-0.32	-0.30	-0.72	-0.88	-0.34	0.09	-0.74	-0.52	0.28	-0.63	-0.06	-0.40
ω_{opt}+2 %	Mean	21.77	15.78	102.04	21.62	21.75	21.65	21.67	14.82	14.79	14.79	14.80	101.33	101.97	101.51	101.60
	Median	21.80	15.78	102.43	21.68	21.78	21.71	21.74	14.80	14.80	14.70	14.80	101.50	102.32	102.07	101.87
	Standard Deviation	0.26	0.52	1.53	0.26	0.30	0.25	0.25	0.35	0.31	0.38	0.29	1.44	1.66	1.52	1.45
	Variance	0.07	0.27	2.33	0.07	0.09	0.06	0.06	0.12	0.10	0.14	0.08	2.08	2.76	2.31	2.10
	Minimum	21.20	14.93	99.18	21.06	21.19	21.19	21.24	14.10	14.20	13.90	14.20	98.09	98.13	98.04	98.60
	Maximum	22.20	16.78	104.42	22.12	22.35	22.13	22.13	15.40	15.30	15.40	15.20	104.05	105.13	103.51	104.09
	Kurtosis	-0.53	-0.79	-0.81	-0.52	-0.49	-0.48	-0.72	-0.73	-1.12	-0.23	-0.78	-0.08	-0.29	-0.35	-0.52
	Skewness coefficient	-0.34	0.12	-0.61	-0.30	0.03	-0.37	-0.21	-0.15	-0.17	-0.01	-0.18	-0.40	-0.36	-0.85	-0.56

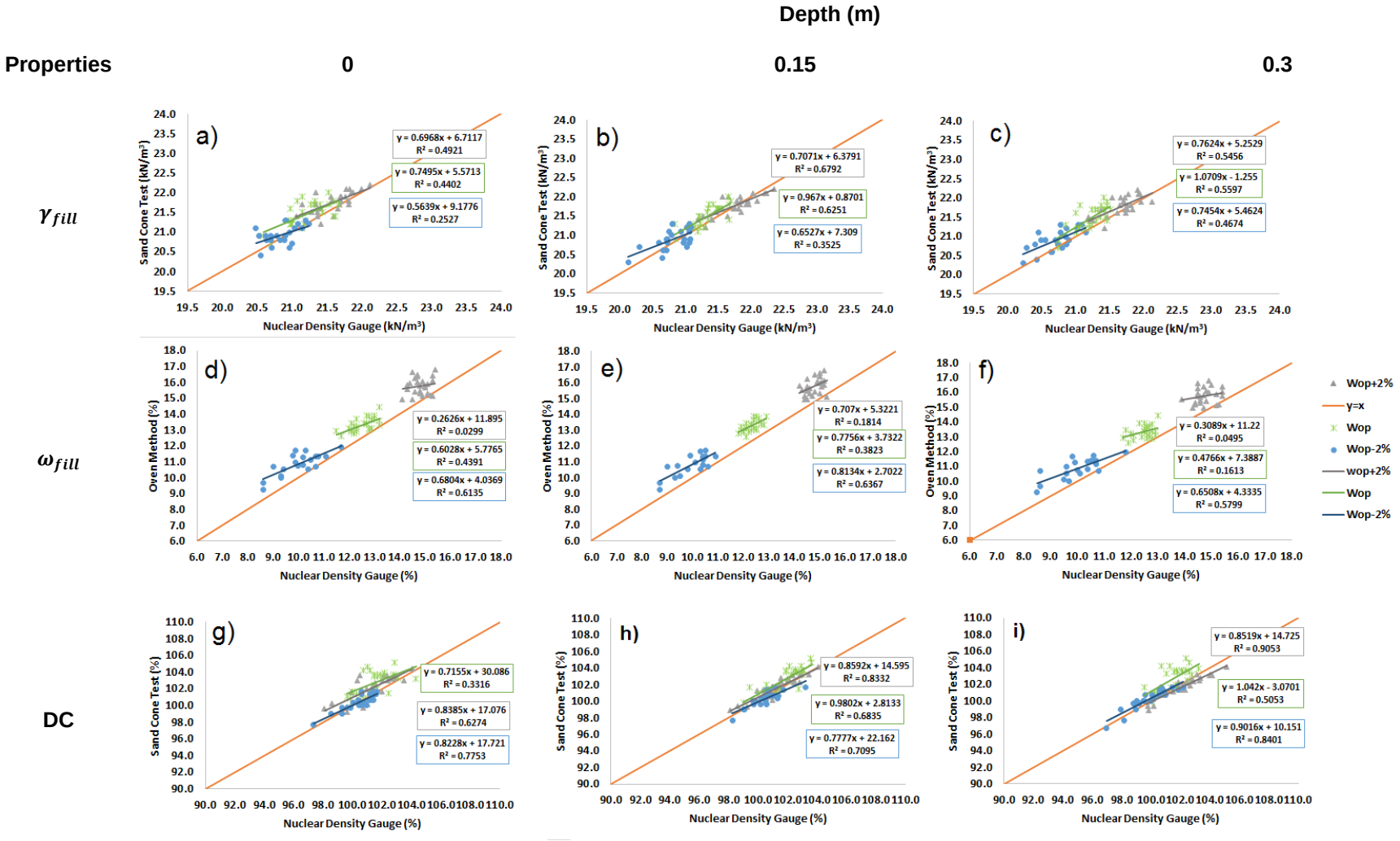

Figure 4.6 – Scattergrams for the $\gamma_{fill}, \omega_{fill}$, and DC parameters obtained with the first analysis, for stage 1 results

Table 4.6 - Correlation matrix for the results from the first analysis that were applied to stage 1 data, considering the measurements taken at different depths, and different placing water contents as individual populations

	Depth (m)	γ_{fill}				ω_{fill}				DC			
		0	0.15	0.3	SC	0	0.15	0.3	SC	0	0.15	0.3	SC
ω_{opt}-2%	0		0.44	0.77	0.50		0.94	0.92	0.80		0.67	0.70	0.86
	0.15	0.44		0.75	0.60	0.94		0.87	0.82	0.67		0.75	0.84
	0.3	0.77	0.75		0.69	0.92	0.87		0.77	0.70	0.75		0.91
	SC	0.50	0.60	0.69		0.80	0.82	0.77		0.86	0.84	0.91	
ω_{opt}%	0		0.69	0.75	0.60		0.56	0.67	0.56		0.67	0.66	0.51
	0.15	0.69		0.77	0.78	0.56		0.46	0.26	0.67		0.78	0.82
	0.3	0.75	0.77		0.75	0.67	0.46		0.32	0.66	0.78		0.72
	SC	0.60	0.78	0.75		0.56	0.26	0.32		0.51	0.82	0.72	
ω_{opt}+2%	0		0.70	0.67	0.69		0.47	0.57	0.16		0.79	0.78	0.79
	0.15	0.70		0.87	0.81	0.47		0.59	0.43	0.79		0.91	0.87
	0.3	0.67	0.87		0.73	0.57	0.59		0.21	0.78	0.91		0.84
	SC	0.69	0.81	0.73		0.16	0.43	0.21		0.79	0.87	0.84	

Relatively to the first type of interpretation, the majority of the correlations coefficients between both methodologies expressed in Table 4.6 represented moderate to very strong correlations (0.5-0.9) for the γ_{fill} and DC. The *r* values for the w_{fill} indicate strong to very strong correlations (0.77-0.82) for the layer compacted with ω_{opt}-2%; moderate to weak (0.32-0.67) for the ω_{opt}% layer; and moderate to very weak (0.43-0.16) for ω_{opt}+2% layer.

The majority of the values presented in Table 4.6 seem to attest the R^2 results since the correlation coefficients between both methodologies tend to be higher for the DC parameter, and the correlations for the ω_{fill} parameter decrease with an increase of water content.

For γ_{fill} and DC, the correlation between both methodologies increased with the depth of measurement (Table 4.6). These results should be expected since the hole from the SCT test reached a depth of 0.25 m, and therefore the best correlations should be achieved for those NDG measurements taken at similar depths. Another aspect that can contribute to this result is the use of a sheepsfoot of roller during the construction of the first stage layers, when a soil is compacted with this type of equipment the lugs from the sheepsfoot rollers penetrate the soils compacting the layer from bottom to top, however this type of rollers are not able to compact the superficial zone of the layer (firsts 0.05-0.06 m), which may explain these lower correlation for the measurements taken with the DM correlations.

The correlations between NDG measurements for the γ_{fill} and DC parameters, have a tendency to be higher for results measured at the depths of 0.15 and 0.3m (DM) than with those measured at the surface (BSM). These correlations coefficients between the results from the measurements taken with the DM express strong to very strong correlations (0.75-0.91). This pattern should be expected since the results from the 0.15 and 0.3m measurements were obtained with the DM and superficial measurements were taken with BSM mode. As explained in Section 3.6.1.2 , this method have significant differences and the BSM only reaches a depth of 0.1 m, as explained in the previous

paragraph the type of roller may have influenced this results. However this tendency cannot be evinced for the ω_{fill} parameter.

From the results presented in Figure 4.6, it can be noted that γ_{fill} and DC parameters have similar behaviours. This should be excepted since the DC results are calculated through Equation 3.27 and therefore dependent on the γ_{fill} results.

As stated in section 4.5.3, a second analysis was established by considering all the measurements taken at different depths and placing water contents as one population. The scatterings and the correlations coefficients between both methodologies for all the control parameters are defined in Figure 4.7 and Table 4.7.

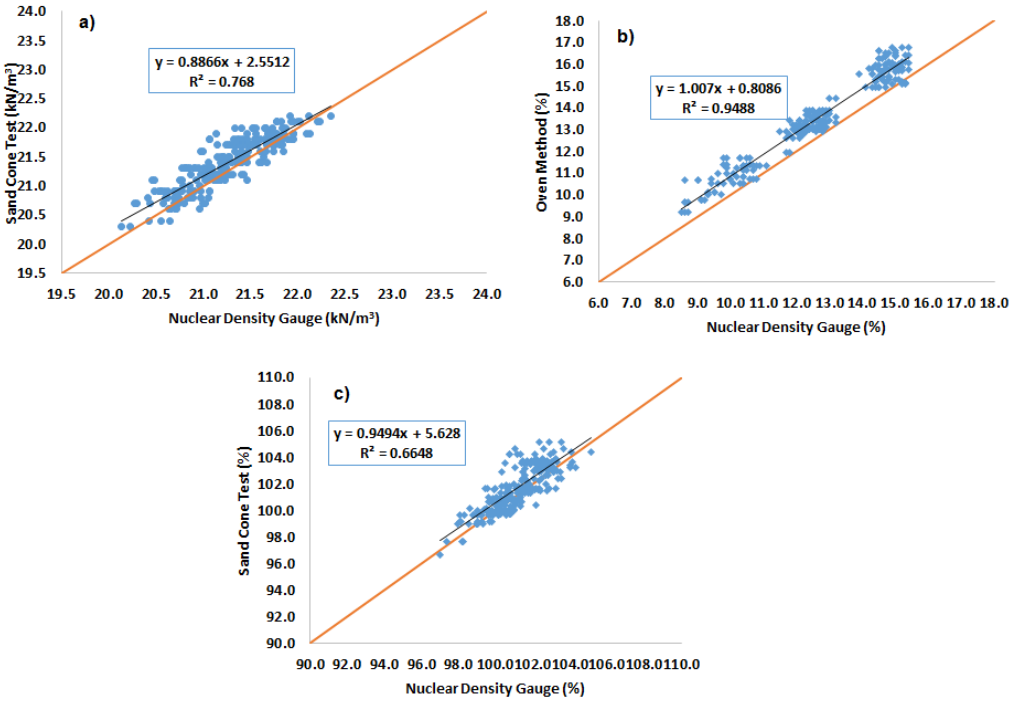

a)γ_{fill}; b) ω_{fill}; c) DC

Figure 4.7 - Scattering for the second analysis of stage 1, considering all the measurements taken at different depths and placing water contents as one population

The purpose of this analysis was to improve the correlations between both methodologies, by considering all the measurements, taken at different depths and water contents as one population. This purpose was fulfilled since all R^2 and *r* values were higher to those obtained in the first analysis, indicating strong to very strong correlations between both methodologies. This increase of correlation had particular incidence for the ω_{fill} parameter (R^2-0.95, Pearson coefficient- 0.97). The correlation coefficients obtained with this analysis indicate very strong correlations between both methodologies for all the compaction parameters, (Table 4.7). The R^2 values obtained for ω_{fill}, this results are in accordance with those expressed in the works of Berney IV et al. (2011).

Table 4.7- Correlation coefficients for the results of the second analysis that was applied to stage 1 data, considering all the measurements taken at different depths and placing water contents as one population

γ_{fill}	0.87
ω_{fill}	0.97
DC	0.82

However, this type of analysis may not be representative, since the populations represented in the scattergrams are defined by grouping three populations into one forming a new population with a larger range of values, which contributes to an increase of correlation. As defined by Howell (2014) the correlation coefficients can be affected by the presence of heterogeneous populations, non-linearity and range restrictions, resulting in overestimated correlations.

This limitation may had a particular significance for the results obtained with the ω_{fill} parameter, since it is possible to identify three distinct populations (each one restricted for a placing water content) with gaps in their distribution. In his works Berney IV et al. (2011) also used a considerable range of water contents, in which three distinct populations can be identified (Figure 3.21) as in this work, this fact could explain the similarities between both works.

The third analysis was defined by grouping all the results from the direct method measurements taken with the NDG into one population, and comparing them with those from methodology A. The scatterings and correlation coefficient from this analysis for each control parameter are illustrated in Figure 4.8 and Table 4.8 respectively.

As in the second analysis, the R^2 (γ_{fill}: 0.81; ω_{fill}: 0.95; DC: 0.72) and *r* (γ_{fill}: 0.9; ω_{fill}: 0.98; DC: 0.85), increased considerably when compared with those from the first analysis, indicating strong to very strong correlations between both methodologies for all the parameters. However, these results were slightly higher in this analysis indicating that the NDG measurements taken with the DM had higher correlations with the SCT than with those from the BSM, corroborating the conclusions from the first analysis, in which was stated that the correlation between both methodologies increased with the depth of the NDG measurement.

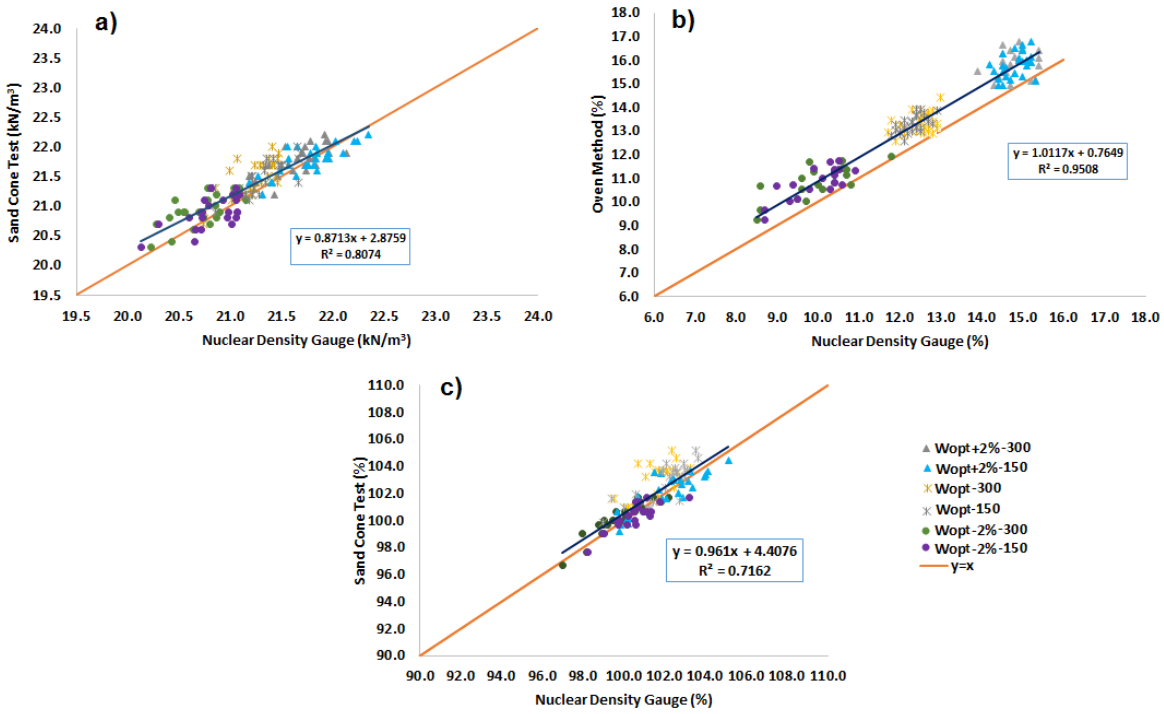

a)γ_{fill}; b) ω_{fill}; c) DC

Figure 4.8 - Scattering for the third analysis of stage 1, considering the NDG results taken with the DM as one population

Table 4.8 - Correlation coefficients for the third analysis of stage 1, considering the NDG results as one population

γ_{fill}	0.90
ω_{fill}	0.98
DC	0.85

4.5.4.2. COMPARISON BETWEEN SCT AND NDG RESULTS FOR STAGE 2

The three layers constructed during the second stage were composed by arkosic materials (SC) and compacted with a smooth wheel roller, the control operations were carried out between 26 of April and 11 of May of 2007. The descriptive statistics from the results obtained by both methodologies are described in Table 4.9, the histograms from the variables defined in this stage are defined in Annex IV.

As in the previous stage, the parameters of central tendency mean and median are higher for methodology A, and this behaviour can also be confirmed by the graphics presented in Figure 4.9 since the majority of methodology A measurements are above the EL.

In terms of dispersion, a distinctive pattern cannot be identified when comparing the results from both methodologies. However when comparing only the standard deviation and variance for the nuclear gauge measurements taken at different depths, it is evident that the results from the superficial measurements (BSM) have greater dispersion than those taken at 0.15 and 0.3 m, with an exception of the ω_{fill} measurements taken in the layer compacted with a ω_{opt}%. As explained in Section 4.5.4.1,

these results may be justified by variations in the soil water content caused by climatic conditions which are more frequent at the surface of the fill.

As verified for the dispersion, a distinctive pattern cannot be identified for the skewness coefficient and kurtosis, showing that the type of data distribution varies with each parameter and placing water content. As can be demonstrated by the histograms in Annex IV, it is not possible to identify a predominant type of distribution for the numerical data.

The R^2 values obtained with this analysis and presented in the graphics from Figure 4.9 range between 0 and 0.51 indicating very weak to weak correlations between both methodologies for all the populations represented in the graphics, being the highest correlation achieved for the γ_{fill} and DC parameters. The correlation matrix for the data presented in this stage is defined in Table 4.10, and as the R^2 and the *r* coefficients demonstrate that the DC parameter presented the highest correlation coefficients, which indicate moderate to strong correlations. The ω_{fill}, correlations increase with an increase of water content being the highest correlation factors reached for the $\omega_{opt} + 2\%$ layer (0.42-0.56), this behaviour is goes against what was observed in stage 1, in which an increase of water content resulted in lower correlations.

In this stage in opposite to what was observed in stage 1, it is impossible to identify a correlation pattern between both methodologies for the γ_{fill} and DC parameters. In some cases the correlations are higher for the NDG measurements taken with BSM and, in others, for those obtained at the depth of 0.3 m. This difference relatively to stage 1 may be explained by the use of the smooth wheel roller as compaction equipment, since this type of equipment compacts the soil by adding pressure to the top of the layer (top to bottom compaction) without causing any disturbance in the superficial zone of the layer, as it is common for the sheepsfoot roller.

This variability of the correlations can also be verified between NDG measurements taken at different depths, since instead of having an evident tendency for higher correlations between DM results as in stage 1, the highest correlations in this stage can be achieved between the results from the measurements taken with BSM method or between those taken at the depth of 0.3 m.

Table 4.9-Descriptive statistics for both methodologies obtained with the stage 2 results

		Methodology A			Methodology B											
		γ_{fill} (kN/m^3)	ω_{fill} (%)	DC (%)	γ_{fill} (kN/m^3)				ω_{fill} (%)				DC (%)			
ω_{opt}-2 %	Depth (m)	0.25	0.25	0.25	0	0.15	0.3	Mean	0	0.15	0.3	Mean	0	0.15	0.3	Mean
	Mean	21.82	11.07	102.38	21.46	21.50	21.27	21.40	10.79	10.86	10.90	10.84	100.76	101.07	100.00	100.57
	Median	21.90	11.10	102.56	21.42	21.47	21.25	21.39	10.80	10.90	10.90	10.80	100.59	100.94	99.93	100.61
	Standard Deviation	0.20	0.23	1.01	0.22	0.18	0.18	0.18	0.40	0.32	0.30	0.28	1.05	0.87	0.98	0.93
	Variance	0.04	0.05	1.07	0.05	0.04	0.03	0.03	0.17	0.11	0.09	0.08	1.16	0.79	0.99	0.90
	Minimum	21.30	10.70	100.09	20.99	21.17	20.97	20.98	10.10	10.30	10.20	10.30	98.64	99.44	98.50	98.59
	Maximum	22.10	11.60	104.20	21.90	21.84	21.68	21.73	11.70	11.60	11.40	11.50	102.87	102.68	102.35	102.33
	Kurtosis	0.35	-0.17	-0.15	-0.22	-0.72	-0.40	-0.10	-0.34	-0.59	-0.07	-0.39	-0.18	-0.57	0.14	-0.30
	Skewness coefficient	-0.84	0.36	-0.54	-0.17	0.04	0.41	-0.07	0.05	0.19	-0.34	0.12	-0.07	0.06	0.54	0.03
ω_{opt}%	Mean	22.05	13.83	105.08	21.47	21.46	21.30	21.41	12.28	12.24	12.35	12.30	102.34	102.27	101.51	102.04
	Median	22.10	13.80	105.11	21.48	21.45	21.28	21.38	12.20	12.10	12.20	12.20	102.37	102.04	101.42	102.02
	Standard Deviation	0.16	0.36	1.23	0.15	0.13	0.14	0.09	0.49	0.56	0.57	0.50	0.92	0.93	0.92	0.77
	Variance	0.03	0.13	1.58	0.02	0.02	0.02	0.01	0.25	0.32	0.33	0.26	0.89	0.91	0.88	0.62
	Minimum	21.70	13.30	102.41	21.18	21.27	21.10	21.24	11.50	11.40	11.30	11.40	99.95	100.85	99.91	100.80
	Maximum	22.30	14.70	107.42	21.85	21.78	21.68	21.59	13.50	13.20	13.50	13.30	104.10	104.29	104.43	104.00
	Kurtosis	-0.85	0.12	-0.18	0.55	-0.09	0.75	-0.68	0.17	-1.33	-0.73	-0.58	0.34	-0.74	3.29	0.36
	Skewness coefficient	-0.32	0.70	-0.04	0.32	0.53	0.66	-0.07	0.63	0.24	0.17	0.46	-0.39	0.57	1.40	0.58
ω_{opt}+2 %	Mean	21.77	15.50	103.09	21.31	21.38	21.31	21.33	13.52	13.55	13.57	13.57	100.77	101.30	100.86	100.97
	Median	21.80	15.48	102.79	21.29	21.42	21.31	21.31	13.50	13.55	13.60	13.50	100.38	101.14	101.02	101.00
	Standard Deviation	0.16	0.39	1.44	0.17	0.15	0.15	0.15	0.38	0.25	0.29	0.28	1.43	1.30	1.24	1.25
	Variance	0.03	0.15	2.18	0.03	0.02	0.02	0.02	0.15	0.07	0.09	0.08	2.13	1.76	1.61	1.64
	Minimum	21.50	14.69	101.55	21.02	21.04	21.00	20.95	12.70	13.00	13.00	13.10	98.25	99.29	98.83	98.88
	Maximum	22.00	16.31	106.33	21.63	21.62	21.62	21.52	14.30	14.10	14.20	14.20	103.85	103.32	102.79	103.32
	Kurtosis	-0.90	-0.52	-0.65	-1.11	-0.37	-0.22	-0.28	0.19	0.45	-0.59	-0.31	-0.33	-1.40	-1.37	-0.98
	Skewness coefficient	-0.33	-0.07	0.76	0.28	-0.64	-0.11	-0.58	-0.04	0.27	0.08	0.60	0.46	0.09	-0.31	0.08

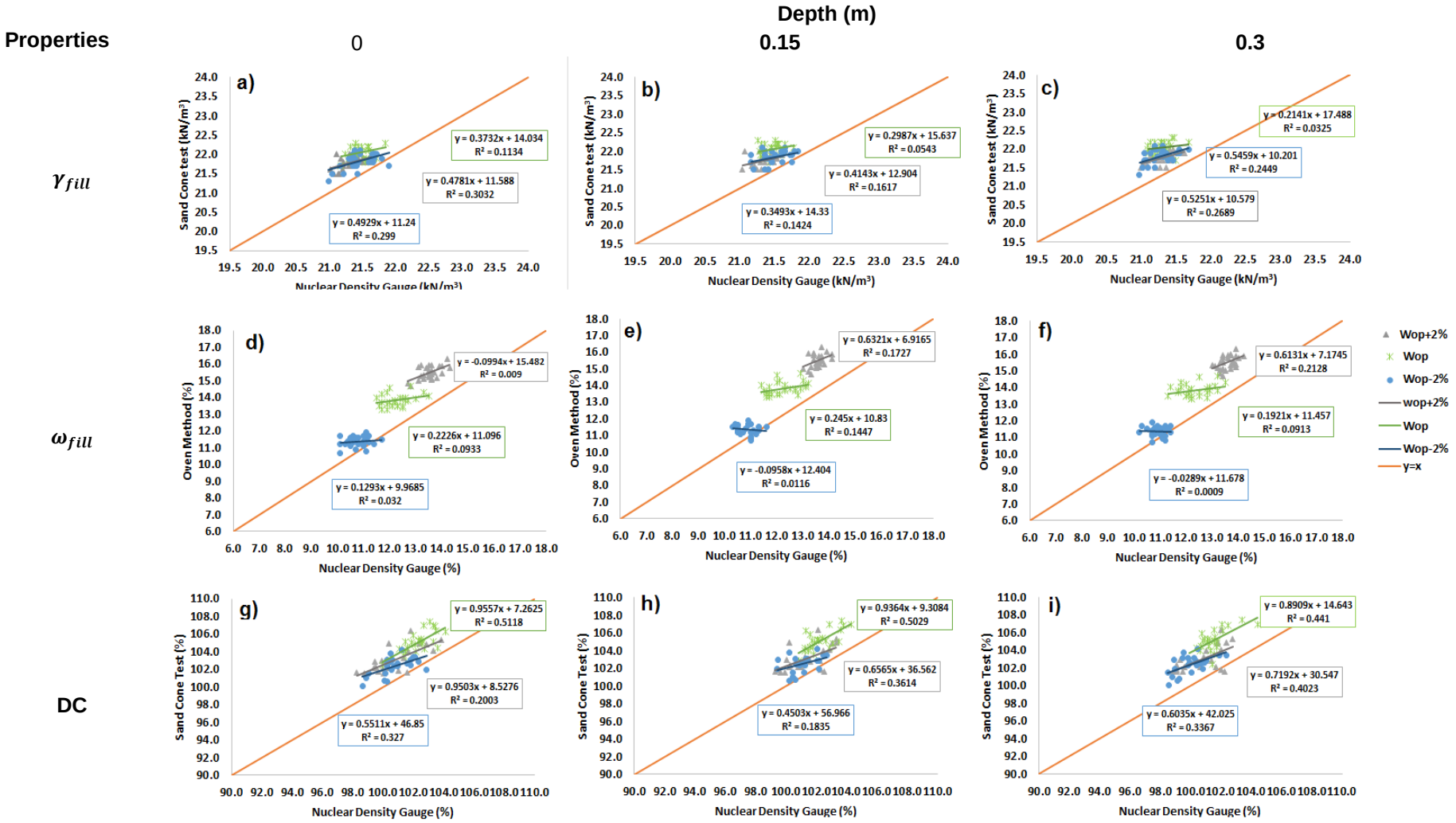

Figure 4.9 - Scattergrams for the $\gamma_{fill}, \omega_{fill}$, and DC parameters obtained with the first analysis, for stage 2 results

Table 4.10- Correlation matrix for the results from the first analysis that were applied to stage 2 data, considering the measurements taken at different depths, and different placing water contents as individual populations

	Depth (m)	γ_{fill}				ω_{fill}				DC			
		0	0.15	0.3	SC	0	0.15	0.3	SC	0	0.15	0.3	SC
ω_{opt}-2%	0		0.53	0.84	0.55		0.48	0.63	0.18		0.59	0.85	0.57
	0.15	0.53		0.76	0.38	0.48		0.68	-0.11	0.59		0.81	0.43
	0.3	0.84	0.76		0.50	0.63	0.68		-0.03	0.85	0.81		0.58
	SC	0.55	0.38	0.50		0.18	-0.11	-0.03		0.57	0.43	0.58	
ω_{opt}%	0		-0.02	-0.04	0.34		0.78	0.79	0.31		0.49	0.44	0.72
	0.15	-0.02		0.38	0.23	0.78		0.75	0.38	0.49		0.71	0.71
	0.3	-0.04	0.38		0.18	0.79	0.75		0.30	0.44	0.71		0.66
	SC	0.34	0.23	0.18		0.31	0.38	0.30		0.72	0.71	0.66	
ω_{opt}+2%	0		0.74	0.42	0.55		0.55	0.58	0.58		0.85	0.80	0.71
	0.15	0.74		0.62	0.40	0.55		0.42	0.42	0.85		0.87	0.60
	0.3	0.42	0.62		0.52	0.58	0.42		0.46	0.80	0.87		0.63
	SC	0.55	0.40	0.52		0.58	0.42	0.46		0.71	0.60	0.63	

The scatterings and the correlations coefficients between both methodologies from the second analysis are defined in Figure 4.10 and Table 4.11.

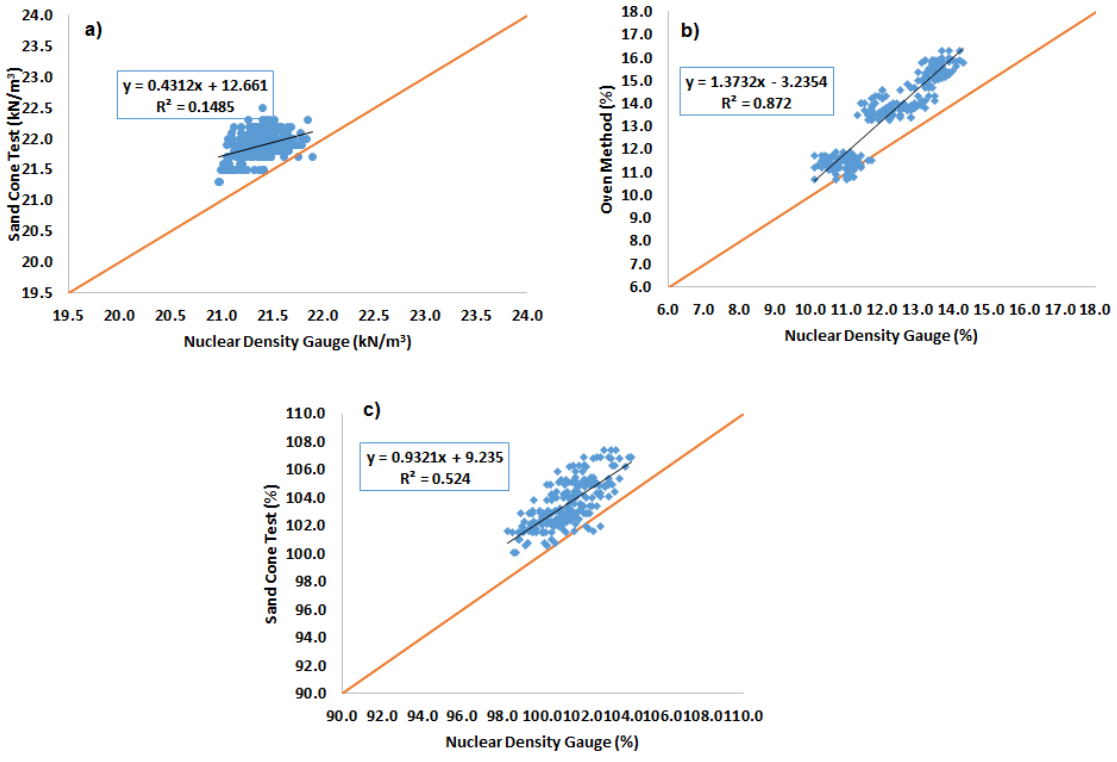

a)γ_{fill}; b) ω_{fill}; c) DC

Figure 4.10- Scattering for the second analysis of stage 2, considering all the measurements taken at different depths and placing water contents as one population

As can be observed from Figure 4.10, the R^2 values when compared with the overall results presented in the first analysis, increased considerably for the ω_{fill} (0.84) and DC (0.52) parameters, and decreased for the γ_{fill}. This decrease may be associated to the fact that all the γ_{fill} populations from the DM have short and similar ranges, therefore the new point cloud formed with this analysis is not composed by a wider range of γ_{fill} values, but by a larger population with higher dispersion and the same range of values, leading to lower values of R^2.

This behaviour is also expressed by the Pearson coefficients presented in Table 4.11, which indicate weak correlations (0.38) for the γ_{fill}, very strong (0.94) for the ω_{fill}, and strong for the DC (0.71). Although this analysis can be used to improve the correlations for ω_{fill} and DC parameters it has some limitations as expressed in Section 4.5.4.1.

Table 4.11-Correlation coefficient for the results of the second analysis that was applied to stage 2 data, considering all the measurements taken at different depths and placing water contents as one population

$\boldsymbol{\gamma_{fill}}$	0.38
$\boldsymbol{\omega_{fill}}$	0.94
DC	0.71

The scattergrams and correlations coefficients for the third analysis are represented in Figure 4.11 and Table 4.12. As in the previous analysis when the results from this analysis are compared with those obtained in the first analysis, it can be observed that the correlations coefficients (R^2 and r) increased considerably for the ω_{fill} (R^2: 0.87, *r:* 0.93*)* and DC (R^2: 0.46, *r: 0.68),* indicating very strong and moderate/good correlations respectively, and decreased for the γ_{fill} (R^2: 0.10 and *r*: 0.32) which presented very weak/weak correlations.

When this results are compared to those from the second analysis and in contrast to what was seen in stage 1 (Table 4.12), the correlations decreased when only the results the from the DM and SCT are compared. This results should be expected, since in the first analysis it was observed that in some cases the correlations are higher for the NDG measurements taken with BSM and, in other cases, for those obtained at the depth of 0.3 m, which may be linked to the use of a smooth wheel roller.

As stated in Section 4.5.4.1, the results from the second and third analysis might have some limitations due to the use of heterogeneous populations.

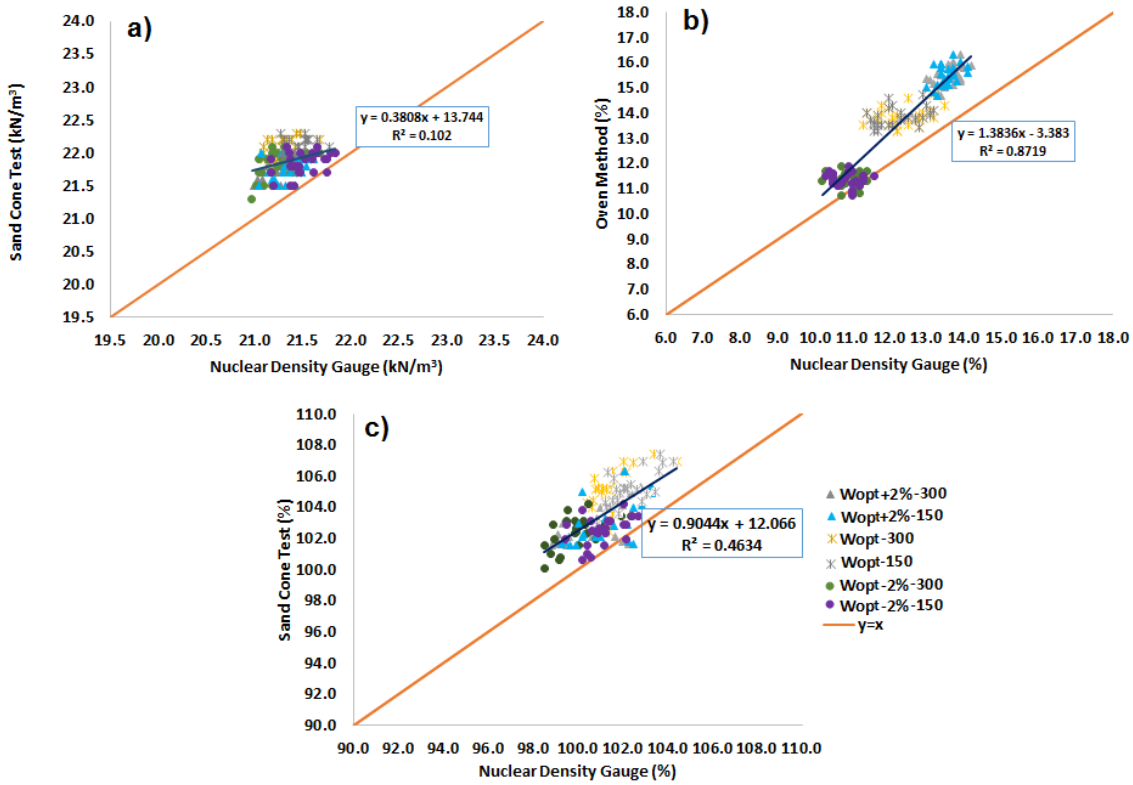

a)γ_{fill}; b) ω_{fill}; c) DC

Figure 4.11 - Scattering for the third analysis of stage 2, considering the NDG results taken with the DM as one population

Table 4.12 - Correlation coefficients for the third analysis of stage 2, considering the NDG results as one population

γ_{fill}	0.32
ω_{fill}	0.93
DC	0.68

4.5.4.3. COMPARISON BETWEEN SCT AND NDG RESULTS FOR STAGE 3

Stage 3 layers were constructed with alluvium materials (SC to GW-GC) and compacted with a smooth wheel roller, the control operations were carried out between 18 and 31 of May 2007. The data was analysed using the same procedures that were presented at the previous stages. The descriptive statistics of the results obtained by both methodologies and the results from the first analysis are described in Table 4.13. The histograms from the variables defined in this stage are defined in Annex IV.

As mentioned in the previous stages, methodology A results tend to be higher to those obtained with methodology B, since the parameters of central tendency, mean and median, are higher for the first.

This aspect can be enhanced by analyzing Figure 4.12 graphics, in which the majority of the points (SCT, NDG) presented in the graphics are above the line defined by the EL.

The results from this stage presented higher dispersion than the previous stages, which may be associated with equipment limitations when applied to coarser grained materials (Section 3.6.1.2), such as those used in this stage, since the samples retrieved during the prospection works were characterized between clayey sands (SC) and well graded gravels wit clay (GW-GC), (Section 4.4.1).

As for the second stage, a distinctive pattern cannot be identified for the skewness coefficient and kurtosis, showing the variability of the data distribution, as can be demonstrated by the histograms in Annex IV.

In this stage the γ_{fill} and DC results did not present a similar behaviour, in particular for the layers compacted with a placing water content of ω_{opt}-2% and ω_{opt}+2%. As can be seen in Figure 4.12 a), b) and c), the point cloud formed by the w_{opt}-2% population has the lowest values γ_{fill} for both methodologies. However, the DC results for the same population are the highest. This contradicts the results from stage 1 and 2, and may also be associated with the type of material used in this stage.

In the comparison between both methodologies for the ω_{fill} parameter, the results are considerably higher for the OVM. When this result are compared with those from stage 1 and 2 it can be observed that the difference between both methodologies is higher in this stage, since in the first stages all the ω_{fill} populations were near the EL. This behaviour may also be associated to the limitation of the NDG when applied to coarse grained materials, which may had led to an underestimation of the ω_{fill} value. R^2 values in Figure 4.12 indicate weak to very weak correlations (0-0.36). The matrix of correlations is defined in the Table 4.14.

From the results expressed in Table 4.14, it can be perceived that both methodologies presented weak to moderate correlations, being the highest ones achieved for the results of DC and γ_{fill} measurements taken at the surface and 0.3m of depth, in the layers compacted with a ω_{opt}-2% and $\omega_{opt} + 2\%$. The correlation between both methodologies for the γ_{fill} and ω_{fill} was directly proportional to an increase of water content.

As in the first stage, the highest correlation coefficients were obtained between nuclear gauge measurements taken with the DM, reaching values up to 0.9, representing very strong correlations.

The results for the second analysis are displayed in Figure 4.13 and Table 4.15. In contrast with what was observed in the last stages, the correlations did not improve considerably with this analysis due to the higher dispersion of the results that was obtained for the alluvial materials, being very weak for the γ_{fill} (R^2: 0; *r*: -0.02), and weak for the ω_{fill} (R^2: 0.17; *r:* 0.41) and DC(R^2: 0.14; *r*: 0.37).

Table 4.13 - Descriptive statistics for both methodologies obtained with the stage 3 results

		Methodology A			Methodology B											
		γ_{fill} (kN/m³)	ω_{fill} (%)	DC (%)	γ_{fill} (kN/m³)				ω_{fill} (%)				DC (%)			
	Depth (m)	0.30	0.30	0.30	0	0.15	0.3	Mean	0	0.15	0.3	Mean	0	0.15	0.3	Mean
ω_{opt}-2 %	Mean	21.72	10.72	102.22	20.32	20.94	21.05	20.78	8.33	8.35	8.15	8.34	96.77	99.54	100.02	98.78
	Median	21.70	10.41	102.52	20.33	20.99	21.05	20.82	8.40	8.30	8.40	8.50	96.96	99.46	99.86	98.91
	Standard Deviation	0.40	0.81	1.62	0.34	0.33	0.30	0.30	0.60	0.45	0.68	0.47	2.22	1.65	1.59	1.69
	Variance	0.16	0.65	2.63	0.12	0.11	0.09	0.09	0.36	0.20	0.46	0.22	4.94	2.72	2.52	2.84
	Minimum	21.00	9.63	97.89	19.75	20.34	20.49	20.27	6.90	7.40	6.50	7.30	92.80	96.92	96.07	95.26
	Maximum	22.60	12.20	103.85	21.14	21.69	21.55	21.50	9.50	9.10	9.20	9.00	101.29	103.33	102.67	102.43
	Kurtosis	-0.14	-1.16	1.51	0.02	-0.06	-0.75	-0.09	0.52	-0.41	0.02	-0.64	-0.76	-0.22	0.39	-0.19
	Skewness coefficient	0.46	0.52	-1.37	0.57	-0.08	-0.39	0.17	-0.60	-0.27	-0.65	-0.44	0.03	0.39	-0.45	-0.02
ω_{opt} %	Mean	22.14	11.64	99.33	20.89	21.88	22.05	21.61	8.29	8.07	8.12	8.20	94.24	98.01	98.76	97.14
	Median	22.10	11.60	99.44	20.81	21.82	22.04	21.65	8.35	8.10	8.10	8.20	94.11	97.85	98.58	97.07
	Standard Deviation	0.43	0.32	1.96	0.57	0.53	0.43	0.42	0.48	0.53	0.52	0.43	1.94	2.15	1.85	1.39
	Variance	0.18	0.10	3.86	0.33	0.28	0.19	0.17	0.23	0.28	0.27	0.18	3.77	4.61	3.44	1.94
	Minimum	21.40	11.10	95.56	19.95	20.76	21.38	20.89	7.30	6.70	6.60	7.50	91.50	94.15	95.02	94.71
	Maximum	23.10	12.20	103.33	21.95	22.98	23.10	22.47	9.00	9.00	8.80	8.90	97.66	102.05	103.13	99.66
	Kurtosis	-0.20	-1.23	-0.05	-0.89	-0.23	-0.18	-0.64	-0.42	0.19	1.46	-0.99	-0.83	-0.62	-0.03	-0.83
	Skewness coefficient	0.18	0.01	0.18	0.16	-0.22	0.38	0.05	-0.51	-0.61	-0.92	-0.19	0.51	0.05	0.29	0.12
ω_{opt}+2 %	Mean	22.29	12.79	100.77	21.60	22.13	22.17	21.99	9.76	9.92	9.67	9.81	97.50	99.72	99.79	99.08
	Median	22.30	12.80	101.00	21.63	22.09	22.19	21.98	9.70	9.95	9.80	9.85	97.30	99.95	99.90	98.87
	Standard Deviation	0.36	0.41	2.02	0.53	0.38	0.43	0.36	0.92	0.66	0.78	0.71	1.87	1.62	1.65	1.48
	Variance	0.13	0.16	4.08	0.29	0.14	0.19	0.13	0.84	0.43	0.61	0.50	3.49	2.61	2.73	2.18
	Minimum	21.30	11.85	97.20	19.78	21.12	21.14	21.30	7.90	8.70	7.80	8.70	94.10	94.50	94.60	95.30
	Maximum	22.80	13.48	105.00	22.40	22.87	22.94	22.66	11.50	11.30	11.10	11.20	101.10	102.60	102.90	101.63
	Kurtosis	0.81	-0.03	-0.12	4.57	1.10	0.06	-0.49	-0.42	-0.14	-0.05	-0.46	-0.57	3.44	3.26	0.63
	Skewness coefficient	-0.85	-0.39	0.22	-1.52	-0.39	-0.25	0.09	0.24	0.15	-0.37	0.30	0.00	-1.09	-1.11	-0.33

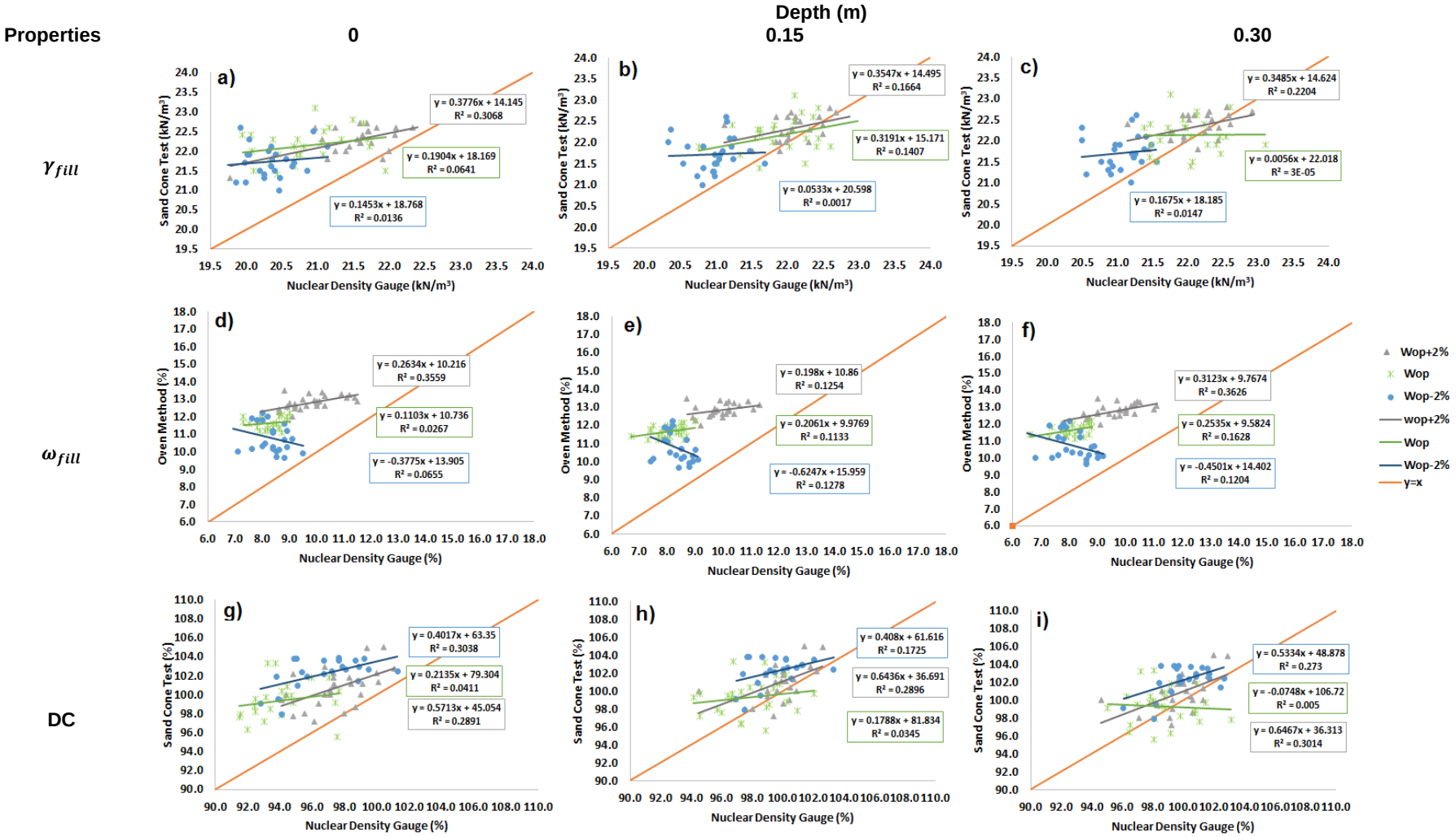

Figure 4.12 - Scattergrams for the $\gamma_{fill}, \omega_{fill}$, and DC parameters obtained with the first analysis, for stage 3 results

Table 4.14- Correlation matrix for the results of the first analysis that were applied to stage 3 data, considering the measurements taken at different depths and with different placing water contents as individual populations

	Depth (m)	γ_{fill}				ω_{fill}				DC			
		0	0.15	0.3	SC	0	0.15	0.3	SC	0	0.15	0.3	SC
ω_{opt}-2%	0		0.50	0.48	0.12		0.75	0.83	-0.26		0.77	0.75	0.55
	0.15	0.50		0.86	0.04	0.75		0.90	-0.36	0.77		0.86	0.42
	0.3	0.48	0.86		0.12	0.83	0.90		-0.35	0.75	0.86		0.52
	SC	0.12	0.04	0.12		-0.26	-0.36	-0.35		0.55	0.42	0.52	
ω_{opt}%	0		0.56	0.28	0.25		0.77	0.73	0.16		0.41	0.00	0.20
	0.15	0.56		0.65	0.38	0.77		0.94	0.34	0.41		0.59	0.19
	0.3	0.28	0.65		0.01	0.73	0.94		0.40	0.00	0.59		-0.07
	SC	0.25	0.38	0.01		0.16	0.34	0.40		0.20	0.19	-0.07	
ω_{opt}+2%	0		0.50	0.44	0.55		0.85	0.87	0.60		0.48	0.45	0.54
	0.15	0.50		0.93	0.41	0.85		0.86	0.35	0.48		0.90	0.54
	0.3	0.44	0.93		0.47	0.87	0.86		0.60	0.45	0.90		0.55
	SC	0.55	0.41	0.47		0.60	0.35	0.60		0.54	0.54	0.55	

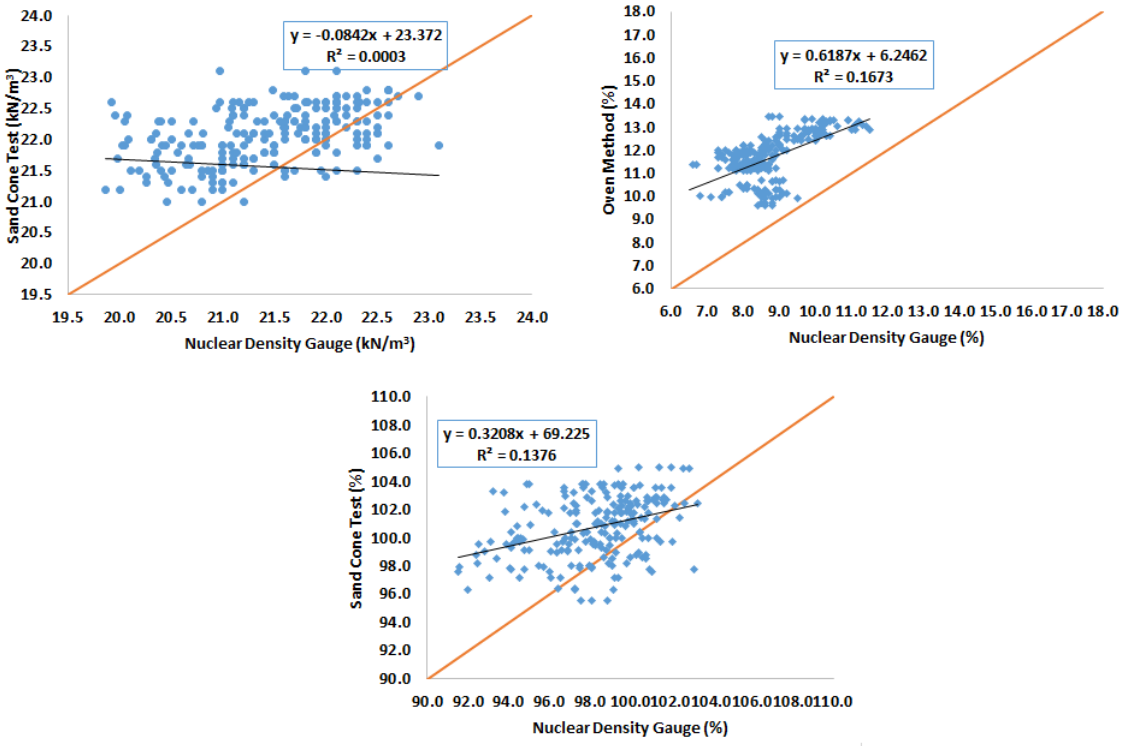

Figure 4.13 Scattering for the second analysis of stage 3, considering all the measurements taken at different depths and placing water contents as one population

Table 4.15- Correlation coefficients for the results of the second analysis that was applied to stage 3 data, considering all the measurements taken at different depths and placing water contents as one population

γ_{fill}	-0.02
ω_{fill}	0.41
DC	0.37

The results from the third analysis are listed in Figure 4.14 and Table 4.16, and show that this analysis did not led to any significant changes, when compared with the overall results from the first analysis, since the R^2 values (γ_{fill}: 0.29; ω_{fill}: 0.36; DC: 0.46) and Pearson coefficients (γ_{fill}: 0.55; ω_{fill}: 0.60; DC: 0.43) indicate weak to moderate correlations.

However and as in the first stage, the correlations obtained with this analysis are higher to those obtained from the previous analysis, demonstrating that the measurements taken with the DM presented better correlations with the SCT results than those taken with the BSM.

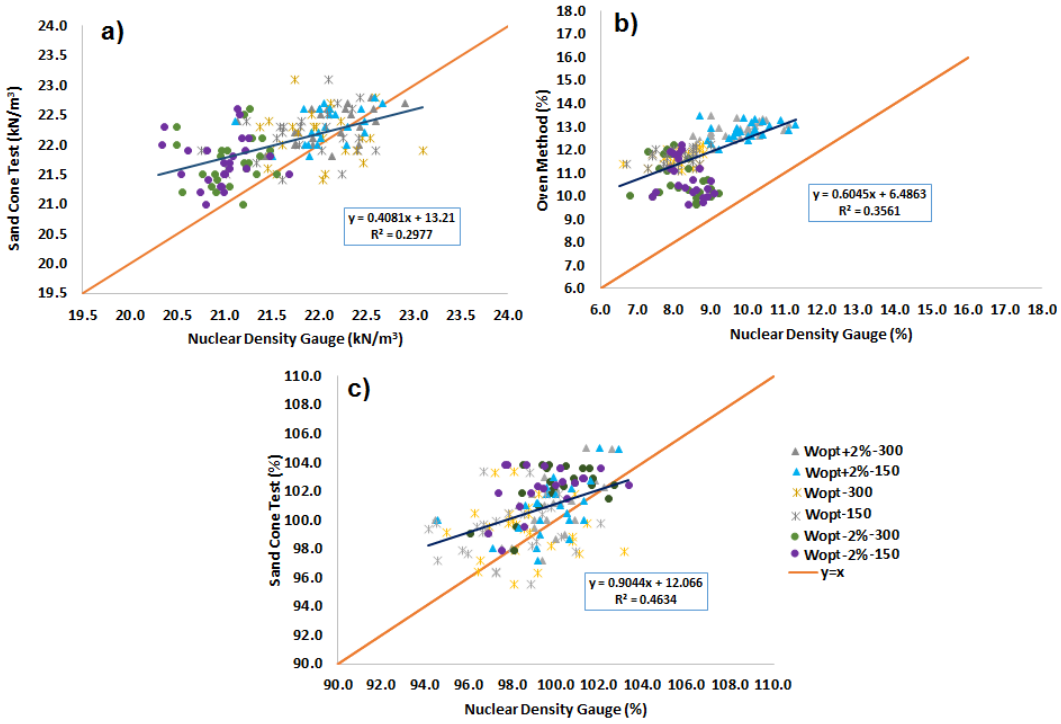

Figure 4.14- Scattering for the third analysis of stage 3, considering the NDG results taken with the DM as one population

Table 4.16 - Correlation coefficients for the third analysis of stage 3, considering the NDG results as one population

γ_{fill}	0.55
ω_{fill}	0.60
DC	0.43

4.5.5. TRIAL EMBANKMENT MAIN CONCLUSIONS

The purpose of the previous sections was to compare the results from the conventional and nuclear methodologies for each one of the trial embankment construction stages, by considering three distinct analyses.

It was observed that methodology A results showed a tendency to be higher to those obtained with the other methodology in all three stages for all the control parameters (Tables 4.5, 4.9 and 4.13). In his

study, Martins (2011) obtained similar results in soils also classified has clayey sands (SC), however it should be considered that his results are only valid for the compaction conditions used.

The results from the third stage presented higher dispersion than the previous stages which may be associated to limitations of the NDG or Hilf method when applied to coarser grained materials, such as those used in this stage (SC to GW-GC)..

The overall R^2 and *r* values obtained with the first analysis were higher for the first stage reaching values up to 0.9 (very strong correlations), however the majority of R^2 values obtained with the analysis in this stage expressed very weak to moderate correlations (Figure 4.6), indicating that both methodologies have substantial differences. In Neves et al., (2013), were obtained similar results for soils also characterized as clayey sands (SC), this authors stated that the differences between both methodologies should be compensated by validating the results for the NDG with the SCT measurements. Maregesi (n.d.) demonstrated that using multiple shift coefficients to calibrate the NDG against the SCT, would improve the R^2 values.

The correlation between methodologies in this stage for the γ_{fill} and DC parameters increased with the depth of measurement, and for the ω_{fill} decreased with an increase of water content (Table 4.6). This increase of correlation with the depth of measurement should be expected, since the SCT reached a depth of 0.25 m, and therefore the best correlations should be achieved for those NDG measurements taken at similar depths (0.3 m).

The correlations between NDG measurements taken at different depths represented in Table 4.6, had a tendency to be higher among those measurements taken at the depths of 0.15 and 0.3 m than with those measured at the surface. This pattern should be expected since the results from the 0.15 and 0.3 m measurements were obtained with the DM, and superficial measurements were taken with BSM mode. However this tendency cannot be evinced for the ω_{fill} parameter. This results are in accordance with those expressed by Neves et al., (2013), which concluded that the measurements taken with the DM were more accurate.

When this analysis was applied to the data from the second stage, the overall R^2 and *r* values decreased (Figure 4.8 and Table 4.10). And it was not possible to identify a correlation pattern between both methodologies, and NDG measurements taken at different depths, as in the first stage.

The results from applying this first analysis to the third stage provided the lowest values of R^2 and *r* graphics, being the highest correlation achieved for the γ_{fill} and DC (Figure 4.12 and Table 4.13). The correlation between both methodologies for the γ_{fill} and ω_{fill} was directly proportional to an increase of water content. As in stage 1, the correlation between NDG measurements taken at different depths had a tendency to be higher between those measurements taken by the DM.

The results from this analysis indicated that the correlation between both methodologies was dependent on the type of material and compaction equipment, since it is not possible to identify a common pattern for the three stages. For example in the first stage, the correlation between both methodologies increased with the depth of measurement for the γ_{fill} and DC parameters, decreased

with an increase of water content and depth of measurement for the ω_{fill}; however this behaviour was not valid for the stage 3 and stage 2 results. Therefore, the results from the construction stages cannot be directly compared between each other since the construction materials and/or compaction equipment differed among stages.

Another possible effect resultant from the variation of compaction equipment that can be observed between stages 1 and 2, is that in the first stage the correlation coefficients between NDG measurements for the γ_{fill} and DC parameters is higher for the DM results, however this pattern cannot be denoted in stage 2. These may be associated with the fact that, in the first stage, it was used a sheepsfoot roller, which produces layers that are not compacted in a superficial zone affecting the measurements taken with the BSM resulting in higher correlations for the DM mode. While in the second stage was used a smooth wheel roller, which compacts the layers by pressure without causing any disturbance in the layer surface and may affect the BSM and DM.

In the first two stages the populations illustrated in the scattergrams presented similar behaviours for the γ_{fill} and DC (Figures 4.6 and 4.9), which can be explained by Equation 3.27, since DC is dependent on the value of γ_{fill}. However, this condition was not valid in stage 3 (Figure 4.12), which may also be associated with limitations of using the NDG or the Hilf method in this type of materials.

When the second analysis was applied to the results from both methodologies, the *r* values increased considerably (comparatively to those from the first stage) for all the parameters in the first stage (Figures 4.7 and Tables 4.7) indicating very strong correlations between both methodologies ((γ_{fill}: 0.9; ω_{fill}: 0.98; DC: 0.85), and for the ω_{fill} and DC in the second stage (Figure 4.10 and Table 4.11) representing strong and very strong correlations respectively (ω_{fill}: 0.94; DC: 0.71).

This improvement in the correlations between both methodologies, relatively to the results from the first analysis, may be explained by the use of populations with larger ranges of values for each control parameter, since in this analysis the three populations defined for each placing water content in the first analysis, were considered as one. Martins (2011) obtained analogous results by considering the same assumption as can be observed in Figures 3.17 and 3.18.

This increase of correlation between methodologies had particular incidence for the ω_{fill} parameter (Tables 4.7 and 4.11). In Berney IV et al., (2011), were obtained similar results for this parameter.

In the third analysis, only NDG results obtained with the DM were compared with the SCT. In the first and third stages the correlations between both methodologies increased comparatively to those from the previous analysis, demonstrating that measurements taken with the DM presented higher correlations with the SCT results than those taken with the BSM in this stages (Figures 4.7 and 4.14; Tables 4.7 and 4.16). However, when the third analysis was applied to the second stage, the R^2 and *r* decreased, as stated in the paragraphs above, this behaviour may be associated with the use of smooth wheel roller; and nevertheless this equipment was applied in stage 3 and this behaviour was not verified. This results are in accordance with the first analysis.

Third stage results presented the lowest correlations with all the analysis, as previously stated this behaviour may be related with the limitations of applying the Hilf method and/or the NDG to coarser grained soils,

It should always be considered that second and third analysis results may not be representative due to the use of heterogeneous populations, since as explained by Berney IV et al. (2011), the R^2 and *r* may be affected by the presence of heterogeneous populations, with particular incidence for the ω_{fill}, since the scattergrams obtained with these analysis presented 3 individual populations (one for each placing water content) with gaps in their distribution.

4.6. CORE FILL

The Coutada/Tamujais dam is a zoned earthfill with central core, as defined in 4.1, however the SCT and NDG were only applied in simultaneously during the core construction. Therefore this dissertation only studies the results from the quality control operations taken during the construction of this structural element, since its purpose is to compare both methodologies.

The core was constructed with arkosic materials classified as clayey sands (SC), defined in Section 4.4.2. The equipment used during the construction of the dam core was defined in Section 4.5.1, and it was tested during the construction of the trial embankment. The construction and control procedures applied in the dam core are defined in the following sections.

4.6.1. CONSTRUCTION PROCEDURES

A summary from the construction procedures is defined in the paragraphs below:

1. The soil for the first layer was placed and spread in a horizontal layer over a previously stripped and compacted platform.
    a. The placing process provided to the layer surface a 2 or 3% dip in the direction of the dam faces, therefore during construction the axis area in each layer is higher than the remnant layer surface;
    b. The project requirements defined that the soil should be placed with an average water content proximate to the $\%\omega_{opt}$ obtained with the standard Proctor test. The tolerance for this parameter varies between $\omega_{opt} - 0.5\%$ and $\omega_{opt} + 1.5\%$.
    c. The soil should be placed on the wet side of the optimum with a water content proximate to the maximum limit ($\omega_{opt} + 1.5\%$), in areas of contact between the embankment, and the concrete structures or the foundation.
    d. A farm tractor equipped with a deposit was used to increase the water content when this parameter was inferior to the project requirements;
    e. The soil was spread using the bulldozer defined in Section 4.5.1, the purpose of this operations was to homogenize the construction material and to uniform the water content.

2. The soil was compacted using the smooth wheel roller defined in Section 4.5.1. In accordance with project requirements the degree of compaction in the embankment should be higher to 98% with a standard deviation of 3% when compared with the value from the standard Proctor test;
3. The final surface of each layer was scarified to a depth of 0.05 m to improve the binding between successive layers;
4. The preceding processes were repeated for the remaining layers.

The soil spreading and compaction equipment circulation were performed in a parallel direction to the dam axis. The layers that did not fulfil the project requirements were removed, and replaced. The core layers should be constructed with a 0.4 m thickness.

A project tolerance between 0 and 0.5 m was established for the embankment walls, for the other limits this tolerance was $\pm$ 0.25 m.

4.6.2. COMPACTION CONTROL

As in the trial embankment, the SCT and the NDG were used in simultaneous during the control operations at the dam core. A total of 684 measurements with the NDG and 102 with the SCT were employed during the core quality control operations. Each SCT executed during the core construction is associated with a variable number of NDGs (Figure 4.15), contrarily to the previous procedure of using three NDG measurements for each SCT. The tests were performed in each layer at the end of the 6 passages. The calibration process for both equipment was described in Section 4.5.2.

The tests were performed in each layer and as recommended in the tender documents with particular incidence in the following areas:

- Equipment manoeuvring areas;
- Areas where could exist a variation of water content and/or construction materials proprieties;
- In places where the number of passes performed by the equipment operator was uncertain;
- Contact areas between the embankment and concrete structures or rockfills;
- Zones compacted with rammers;
- Areas corresponding to layers with a higher thickness.

Since the degree of compaction achieved in this areas could be doubtful due to their construction characteristics. The Hilf method was applied to the results from both methodologies, during the quality control stages.

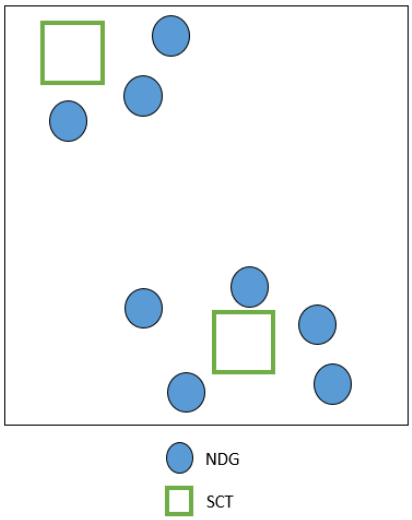

Figure 4.15- Generic representation for the compaction control process used: one SCT is associated with a variable number of NDGs

4.6.3. DATA ANALYSIS – METHODOLOGY

As in the trial embankment, the calculus of applying Hilf method to both methodologies were all redone. Only results that fall within the project specifications were considered in this study (Section 4.6.1), the results from 83 SCTs and 487 NDGs fulfilled those specifications.

Three types of analysis were considered:

- *Point to vicinity points comparison*: each one of the methodology A observations is individually compared with all the results from NDG that were performed in its vicinity;
- *Point to mean of vicinity points comparison*: comparison between the results from each SCT and the mean of all NDGs performed in its vicinity;
- *Closest point comparison:* each one of the methodology A observations is individually compared with the results from NDG that was performed at a closest distance.

As in the trial embankment, the results of the comparisons between both methodologies were established by plotting in SCT/OVM Vs NDG scattergrams, a linear regression was applied to each one of the populations represented in those scatters, and the R^2 and *r* coefficients were determined. The results from the core analysis were compared with those from stage 2.

A complementary analysis for the comparison between both methodologies was defined by creating nine three dimentional models. This nine models were divided into three sets of three models (one for each control parameter):

- SCT results
- NDG results;
- SCT and NDG results.

With these models it was also possible to study the spatial variability of each control parameter in the dam core.

4.6.4. RESULTS

4.6.4.1. POINT TO VICINITY POINTS COMPARISON

The descriptive statistics from the results obtained during the compaction control operations, are represented in Table 4.17, and the histograms from the variables defined in this stage are defined in Annex V. The scattergrams from the comparison between both methodologies, are given in Figure 4.16.

Table 4.17 – Descriptive statistics for the core results obtained with the point to vicinity points comparison

	Methodology A			Methodology B		
	γ_{fill} (kN/m³)	ω_{fill} (%)	DC (%)	γ_{fill} (kN/m³)	ω_{fill} (%)	DC (%)
Mean	21.52	11.02	100.09	21.34	10.87	99.27
Median	21.52	10.90	100.19	21.34	10.87	99.27
Standard Deviation	0.22	0.79	0.94	0.21	0.67	0.96
Variance	0.05	0.64	0.89	0.05	0.45	0.93
Minimum	20.90	9.10	98.06	20.74	9.20	97.52
Maximum	21.90	12.80	101.50	21.97	12.60	101.50
Kurtosis	-0.24	-0.42	-0.89	-0.17	-0.49	-0.72
Skewness Coefficient	-0.40	0.11	-0.34	-0.11	0.10	0.16

The results presented in Table 4.17 and Figure 4.16 show that, as in the trial embankment, methodology A results have a tendency to be higher, since the parameters of central tendency are higher, and the majority of the points in the Figure 4.16 graphics are above the EL. The γ_{fill} and ω_{fill} data have higher dispersion for methodology A results, and the DC data for methodology B.

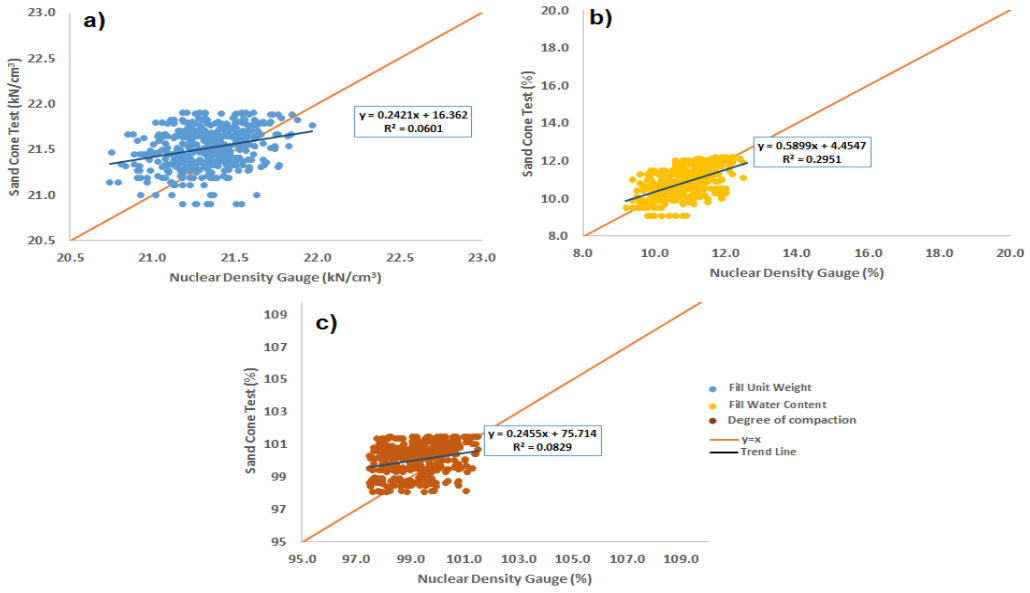

a)γ_{fill}; b) ω_{fill}; c) DC

Figure 4.16- Scattergrams for the point to vicinity points comparison

All the populations studied in this section have negative values of kurtosis, which indicates that the distribution curve is flatter. The data distributions illustrated by the histograms in Annex V have a tendency to be multimodal for the SCT results, and symmetrical for the NDG; this difference can be explained by the considerably larger NDG population, creating more uniform distributions.

In Figure 4.16 it is possible to identify horizontal alignments in the graphics due to the comparison between the results from one SCT or OVM measurement with the results from several NDG measurements that were made in its proximity.

The correlations between methodologies for each one of the control parameters were measured using the Pearson coefficient and are expressed in Table 4.18.

Table 4.18 - Correlation between methodologies A and B for the point to vicinity points comparison

γ_{fill}	0.29
ω_{fill}	0.54
DC	0.26

From the *r* and R^2 values obtained during this analysis it can be observed that the core results present weak correlations between the SCT and NDG, since the correlation is lower for the parameters based on the results from these tests (γ_{fill}: 0.29 and DC: 0.26), and moderate correlations between the NDG and OVM (ω_{fill}: 0.59).

4.6.4.2. POINT TO MEAN OF VICINITY POINTS COMPARISON

The descriptive statistics from the NDG results and the respective scattergrams obtained with this analysis are represented in Table 4.19 and Figure 4.17, and show that the dispersion of the NDG results decreases in this analysis. This can be justified due to the use of a smaller population representing a mean from a set of results, grouping the set into a central value and reducing the respective overall dispersion. The histograms presented in Annex V indicate that the studied populations for each parameter have a symmetrical distribution.

The correlations between both methodologies are expressed in Table 4.20.

Table 4.19 - Descriptive statistics for the Point to mean of vicinity points analysis for the NDG results

	γ_{fill}(kN/m^3)	ω_{fill} (%)	DC (%)
Mean	21.33	10.94	99.26
Median	21.34	10.94	99.26
Standard Deviation	0.13	0.52	0.73
Variance	0.018	0.28	0.54
Minimum	20.95	9.72	97.88
Maximum	21.67	11.99	101.36
Kurtosis	0.83	-0.42	0.81
Skewness coefficient	-0.32	0.14	0.73

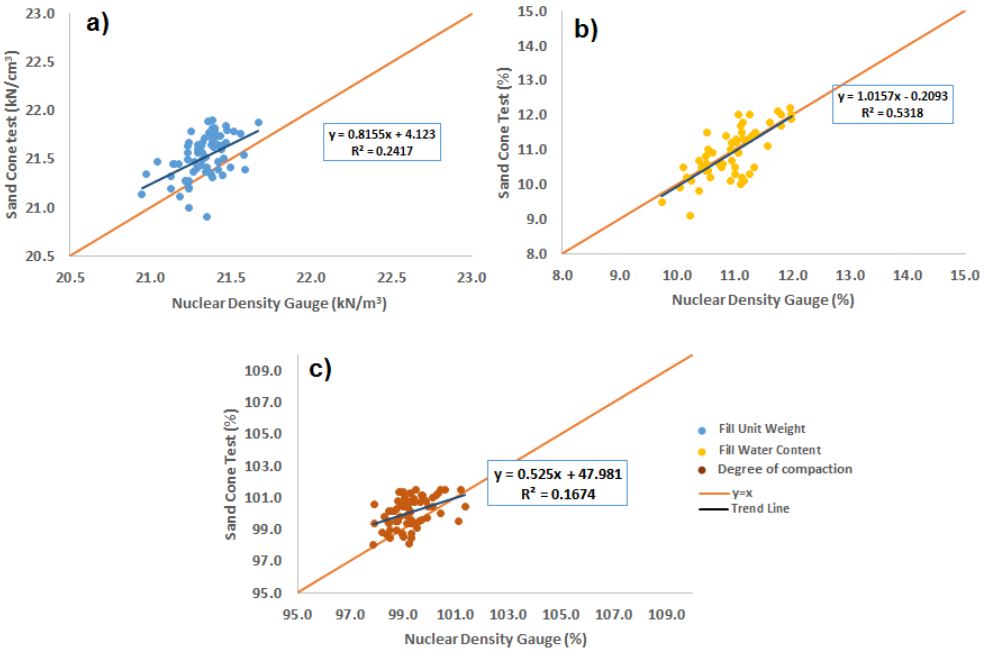

a)γ_{fill}; b) ω_{fill}; c) DC

Figure 4.17- Scattergrams for the point to mean of vicinity points analysis

Table 4.20 - Correlation coefficients between both methodologies for point to mean of vicinity points analysis

γ_{fill}	0.46
ω_{fill}	0.72
DC	0.41

Figure 4.17 graphics and the correlations coefficients in the Table 4.20 express that both indicators increased in this analysis due to decrease of dispersion, corresponding to the highest values of Pearson coefficient and R^2 (0.53 and 0.72) achieved for the ω_{fill}. The values of this parameters indicate a moderate to strong correlation. This growth was particular incident in γ_{fill} and DC; however, they still present an average correlation between methodologies.

4.6.4.3. CLOSEST POINT COMPARISON

The results from this comparison are expressed in Figure 4.18 and the correlation coefficients in Table 4.21. The R^2 parameter reached its highest value for all the control parameters in this study. As in the previous analyse, this indicator increased particularly for the γ_{fill} and DC parameters; (γ_{fill}: 0.46; ω_{fill}: 0.64; DC: 0.35). The correlation coefficients between both methodologies (Table 4.21) express a strong correlation for the ω_{fill} (0.8) parameter and strong for γ_{fill} (0.68) and DC (0.54).

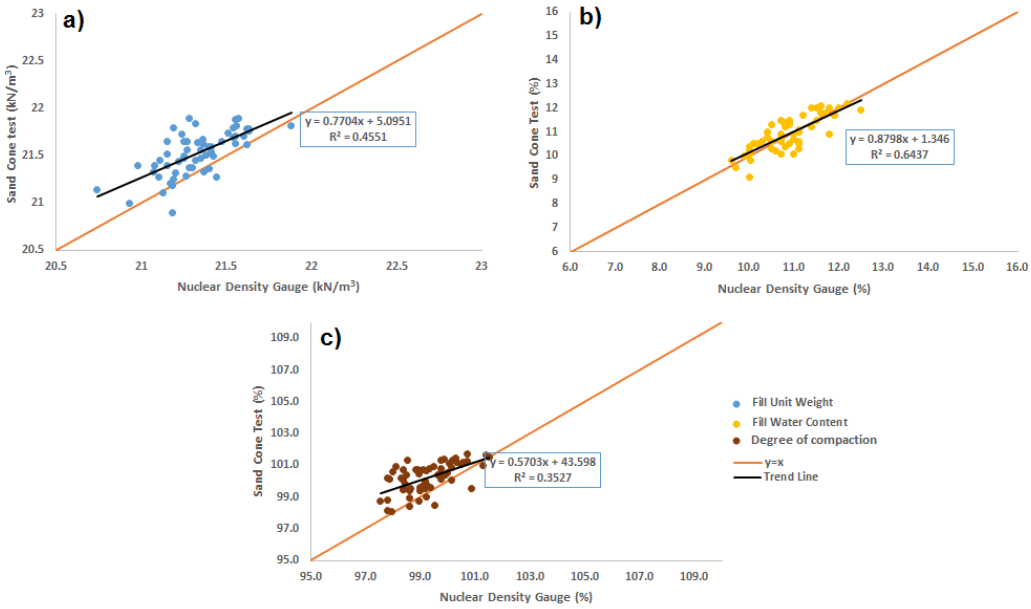

a)γ_{fill}*; b)* ω_{fill}*; c) DC*

Figure 4.18- Scattergrams for the closest point analysis

Table 4.21 - Correlation between both methodologies for the closes point analysis

γ_{fill}	0.68
w_{fill}	0.80
DC	0.54

The R^2 and correlations coefficients results achieved with this analysis show that the control tests performed at a shortest distance presented higher correlations than those performed at higher distances, as it should be expected since it is impossible to guarantee that an embankment layer is completely homogeneous, in a way that control tests performed at different locations provide equal results. Therefore, tests performed at closer distances should usually provide better correlations, as it was verified here.

The results from the first and third analysis are published in article by Blanco et al. (2015), which was accepted to be presented in the European Conference in Geo-Environment and Construction.

4.6.4.4. CORE AND STAGE 2 TRIAL EMBANKMENT RESULTS COMPARISON

The results obtained during the core analysis can be compared with those from the second stage of the trial embankment between SCT and NDG measurements made at the depth of 0.30 m, once both measurements were taken with similar conditions.

In Table 4.9, the central tendency indicators show that the results from the second stage tend to be higher for methodology A, and the core results present similar behaviour as can be seen in Table 4.17.

This tendency for methodology A results to be higher can be sustained by Figures 4.6, 4.9 and 4.12 graphics, showing the majority of the results located above the EL, as can also be observed in the graphics form Figures 4.16, 4.17 and 4.18.

In each one of the analyses undertaken (core and trial embankment), the cloud point formed by the γ_{fill} data is similar to the one obtained with the DC results. This outcome was expected since the DC is dependent on the γ_{fill}.

Stage 2 results (Table 4.10) demonstrate that the correlation coefficients between both methodologies were greater for the γ_{fill} and DC results, and lower for the ω_{fill} data. However, core results contradict this behaviour since they presented higher correlation coefficients for the ω_{fill} parameters. This difference may be explained by the fact that the R^2 values were calculated for each one of the three individual populations for each one of the placing water contents of stage 2 and the dimensions of the populations used in this stage were considerably smaller. The increase in the dimension of the population may accentuate some characteristics that cannot be visible for smaller populations.

4.6.5. SPATIAL VARIABILITY MODELLING

A total of nine models were developed to study the spatial variability of the control parameters in the dam core. These models were developed using the software RockWorks®, version 15. The method of estimation used to develop those models was the inverse distance weighting (IDW), with vertical and horizontal weighting exponentials of 2.

In the IDW method, the voxel node value is determined with the weighted average of the neighbouring data points; the value of each one of these points is weighted according to the inverse distance from the voxel node taken to an exponent. The higher the exponent, the less influence distant control points will have on the voxel node value (Roberts et al. 2004).

As explained in Section 4.6.3, the nine models were divided in three sets:

- SCT results (Figures 4.19, 4.20, and 4.21);
- NDG results (Figures 4.22, 4.23, and 4.24);
- SCT and NDG results (Figures 4.25, 4.26 and 4.27).

Each one of these sets is composed by three models, one for each control parameter. The γ_{fill} model for the SCT results (Figure 4.19) presented highest values for this parameter in both abutments (22 kN/m^3) and lower values in the centre (21 kN/m^3).

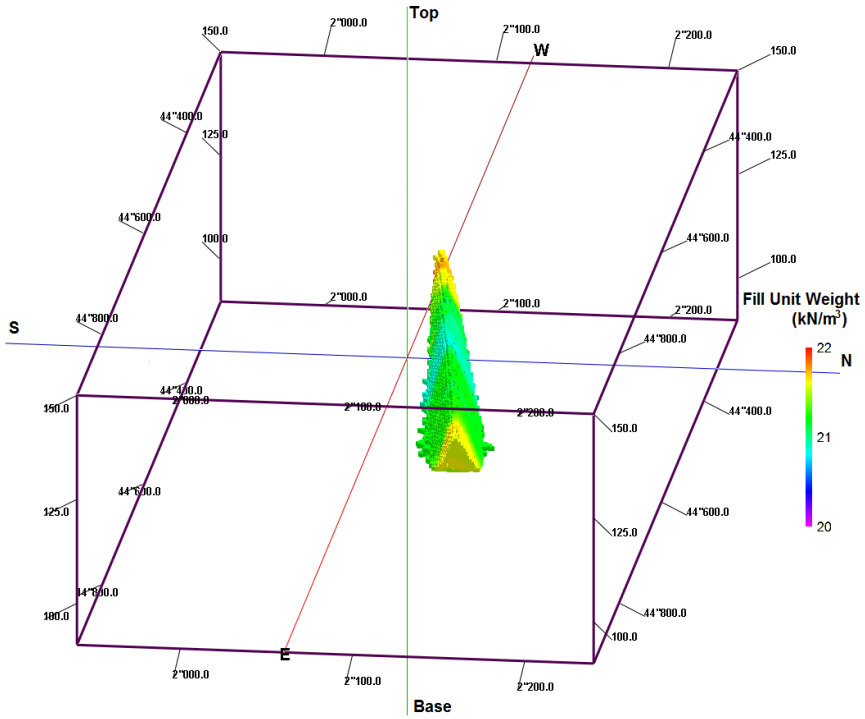

Figure 4.19 - Fill unit Weight model for the SCT results with a vertical exaggeration of 2.5

In the ω_{fill} model (Figure 4.20), the lowest values of water content were achieved in both extremes (11%), and the highest in the center (12%). Singh & Varshey (1995) stated that earthfills compacted with higher water contents tend to have lower permeability, higher flexibility, and lesser compressibility when saturated. These higher flexibility will prevent the center of core from cracking, preventing the dam failure.

Figure 4.21 shows that the maximum DC values (101%) were reached in the East abutment and in a stripe near the West abutment, the minimum values for this parameter were reached in the center and west abutment (99%).

The NDG models for all the compaction parameters tended to be more uniform than those from the SCTs; these behaviour can be explained by the smaller number of SCT tests that were performed during the core construction

Figures 4.22 and 4.23 show that the γ_{fill} and ω_{fill} achieved in the dam core were uniform in all its extension, reaching values of 21 kN/m^3 and between 11-12 %, respectively.

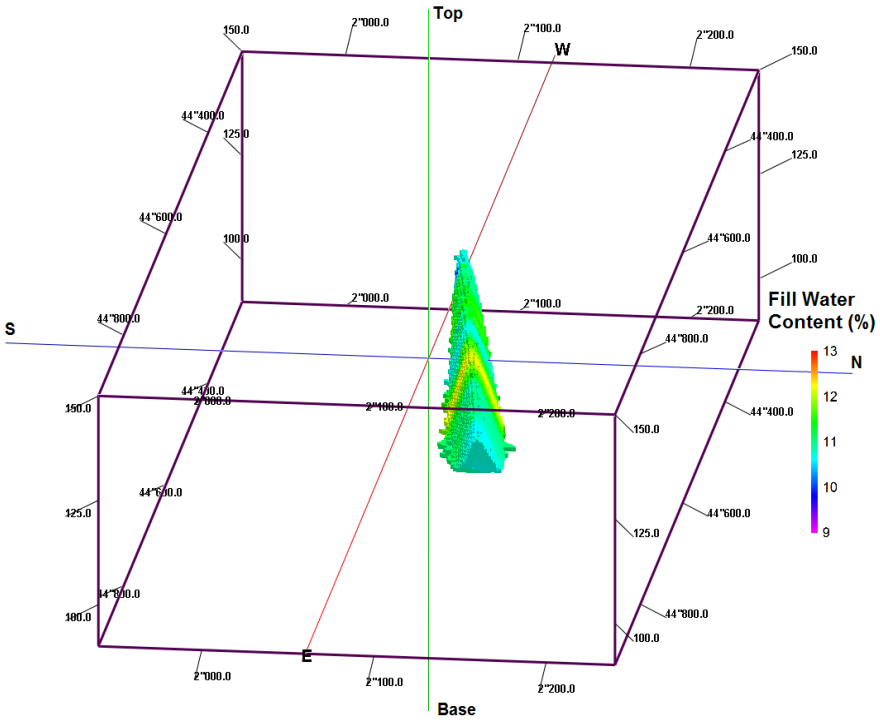

Figure 4.20 - Fill water content model for the SCT results with a vertical exaggeration of 2.5

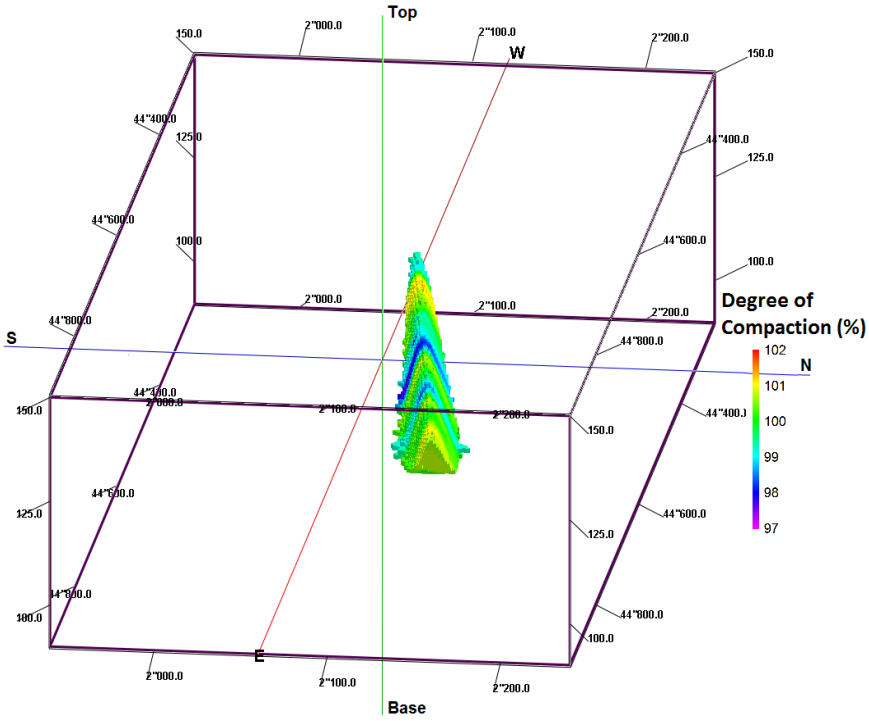

Figure 4.21 - DC model for the SCT results with a vertical exaggeration of 2.5

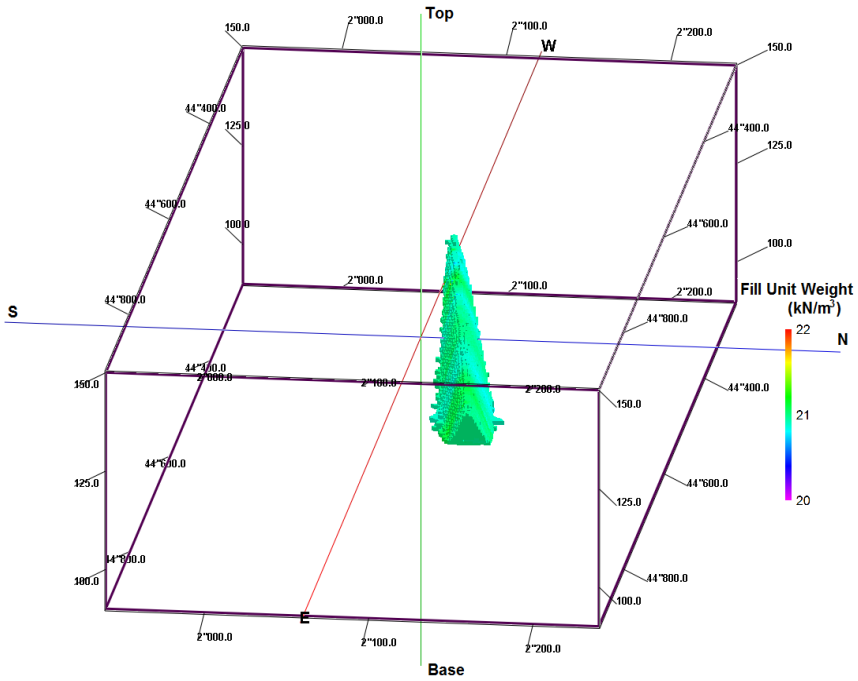

Figure 4.22 - Fill unit weight model for the NDG results with a vertical exaggeration of 2.5

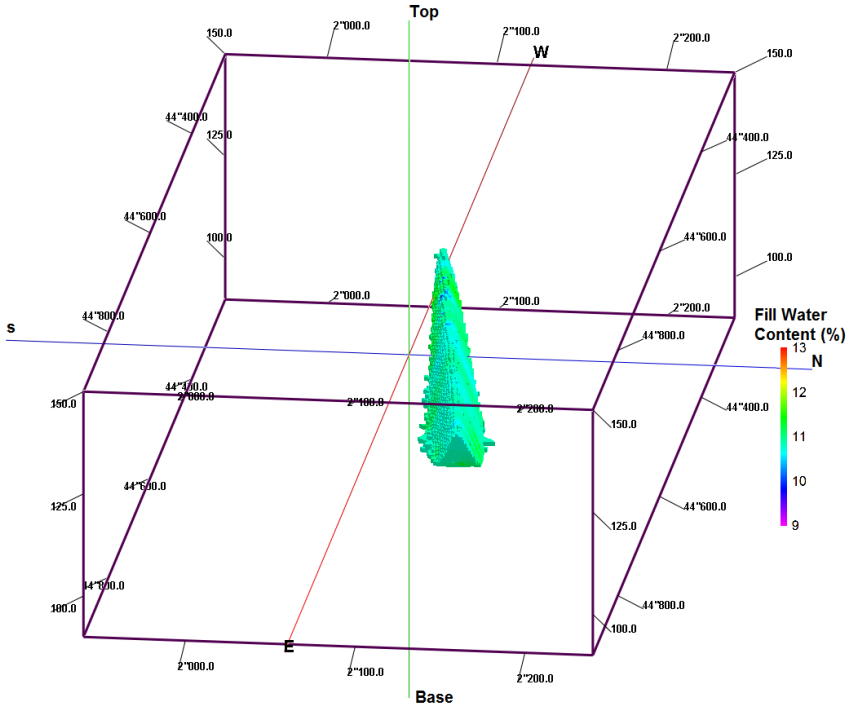

Figure 4.23 - Fill water content model for the NDG results with a vertical exaggeration of 2.5

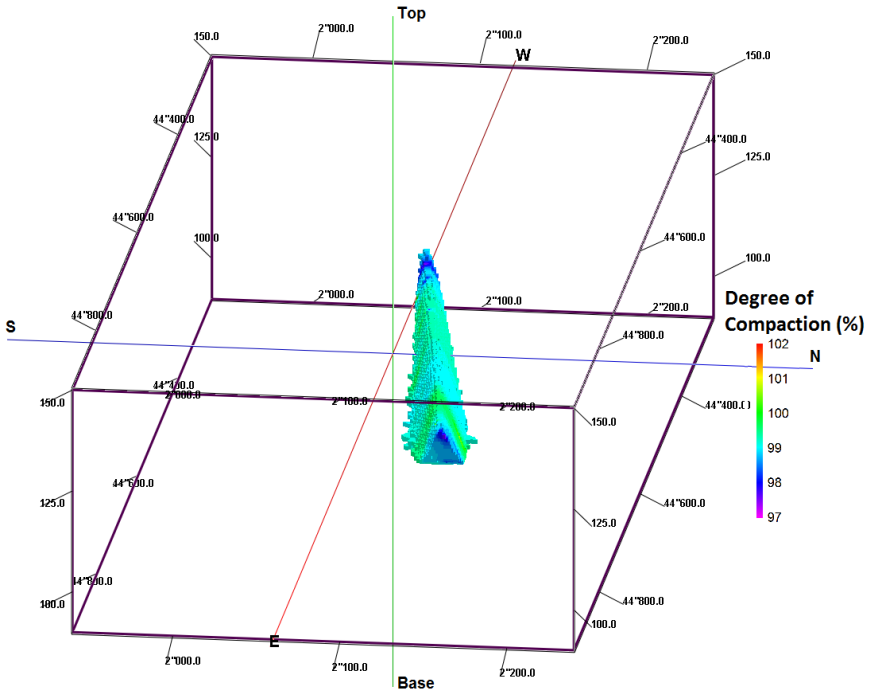

Figure 4.24 - DC model for the NDG results with a vertical exaggeration of 2.5

The DC achieved in the dam core (Figure 4.24) falls between the project specifications (99-100%) and is also uniform through the extension of the embankment, with an exception for both abutments which present lower values that correspond to the lower limit defined in the project specifications (98%). This lower values may not represent any significant problem to the structure, since the region of the embankment that need higher DC to prevent appearance of cracks is the center. According to Fell et al. (2015) this behaviour may be associated with an inability of the rollers to compact the edges of the fill.

The models obtained by adding the results from both methodologies (Figures 4.25, 4.26 and 4.27) were similar to the ones achieved with the NDG results, γ_{fill} and ω_{fill} uniform in all its extension, reaching values of 21 kN/m3 and between 11-12 % respectively. The DC models were also uniform through the core extension, with an exception for both abutments which present lower values (98%),

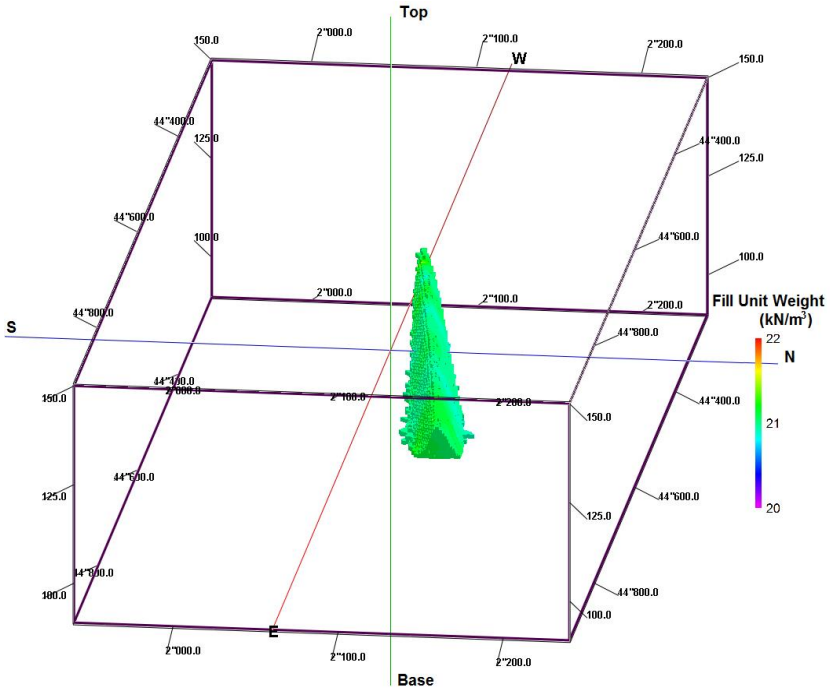

Figure 4.25 - Fill unit weight model for the NDG and SCT results with a vertical exaggeration of 2.5

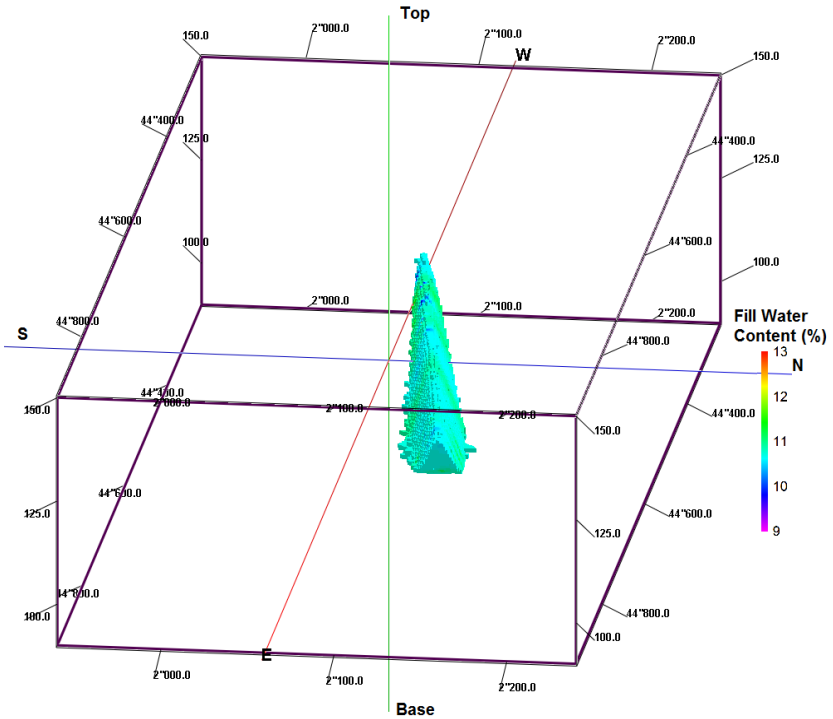

Figure 4.26 - Fill water content model for the NDG and SCT results with a vertical exaggeration of 2.5

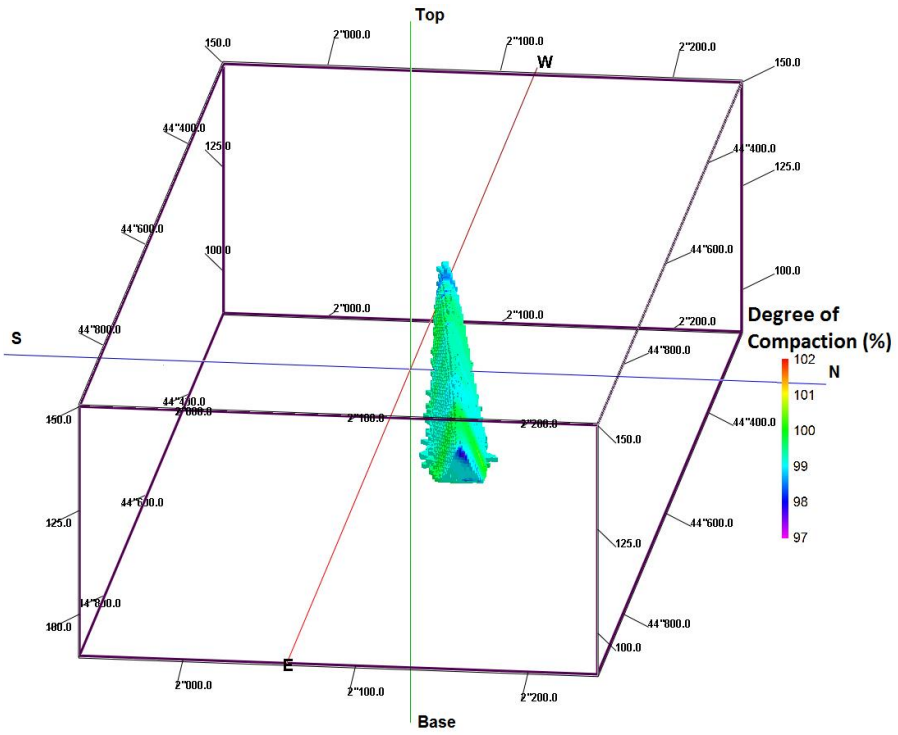

Figure 4.27- DC model for the NDG and SCT results with a vertical exaggeration of 2.5

This small difference between NDG models and those obtained by adding the SCT and NDG results can be justified by the fact that, from the total of points used to produce those models, only 13% were SCT results.

4.6.6. CORE FILL CONTROL MAIN CONCLUSIONS

The purpose of the previous sections was to compare both methodologies using the results from the construction of the dam core by considering three distinct comparative analysis (point to vicinity of points comparison, point to mean of vicinity points comparison, closest point comparison), and to study the spatial variability of the compaction parameters in the core.

Through the comparison between both methodologies it was possible to notice that as in the trial embankment, methodology A has a tendency to provide higher results in all the analysis performed in this study (Figures 4.16, 4.17 and 4.18). The results from the first analysis (point to vicinity point comparison), showed horizontal alignments that were originated by comparing the results from one SCT or OVM measurement with the data from several NDG measurements made in their proximity.

R^2 results from the first analysis (Figure 4.16) indicate low correlations between the results from both methodologies, being the lowest values achieved for the parameters that express the relation between SCT and NDG test (γ_{fill}: 0.06 and DC: 0.08); this relation was considerably higher for the ω_{fill} (0.29).

The Pearson coefficients were in accordance with this results since it expressed low correlations for γ_{fill} and DC data (respectively, 0.29 and 0.26) and average for the ones of ω_{fill} (0.54).

When the second and third analyses were applied to the core results, the R^2 and Pearson coefficients increased substantially due to a decrease of the dispersion (Figures 4.17 and 4.18 and Table 4.20 and 4.21). As in the first analysis, the highest values of R^2 and Pearson coefficient were obtained for the ω_{fill} and the lowest for DC and γ_{fill} data.

In the second analysis, the values of R^2 (γ_{fill}: 0.24; ω_{fill}: 0.53; DC: 0.16) and Pearson coefficient increased considerably (Figure 4.17). The Pearson coefficient indicated low/average correlations (0.46 and 0.41) for γ_{fill} and DC parameters and average/good correlations (0.72) for ω_{fill} data (Table 4.20).

The third analysis undertaken, provided the highest values for the R^2 (γ_{fill}: 0.45; ω_{fill}: 0.64; DC: 0.35) and *r* (γ_{fill}: 0.68; ω_{fill}: 0.80; DC: 0.54), indicating weak/average correlation for the γ_{fill} (R^2:0.45, *r*. 0.68) and DC (R^2:0.35, r:0.54), and strong/very strong for the ω_{fill} (R^2:0.64, *r*:0.8), Figure 4.18 and Table 4.21. The results from the closest point analysis showed that the control tests performed at a shortest distance presented higher correlations than those performed at higher distances. This should be expected since it is impossible to guarantee that an embankment layer is completely homogeneous in a way that control tests performed at different locations provide similar results. Therefore, tests performed at closer distances should usually provide better correlations, as it was verified here.

As in the trial embankment, the overall R^2 values indicate that the results obtained with both methodologies had substantial differences since Pearson coefficients and/or R^2 near 1 could not be achieved. This enhances the fact that NDG results should be validated against SCT results as sustained by Neves et al. (2013)

The core models obtained with the SCT results present a higher spatial variability comparatively to those from the NDG results, which can be explained by the smaller number of SCT tests that were performed during the core construction, therefore the results from both types of models cannot be directly compared.

The models elaborated by adding the results from both methodologies did not had considerable differences relatively to those achieved with the NDG results, since from the total of points that were used to produce those models, only 13% were SCT results.

These models indicate that the γ_{fill} and ω_{fill} achieved in the core were uniform in all its extension, reaching values of 21 kN/m^3 and 11-12% respectively (Figures 4.25 and 4.26). The DC models (Figure 4.27) were also uniform through the extension of the embankment, with an exception for both abutments which present lower values, that correspond to the lower limit defined in the project specifications (98%). However this lower values may not represent any significant problem to the structure, since the region of the embankment that needs higher DC to prevent appearance of cracks is the centre.

The γ_{fill} and ω_{fill} quality control 3D models had low variability, and the DC model presents lower values in both extremes, wich may be associated with an inability of the rollers to compact the edges of the fill.

5. FINAL CONSIDERATIONS AND FUTURE WORKS

This dissertation addresses the suitability of using the conventional (SCT and OVM) and nuclear (NDG) methodologies during the fill compaction quality control / quality assurance operations in an earth dam. The results obtained during the control operations employed at the construction of the Coutada/Tamujais dam core and trial embankment were used to establish a comparison between both methodologies. Additionally, the spatial variability of the control parameters in the dam core was also studied using 3D models.

Each one of the methodologies (SCT and NDG) have their own disadvantages and advantages, the NDG is a non-destructive and a fast way to access the control parameters, however it may cause health damages to the operator, and is more susceptible to operator errors. On the other hand, the SCT is a destructive and time consuming technique; therefore, in the time required to perform a SCT several NDG measurements can be obtained, increasing the amount of information about the spatial variability of the compaction parameters. However, this information can only be useful if the results provided by the NDG are representative and thus the question about the accuracy of the NDG relatively to the SCT remains.

To solve this problem, is a common practice in Portuguese dams to validate the NDG measurements against the SCT results as stated by Neves et al. (2013). However as stated by Maregesi (n.d.), the usual procedure for calibrating the NDG against the SCT can be improved by using multiple shift coefficients. This procedure should have been followed in the construction of the Coutada/Tamujais dam.

The trial embankment was considered to be divided in three stages. In the first stage, three layers formed by arkosic materials (SC) were compacted with the sheep foot roller. In the next stage, three layers composed by the same materials were compacted with a smooth wheel roller. In the last stage, three layers were built with alluvial materials (SC to GW-GC), and compacted with a smooth wheel roller.

The data from a total of 324 measurements (81 with the conventional methodology, and 243 with the nuclear methodology) employed to access the fill unit weight and water content were analyzed in this work. The γ_{fill}, ω_{fill}, and DC were defined as the quality control parameters, and the Hilf method was applied to the results from both methodologies to access the DC.

Three types of analysis were applied to trial embankment data to establish a comparison between the results from both methodologies:

- Comparison between each methodology A measurement and all the NDG measurements taken in the vicinity of the SCT testing site, by considering the measurements taken at different depths, and different placing water contents as individual populations;
- Comparison between both methodologies, by considering all measurements taken at different depths and different placing water contents as a single population;

- Comparison between each methodology A measurement and the NDG measurements taken in its vicinity at depths of 0.15 and 0.30 m (DM), the measurements taken at different depths, and different placing water contents were considered as a single population.

The overall R^2 and *r* values obtained with the first analysis (Figures 4.6, 4.9 and 4.13 and Tables 4.6, 4.10, and 4.14) were inferior to those obtained with the second and third (single population for all the placing water contents), due to the smaller dimensions of the populations considered in the first (one for each placing water content). Being the highest correlations for this parameters reached for stage 1, and the lowest in stage 3.

The R^2 and *r* values obtained in first stage (Figure 4.6 and Table 4.6) reached values up to 0.9 (very strong correlations); however, the majority of the R^2 values obtained with this analysis in this stage expressed very weak to moderate correlations, indicating that the results from both methodologies have substantial differences. Neves et al. (2013) obtained similar results to those verified in stage 1, and stated that this differences should be compensated by validating the NDG measurements with the SCT results.

The correlations between both methodologies increased with the depth of measurement for the γ_{fill} and DC parameters, and decreased with an increase of water content for the ω_{fill} (Table 4.7). This increase of correlation with the depth of measurement can be explained by the fact that the SCT reached a depth of 0.25 m. Thus, the best correlations should be achieved for those NDG measurements taken at most proximate depths (0.3m). This results are in accordance with those expressed by Neves et al. (2013), which concluded that the measurements taken with the DM were more accurate.

The correlations between NDG measurements taken at different depths showed a tendency for being higher between the measurements taken at the depths of 0.15 and 0.3m than those measured at the surface. This pattern should be expected since the results from 0.15 and 0.3 m depth measurements were obtained with the DM, and superficial measurements were taken with BSM mode. However, this tendency cannot be evinced for the ω_{fill} parameter.

When this first analysis was applied to the data from the second stage, the overall R^2 and *r* values decreased (Figure 4.9 and Table 4.10) and it was not possible to identify a correlation pattern between both methodologies and NDG measurements taken at different depths, in opposite to the previous stage.

The results from applying this analysis to the third stage provided the lowest values of R^2 and *r* graphics being the highest correlation achieved for the γ_{fill} and DC parameters (Figure 4.12 and Table 4.14). The correlation between both methodologies for the γ_{fill} and ω_{fill} was directly proportional to an increase in water content. As for stage 1, the correlation between NDG measurements taken at different depths had a tendency to be higher between those measurements taken by the DM.

The results from the first analysis showed that the correlation between both methodologies was dependent on the type of material and compaction equipment, since it is not possible to identify a

common behaviour between the three stages. For example and for the first stage, the correlation increased with the depth of measurement for the γ_{fill} and DC, and decreased with an increase of water content and depth of measurement for the ω_{fill}; however, this behaviour was not valid for the stages 3 and 2 results. Thus, the results from the construction stages cannot be directly compared between each other since the construction materials and/or compaction equipment differed between them.

The effects from the variation of compaction equipment can be observed by comparing the results from the second and first stages. For the first stage, the correlation coefficients between NDG measurements for the γ_{fill} and DC parameters were higher for the DM results (Table 4.6); however, this pattern cannot be observed in stage 2 (Table 4.10). This behaviour may be associated with the fact that a sheepsfoot roller was used in the first stage and a smooth wheel roller, in the second. Since the first produces layers that are not compacted in a superficial zone, which may affect the measurements taken with the BSM, and thus resulting in higher correlations for the DM mode. While for the second stage, it was used a smooth wheel roller, which compacts the layers by pressure without causing any disturbance in the layer surface that may affect the BSM or DM readings.

For the first two stages, the populations illustrated in the scattergrams presented similar behaviours for the γ_{fill} and DC parameters (Figures 4.6 and 4.9), which can be explained by Equation 3.27, since DC is dependent on γ_{fill} value. However, this condition was not valid in stage 3 (Figure 4.12), which may also be associated with limitations of using the NDG or the Hilf method for those coarser materials.

When the second analysis was applied, the overall values of R^2 and *r* increased due to the use of populations with larger ranges of values. Once all the results from the different placing water contents were considered as a single population, in opposite to the first analysis, where it was defined one population for each placing water content. The results from this analysis are summarized in Table 5.1.

This increase of correlation between methodologies had particular incidence for the ω_{fill} parameter reaching values of 0.97 and 0.94 for the first and second stages respectively (Table 5.1). In Berney IV *et al*. (2011), similar results were obtained for the ω_{fill} parameter. Nevertheless, their results may have the some limitations, since they also used (Figure 3.21) a considerable range of water in which three populations can be identified.

Table 5.1- Summary of the R^2 and r results obtained with the second analysis applied to the trial embankment data

	Parameter					
	γ_{fill}		ω_{fill}		**DC**	
Construction stage	R^2	*r*	R^2	*r*	R^2	*r*
1	0.77	0.87	0.95	0.97	0.66	0.82
2	015	0.38	0.87	0.94	0.52	0.71
3	0	-0.02	0.17	0.41	0.14	0.37

Nevertheless, it should be considered that these results may not be representative due to the use of heterogeneous populations, with particular incidence for the ω_{fill}, since it is formed by two individualized populations.

The results from the third analysis for the R^2 and *r* coefficients are summarized in Table 5.2. When this analysis was applied to the quality compaction control results, higher R^2 values and Pearson coefficients were obtained for all the parameters in the first stage, and for the DC and ω_{fill} in the second stage. This behaviour indicates that whenever only NDG results from the DM are considered, the correlation between both methodologies increases for those parameters. Therefore, the DM results are more accurate for this parameters in this stages. However, this results may have the same limitations that were defined for stage 2.

Table 5.2- Summary of the R^2 and r results obtained with the third analysis applied to the trial embankment data

	Parameter					
	γ_{fill}		ω_{fill}		**DC**	
Construction Stage	R^2	*r*	R^2	*r*	R^2	*r*
Stage 1	0.81	0.90	0.95	0.98	0.71	0.85
Stage 2	0.1	0.32	0.87	0.93	0.46	0.68
Stage 3	0.3	0.55	0.36	0.6	0.46	0.43

In all the analysis stage 3 materials (SC to GC) presented the lowest correlations, which may be associated to limitations of applying the NDG and/ or the Hilf method in coarser grained materials.

From the trial embankment results, it can be concluded that any variation of the compaction conditions will affect the results and therefore the correlation between both methodologies, demonstrating that the results from the quality control operations under certain compaction conditions may only be valid for those conditions. As a result, the conclusions presented in this study shall only be valid under conditions used during the construction of the Tamujais/Coutada dam trial embankment and core.

The dam core built with arkosic materials (SC) and only results that fall within the project specifications were considered in this stud. The results from a total of 786 measurements that were employed during the control operations (684 with the NDG and 102 with the SCT) were considered in this work, and the data from both methodologies obtained were compared. The Hilf method was applied to the results from both methodologies to access the DC. The project specifications were defined as follow:

$$98\% \leq DC \leq 101\%$$

$$\omega_{op}\text{-}0.5\% \leq \omega_{fill} \leq \omega_{op}\text{+}1.5\%$$

Three types of comparative analyses between both methodologies were established: a point to point analysis, point to average of points comparison, and a closest point comparison.

As in the trial embankment conventional methodology results showed a tendency to be higher for all the comparative analysis that were applied to the core data (Figures 4.16, 4.17 and 4.18, and Tables 4.17 and 4.19). The R^2 and *r* coefficients obtained in each analysis, are summarized in Table 5.3.

Table 5.3 - Summary of the R^2 and *r* results obtained for all the analysis that were applied to the data

	Parameter					
	γ_{fill}		ω_{fill}		**DC**	
Analysis	R^2	*r*	R^2	*r*	R^2	*r*
Point to vicinity points comparison	0.06	0.29	0.3	0.54	0.08	0.26
Point to vicinity points average comparison	0.24	0.46	0.53	0.72	0.17	0.41
Closest point comparison	0.46	0.68	0.64	0.8	0.35	0.54

In the point to vicinity points comparison, R^2 and *r* expressed weak correlations for the γ_{fill} and DC and moderate for the ω_{fill} (Table 5.3). When the second and third analyses were applied, the R^2 and Pearson coefficients increased substantially due to a reduction of the population dispersion. The Pearson coefficient in the second analysis indicated moderate correlations (0.46 and 0.41) for γ_{fill} and DC parameters and strong correlations (0.72) for ω_{fill} data.

The highest correlations were achieved for the closest point analysis, indicating that the results from the control tests performed at a shortest distance presented higher correlations than those performed at greater distances. The R^2 and *r* values for this analysis indicate weak/average correlation for the γ_{fill} (R^2: 0.45, *r*: 0.68) and DC (R^2: 0.35, *r*: 0.54), and strong/very strong for the ω_{fill} (R^2: 0.64, *r*: 0.8). This result can be justified due to the impossibility of constructing a homogeneous layer that provides similar results in all the control tests performed at different locations. Therefore, it seems consistent that tests performed at shortest distance have more similar results.

As in the first analysis of the trial embankment, the overall values of R^2 for all analyses in the core indicate that the results obtained with both methodologies present substantial differences. Since a Pearson coefficient and/or R^2 correlation near 1 could not be achieved, this enhances the fact that NDG results should be validated against the ones from SCT. The main results obtained during the core and trial embankment analysis are expressed in Table 5.4.

The core models obtained with the SCT results showed higher spatial variability when compared to those from the NDG (Figures 4.19, 4.20, and 4.21). This behaviour can be justified by the smaller number of SCT that were performed during the quality control operations.

The 3D models elaborated by grouping the results from both methodologies did not generate any substantial differences from those obtained with only the NDG data, since only 13% of the control points were SCT results. These models indicate that the γ_{fill} and ω_{fill} achieved in the core were uniform in all its extension, reaching values of 21 kN/m3 and 11-12% respectively. The DC models were also uniform through the extension of the embankment, with an exception for both abutments which presented lower values (98%); this behaviour may be related with an inability of the rollers to

compact the edges of the fill. This DC model shows that the compaction specifications were fulfilled during the construction of the core.

Table 5.4 - Main results obtained during the core and trial embankment analysis

Structure	Analysis	Main results
Trial Embankment	**First analysis**	The majority of the R^2 values obtained with first analysis for stage 1 expressed very weak to moderate correlations; The correlations between both methodologies achieved with this first analysis increased with the depth of measurement for the γ_{fill} and DC parameters, and decreased with an increase of water content for the ω_{fill}; When the first analysis was applied to the data from the second stage, the overall correlations decreased (relatively to stage 1), and a correlation pattern between both methodologies, or NDG measurements taken at different depths, could not be identified; The overall R^2 and *r* values obtained with the first analysis were inferior to those obtained with the other two;
	Second analysis	When the Second analysis was applied R^2 and *r* values for the first and second stages increased relatively to those from the previous analysis with particular incidence for the ω_{fill}, due to the use of populations with larger ranges of values;
	Third analysis	The results from the third analysis for the R^2 and *r* coefficients expressed the highest correlations between both methodologies for all the parameters in the first stage; In the third analysis for stage 2 the DC and ω_{fill} reached their highest correlations; This results show that for this parameters in this stages the correlation between both methodologies increases when only NDG measurements taken with the DM are considered;
	Overall conclusions	Conventional methodology results showed a tendency to be higher in all the analysis that were applied to the trial Embankment data; The Correlation between both methodologies is dependent on the type of soil and compaction equipment; The second and third analysis may have some limitations, due to the use of heterogeneous populations; In all the analysis stage 3 materials (SC to GW-GC) presented the lowest correlations;
Core	**Point to point comparison**	The lowest correlations were achieved with this analysis, being weak for the γ_{fill} and DC and moderate for the ω_{fill}
	Point to average of points comparison	When this analysis was applied, correlations increased substantially due to a reduction of the population size; The Pearson coefficient indicated moderate correlations (0.46 and 0.41) for γ_{fill} and DC parameters and strong correlations (0.72) for ω_{fill} data;
	Closest point comparison	The R^2 and *r* values for this analysis indicated weak/average correlation for the γ_{fill} and DC, and strong/very strong for the ω_{fill}. The highest correlations were achieved with this analysis, therefore the results from the control tests performed at a shortest distance presented higher correlations than those performed at greater distances
	Overall conclusions	As in the trial embankment conventional methodology results showed a tendency to be higher in all the comparative analysis that were applied to the core data

The results obtained in this dissertation confirm that the results from both methodologies have substantial differences and thus the best solution may be to use both methodologies, as it is common practice in Portuguese earth dams during compaction control operations. Since with this practice the NDG measurements can be validated against those from the SCT and the amount of knowledge about

the spatial variability of the compaction parameters obtained by using both methodologies is considerably higher than when just the SCT are used, as can be verified by the core models.

The propositions for future research works on this subject are the following:

- Implementation of studies in Portugal to verify the suitability and economic viability of implementing another methodologies such as the MDI, SDG, and EDG to access the quality compaction control parameters;
- Establishment of a study on the effects of using multiple shift coefficient for calibrating the NDG against the SCT results in a future construction project.

REFERENCES

AASHTO T272. (2004). Standard Method of Test for Family of Curves—One Point Method. Standard Specifications for Transportation Materials and Methods of Sampling and Testing, Part II: Methods of Sampling and Testing. Washington, D. C.: AASTHO.

Abadi, Shahriar Shahrokh Armin, Y., & Mohammad, B. K. R. (2010). Determining Compaction and Water Content Ratio of Compacted Soil Using Hilf Rapid Method. Proceedings 4th International Conference on Geotechnical Engineering and Soil Mechanics, Iran.

Altun, S., Gokpete, A. B., & Sezer, A. (2008). Investigation of Parameters of Compaction Testing. Turkish Journal Of Engineering, Environment and Science, 32, 201–209.

AS 1289.5.7.1 (2006). Methods of Testing Soils For Engineering purposes Method 5.7.1: Soil Compaction and Density Tests—Compaction Control Test—Hilf density ratio and Hilf Moisture Variation (Rapid Method). AS.

ASBNT MB-3443. (1991). Solo - Controle de Compactação Pelo Método de Hilf. Rio de Janeiro: ABNT.

ASTM D422-63e2 (2007). Standard Test Method for Particle-Size Analysis of Soils. West Conshohocken, PA: ASTM International.

ASTM D4643 (2008). Standard Test Method for Determination of Water (Moisture) Content of Soil by Microwave Oven Heating. West Conshohocken, PA: ASTM International.

ASTM D2216-10 (2010a). Standard Test Methods for Laboratory Determination of Water (Moisture) Content of Soil and Rock by Mass. West Conshohocken, PA: ASTM International.

ASTM D4318-10e1(2010b). Standard Test Methods for Liquid Limit, Plastic Limit, and Plasticity Index of Soils. West Conshohocken, PA: ASTM International.

ASTM D6938-10(2010c). Standard Test Method for In-Place Density and Water Content of Soil and Soil Aggregate by Nuclear Methods (Shallow Depth). West Conshohocken, PA: ASTM international.

ASTM D2487-11 (2011a). Standard Practice for Classification of Soils for Engineering Purposes (Unified Soil Classification System). West Conshohocken, PA: ASTM International.

ASTM D4944(2011b). Standard Test Method for Field Determination of Water (Moisture) Content of Soil by the Calcium Carbide Gas Pressure Tester. West Conshohocken, PA: ASTM International.

ASTM D698-12e1(2012a). Standard Test Methods for Laboratory Compaction Characteristics of Soil Using Standard Effort (12,400 ft-lbf/ft3(600 kN-m/m3)). West Conshohocken, PA: ASTM International.

ASTM D1557 (2012b). Standard Test Methods for Laboratory Compaction Characteristics of Soil Using Modified Effort (56,000 ft-lbf/ft3 (2,700 kN-m/m3)). West Conshohocken, PA: ASTM International.

ASTM D1556-15 (2015). Standard Test Method for Density and Unit Weight of Soil in Place by the Sand-Cone Method. West Conshohocken, PA: ASTM International.

Berney IV, E. S., Kyzar, J. D., & Oyelam, L. O. (2011). Device Comparison for Determining Field Soil Moisture Content. Vicksburg.

Berney IV, E. S., & Kyzar, J. D. (2012). Evaluation of Non-Nuclear Soil Moisture and Density Devices For Field Quality Control. Transportation Research Board, 2310(1), 18–26.

Blanco, L., Santos-Ferreira, A., & Silva, P. F. da. (2015). Control of Compaction on Embankment Dam Core by Nuclear Density Meter and Sand Cone test. Geo-Environment and Construction European Conference, Tirana (Albania) - in press.

Braja, M. D. (2007). Fundaments of Geothechnical Engineering (Third Ed.). Madrid: Chris Carson.

Bretas, E. M., Lemos, J. V., & Lourenço, P. B. (2012). Mansonary Dams- Analysis of the historical profiles of Sazilly, Delocre and Rankine (copy).

Budhu, M. (2011). Soil Mechanics and Foundations (Third Edit.). USA: Jonh Wiley & sons, Inc.

Caldeira, L., & Brito, A. (2011). The Use of Soil-Rock Mixtures in Dams in Portugal. In: IX Jornadas Españolas de Presas, Valladolid: Comité Nacional Español de Grandes Presas.

CIGB. (2008). 80 anos- Barragens Para o Desenvolvimento Humano Sustentável. Lisboa: CIGB.

Colorado Department of Transportation - DOT (2003). Family of curves – one-point method fop for AASHTO T 272. Colorado: Colorado DOT.

CPNI. (2015). Testing Soil Conditions For Vehicle Security Barrier Tests. United Kingdom: CPNI.

Decreto-Lei n.º 344/2007. (2007). Regulamento de Segurança de Barragens. Diário da Republica, I Série. N.º 198 (15-10-2007).

Department of Transport. (1982). Technical Recomendations For Highways 9-Construction of Road Embankments. Pretoria: Department of Transport.

Distribution & Pipeline Technology Division-Gas Technology Institute. (2005). Evaluation of Soil Compaction Measuring Devices. Ilinois.

E196 (1966b). Solos Análise Granulomética. Lisboa: LNEC.

E197 (1966a). Solos. Ensaio de compactação. Lisboa: LNEC.

E204 (1967). Determinação da baridade seca “in situ” Pelo Método da Garrafa de Areia. Lisboa: LNEC.

E239 (1970). Análise Granulométrica por Peneiração Húmida. Lisboa: LNEC.

Emiroglu, M. E. (2008). Influences on Selection of the Type of Dam. International Journal of Science & Technology, 3(2), 173–189.

Environment Agency. (2014). Compliance Testing Earthworks on Landfill Sites Using Nuclear Density Gauges: LFE9 (copy).

Evans, J. (1996). Straightforward Statistics for the Behavioural Sciences. California: Brooks/Cole Publishing.

Faustino, V. (2009). Uma Contribuição Para a Divulgação das Barragens de Enrocamento com Cortina Interior de Betão Betuminoso em Portugal. Dissertação para obtenção do grau de Mestre, Lisboa: IST - UTL.

Fell, R., Macgregror, P., & Stapledon, D. (1992). Geotechnical Engineering of Embankment Dams (First Ed.). Rotterdam: A.A. Balkema Publishers.

Fell, R., Macgregror, P., & Stapledon, D. (2015). Geotechnical Engineering of embankment dams (Second ei.). London: Taylor & Francis Group.

Fernandes, M. de M. (2011). Mecânica dos Solos-Introdução à engenharia geotécnica, Volume 2. Faculdade de Engenharia da Universidade do Porto, Ed. (First Edit.). Porto: Norprint.

Foster, M. A., Fell, R., & Spannangle, M. (2000). The Statistics of Embankment Dam Failures and Accidents. Canadian Geotechnical Journal, 37:1000-10.

Foster, M. A., Fell, R., Davidson, R., & Wan, C. F. (2002). Estimation of The Probability of Failure of Embankment Dams by Internal Erosion and Piping Using Event Tree Methods. ANCOLD, Bulletin 121.

Galopim de Carvalho, A. M. (2003). Geologia Sedimentar-Volume I-Sedimentogénese (First Edit.). Lisboa: Âncora, Ed.

Gardner, R. P., Roberts, K. F., & Anday, M. C. (1967). Calibration Model for Optimizing Air-Gap Method of Compensating Nuclear Gages for Soil Composition Variation. Journal of Materials, 2(1), 3–19.

Gnaedinger, J. P. (1960). Experiences with Nuclear Moisture and Density Surface Probes on O'Hare Field Project. Symposium on Nuclear Methods for Measuring Soil Density and Moisture, (293), 36–44.

Guedes de Melo, F. (1985). Compactação de Aterro de Barragens de Terra. Lisboa: LNEC.

Gulhati, K. S., & Datta, M. (2008). Geotechnical Engineering (Fifthe Edi.). London: McGraw-Hill.

Hall, R. M., Lindsay, R., & Krayenhoff, M. (2012). Modern Earth Buildings (First Edit.). Cambridge: Woodhead.

Hatano, M. M., Hirsch, A. D., & Forsyth, R. A. (1973). Structure Backfill Testing. California.

Hilf, J. W. (1959). A Rapid Method of Construction Control For Embankments of Cohesive Soil. Engineering Monographs, (26).

Holtz, R. D., & Kovacs, William, D. (1981). An Introduction to geotechnical engineering. New Jersey: Pretence Hall, INC.

Howell, D. C. (2014). Fundamental Statistics for the Behavioural Sciences (Eighth Ed.). Belmont: Wadsworth.

ICOLD - International Comission of Large Dams. (1983). Deterioration of Dam Design. International Comission of Large Dams, (46).

ICOLD. (2011). Constitution. Paris.

ICOLD - European Group. (2012). Working group on Safety of Existing Dams. Paris: ICOLD.

ICOLD. (2014). General Synthesis. Retrieved December 31, 2014, from http://www.icold-cigb.org/GB/World_register/general_synthesis.asp

ISO/TS 17892-4:2004/Cor 1:2006 (2006). Geotechnical Investigation and Testing - Laboratory Testing of Soil - Part 4: Determination of Particle Size Distribution. Brussels: Comité Européen de Normalisation.

ISO/TS 17892-12:2004 (2006). Geotechnical Investigation and Testing - Laboratory Testing of Soil - Part 12: Determination of Atterberg Limits. Brussels: Comité Européen de Normalisation.

ISO 14688-2:2004/Amd 1:2013 (2013). Geotechnical Investigation and Testing - Identification and Classification of Soil - Part 2: Principles for a Classification - Amendment 1. Brussels: Comité Européen de Normalisation.

ISO 17892-1:2014 (2014). Geotechnical Investigation and Testing - Laboratory Testing of Soil - Part 1: Determination of Water Content. Brussels: Comité Européen de Normalisation.

Jesus, Diegues, R. (2011). Optimização da Forma Estrutural de uma Barragem. Dissertação de Mestrado, Universidade do Porto - Faculdade de Engenharia, Porto.

Kim, Y.-R., Kabassi, K., Zhuang, Z., Im, H., Wang, C., & Bode, T. (2011). Non-Nuclear Method for Density Measurements. Lincoln: Nebraska.

Kuhn, S. H. (1963). Effects of Material on Nuclear Density Measurements. Highway Research Record, 66, 1–14.

Lambe, T. W., & Robert, V. W. (1969). Soil Mechanics (First Ed.). Massachusetts Institute of Technology.

LeFevre, E. W. (1984). Determination of the Correlation Between Nuclear Mositure/Density Test And Standard Tests on Certain Gravel Bases in South Arkansas. University of Arkansas.

Maregesi, G. R. (n.d.). Validation of nuclear gauge density-meter readings against sand replacement method. AESL Site (http://www.aesl.co.tz/publication-dtl.php?pID=23), Consulted in February 4, 2015.

Martini, I, P., & Cesworth, W. (1992). Weathering, Soils and Paleosols. Amesterdam: Elsevier.

Martins, J. P. (2011). Compaction and its influence on the structural behaviour of high speed railways. Dissertação de Mestrado, Guimarães: Universidade do Minho.

Mejia, L. H., Sun, J. I., & Leung, K. k. (2005). Seismic Upgrade of Hydraulic Fill Dam by Buttressing. Soil Dynamics and Earthquake Engineering, 25(7-10), 571–579.

Mejías-Santiago, M., Berney IV, E. S., & Bradley, C. T. (2013). Evaluation of a Non-Nuclear Soil Density Gauge on Fine-Grained Soils. Vicksburg.

Ministério da Agricultura do Desenvolvimento Rural e das Pescas. (2000). Aproveitamento Hidroagricola de Coutada/Tamujais Barragem - Projecto de execução, Volume I - Memória descritiva Tomo I.2 - Estudo geológico-geotécnico. Lisboa, relatório não publicado.

Ministry of Railways. (2005). Study report on compaction equipments. Manak Nager.

Mooney, M., ASCE, A. M., & Dietmar, A. (2007). Vibratory Roller Integrated Measurement of Earthwork Compaction: An Overview. 7th International Symposium on Field Measurements in Geomechanics, Boston, Massachusetts. ASCE.

Moum, A. R., Frink, D. L., & Pope, E. J. (1985). North Dakota Dam Design Handbook (Second Ed.). Bismarck, North Dakota: North Dakota State Engineer.

National Research Council. (1983). Safety of Existing Dams, Evaluation and Improvement. National Academy Press.

Neves, J., Duarte, A., & Silva, C. (2013). Study of Laboratory and Field Tests Related to Soil Compaction Based on Proficiency Testing Schemes. Journal of Materials Science and Engineering, 3(12), 772–779.

NP 84 (1965). Solos. Determinação do Teor em Água. Lisboa: LNEC.

NP143 (1969). Determinação dos Limites de Consistência. Lisboa: LNEC.

Pimenta, L. (2008). Abordagens de Riscos em Barragens de Aterrro. IST UTL.

Quintela, António, de C., Cardoso, João, L., & Mascarenhas, J. M. (1989). Barragens Antigas em Portugal a Sul do Tejo. Encontros Sobre El Tajo: El Agua Y Los Asentamientos Humanos, Cuadernos.

Rahardjoa, H., Aungb, K. K., Leongc, E. C., & Rezaurd, R. B. (2004). Characteristics of residual soils in Singapore as formed by weathering. Engineering Geology, 73, 157–169.

Raj, P. P. (2008). Soil Mechanics & Foundation Engineering (First Ed.). New Delhi: Dorling Kindersley (India).

Ralston, H. H., & Anday, M. C. (1963). Nuclear Measurements of Soil Properties. Highway Research Record, (66), 14–50.

Ranjan, G., & Rao, A. S. R. (2005). Basic and Applied Soil Mechanics. New Delhi: New Age Internation Publishers.

Ribeiro, O., Teixeira, C., Ferreira, C. R., & Alves, C. A. de M. (1967). Carta geológica de Portugal na Escala de 1/50.000 : Notícia Explicativa da folha 24-D, Castelo Branco : Estudos Petrográficos. Lisboa: Serviços Geológicos de Portugal.

Roberts, E. A., Sheley, R. L., & Lawrence, R. L. (2004). Using Sampling and Inverse Distance Weighted Modeling for Mapping Invasive Plants. Western North American Naturalist, 64(3), 312–323.

Santos, Jaime., A. (2008). Compactação - Elementos Teóricos. Notas de aula. Lisboa: Instituto Superior Técnico - Departamento de Engenharia Civil e Arquitectura.

Santos-Ferreira, A., & Dias, E. (2007a). Aproveitamento Hidroagrícola de Coutada / Tamujais Memória Descritiva: Aterro Experimental, Procedimentos de Excução do Aterro Experimental da Barragem da Coutada/Tamujais. Lisboa, relatório não publicado.

Santos-Ferreira, A., & Dias, E. (2007b). Memorando Técnico- Aproveitamento Hidroagrícola de Coutada/Tamujais-Barragem. Lisboa, relatório não publicado.

Seed, H. B., & Chan, C. K. (1959). Structure and Strength Characteristis of Compacted Clays. Journal of the Soil Mechanincs and Foundations Division, ASCE, 85(5), 87–128.

Selley, R. C. (2000). Applied Sedimentology (Second Ed.). San Diego, California: Academic Press.

Singh, B., & Varshey, R. S. (1995). Engineering for Embankments Dams (First Ed.). Rotterdam: A.A. Balkema Publishers.

Singh, V. P. (1996). Dam Breach Modeling Technology (First Edit.). Springer Science+Business Media Dordrecht.

Solava, S., & Delatte, N. (2003). Teton Dam Failure Case Study. Procedings 3rd ASCE Forensics Congress, 1–9.

Terzaghi, K., & Peck, R. (1996). Soil Mechanics in Engineering Pratice (Third Ed.). Urbana Ilinois: Wiley International.

Todor, P. C., & Gartner Jr., W. (1966). Evaluation of Direct Transmission - Type Nuclear Density Gage for Measuring In-Place Densities of Soils. Highway Research Record, (107), 13–24.

Truesdale, W. B., & Selig, E. T. (1967). Evaluation of Rapid Field Methods for Measuring Compacted Soil Properties. Highway Research Record, (177), 58–97.

USACE. (2004). General Design and Construction Considerations for Earth and Rock-Fill Dams. USACE.

USBR- United States Bureau of Reclamation. (1987). Design of Small Dams (Third Edit.). Washington, DC: United States Department of the interior.

USBR. (1991). Design Standards. Embankment dams, No. 13, Chapter 10. Embankment construction. Denver,Colorado: US Bureau of Reclamation (USDI - BR).

USBR. (1998). Earth manual-Part I. Revised (First Ed). Washington, DC (Third Edit.). Denver, Colorado: USDI - BR.

USBR. (2011a). Design Standards No.13, Embankment Dams. USDI-BR.

USBR. (2011b). Embankment Dams. (U. S. D. of T. Interior, Ed.) (First Edti., Vol. 4). Washington, DC: United States Department of the interior.

USBR. (2014). Using Intelligent Compaction for Better Earthwork Construction Control. Bulletin USBR, (6).

Venkatramaiah, C. (2006). Geotechnical Engineering (Third Ed.). New Delhi: New Age International.

Vicroads. (2011). Technical Note-Surveillance of Field Density Testing by Nuclear Density Gauge. Victoria: State Goverment of Vitoria.

Wan, Fai, C., & Fell, R. (2004). Investigation of Rate of Erosion of Soils in Embankment Dams. Journal of Geotechnical and Geoenvironmental Engineering, 130(4), 373–380.

Weber, J. W. G. (1963). Laboratory and Field Evaluation of Nuclear Gages for Determining Soil Moisture and Density. Highway Research Record, 66, 51–72.

Weslie, L. (2009). Behaviour and Geotechnical Properties of Residual Soils and Allophane Clays. Obras y Projectos, (6), 5–10.

Xu, Y., Zhang, L. M., & Jia, J. S. (2007). Analysis of Earth Dam failures - a Database Approach. In: First international Symposium on Geotechnical Safety & Risk (pp. 293–302). Shanghai.

ANNEXES

ANNEX I - HILF METHOD

I.a. DRY DENSITY

Considering an in situ SCT test for measuring the fill unit weight, the sample retrieved from this test was protected against evaporation. The Proctor test will be applied to the sample material compacting it at its fill water content (ω_{fill}) to achieve the "cylinder" wet unit weight (γ_{ω_c}). The curves of wet unit weight *versus* water content and dry unit weight versus water content can be obtained with the test results, both curves are illustrated in Figure I.A.

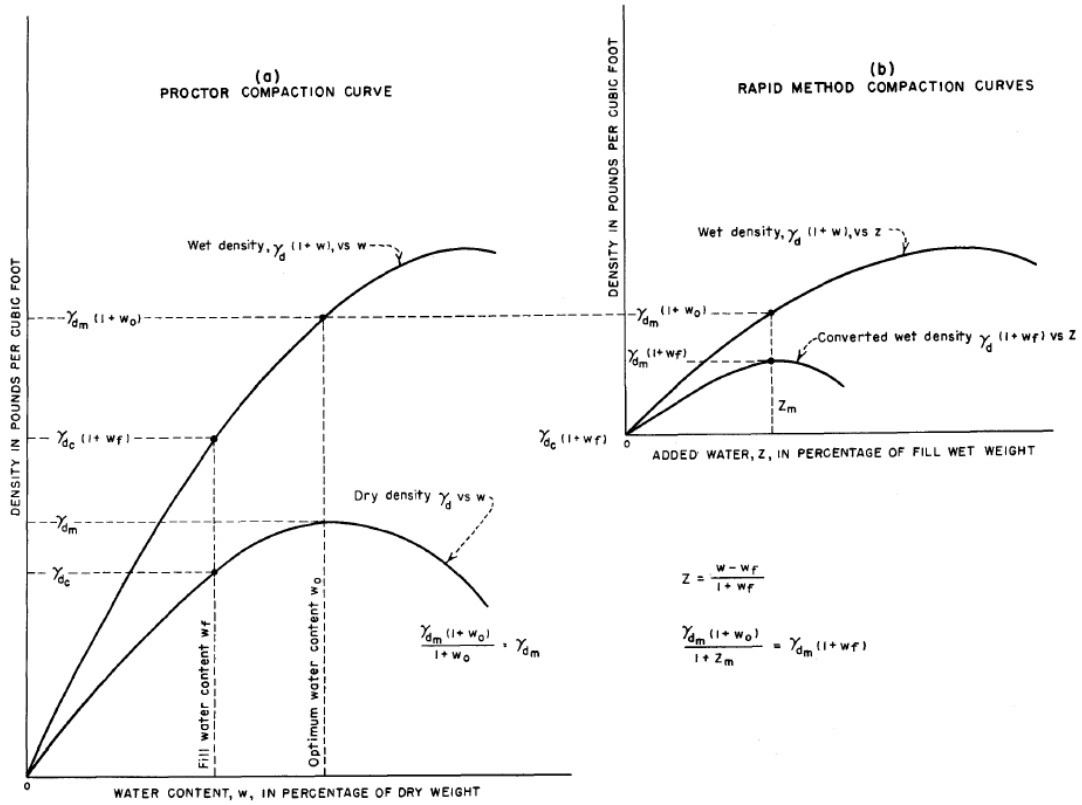

Figure I.A – Comparison between the curves obtained with the Hilf method and the Proctor test (Hilf, 1959).

As can be observed form Figure I.A, every value of fill wet weight and cylinder wet unit weight have the same water content. A parameter C can be defined considering a ratio between both unit weights (Equation I.A); this parameter expresses a relation between the fill and laboratory compactive efforts.

$$\frac{\gamma_{\omega_{fill}}}{\gamma_{w_c}} = \frac{\gamma_{d_{fill}} \times (1+\omega_{fill})}{\gamma_{d_c} \times (1+\omega_{fill})} = \frac{\gamma_{d_{fill}}}{\gamma_{d_c}} = C \qquad (I.A)$$

Where:

$\gamma_{\omega_{fill}}$- Fill wet unit weight;

γ_{ω_c}- Cylinder wet unit weight;

ω_{fill}- Fill water content;

$\gamma_{d_{fill}}$- Fill dry unit weight;

γ_{d_c}- Cylinder dry unit weight.

The degree of compaction can also be obtained from this curves using the cylinder maximum density, through Equation I.B.

$$DC = \frac{\gamma_{d_{fill}} \times (1 + \omega_{fill})}{\gamma_{d_m} \times (1 + \omega_{fill})} = \frac{\gamma_{d_{fill}}}{\gamma_{d_m}} \qquad (IIB)$$

Where:

γ_{d_m}- Cylinder maximum unit weight.

The Hilf's rapid method is an expedite method used to obtain the value of Equation I.C.

$$y_\omega = \gamma_{d_m}(1 + \omega_{fill}) \qquad (\mathrm{I.C})$$

Where:

w_{fill} - Water content in the fill.

The cylinder wet unit weight (γ_{ω_c}) for any soil sample with an water content inferior to the optimum and compacted in a specified manner, can be calculated with Equation I.D.

$$y_{\omega_c} = \gamma_{d_c}(1 + \omega_{fill}) \qquad (\mathrm{I.D})$$

The cylinder wet unit weight can be obtained by the Proctor test at any water content, therefore this point will be used as the origin of new curves obtained by translating the origin of abscissas to fill water content, (Figure I.A). The abscissa of the new curves will be defined as z, which represents the amount of water added to the soil in percentage of fill unit weight, this modification is the same as considering the soil retrieved from the fill to be dry, in other words the water content is considered as solid material.

A wet unit weight *vs* z curve can be obtained by adding water and applying the proctor methodology to the fill sample, as the one illustrated by the upper curve in the Figure I.A. The ordinate values are the same for both wet unit weight curves represented in a) and b).

The curve equivalent to the Proctor dry unit weight curve illustrated in Figure I.A can be obtained by dividing the ordinates from the upper curve by $(1 + z)$ and is known as converted wet density, this curve is illustrated by the lower curve represented in the Figure I.A. The ordinate values for this curve correspond to $\gamma_d(1 + \omega_{fill})$. This can be demonstrated by the paragraphs bellow.

The ordinated of the converted dry density were calculated by dividing $\gamma_d(1 + \omega)$ by $(1 + z)$, z can be defined by Equation I.E.

$$z = \frac{\Delta W_\omega}{W} = \frac{\omega W_s - \omega_{fill} W_s}{W_s(1 + \omega_{fill})} = \frac{\omega - \omega_{fill}}{1 + \omega_{fill}} \qquad (I.E)$$

So $(1 + z)$ is equal to:

$$1 + z = 1 + \frac{\omega - \omega_{fill}}{1 + \omega_{fill}} = \frac{1 + \omega}{1 + \omega_{fill}} \qquad (I.F)$$

Dividing $\gamma_d(1 + \omega)$ by $(1 + z)$:

$$\frac{\gamma_d(1 + \omega)}{1 + z} = \frac{\gamma_d(1 + \omega)}{\frac{1 + \omega}{1 + \omega_{fill}}} = \gamma_d\left(1 + \omega_{fill}\right) \qquad (I.G)$$

Therefore the maximum converted wet density can be obtained by $\gamma_{d_m}\left(1 + \omega_{fill}\right)$, $\left(1 + \omega_{fill}\right)$ is constant.

The proctor curves illustrated in the Figure I.A, which represent the classical approach for control of compaction operations are dependent on the determination of the water content, however the curves defined in Figure I.A can be obtained without knowing the water content since the values of z are a ratio of known water masses added to a soil sample retrieved from the fill.

Once knowing the ordinate of the converted wet density curve peak point, it is possible to determinate the degree of compaction by Equation I.H.

$$DC = \frac{\gamma_{d_{fill}}}{\gamma_{d_m}} \qquad (I.H)$$

For the determination of the peak point needs at least three points need to be plotted.

I.b. WATER CONTENT

The peak point of the converted wet densities indicates if the soil is at the optimum water content or not, however the magnitude of the difference between the soil water content and the optimum water content $\left(\omega_{opt}\right)$ is unknown. From the Equation I.I comes that:

$$z_m = \frac{\omega_{opt} - \omega_{fill}}{1 + \omega_{fill}} \Leftrightarrow \omega_{opt} - \omega_{fill} = z_m(1 + \omega_{fill}) \qquad (I.I)$$

Where:

z_m - Abscissa correspondent to the peak point.

Through Equation I.J follows that:

$$1 + \omega_{fill} = \frac{1 + \omega_{opt}}{1 + z_m} \qquad (I.J)$$

Therefore $\omega_{opt} - \omega_{fill}$can also be calculated by Equation I.L.

$$\omega_{opt} - \omega_{fill} = \frac{z_m}{1 + z_m}\,(1 + \omega_{0pt}) \qquad (I.L)$$

The values of ω_{opt} and ω_{fill} are not known, however this values can determined by estimation. A set of curves was developed to estimate ω_{opt} from the coordinates of the peak point of the converted wet unit weight curve. The relation between the peak point of the converted curve and the wet unit weight at optimum water is illustrated in Figure I.A. These curves are defined in the work of (Hilf, 1959).

ANNEX II - CHARACTERIZATION TEST FOR ALLUVIAL MATERIALS

II.a. SIEVE ANALYSIS AND CONSISTENCY LIMITS

Laboratory tests used to characterize the particle size distribution, and consistency limits were taken on those samples, the results and the respective soil classification according to AASHTO and ASTM classification systems are defined in the Table II.A.

Table II.A - Identification tests in the samples retrieved from area A (adapted from MADRP, 2000).

Site	Well	Phase	Depth (m)	Grading			Consistency limits			Classifications	
				Mud+ Silt (%)	Sand (%)	Gravel (%)	LL (%)	LP (%)	IP (%)	ASTM	AASHTO
Flood Plain	P7	1ª (E.V.)	0,5 - 1,5	5	--	--	22	15	7	GW-GC-GM	A-2-4(0)
	P9		1,5 - 2,5	6	--	--	22	14	8	GP-GC	A-2-4(0)
	P1	2ª	0,7 - 2,0	24	59	17	19	14	5	SC-SM	A-2-4(0)
	P2		0,2 - 1,4	10	30	60	25	14	11	GW-GC	A-2-6(0)
	P3		0,2 - 2,4	19	44	37	23	18	5	SC-SM	A-1-b(0)
	P4		0,3 - 2,5	16	36	48	21	14	7	SC	A-2-4(0)
	P8		0,3 - 2,8	6+7	24	63	24	18	6	GC-GM	A-1-a(0)
	P9		0,3 - 3,0	10	18	72	27	18	9	GP-GC	A-2-4(0)
	P10		0,4 - 4,7	7+13	30	50	20	13	7	SC	A-2-4(0)
	P11		0,4 - 4,0	22	33	45	NP	NP	NP	SM	A-1-b(0)
	P12		0,3 - 2,8	14	31	55	23	16	7	GC-GM	A-2-4(0)
	P13		0,3 - 2,9	35	32	34	25	18	7	SC	A-2-4(0)
	P14		0,5 - 2,5	17	36	47	20	13	7	SC-SM	A-2-4(0)

The grading curves for the samples retrieved in the area A and listed in the Table II.A are defined in the Figure II.A, the hydrometer test was applied to the samples retrieved from the wells P8 and P10.

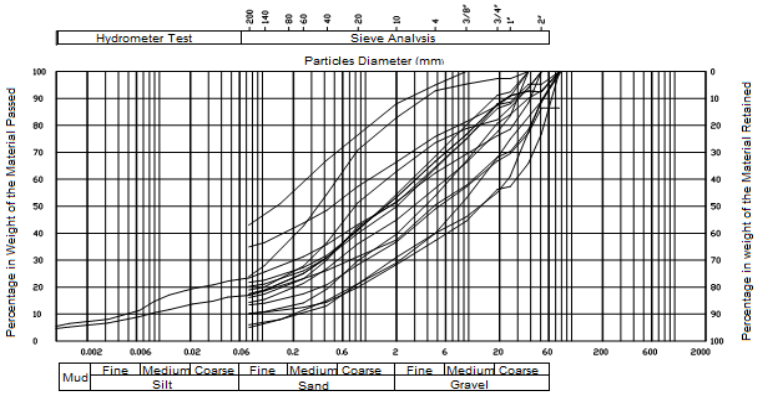

Figure II.A - Gradation curves from the samples retrieved in the borrow area A (adapted from MADRP, 2000).

The location of this samples on the plasticity chart is defined bellow:

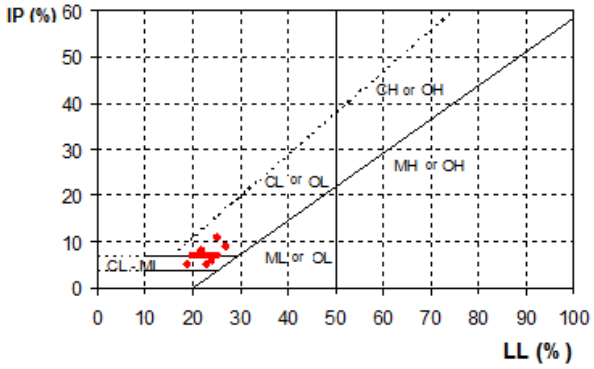

Figure II.B - Location of the samples retrieved from borrow area A in the plastic chart (MADRP, 2000)

II.b. COMPACTION TEST

The Proctor test was executed on the samples retrieved from the pits P3, P8, P9, P10, and P13. The results are defined in the Table II.B.

Table II.B - Results from the standard Proctor Test in the Samples at Area A (adapted from MADRP, 2000).

Well	Depth (m)	Standard Proctor		γ (kN/m³)	γ_{sat} (kN/m³)	S (%)	e (--)	n (--)
		γ_{dmax} (kN/m³)	ω opt (%)					
P3	0,2 - 2,4	19,8	9,8	21,74	22,18	81,37	0,31	0,24
P8	0,3 - 2,8	20,1	9,2	21,95	22,37	81,49	0,29	0,23
P9	0,3 - 3,0	20,1	9,8	22,07	22,37	86,80	0,29	0,23
P10	0,4 - 4,7	20,6	8,7	22,39	22,68	86,29	0,26	0,21
P13	0,3 - 2,9	20,1	8,8	21,87	22,37	77,95	0,29	0,23

The $(\gamma_{d\,max}, \omega_{opt})$ points obtained for each sample are represented in the Figure II.C.

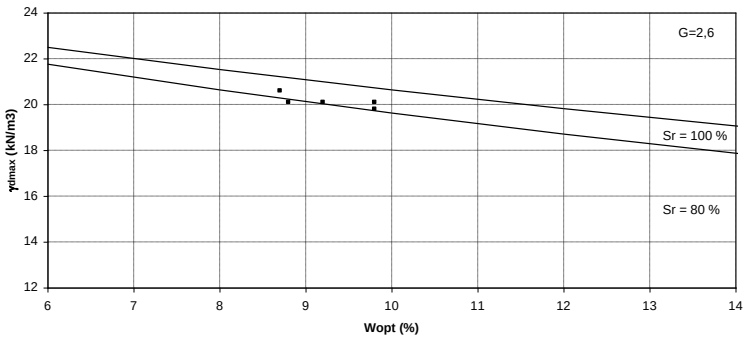

Figure II.C - Results of the Standard Proctor test plotted in a $(\gamma_{d\,max}, \omega_{opt})$ graphic (adapted from MADRP, 2000)

ANNEX III - CHARACTERIZATION TEST FOR ARKOSIC MATERIALS

III.a. SIEVE ANALYSIS AND CONSISTENCY LIMITS

Laboratory tests to identify the particle size distribution, and the Atterberg limits were taken on those samples, the results and the respective soil classification according to AASHTO and ASTM classification systems are defined in the Table III.A.

Table III.A - Identification tests taken in the samples retrieved from area B (adapted from MADRP, 2000).

Site	Well	Phase	Depth (m)	Grading			Consistency limits			Classifications	
				Mud + Silt (%)	Sand (%)	Gravel (%)	LL (%)	LP (%)	IP (%)	ASTM	AASTHO
ME	P5	1ª	0,5 - 2,2	91	--	--	73	35	38	MH	A-7-5(20)
	P5	2ª	0,3 - 3,5	12	31	57	20	13	7	SP-SC	A-2-4(0)
	P6		0,2 - 3,0	14	34	52	18	11	7	SC	A-2-4(0)
	P7		0,4 - 2,0	21	40	39	30	14	16	SC	A-2-6(0)
MD	P10	1ª	0,3 - 1,5	16	--	--	30	20	10	SC	A-2-4(0)
	P11		0,5 -2,0	10	--	--	26	19	7	GP-GC-GM	A-2-4(0)
	P15	2ª	0,2 - 3,7	26	74	0	27	16	11	SC	A-2-6(0)
	P16		0,5 - 3,5	23	60	17	29	19	10	SC	A-2-4(0)
	P17		0,1 - 3,6	25	58	17	35	17	18	SC	A-2-6(1)
	P18		0,4 - 3,7	29	54	17	40	18	22	SC	A-2-6(2)
	P21		0,4 - 3,1	51	49	0	39	19	20	CL	A-6(7)
	P22		0,4 - 3,2	36	39	25	28	14	14	SC	A-6(1)
	P23		0,9 - 3,6	14+15	58	13	42	23	19	SC	A-2-7(1)
	P24		0,3 - 3,5	17+10	51	22	38	18	20	SC	A-2-6(1)
	P25		0,3 - 3,7	23	54	23	35	16	19	SC	A-2-6(1)
	P27		1,2 - 3,5	22	24	54	25	16	9	GC	A-2-4(0)
	P29		0,5 - 4,0	37	63	0	42	21	21	SC	A-7-6(3)
	P19		1,6 - 3,6	29	27	44	26	16	10	SC	A-2-4(0)
	P20		0,2 - 3,8	52	45	3	37	19	18	CL	A-6(6)

The grading curves for the samples retrieved in the area A and listed in the Table III.A are defined in the Figure III.A, the hydrometer test was applied to the samples retrieved from the wells P23 and P24.

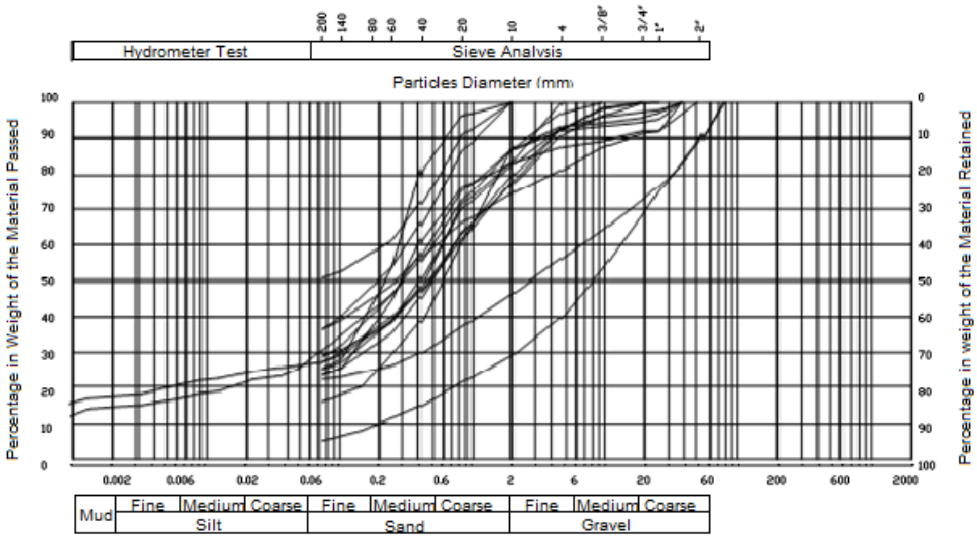

Figure III.A - Gradation Curves from the samples retrieved in the borrow area B (adapted from MADRP, 2000).

The location of this samples on the plasticity chart is defined bellow.

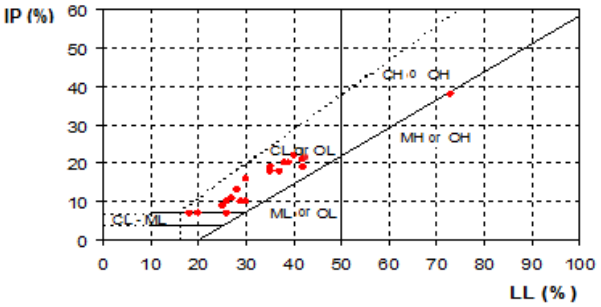

Figure III.B - Location of the samples retrieved from borrow area A in the plasitic chart (MADRP, 2000)

III.b. COMPACTION TEST

The Proctor test was executed on the samples retrieved from the wells P23, P24, P25, and P29. The results are defined in the Table III.B below.

Table III.B - Results from the Standard Proctor Test in the Samples from the Area B (adapted from MADRP, 2000)

Well	Depth (m)	Standard Proctor		γ (kN/m³)	γ_{sat} (kN/m³)	S (%)	e (--)	n (--)
		d máx (kN/m³)	ω opt (%)					
P23	0,9 - 3,6	18,7	11,7	20,89	21,51	77,93	0,39	0,28
P24	0,3 - 3,5	18,7	13,5	21,22	21,51	89,91	0,39	0,28
P25	0,3 - 3,7	18,7	10,9	20,74	21,51	72,60	0,39	0,28
P29	0,5 - 4,0	18,8	12,3	21,11	21,57	83,50	0,38	0,28

The $(\gamma_{d\,max}, \omega_{opt})$ points obtained for each sample are represented in the Figure 4.8.

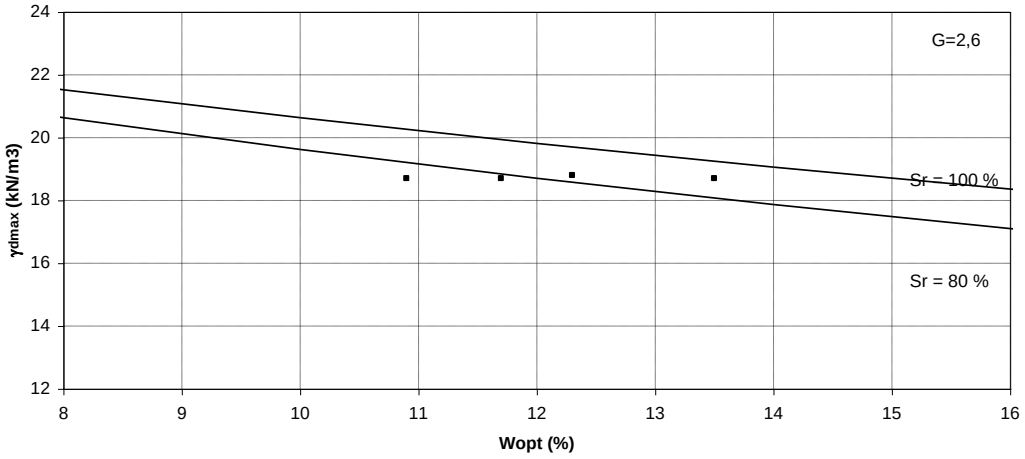

Figure III.C - Results of the Standard Proctor test plotted in a $(\gamma_{d\,max}, w_{opt})$ graphic (adapted from MADRP, 2000).

ANNEX IV - HISTOGRAMS FOR THE TRIAL EMBANKMENT RESULTS

IV.a. Stage 1 - HISTOGRAMS FOR THE ω_{OPT}-2% LAYER

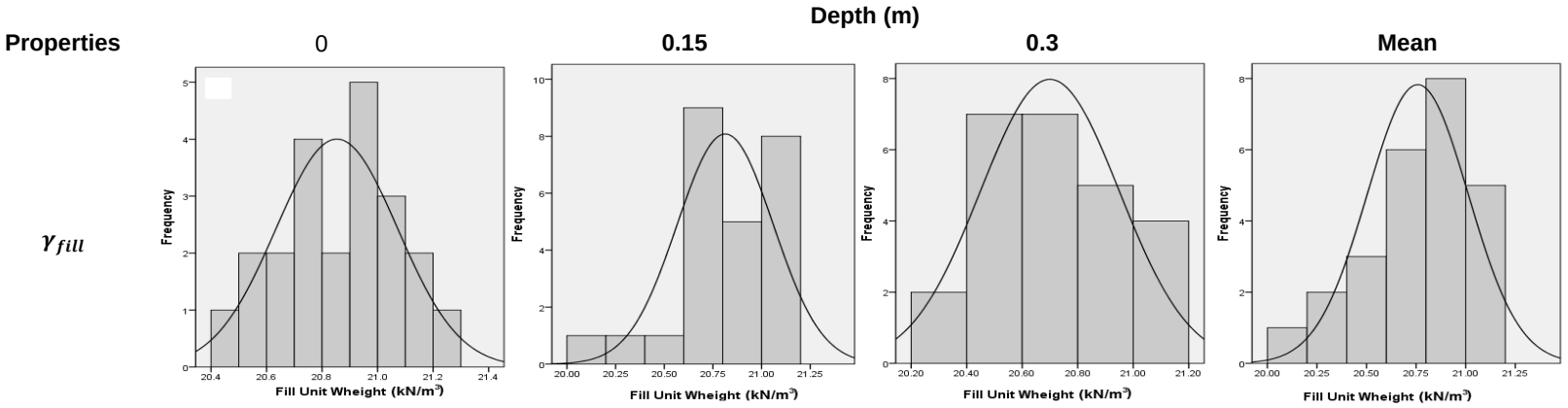

Figure IV.A - Histograms for the γfill results obtained in stage 1, with the NDG in the ωopt-2% layer.

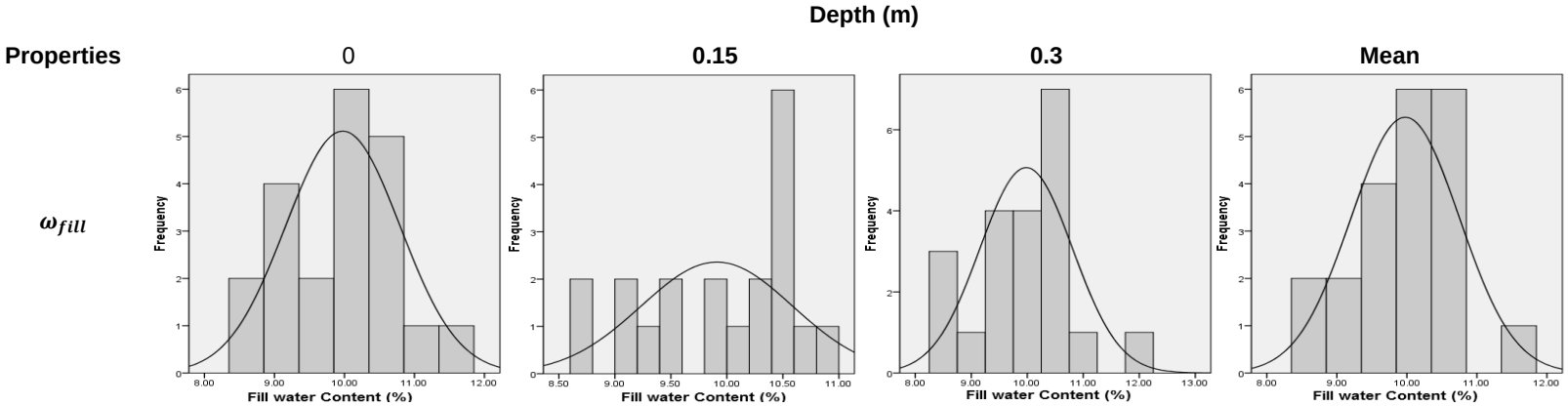

Figure IV.B - Histograms for the ω_{fill} results obtained in stage 1, with the NDG in the ωopt-2% layer.

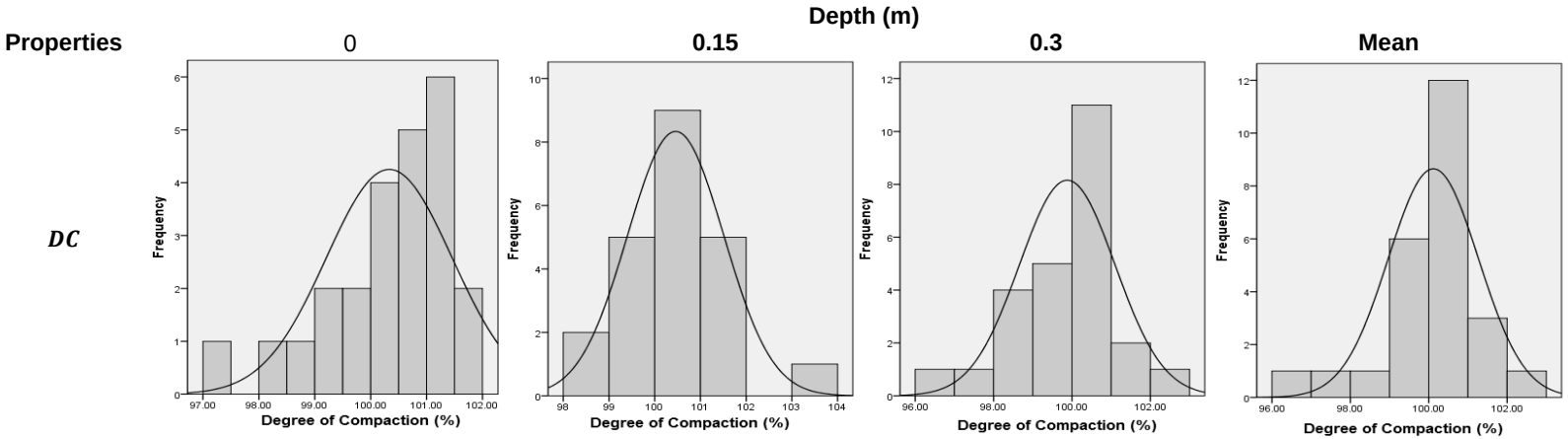

Figure IV.C - Histograms for the DC results obtained in stage 1, with the NDG in the ωopt-2% layer.

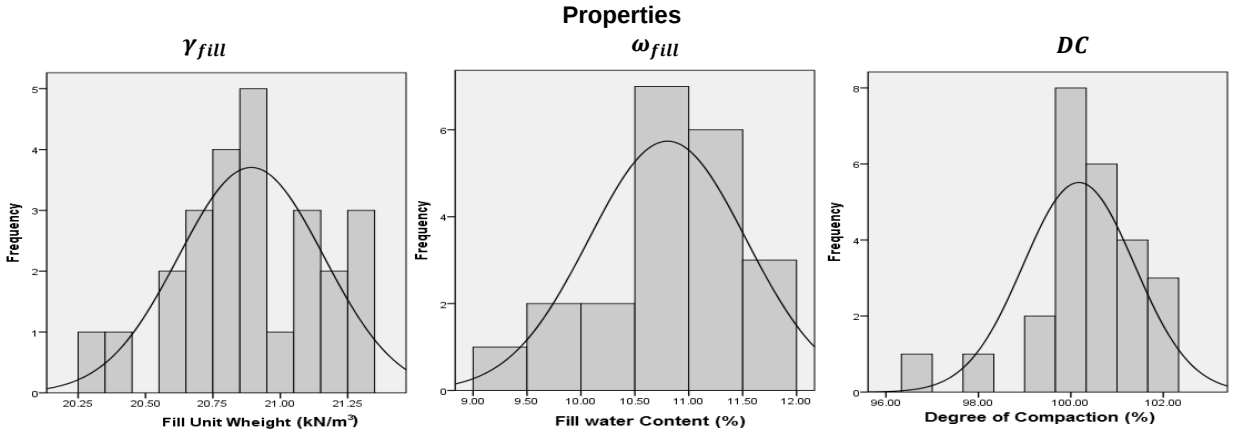

Figure IV.D - Histograms for the results obtained in stage 1, with the SCT in the ωopt-2% layer.

IV.b. STAGE 1 - HISTOGRAMS FOR THE ω_{OPT}% LAYER

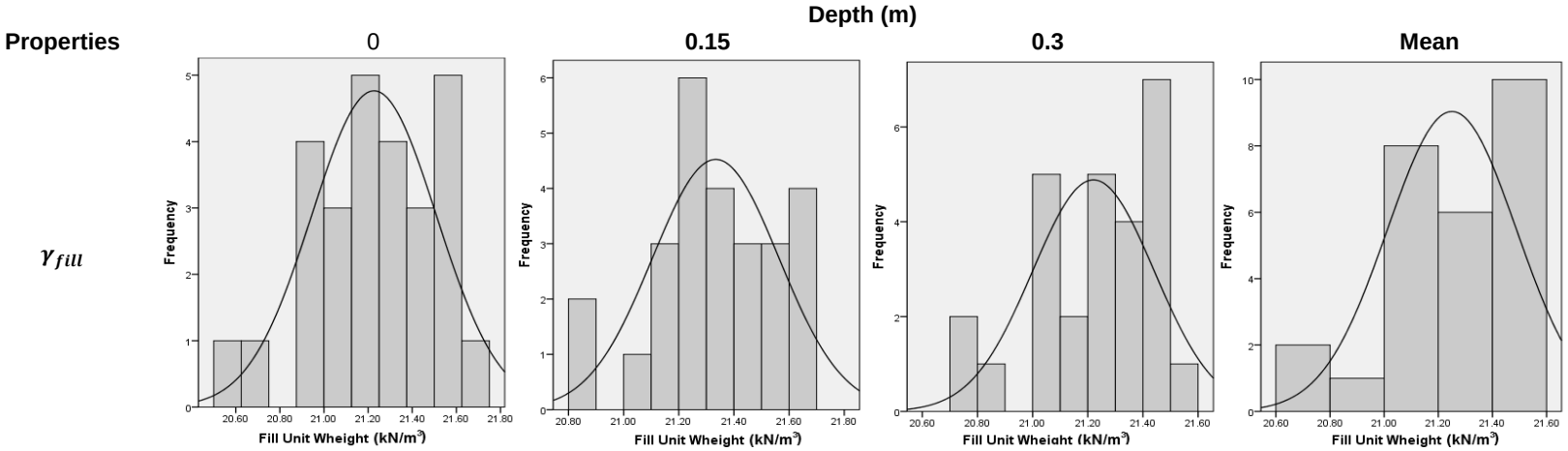

Figure IV.E - Histograms for the γ_{fill} results obtained in stage 1, with the NDG in the ωopt% layer.

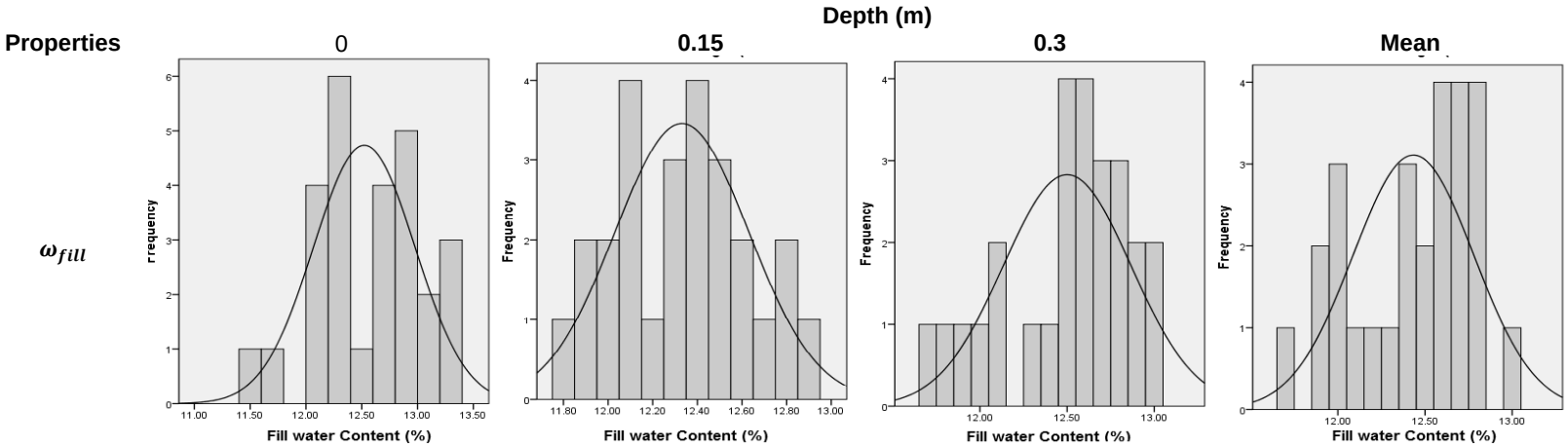

Figure IV.F - Histograms for the ω_{fill} results obtained in stage 1, with the NDG in the ωopt% layer.

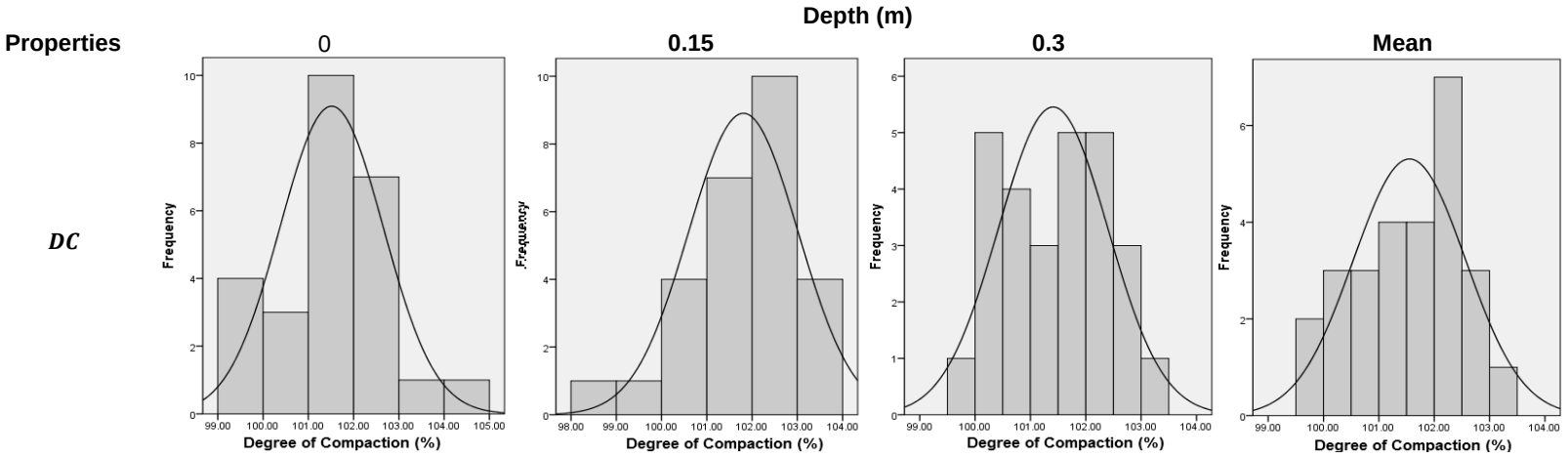

Figure IV.G - Histograms for the DC results obtained in stage 1, with the NDG in the ωopt% layer.

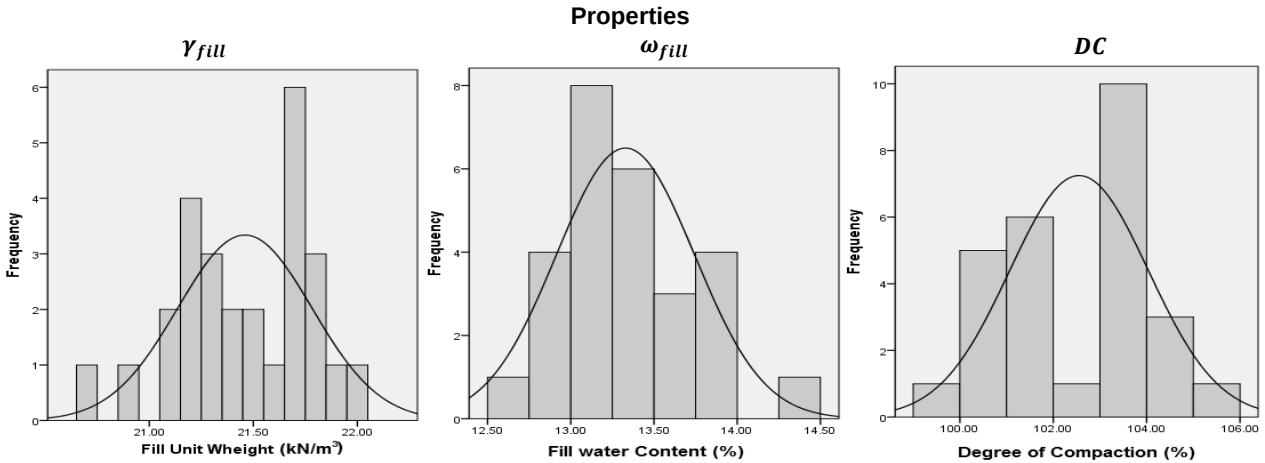

Figure IV.H - Histograms for the results obtained in stage 1, with the SCT in the ωopt% layer.

IV.c. STAGE 1 - HISTOGRAMS FOR THE ω_{OPT}+2% LAYER

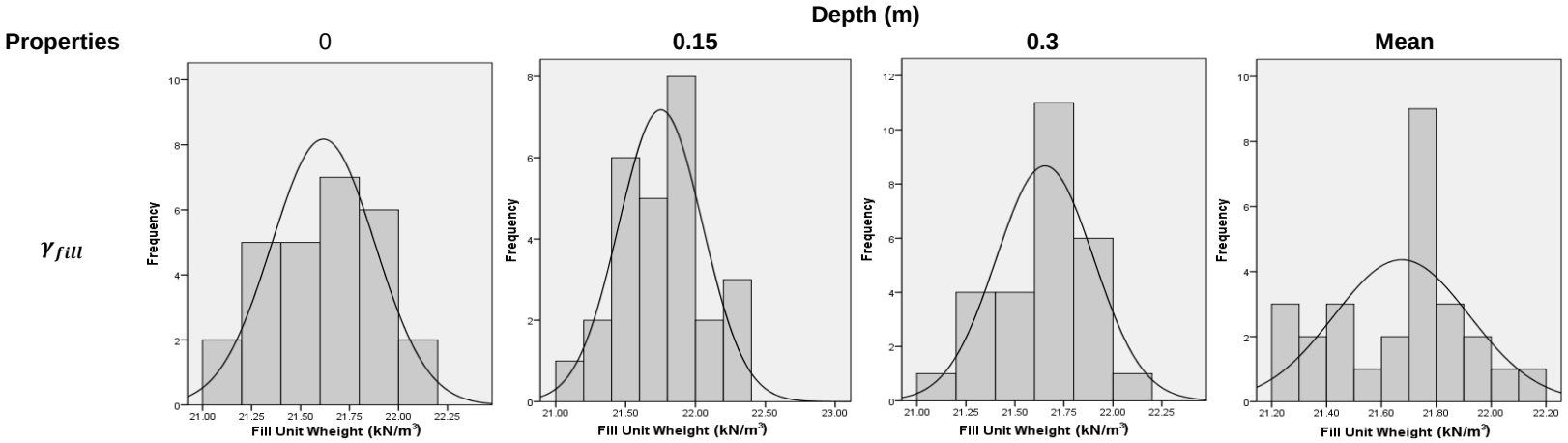

Figure IV.I - Histograms for the γ_{fill} results obtained in stage 1, with the NDG in the ωopt+2% layer.

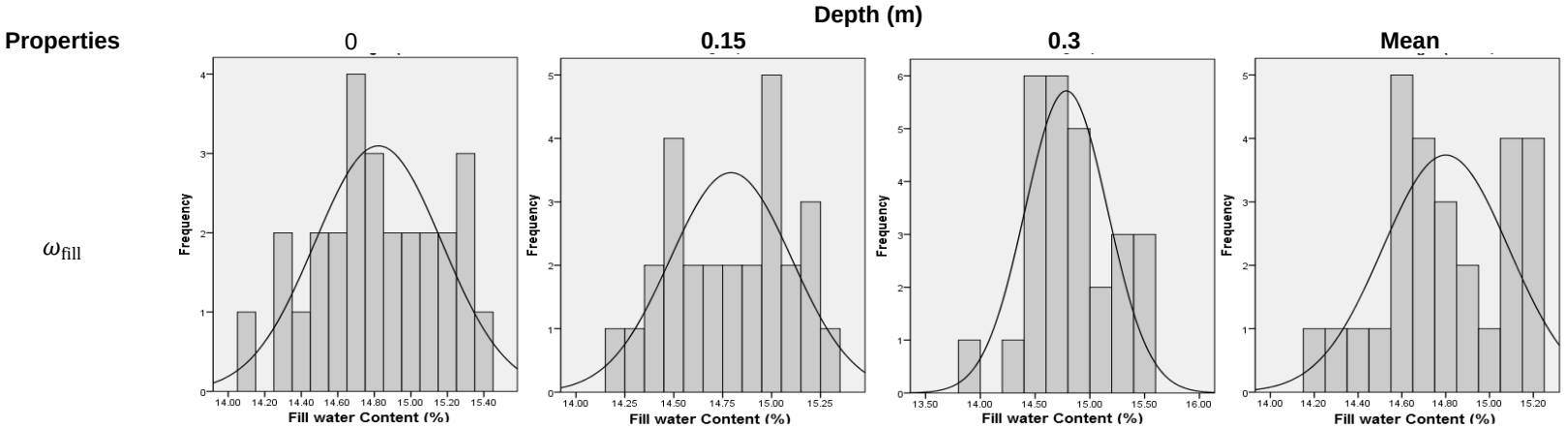

Figure IV.J - Histograms for the ω_{fill} results obtained in stage 1, with the NDG in the ωopt+2% layer.

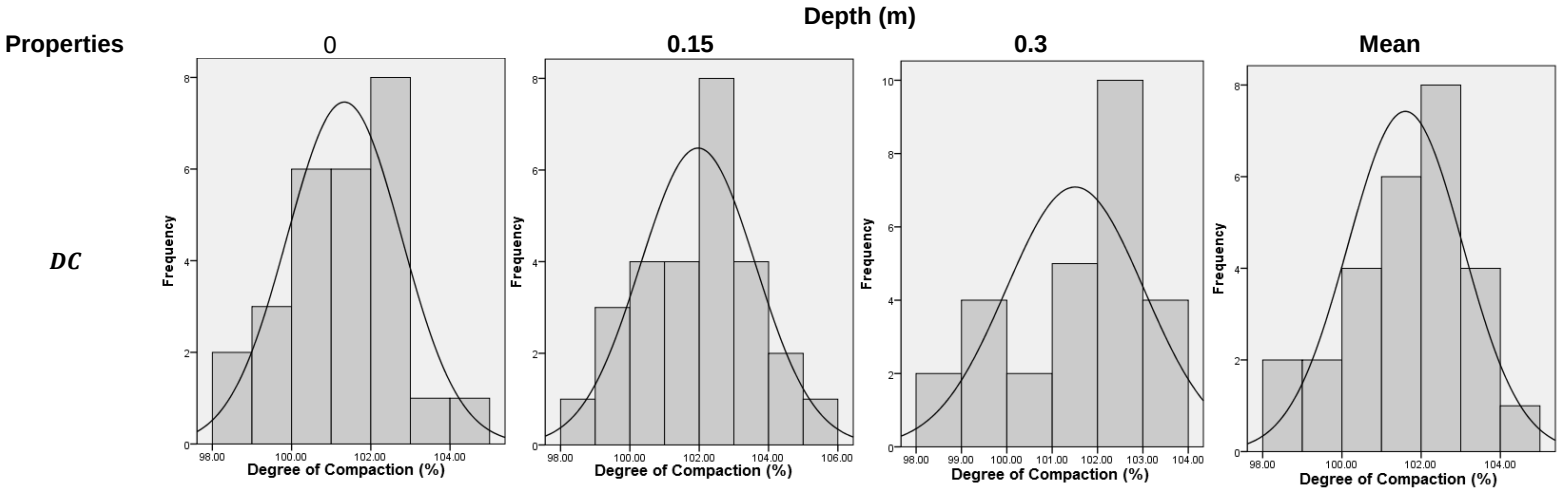

Figure IV.K - Histograms for the DC results obtained in stage 1, with the NDG in the ωopt+2% layer.

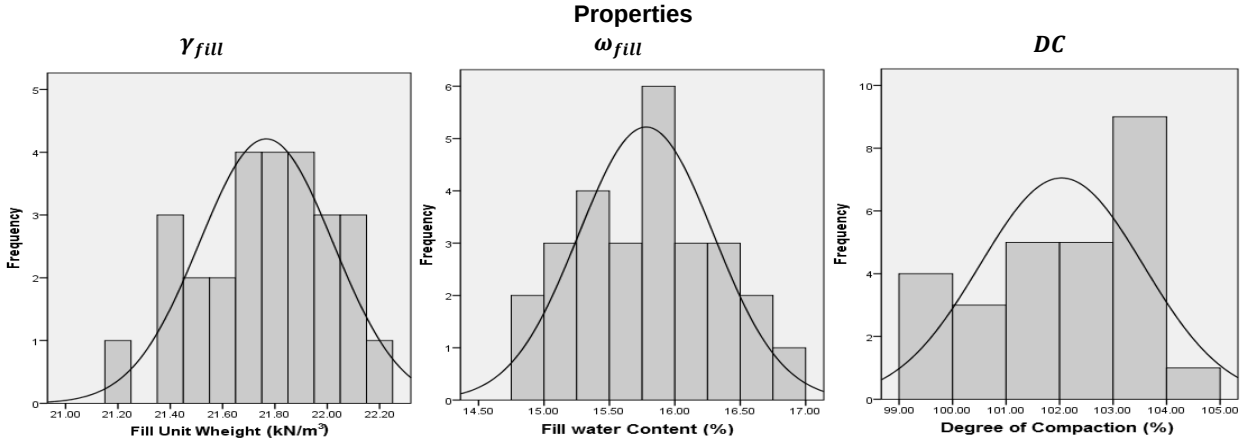

Figure IV.L - Histograms for the results obtained in stage 1, with the SCT in the ωopt+2% layer.

IV.d. STAGE 2 - HISTOGRAMS FOR THE ω_{OPT}-2% LAYER

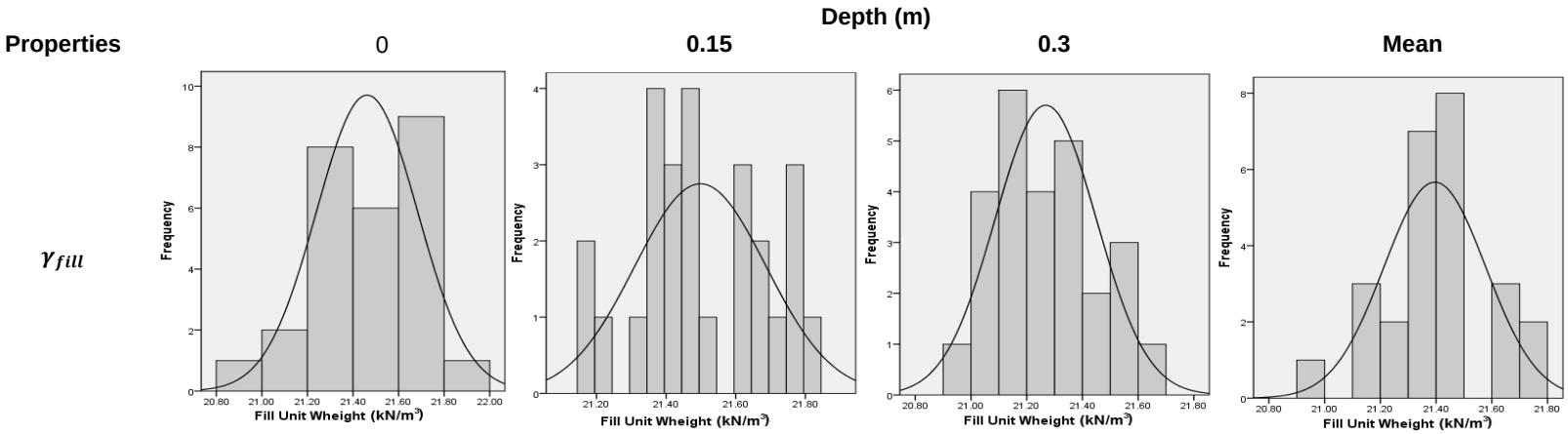

Figure IV.M - Histograms for the γ_{fill} results obtained in stage 2, with the NDG in the ωopt-2% layer.

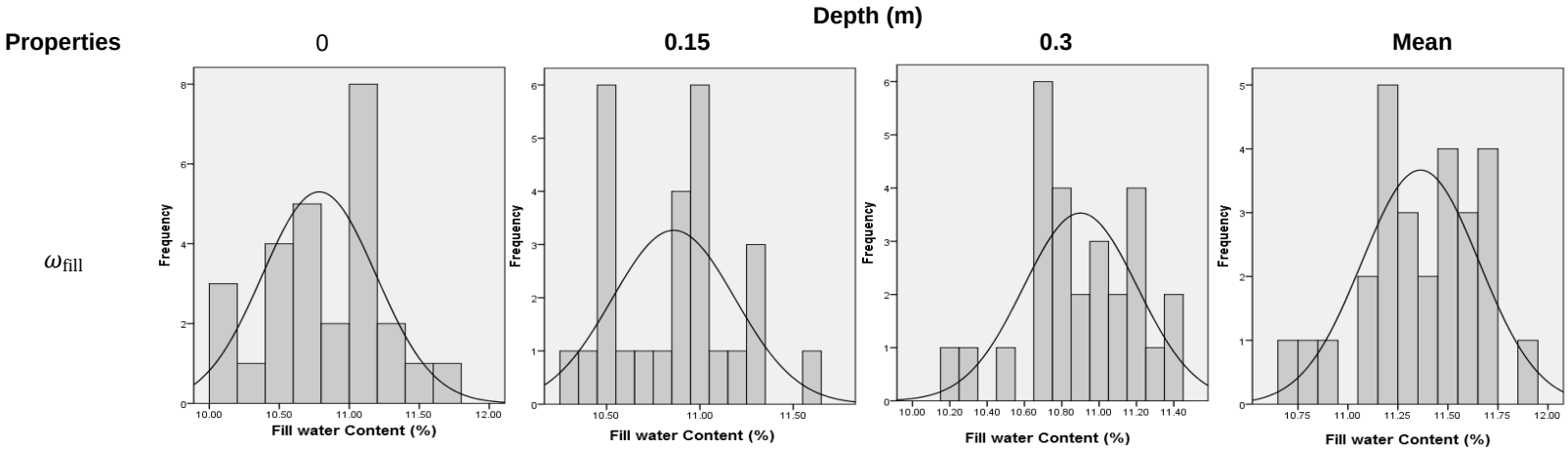

Figure IV.N - Histograms for the ω_{fill} results obtained in stage 2, with the NDG in the ωopt-2% layer.

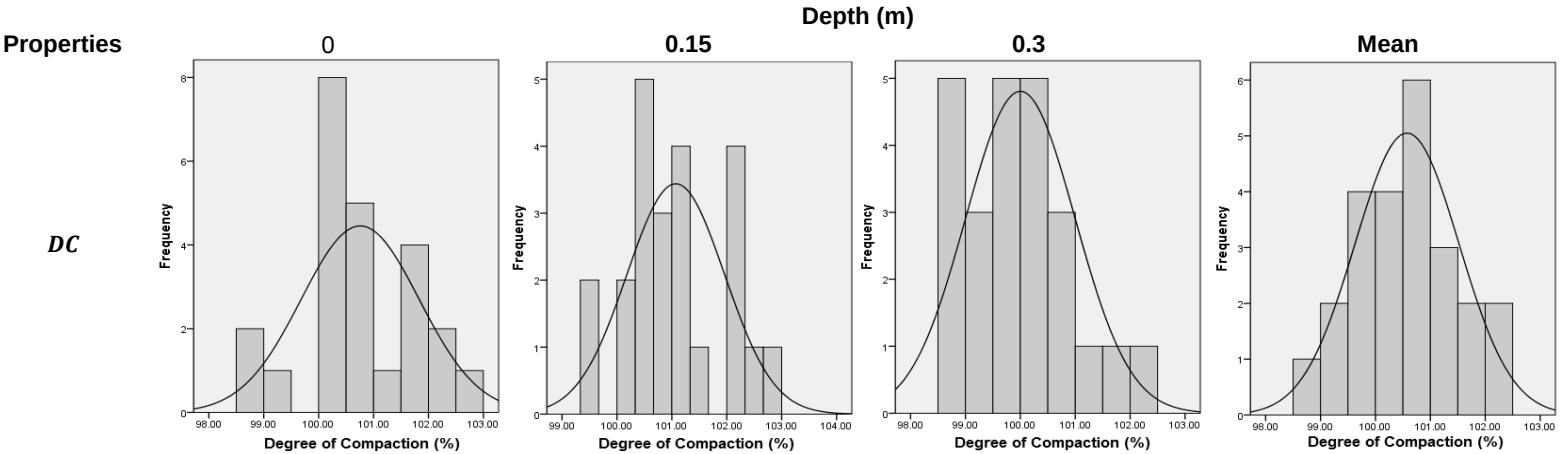

Figure IV.O - Histograms for the DC results obtained in stage 2, with the NDG in the ωopt-2% layer.

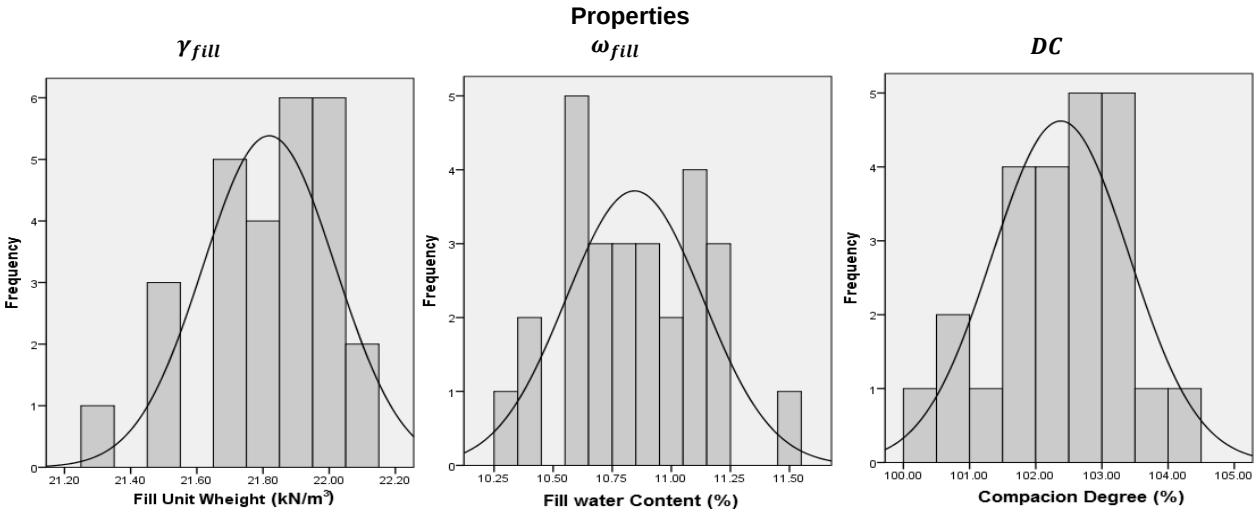

Figure IV.P1 - Histograms for the results obtained in stage 2, with the SCT in the ωopt-2% layer.

IV.e. STAGE 2 - HISTOGRAMS FOR THE ω_{OPT}% LAYER

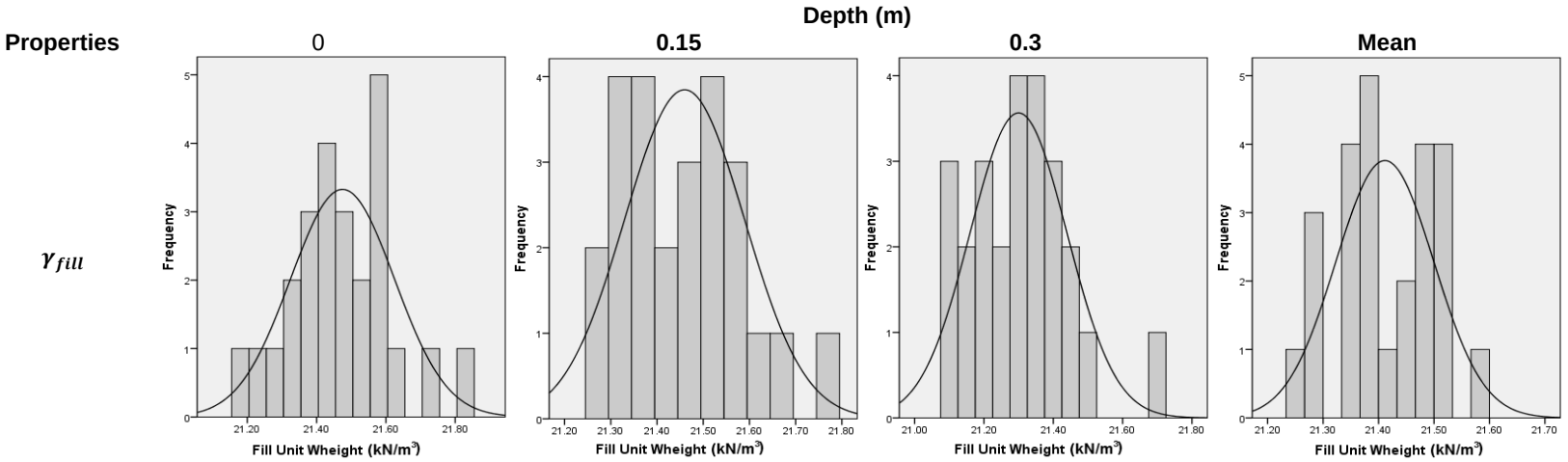

Figure IV.Q - Histograms for the γ_{fill} results obtained in stage 2, with the NDG in the ωopt% layer.

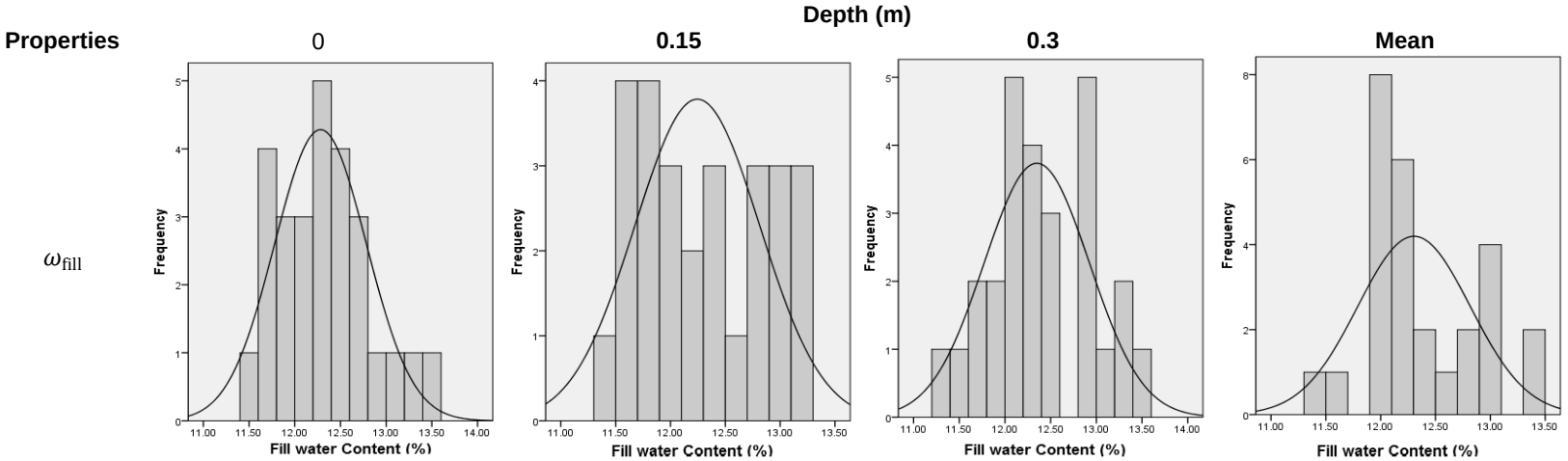

Figure IV.R - Histograms for the ω_{fill} results obtained in stage 2, with the NDG in the ωopt% layer.

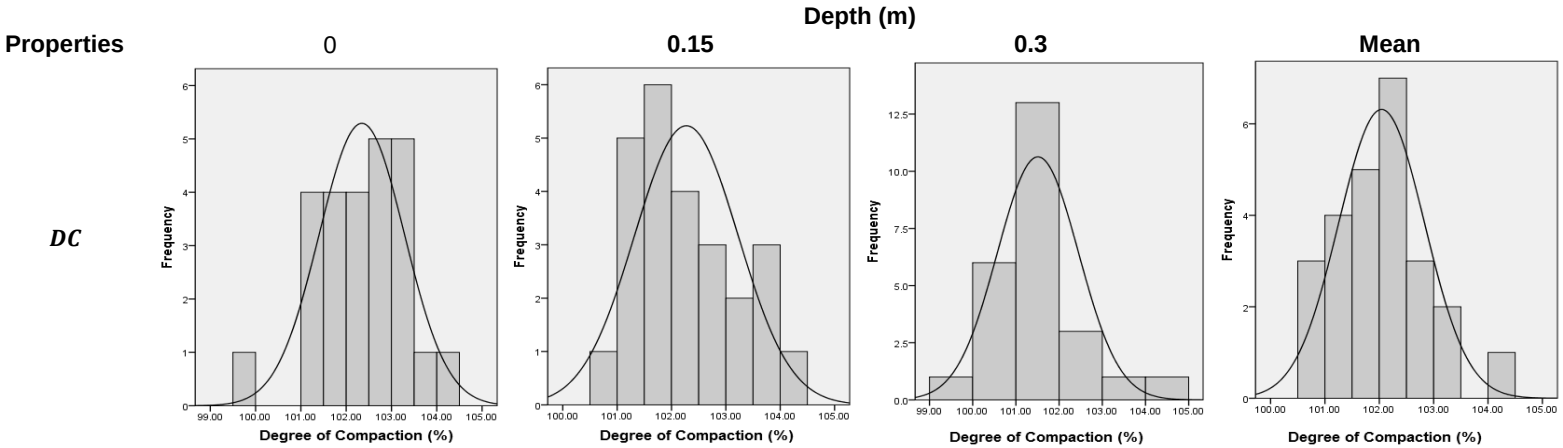

Figure IV.S - Histograms for the DC results obtained in stage 2, with the NDG in the ωopt% layer.

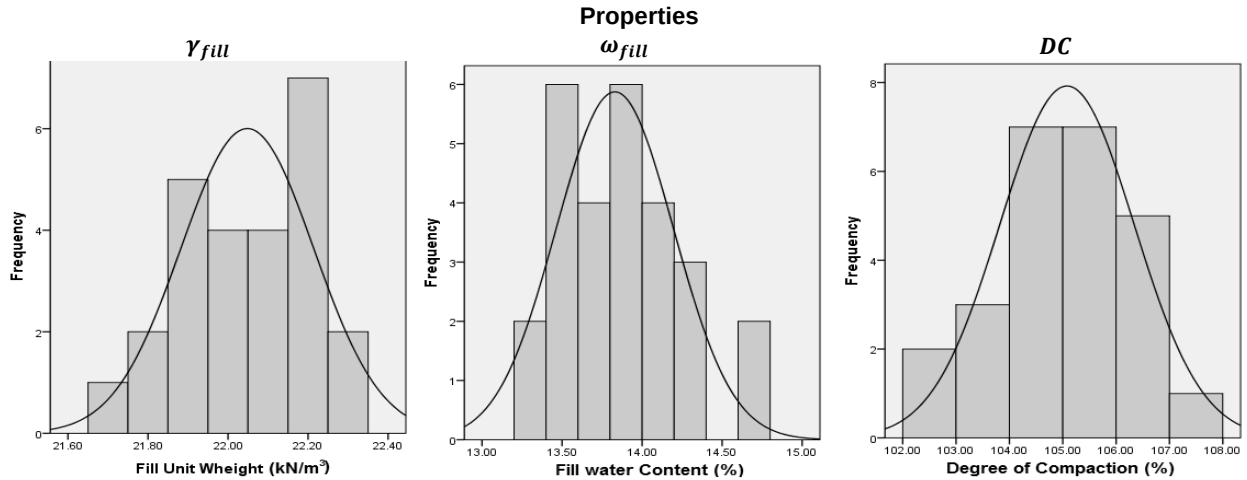

Figure IV.T - Histograms for the results obtained in stage 2, with the SCT in the ωopt% layer.

IV.f. STAGE 2 - HISTOGRAMS FOR THE ω_{OPT}+2% LAYER

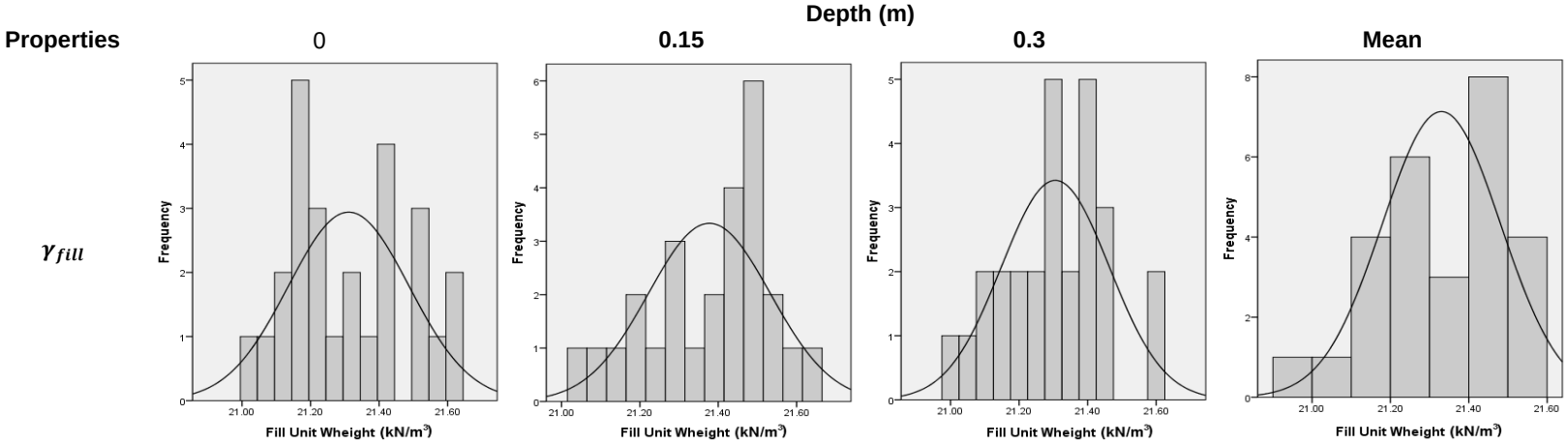

Figure IV.U - Histograms for the γ_{fill} results obtained in stage 2, with the NDG in the ωopt+2% layer.

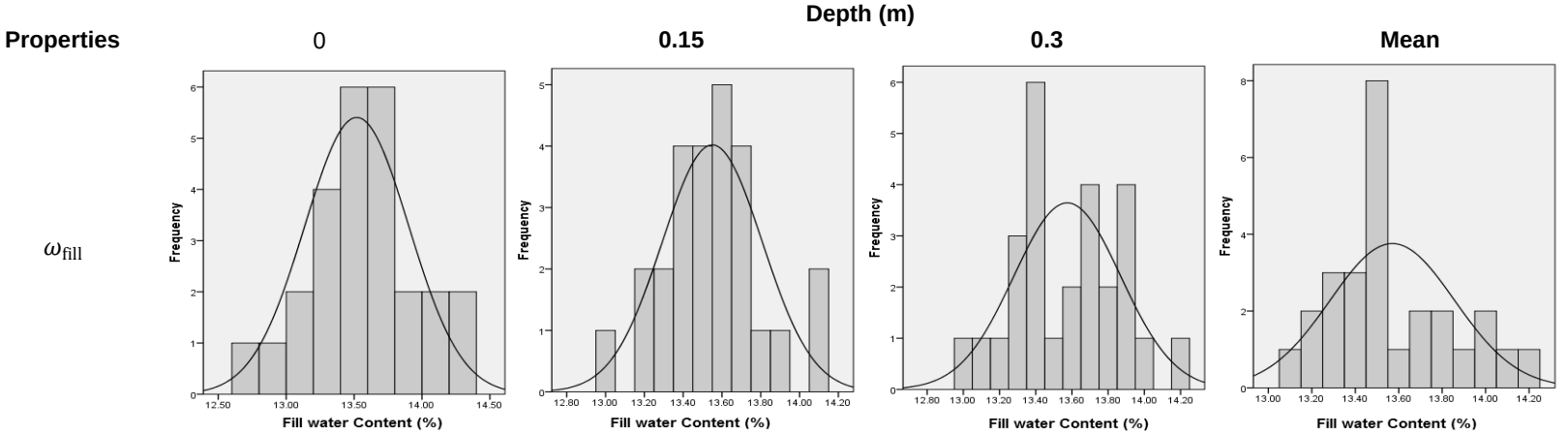

Figure IV.V - Histograms for the ω_{fill} results obtained in stage 2, with the NDG in the ωopt+2% layer.

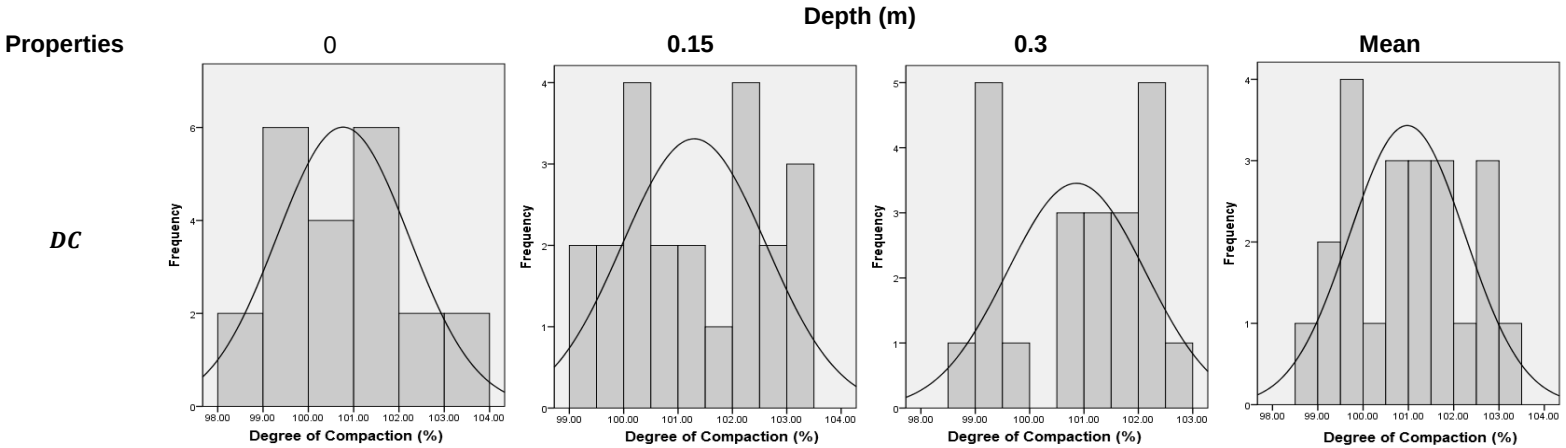

Figure IV.W - Histograms for the DC results obtained in stage 2, with the NDG in the ωopt+2% layer.

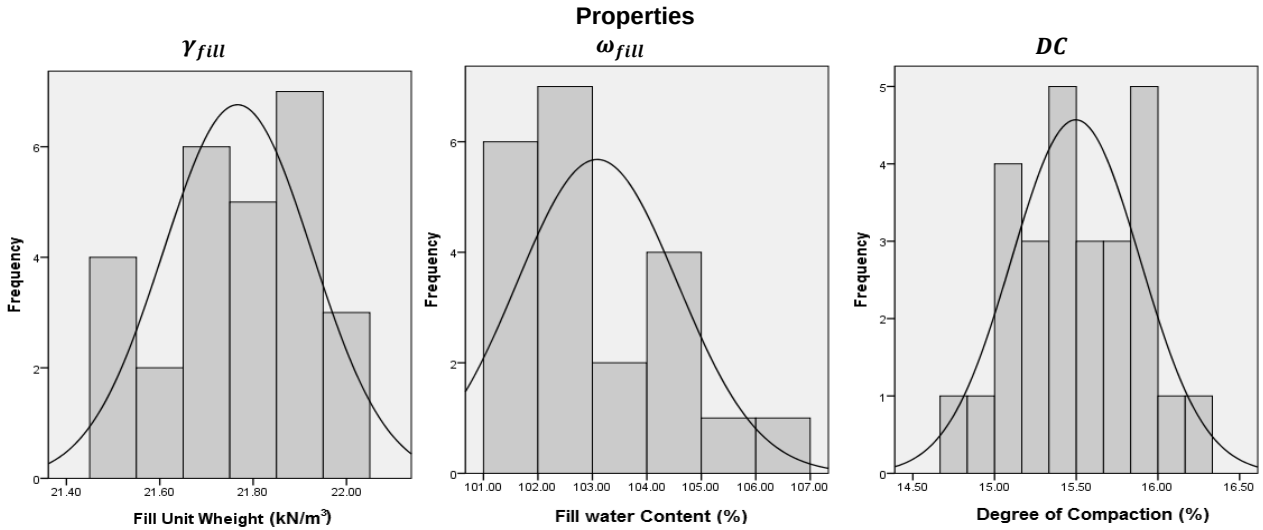

Figure IV.X - Histograms for the results obtained in stage 2, with the SCT in the ωopt+2% layer.

IV.g. STAGE 3 - HISTOGRAMS FOR THE ω_{OPT}-2% LAYER

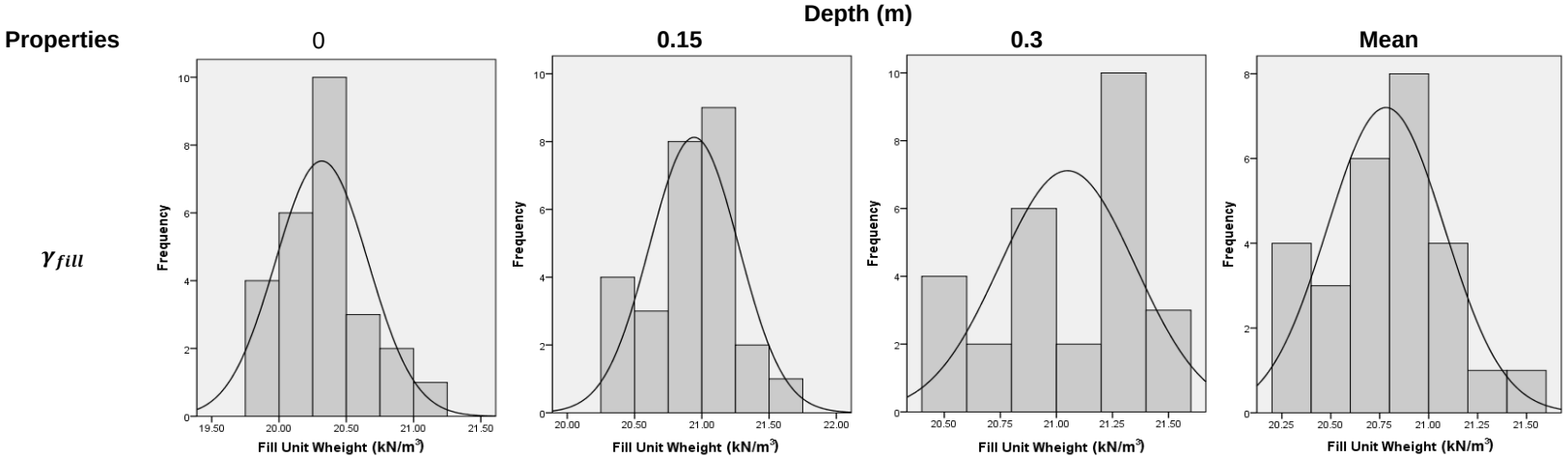

Figure IV.Y - Histograms for the γ_{fill} results obtained in stage 3, with the NDG in the ωopt-2% layer.

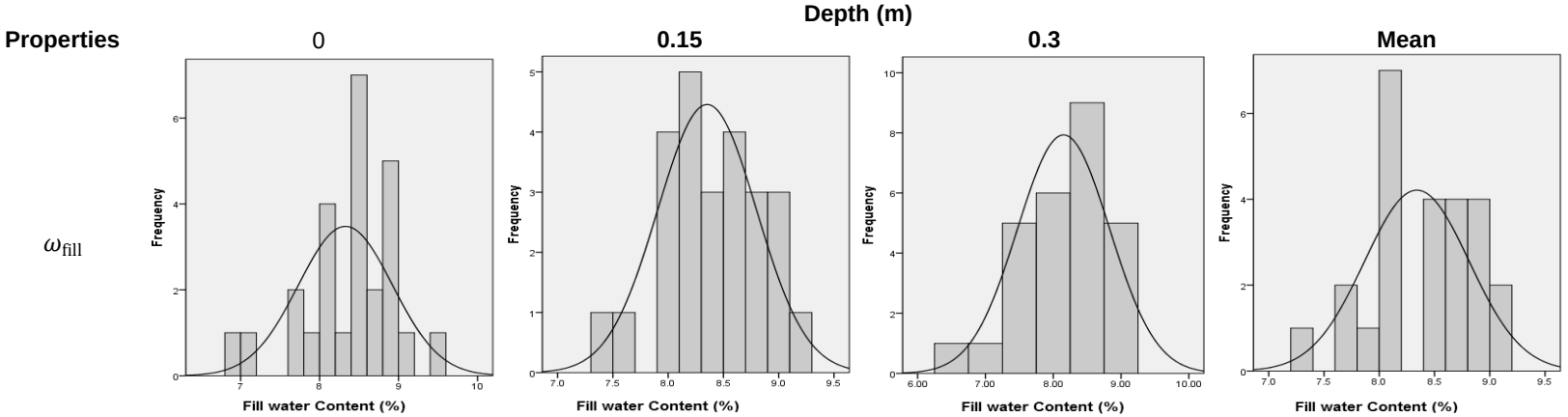

Figure IV.Z - Histograms for the ω_{fill} results obtained in stage 3, with the NDG in the ωopt-2% layer.

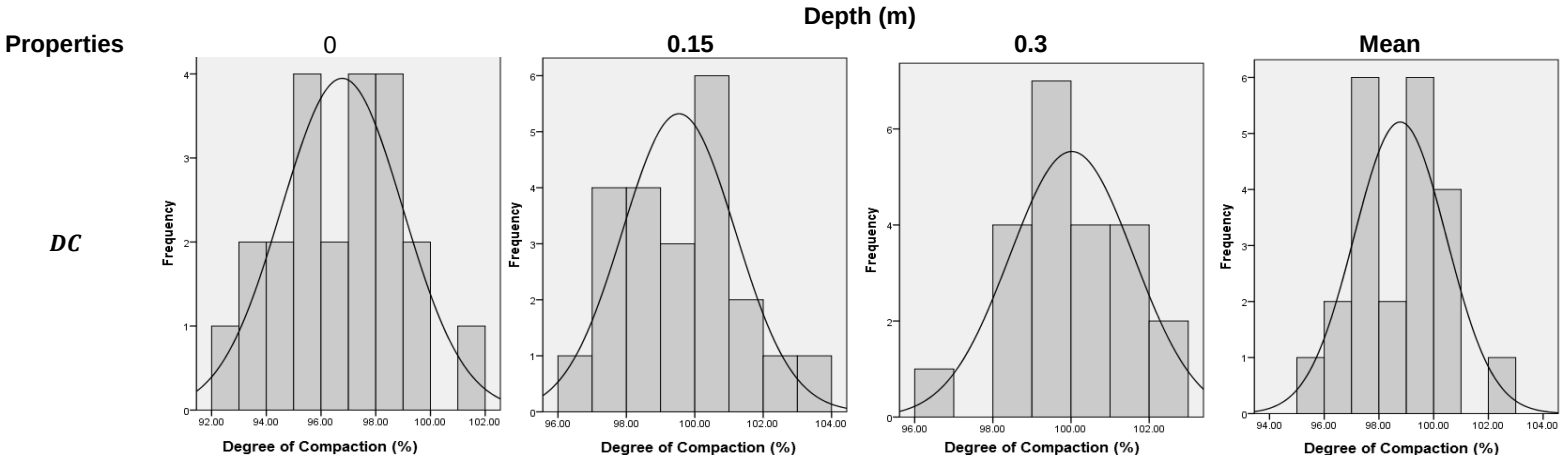

Figure IV.AA - Histograms for the DC results obtained in stage 3, with the NDG in the ωopt-2% layer.

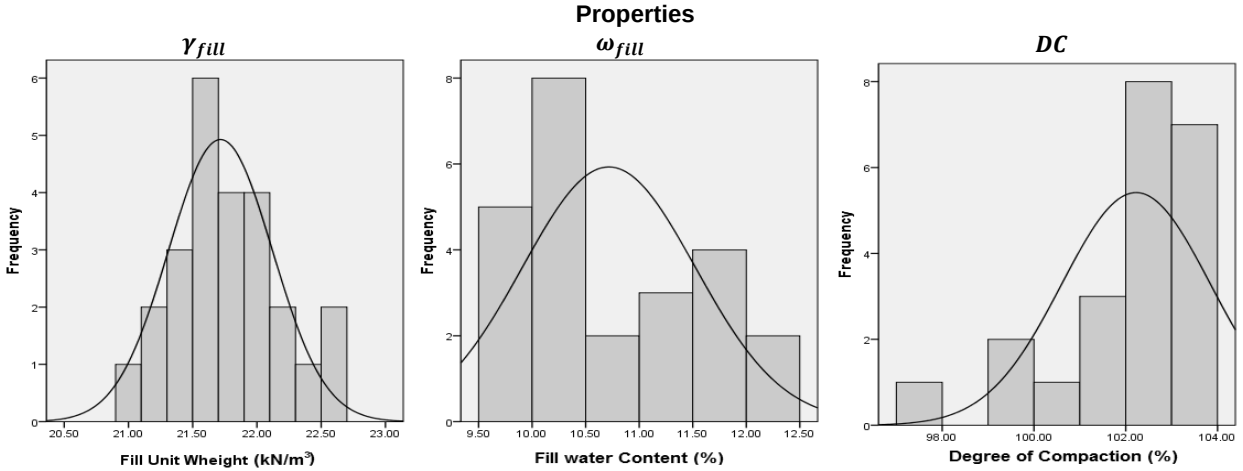

Figure IV.BB - Histograms for the results obtained in stage 3, with the SCT in the ωopt-2% layer.

IV.h. STAGE 3 - HISTOGRAMS FOR THE ω_{OPT}% LAYER

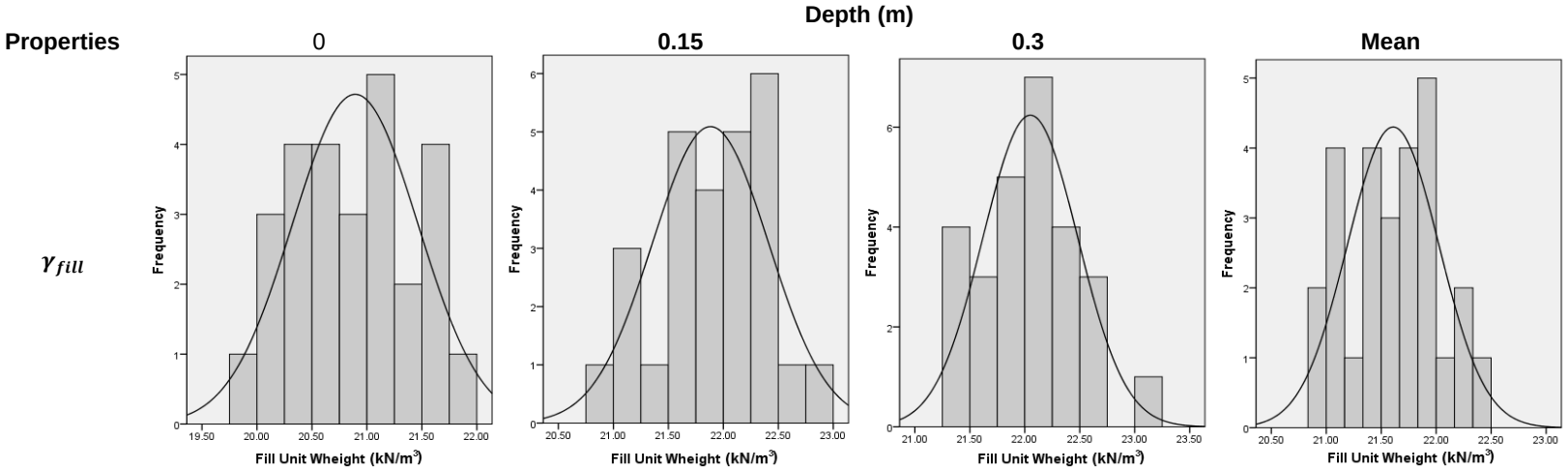

Figure IV.CC - Histograms for the γ_{fill} results obtained in stage 3, with the NDG in the ωopt% layer.

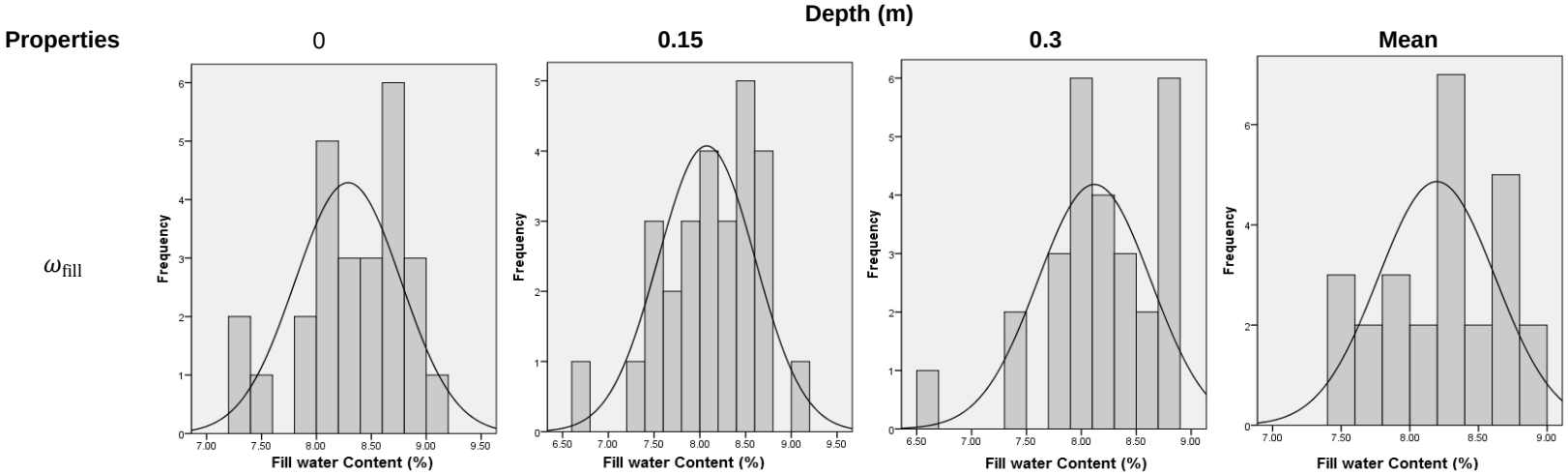

Figure IV.DD - Histograms for the $\boldsymbol{\omega_{fill}}$ results obtained in stage 3, with the NDG in the ωopt% layer.

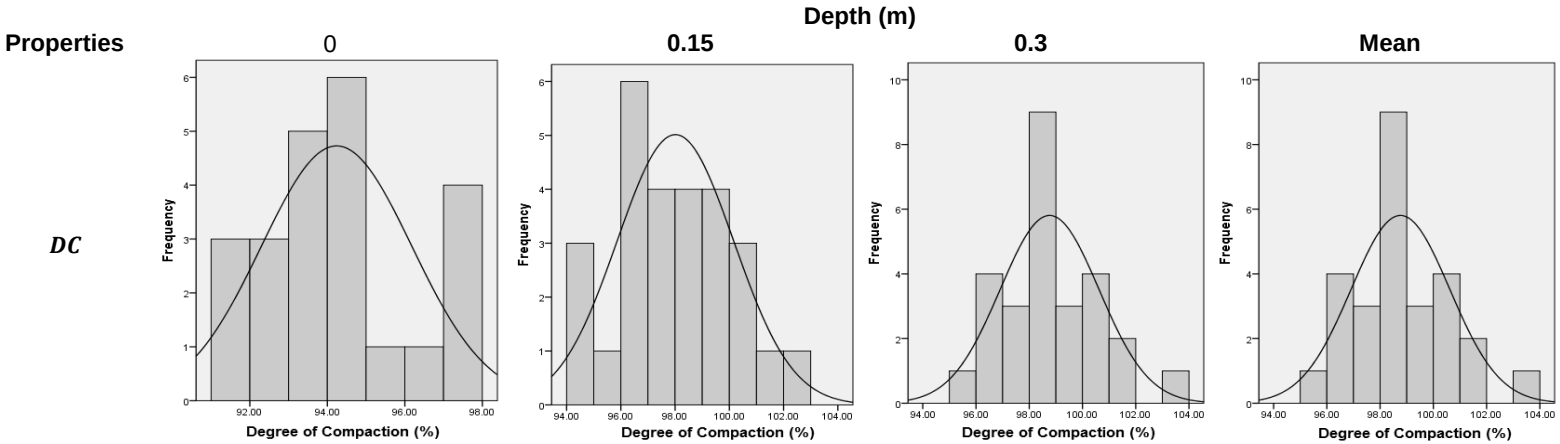

Figure IV.EE - Histograms for the DC results obtained in stage 3, with the NDG in the ωopt% layer.

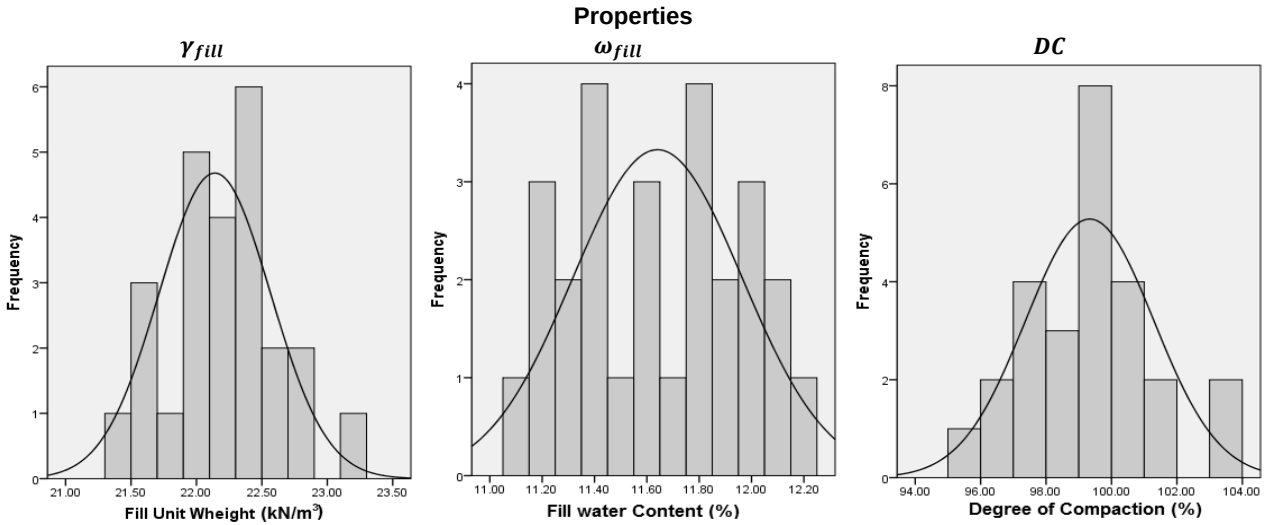

Figure IV.FF - Histograms for the results obtained in stage 3, with the SCT in the ωopt% layer.

IV.i. STAGE 3 - HISTOGRAMS FOR THE ω_{OPT}+2% LAYER

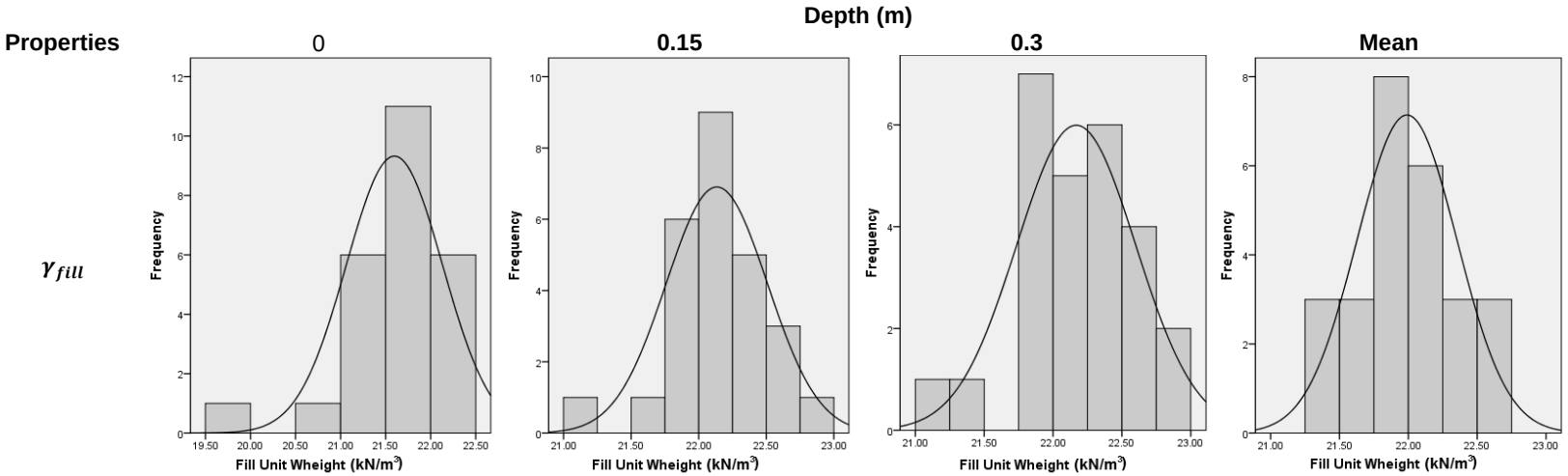

Figure IV.GG - Histograms for the γ_{fill} results obtained in stage 3, with the NDG in the ωopt+2% layer.

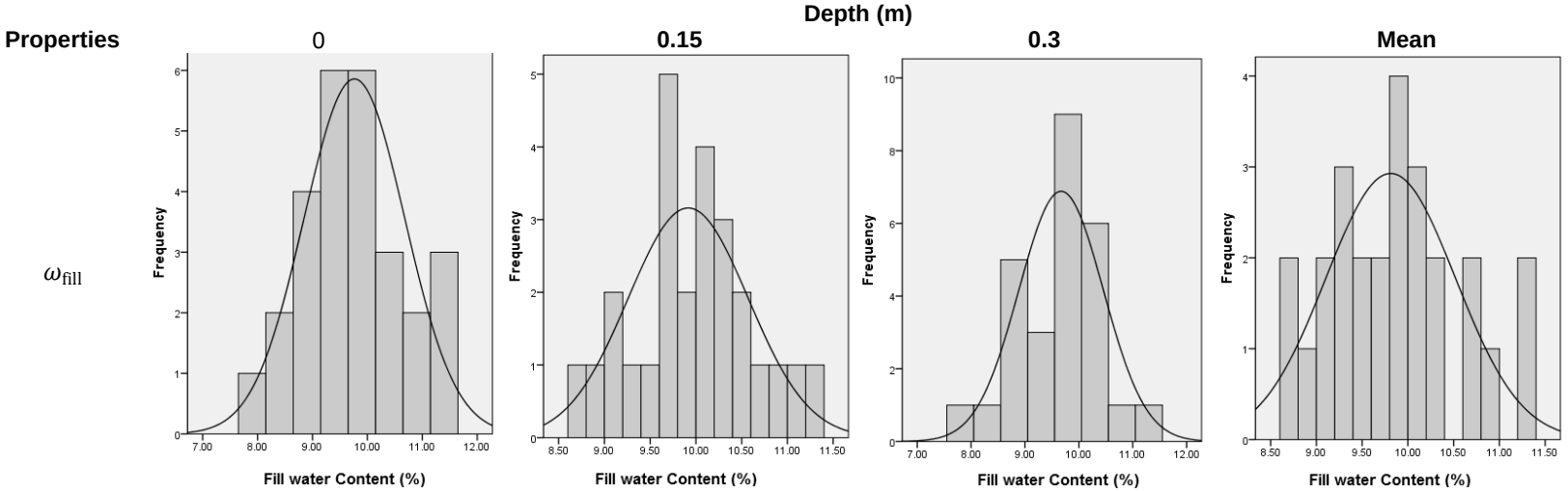

Figure IV.HH - Histograms for the ω_{fill} results obtained in stage 3, with the NDG in the ωopt+2% layer.

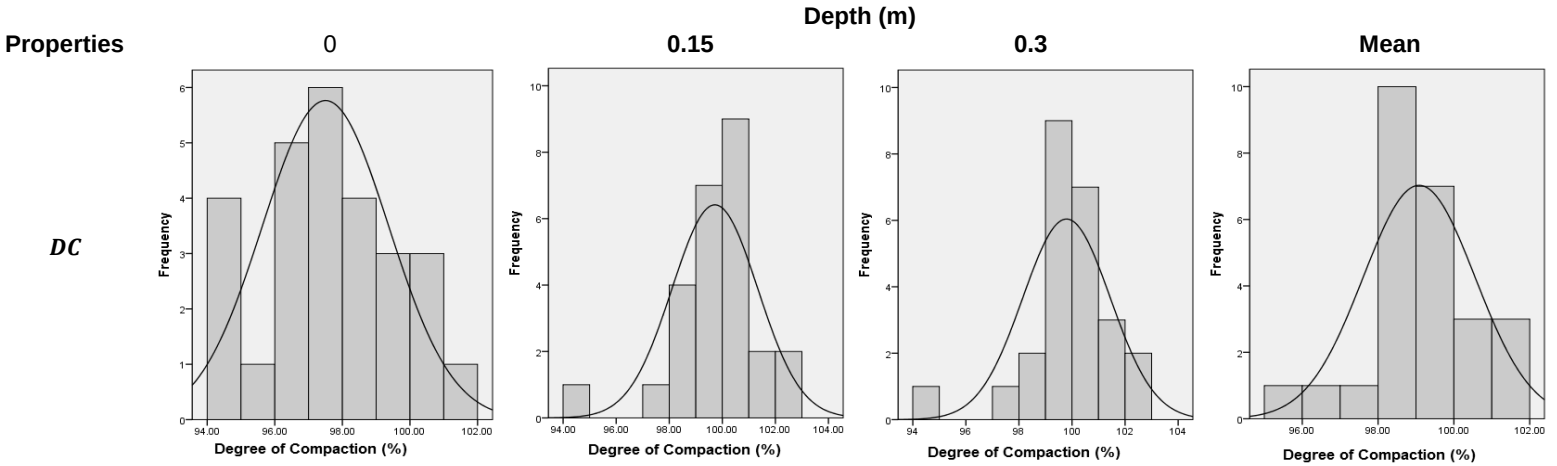

Figure IV.II - Histograms for the DC results obtained in stage 3, with the NDG in the ωopt+2% layer.

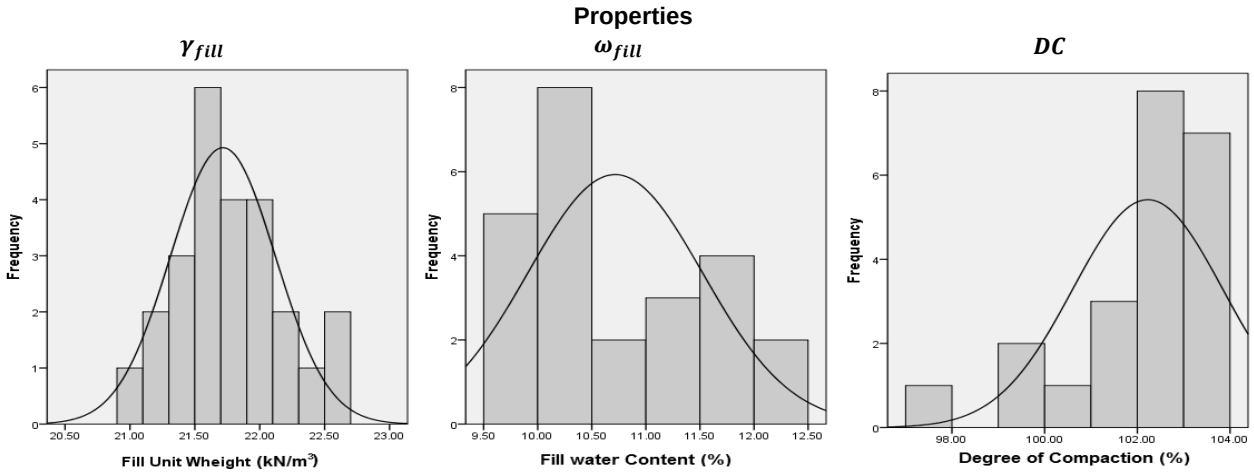

Figure IV.JJ - Histograms for the results obtained in stage 3, with the SCT in the ωopt+2% layer.

ANNEX V - HISTOGRAMS FOR THE CORE RESULTS

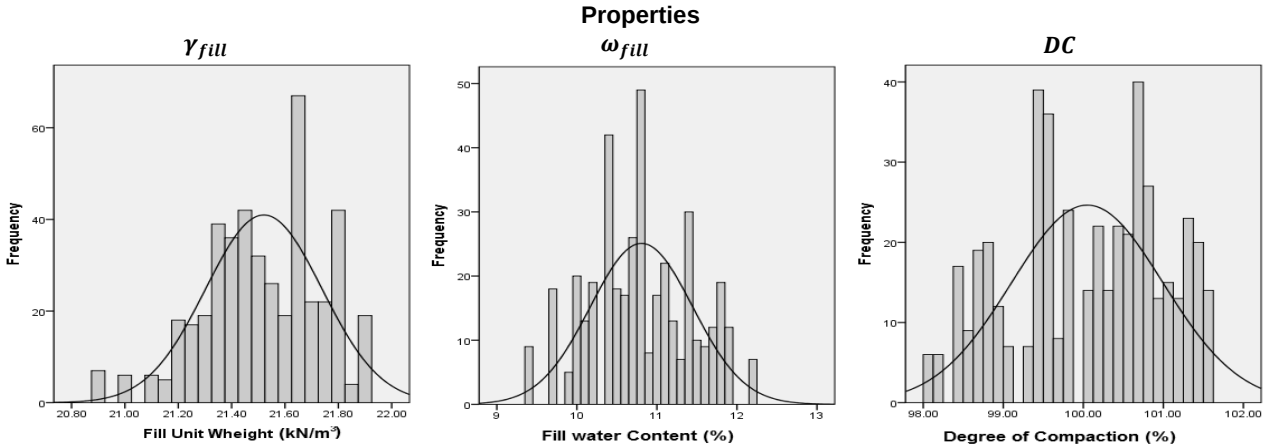

Figure V.A - Histograms for the core results obtained with the SCT.

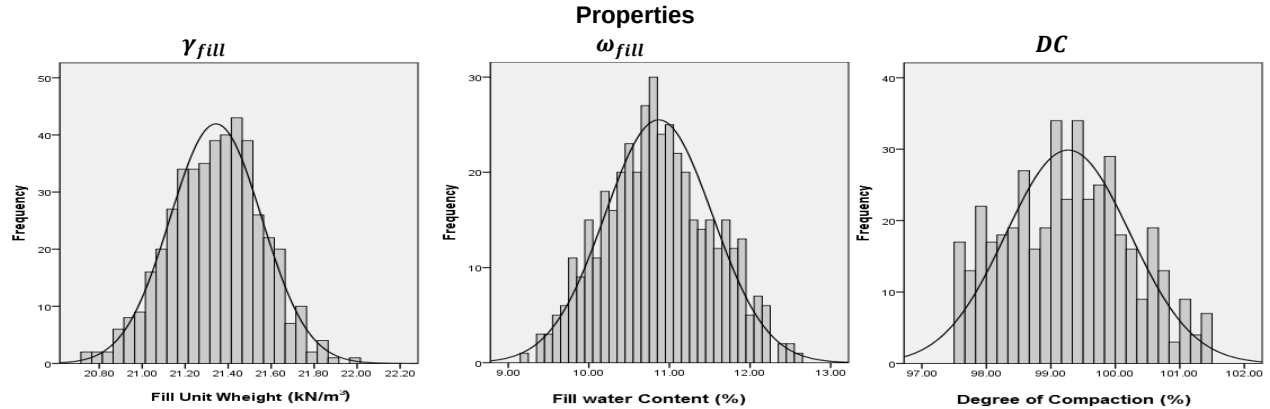

Figure V.B - Histograms for the core results obtained with the NDG.

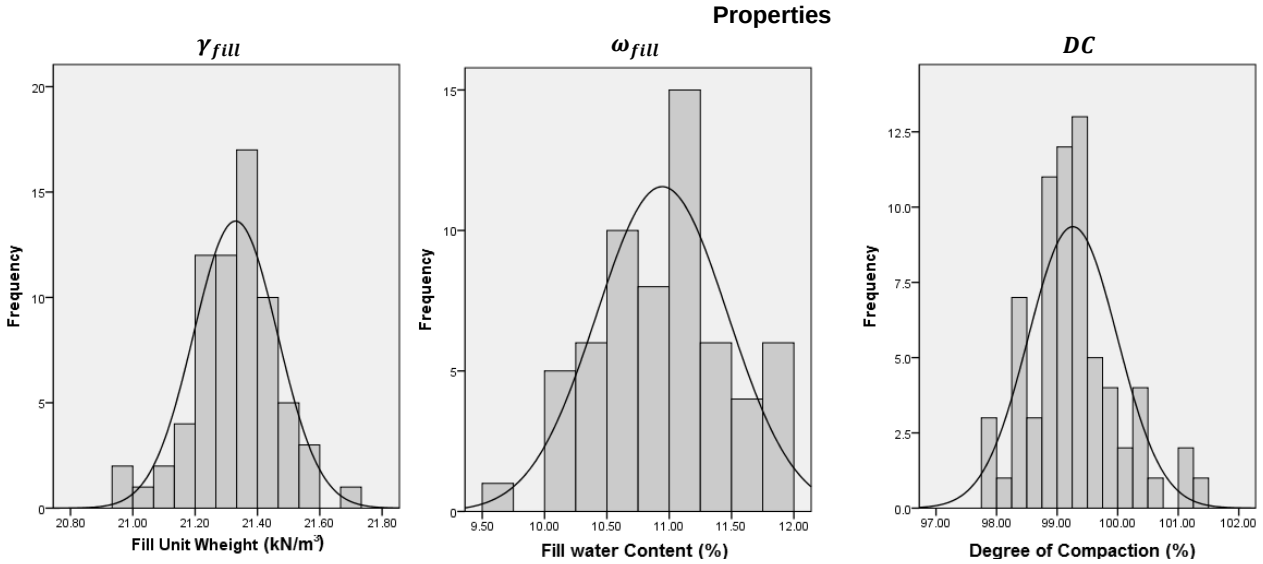

Figure V.C - Histograms for the core results obtained by considering the mean of all NDG measurements that can be compared with each SCT.